Geological Survey of Finland, Bulletin 359

GLACIAL DEPOSITS, THEIR ELECTRICAL PROPERTIES AND SURVEYING BY IMAGE INTERPRETATION AND GROUND PENETRATING RADAR

by

RAIMO SUTINEN

with 108 figures and 5 tables

ACADEMIC DISSERTATION

Academic Dissertation to be presented with the assent of the Faculty of Science, University of Oulu, for public discussion in the Auditorium GO 101, Linnanmaa, on May 22nd, 1992, at 12 o'clock noon

GEOLOGIAN TUTKIMUSKESKUS
ESPOO 1992

Sutinen, R. 1992. Glacial deposits, their electrical properties and surveying by image interpretation and ground penetrating radar. *Geological Survey of Finland, Bulletin 359.* 123 pages, 108 figures and 5 tables.

Genetical, textural and electrical classification has been presented for glacial materials in northern Finland, Wisconsin and Glacier Bay, southeast Alaska. Electrical properties (dielectrics and conductivity) have been used as a »ground truth» reference for interpretation and classification of remotely sensed data, such as SPOT satellite data, airborne electromagnetic and gamma-radiation data. Ground penetrating radar (GPR) surveys were applied to evaluate raw materials potential of different morphogenetic landform types, and GPR profiling was used in northern Finland to determine meltwater paleoflow patterns in eskers and end moraines to reconstruct the Weichselian Glacial Episode.

The genetic classification: lodgement till, melt-out till, flow sediments, glaciofluvial infill and openwork sediments and fluvial sediments, was demonstrated to be consistent with the textural classification expressed by moment kurtosis and graphic standard deviation (sorting coefficient) grain size parameters. Dielectric properties of glacial deposits, determined *in situ* by the time domain reflectometry (TDR) and radar surface arrival detection (RSAD) techniques (in the frequency range from 1 MHz to 1 GHz), are strongly dependent on the contained volumetric water, and an empirical relationship $\varepsilon_r = 3.2 + 35.4*\Theta_v + 101.7*\Theta_v^2 - 63*\Theta_v^3$ is given. Because the amount of free water ($\varepsilon_r \approx 80$) was shown to strongly dominate over bound water ($\varepsilon_r \approx 3.5$) also in unsaturated materials, and volumetric water content is sediment specific, the dielectric classification is valid. Conductivity of unfrozen glacial materials is dependent on the moisture content and textural characteristics, but ground water salinity and mineralogic composition of some local tills increase the overall conductivity.

Grussification detected by GPR in Central Finnish Lapland, is one indication of low glacial erosion rate in the center area of former ice sheet(s). Streamlined forms tend to increase in size and volume downice, but practically lack near the end moraines. Drumlins exhibit both erosional and depositional features. Contrary to Wisconsin drumlins in Finland do not contain significant gravel and sand resources presumably because of absence of outwash deposition prior to drumlinization. Eskers and end moraines are the most valuable raw materials reserves and ground water sources, but also coarse-textured flow sediments found in the hummocky moraines are potential substitute reserves.

Based on the ground penetrating radar data, glacial dispersal patterns, till stratigraphy and palynological evidences three Weichselian ice advances have been identified in northern Finland. The Pudasjärvi stage, correlated with the Early Weichselian, is demarcated by the Pudasjärvi end moraine south from the Arctic Circle. The second Early Weichselian (or Mid Weichselian) stage, the Lapland ice flow stage is demarcated by the Kuusanjärvi-Nunospuljut and Niliharju end moraines north from the Arctic Circle. During the Late Weichselian northern Finland was entirely covered by ice.

Key words (GeoRef Thesaurus, AGI): glacial features, glaciofluvial features, moraines, radar methods, electrical properties, remote sensing, textures, water content, stratigraphy, Quaternary, northern Finland, United States, Wisconsin, Alaska.

Raimo Sutinen
Geological Survey of Finland
SF-96400 Rovaniemi, Finland

ISBN 951-690-454-8
ISSN 0367-522X

Vammala 1992 Vammalan Kirjapaino Oy

To Marja-Liisa, Salla and Einari

Preface

This thesis synthesizes genetical, textural and electrical characteristics of glacial deposits in northern Finland, southern Wisconsin and Glacier Bay, southeast Alaska. Morphogenetic and stratigraphic classification of landforms is based on image interpretation and ground penetrating radar surveys. The material for this study was collected during the Quaternary mapping program of the Geological Survey of Finland, as a member of the Nordkalottproject 1980 — 1986 and as an Honorary Fellow at the University of Wisconsin-Madison, Dept. of Geology and Geophysics between 1987 and 1989. The work was financially supported by the Academy of Finland, the Research Council for the Environmental Sciences (grant no. 29/010) and by the grant to the University of Wisconsin-Madison (grant no. 133-M939) from Wisconsin DOT.

I express my gratitude to my supervisors, Professors Risto Aario and Sven-Erik Hjelt at the University of Oulu and Professor David M. Mickelson at the University of Wisconsin-Madison for the advices and constructive criticism during the study. I also would like to thank Professor Raimo Kujansuu for his support and advices, and Professor Frank Scarpace and Dr Ahti Silvennoinen for encouraging me to apply digital image processing techniques to glacial deposits.

Several people, as a staff and students, have been involved in applications and developing of measuring techniques, laboratory testing of materials and field reconnaissance. Their efforts are highly appreciated. Particularly I would like to mention Pekka Hänninen, Veikko Musta, Risto Pollari, Paula Haavikko and Andrea Sutherland. Päivi Heikkilä prepared the illustrations. Ardith Hansel and Rowland Cromwell corrected my English.

CONTENTS

INTRODUCTION

General

Unconsolidated glacial materials cover over 30 % of the continents and till probably is the most widespread sediment type in the world (Flint 1971). Since those deposits are on one hand important raw materials and on the other hand largely vary in geotechnical, hydrogeological and geochemical properties, lateral mapping of surface materials and surveying the thickness and volumes of raw materials are the main objectives in the glacial geological mapping. The earliest maps were mainly focused on geomorphology (Tanner 1915, Alden 1918), but later also stratigraphic information has been included.

Presently there is, however, no unambiguous way to classify tills and other glacial sediments *in situ* by numerical parameters, which could be effectively utilized as a »ground truth» for digital interpretation of remotely sensed data. Because those data either directly (airborne gamma radiation data) or indirectly (optical airborne and space borne data) are related to the earth surface water content, new fast field techniques are needed for measuring the properties that are related both to the textural characteristics as well as the water content of the earth materials. The other problem has been the lack of fast techniques to detect thicknesses and stratigraphy of the Quaternary deposits. Therefore new survey methods are needed to minimize high cost of drillings.

The objective of this study

The first objective of this thesis is to classify glacial materials by the electrical properties; dielectrics and conductivity. To put emphasis on the *in situ* characteristics of materials, two relatively new techniques, time domain reflectometry (TDR) and ground penetrating radar (GPR) have been applied to determination of dielectric properties of glacial materials. The effects of the texture, moisture content, salinity, mineralogy and temperature on the electrical properties have been studied to evaluate the feasibility of the electrical classification of glacial deposits.

The second objective is to apply the electrical data for mapping of surface materials and also use those characteristics to interpret radar and resistivity survey data. Digital image processing (DIP) and interpretation of different remotely sensed data, such as SPOT HRV satellite images, airborne electromagnetic/ gamma radiation data and low- and high-altitude photos have been tested for mapping of glacial materials. Since GPR allows fast and continuous subsurface profiling, it has been applied to evaluate the potential of coarse-textured raw materials within different glacial landforms, such as drumlins, Rogen moraines, eskers and end moraines. Genesis and stratigraphy of glacial deposits have been discussed based on the radar surveys, as well. DIP of Landsat TM images and conventional air photo interpretation (API) have been used to direct radar surveys for locating »old» gravel and sand reserves buried beneath »younger» tills.

Previous studies

Image interpretation

Air photo interpretation has been used in mapping of glacial deposits for decades (Kujansuu 1967, Prest 1968, Kihlblom 1970, Aario & Forsström 1979, Nordkalottproject 1986b, 1986c, Aylsworth & Shilts 1989). Even though the conventional stereoscopic API is based on the intuition (and of course the expertise) of the interpreter, it is in practice the easiest way to recognize different glacial morphological features. Also SPOT HRV images allow stereoscopic viewing but is more expensive.

Landsat MSS data has been used to map streamlined morainic landforms and eskers (Punkari 1982, 1984, 1985). Despite the exponential increase of digital image processing and interpretation (described thoroughly in the textbooks by Lillesand and Kiefer (1987) and Gonzales and Wintz (1987) of satellite (Landsat TM and SPOT HRV) data in tectonic lineament and bedrock mapping, geobotany and mineral exploration (most of the case studies presented from arid and semiarid areas), only a few attempts of mapping of glacial terrains (Denny et al. 1984) and attributed aggregates (Edwards & Richardson 1989, Gorecki et al. 1989) have been conducted. Airborne magnetic, electromagnetic and gamma radiation data have been applied almost exclusively in Finland (Peltoniemi 1982, Aarnisalo 1984, Lanne 1986, Gaál, 1988) to the mapping of igneous and metamorphic rocks as well as to ore exploration. Gamma-ray spectrometry has been applied to rock and soil discrimination (Schwarzer & Adams 1973) and to snow water equivalent measurements (Kuittinen & Vironmäki 1980). Several investigations (Grasty 1977, Burson 1973, Lanne 1986) suggest that airborne gamma ray information indicates earth surface moisture content — a very important observation in terms of surface mapping of glacial materials.

Electrical properties

The time domain reflectometry technique was introduced by Fellner-Felldeg (1969) for determining dielectric properties, also allowing simultaneous determination of electrical conductivity of soil (Dalton et al. 1984, Dasberg & Dalton 1985). TDR has been applied to measure dielectric properties of soils in laboratory (Topp et al. 1980, Delaney & Arcone 1982, Topp et al. 1982) and *in situ* (Davis 1975, Davis & Chudobiak 1975, Davis & Annan 1977, Davies et al. 1977, Topp & Davis 1982). Dielectric properties of a variety of soils have been studied as a function of electromagnetic wave frequency, volumetric moisture content and temperature (Leschanskii et al. 1971, Cihlar & Ulaby 1974, Hipp 1974, Hoekstra & Delaney 1974, Selig & Mansukhani 1975, Wobschall 1977, Wang & Schmugge 1980, Delaney & Arcone 1982, de Loor 1983, Hallikainen et al. 1985, Dobson et al. 1985, Ulaby et al. 1986). Electromagnetic measurement of soil moisture is based on the well-documented (Topp et al. 1980, Hallikainen et al. 1985, Alharthi & Lange 1987) dependence of the dielectric constant to the volumetric moisture content. That relationship has also been utilized in determining the moisture content in field (Topp et al. 1984, Baker & Allmaras 1990). A fairly new application of TDR is to locate the frozen — unfrozen interface in soils (Baker et al. 1982, Hayhoe et al. 1983) and measure water content and dielectric properties of frozen soils (Arcone & Delaney 1984, Patterson & Smith 1980, 1981, Stein 1985). Only a few attempts have been made to characterize tills by dielectric properties (Morey & Harrington 1972, Mickelson & Sutinen 1989, Sutinen 1989, Sutinen & Hänninen, Pekka 1990).

Electrical conductivity is dependent on the texture, porosity, moisture content and particle shape of earth materials as well as the concentration of electrolytes in the water that are either partially (unsaturated deposits) or totally (saturated deposits) filling the pore spaces between the

grains (Smith-Rose 1933, Todd 1964, Hoekstra & McNeill 1973, McNeill 1990, Ward 1990). Conductivity has been shown to increase with finer texture (Culley et al. 1975, Jackson et al. 1978, Pernu 1979, 1991) as well as being dependent on EM wave frequency (Parkhomenko 1967, Hipp 1974). Resistivity soundings have been applied to aggregate surveys since 1940's (Wilcox 1944).

Ground penetrating radar

Several hundreds of ground penetrating radar investigations have been conducted since 1930's as reviewed by Pilon (1983) and Olhoeft (1988). Since commercially manufactured GPR systems became available in the early 1970's (Morey & Harrington 1972), those have been applied to a great number of topics, including the measuring of thickness and structures of ice, glacier and polar ice (Annan & Davis 1976, Jezek et al. 1978, Kovacs et al. 1982, Bogorodsky et al. 1985), frozen ground and permafrost (Annan & Davis 1976, Arcone 1984), measuring fresh water depth (Annan & Davis 1977a, Kovacs 1990), monitoring ground water (Shih et al. 1986), detecting rock fractures (Holloway et al. 1985), peat investigations (Marttila 1982, Ahokas 1984, Lappalainen et al. 1984), investigation of glacial landforms (Sutinen 1985b, Pekka Hänninen 1991) engineering geological studies (Ulriksen 1982, Sakayama et al. 1983, Berg et al. 1983, Arcone & Delaney 1984), locating cavities beneath pavements (Kovacs & Morey 1983, Mickelson & Sutinen 1989) as well as more recently environmental and contamination studies (Olhoeft 1986, Inkster et al. 1989). GPR is an extremely versatile and rapid method for shallow depth investigations. The primary disadvantage of GPR is its extremely site specific applicability; the presence of high clay content in near subsurface will generally defeat the application of GPR (Olhoeft, 1986). However, the digital data processing will improve the quality of the GPR records (Daniels 1989, Maijala 1991), and thus help interpretation.

Study areas

Since glacial materials largely vary in genesis (deposited by glacier ice, by meltwater or by gravity), texture, lithologic composition and stratigraphy from one area to another, the electrical classification, if relevant, must be applicable everywhere in the glaciated terrains. Therefore electrical data for this study have been collected near modern glacier (Burroughs Glacier, Alaska) and from different Pleistocene materials deposited by the Laurentide and Scandinavian Ice Sheets in Wisconsin and northern Finland. Since electromagnetic wave propagation is governed by the dielectric properties and conductivity, the feasibility of ground penetrating radar has been evaluated for different glacial materials.

Glacier Bay, Alaska

Glacier Bay in the southeastern Alaska (Fig. 1) provides an excellent opportunity to study glacial processes and till deposition. The glacial history and the retreat of the Neoglacial ice in the area have been well documented since late 1800's (Reid 1896, see Goldthwait 1986). The field work for this study was done between Aug. 19 — 24, 1987 and Sept. 12 — 18, 1988 at the SE-margin of the Burroughs Glacier, previously studied by Taylor (1962), Mickelson (1971) and Larson (1978). The purpose was to characterize the Glacier Bay till by the electrical properties and apply those features to explain till deposition mechanisms in the Late Pleistocene terrains in Finland and Wisconsin. Since recent landslides and earthquakes are common in the Glacier Bay area (Horner 1990), the relationship between the landslides and postglacial rebound and attributed earthquakes (see Kujansuu 1972, Lagerbäck 1990) is discussed.

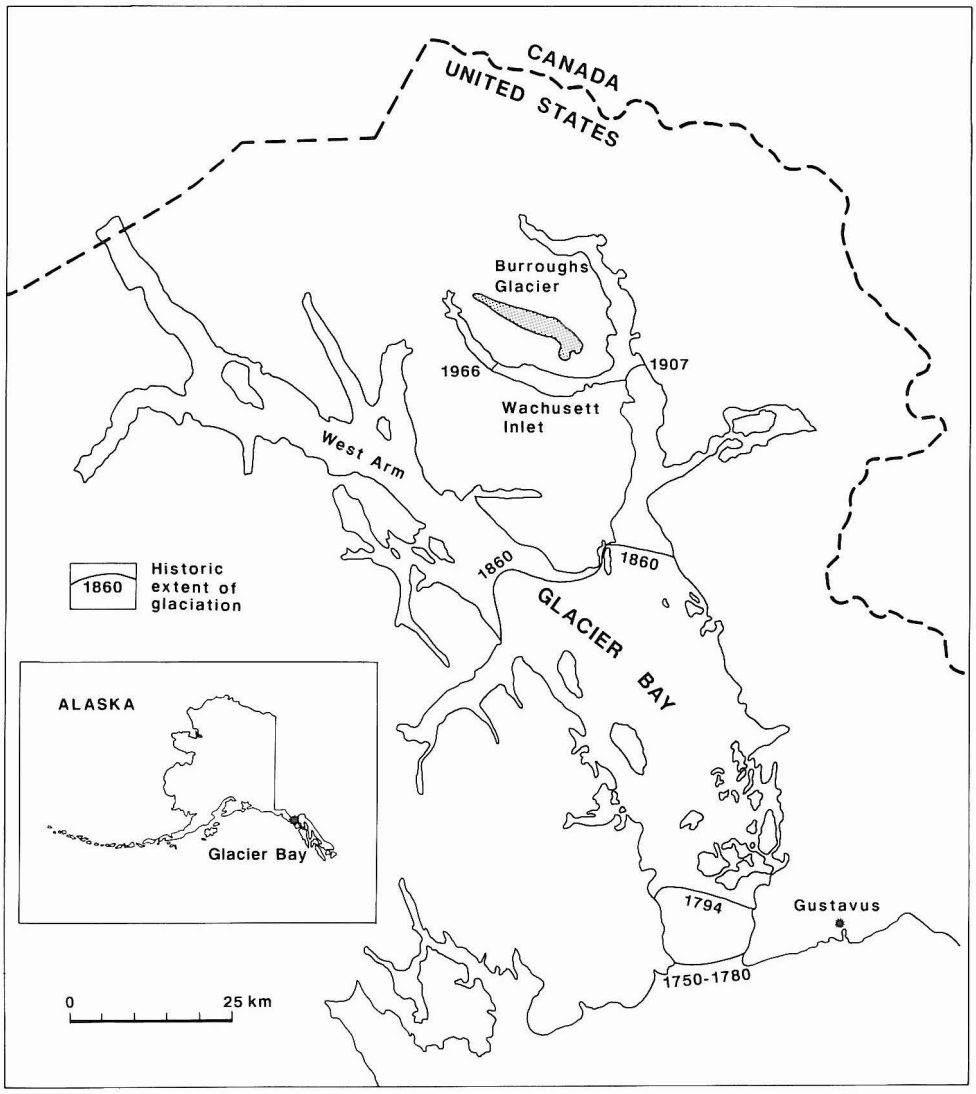

Fig. 1. Location of the Burroughs Glacier in Glacier Bay, southeastern Alaska.

Wisconsin

Drumlins and end moraines are the most prominent glacial features in Wisconsin (Fig. 2, Alden 1918). The drumlins particularly in the southeastern part of the state are of significant economic value due to large amounts of exploitable gravel (Whittecar & Mickelson 1979). If glaciofluvial activity is attributed to the deposition of the drumlins (see Shaw & Kvill 1984, Shaw et al. 1989), gravels should be found also in the cores of the drumlins in Finland. But, if the erosion mechanism (Whittecar & Mickelson 1979) is true, the »gravel drumlins» would be absent in Finland, because of the lack of the outwash deposits prior to drumlinization. One of the drumlins, the Door Creek drumlin, was studied in detail using GPR and the electrical characteris-

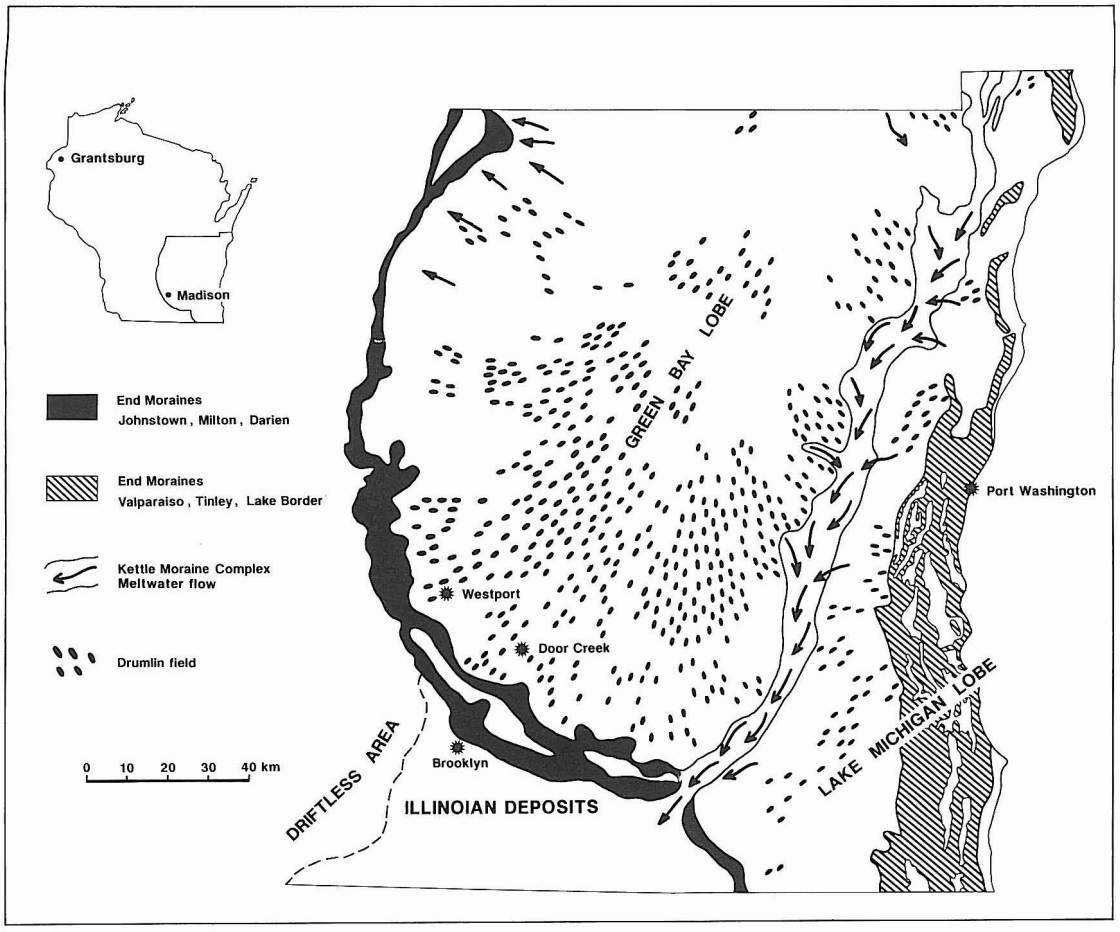

Fig. 2. Air photo interpreted stramlined features in southeastern Wisconsin. End moraines and the Kettle moraine complex adopted from Hadley and Pelham (1976) and Schneider (1983). Locations of the study sites also shown.

tics were applied to differentiate the drumlin sediments. Since the tills in southern and southeastern Wisconsin vary largely in texture as summarized by Schneider (1983) the electrical properties were determined for clayey, silty and sandy tills. Feasibility of SPOT HRV image processing and terrain geophysics were tested for sand and gravel reserves mapping in the Westport study site.

Northern Finland

Glacial landforms and materials in northern Finland were studied partially within the Quaternary mapping program of the Geological Survey of Finland and partially within the Nordkalott-project 1982 — 1986. In northern Finland the streamlined morainic landform patterns (Fig. 3), as recognized by the API and interpretation of satellite (Landsat TM and SPOT HRV) images, are presumably resulted from several glaciations (see Nordkalottproject 1986b, 1986c), and therefore glacial stratigraphy is emphasized dealing with the surveys there. GPR was extensively applied to different landforms to evaluate their raw material potential, genesis and stratigraphic context.

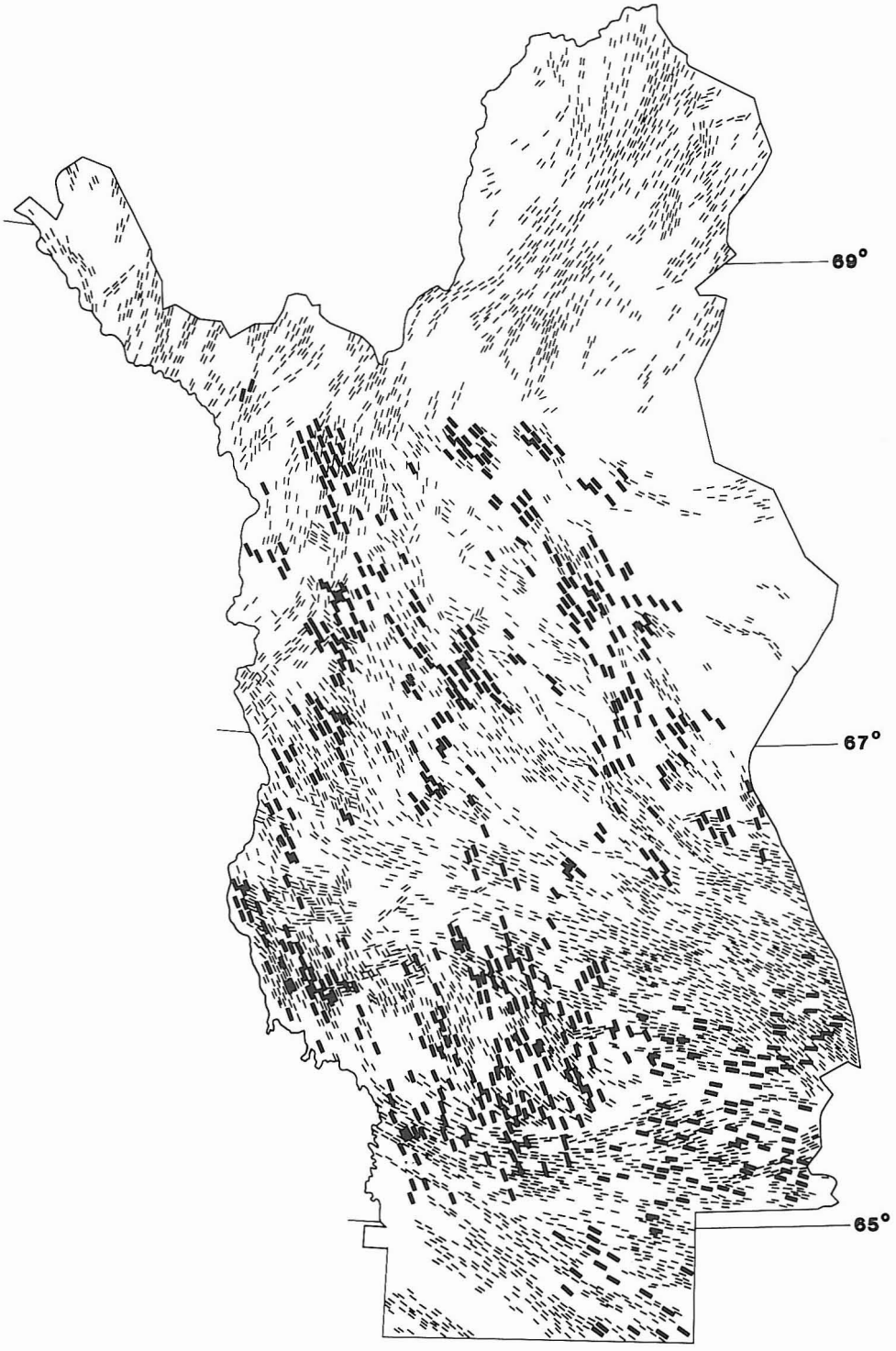

Fig. 3. The northern Finland study area and the air photo interpreted streamlined morainic landforms (partially published in Nordkalottproject 1986c). Thick stripes indicate large-scale drumlinoid forms (predominantly pre-Late Weichselian) and thin stripes flutes, drumlins and drumloids (predominantly Late Weichselian).

METHODOLOGY

Image interpretation

Glacial landforms were classified by using stereoscopic air photo interpretation (API). The material predominantly composed of black-and-white photos varying in the scales of 1 : 20 000 to 1 : 60 000, most prevalent being 1 : 30 000. Stereopairs had 60 % stereo coverage and 30 % overlapping with flight lines.

The following remotely sensed images were tested for mapping of glacial landforms and surface materials: SPOT HRV, June 3, 1986, Madison scene, Wisconsin; SPOT HRV June 24, 1986, Sokli scene, Finland; SPOT HRV, June 24, 1990, Savukoski scene, Finland; Landsat TM, June 2, 1984, Kemijärvi scene, Finland and Landsat TM, June 2, 1984, Savukoski scene, Finland; Airborne electromagnetic and gamma radiation data, Oulunsalo map sheet 2444 08, Finland; high-altitude color IR photo, Jun 6, 1979, Burroughs Glacier, Glacier Bay, Alaska; low-altitude low-angle color photo, Aug. 24, 1988, Burroughs Glacier, Alaska.

Air photos were digitized (by Optronics Model P-1700 densitometer) using 50 μm pixel size. SPOT composite was created by merging 10-meter resolution panchromatic band to 20-meter resolution multispectral bands. The following image processing routines (see Lillesand & Kiefer 1987, Scarpace 1989) were used for satellite images: geometric correction using cubic convolution, linear stretch, creating polygons and training sets and classification using maximum likelihood classification. Airborne geophysics data were processed as presented by Peltoniemi (1982), Gaál (1988) and Hyvönen et al. (1991). The image processing was partially performed at the Environmental Remote Sensing Center (ERSC), University of Wisconsin-Madison and partially at the Geological Survey of Finland (GSF). ERSC has PC-based image processing routines developed at the university, and at the GSF the Australian Disimp software and Apollo workstation were used.

Constitutive electrical parameters

The electromagnetic properties of materials are described by permittivity (ε), permeability (μ) and conductivity (σ). This thesis deals with glacial materials, which has a practically constant permeability equal to the free space permeability, $\mu_o = 4\pi * 10^{-7}$ Henry/m. Therefore permittivity and conductivity are the constitutive parameters described in this section.

The dielectric properties of materials describe its ability to store electrical potential energy under the influence of an electrical field, relative to that of air. Soils and parent glacial deposits are dielectric materials. In many applications these materials can be treated as linear dielectrics, meaning that the vector volume density of electrical current and vector volume density of polarization are proportional to the applied electrical field. The proportionality constant relating the vector volume density of current to the electrical field is called the conductivity and is, in general, a complex value, given (King & Smith 1981) by

$$\sigma = \sigma' + i\sigma''$$

The proportionality constant relating the vector volume density of polarization to the electrical field is $\varepsilon - \varepsilon_o$ where

$$\varepsilon = \varepsilon' + i\varepsilon''$$

is the permittivity of the material and $\varepsilon_o = 8.854*10^{-12}$ Farad/m is the permittivity of free

space. The relative permittivity, ε_r, is a dimensionless parameter defined such that

$$\varepsilon = \varepsilon_r \varepsilon_o$$

The imaginary portion of the conductivity σ'', accounts for time lags in the conduction response of the material to a time-varying electrical field. Similarly, ε'' accounts for the time lags in the polarization response of the material.

In Maxwel's equations (which govern the propagation of electromagnetic energy) the above parameters appear in the following combinations:

$$\sigma_e = \sigma' + \omega\varepsilon''$$

and

$$\varepsilon_e = \varepsilon' - \sigma''/\omega$$

where ω is the angular frequency of the electrical field. The parameters defined in the above equations are called the real effective conductivity and the real effective permittivity, respectively. The relative real effective permittivity (ε_{er}) is defined such that

$$\varepsilon_e = \varepsilon_{er} \varepsilon_o$$

Over the frequencies (between 1 MHz and 1 GHz) operated by the time domain reflectometer and ground-penetrating radar the imaginary part of the conductivity σ'' equals zero, so that ε_{er} is approximately equal to the real part of the dielectric constant (King & Smith 1981, Ulriksen 1982). Further in the text the term dielectric constant refers to the real part of the dielectric constant.

TDR instrumentation

TDR is relatively new method for soils surveys, first introduced by Fellner-Feldegg (1969) that allows dielectric constant determinations and indirect calculation of volumetric water content (Davis & Annan 1977, Davies et al. 1977, Topp et al. 1980). The time domain reflectometer consists of a pulse generator which produces a fast rise time step, a sampler and an oscilloscope or any other display or recording device. The frequency output contains frequencies between 1 MHz and 1 GHz. In the time domain, a pulse is sent which contains all frequencies simultaneously. The pulse travels along the transmission line, and any discontinuity such as change in dielectric, change in dimensions in transmission lines (e.g. Davis & Chudobiak 1975) or open circuit, will send a reflected pulse to the generator. The reflected pulses are visible on the recording display and this permits the determination of the end of the probe. The TDR trace can be printed by an XY-recorder or it can be photographed (e.g. polaroid film) for later analysis. In this study portable TDR units manufactured by Tektronix and SOILMOISTURE EQUIPMENT CORP. (Trase System I) were used. Figure 4 shows a TDR field instrumentation.

Transmission lines

TDR involves inserting a transmission line into the ground and measuring the time required for an electromagnetic pulse to travel to the end of the guide, giving a measure of pulse velocity in the soil material. There are two basic line configurations, parallel line (using probes) (e.g. Davies et al., 1977) and coaxial line / tube (e.g. Topp et al., 1980) and there are two basic design considerations, cross-sectional geometry and line length.

In this study a coaxial transmission line with characteristic impedance of 50 ohm was attached to a parallel transmission line composed of two steel probes inserted into the sediment. The velocity of a pulse (v) along the transmission line of known length (L, in meters) is given for low loss materials as follows:

$$v = L / t = c / \sqrt{\varepsilon_r}$$

where t is the travel time and c is the free space

velocity ($3 * 10^8$ m s^{-1}). Hence ε_r is

$$\varepsilon_r = (c * t / L)^2$$

To measure the pulse travel time (t) on the trace, the beginning and the end of the probe has to be determined. Figure 5 shows an XY-print of the TDR trace, where the beginning of the probe (A) is at the top of the peak. The end of the probe (B) has been determined with tangents described by Patterson and Smith (1980, also Stein 1985).

There are some limitations for the length of the probes. In electrically conductive materials, such as marine clay, the high signal attenuation makes it difficult to define the transition point B (Fig. 5), because the magnitude of the reflected wave is low, and the trace lies near horizontally or bends down. The following steel probes were used: 20 cm probes, 6 mm in diameter for majority of the determinations, 15 cm, 2 mm in diameter for some laboratory tests and 1,5 m to 3 m, 25 mm in diameter as well as up to 7 m, 15 mm in diameter for some field tests. The maximum probe spacing, distance between centers of the probes, depends upon the wavelength of the electromagnetic signal. It should be smaller than one tenth of the wavelength (Davis & Chudobiak 1975). The volume sampled is approximately equal to the square of the spacing between the probes (Topp et al. 1980) and the shape of volume sampled resembles a flattened cylinder with an ellipsoid cross section.

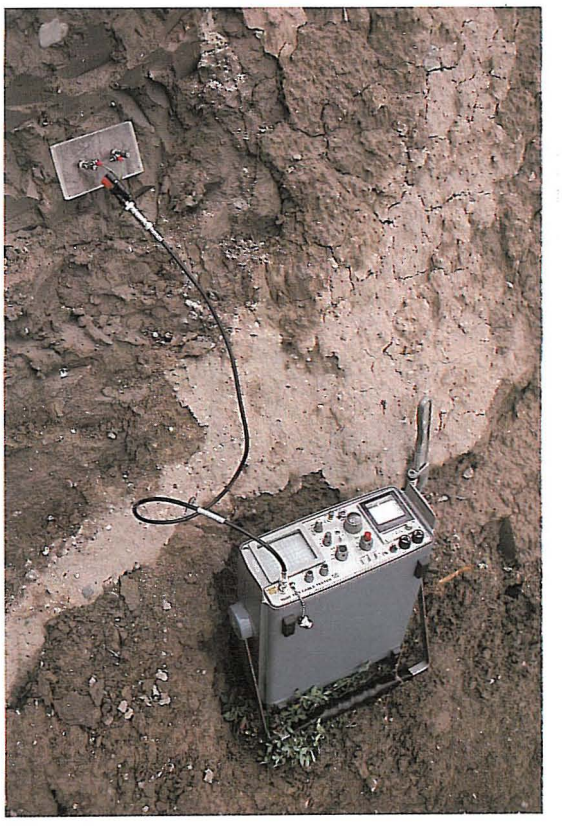

Fig. 4. Instrumentation for determination of dielectric constant using the time domain reflectometry technique (Tektronix 1502, commercially known as cable tester) and parallel transmission line, composed of two 20-cm-long steel probes, 6 mm in diameter. PVC-block is to maintain constant probe spacing of 5 cm.

GPR instrumentation

The GPR system consists of a control unit, transducer (antenna and transmit / receive electronics), power source and graphic and/or tape recorder (GSSI 1980). Both electronics components and bowtie-type antenna usually are packed into same fiberglass console, but also the transmitter and receiver can be placed in different consoles. The majority of the radar data for this study was collected by an 80 MHz (center frequency, c.f.) antenna. The transducer electronics mounted on the top of the console generates a pulse 6 ns wide at a repetition frequency of 50 kHz. This pulse is fed through the bow-tie antenna, which radiates a wavelet with a c.f. of 80 MHz and then receives the reflected energy from subsurface interfaces. The receiver uses amplitude samples from successive returning wave forms to create an audio analog of the returning

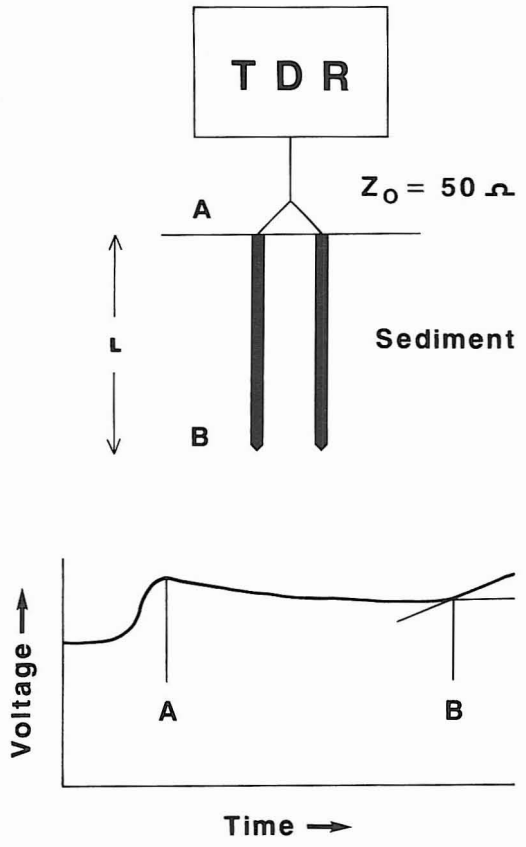

Fig. 5. A TDR trace for the 50 ohm line for determining dielectric constant.

signal. The analog signal is then transmitted to the system's control unit, where the signal can be transferred for digital recording, and/ or printed on a graphic recorder. The graphic recorder represents deflections of the return signal from zero amplitude in shades of gray, with darkness increasing in proportion to signal amplitude.

The radar system used in this study was manufactured by GSSI, Inc. of Hudson, New Hampshire. The major components of the system SIR-8 included the model 4800 radar control unit, model SR-8004H graphic recorder, model DT-6000 digital tape recorder as well as transducers: model 101C (900 MHz), model 3102 (500 MHz), model 3110 (120 MHz) and a model 3112 (80 MHz). Also another graphic recorder, model Honeywell 1856 A Visicorder, tape recorder model TEACH R-61D Cassette Data Recorder, as well as, oscilloscope model Hitachi Oscilloscope V-209, were additionally used. Power was supplied by a 12-V car battery through power distribution unit.

Radar surface arrival detection (RSAD)

There are several ways to determine dielectric properties of materials by applying GPR: wide angle reflection and refraction (WARR) sounding (Jezek et al. 1978, Annan & Davis 1976, Kovacs et al. 1982, Arcone 1984, Bogorodsky et al. 1985) and reflection coefficient determination (Kowacs & Gow 1977), for example. The primary quantity measured by GPR is the difference in travel time between different arrivals. Besides the travel time the amplitude of the reflected signal provides additional information about the material being probed. Since GPR is similar to TDR, the radar data could be analyzed by using TDR formulas.

In this study GPR dual antenna configuration was applied to determine dielectric properties of coarse-textured glacial materials, such as gravel and stony diamictic flow-type sediment. In those materials GPR was considered to be more relevant than TDR, because inserting the steel probes is very difficult or impossible. The principle of the dual antenna method is called the radar surface arrival detection (RSAD, Sutinen & Pekka Hänninen 1990), where the travel time of the refracted radar signals (along the surface of ground or pit wall) between transmitter and receiver units of known spacing (L) is detected (see also Arcone 1990). Dielectric constant is then determined $\varepsilon_r = (c * t / L)^2$. Figure 6 shows the antenna configuration and an example typical radar signal for till.

GPR performance

The most important factors affecting the results of GPR profiling are the propagation velocity (determined by dielectric properties), at-

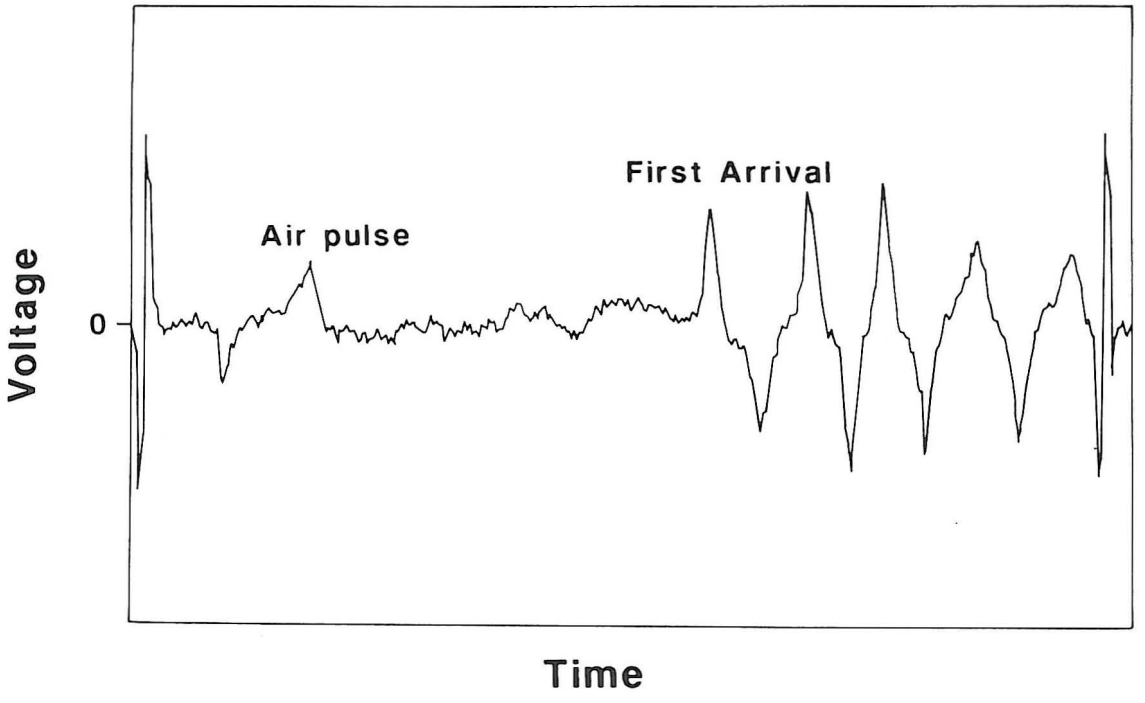

Fig. 6. Determination of dielectric constant for till in the core of Rogen moraine ridge in Kemijärvi, northern Finland by using GPR-RSAD technique (Sutinen & Pekka Hänninen 1990), and the radar signal showing the air pulse (directly from the transmitter to the receiver) and first arrival along the till surface.

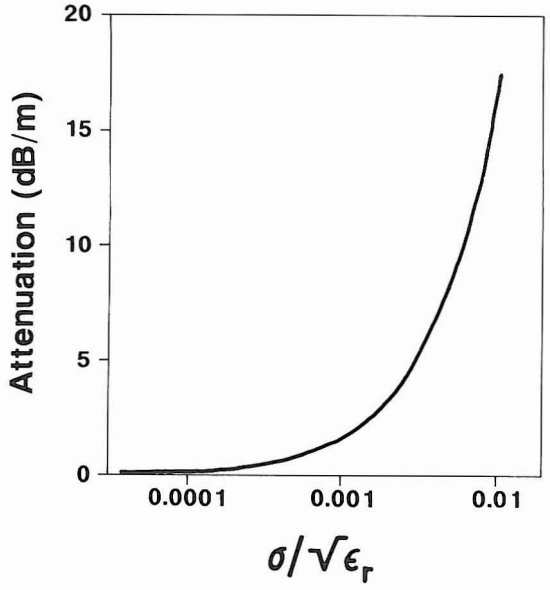

Fig. 7. Attenuation of the radar signal as a function of the electrical properties of glacial materials.

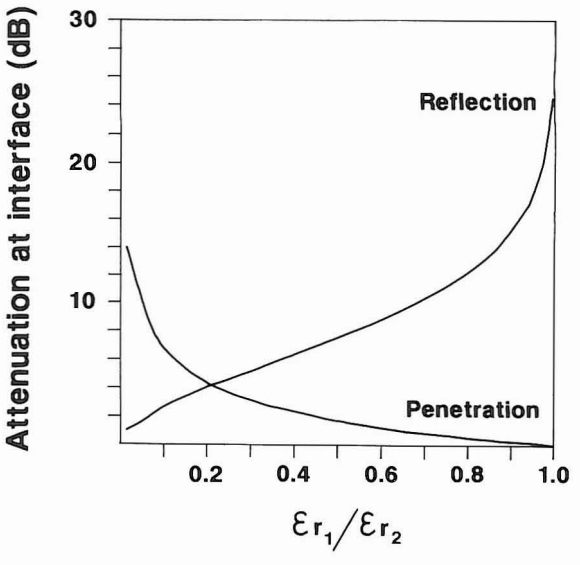

Fig. 8. Attenuation of reflected and penetrated wave at the sediment interface according to Pekka Hänninen (1991).

tenuation (determined by electrical conductivity of the materials, the amount of internal layers and the distance of interfaces from the antenna) and resolution (determined by the applied frequency content of the pulse and dielectric properties of the materials) of the radar signal in the subsurface glacial materials and the strength of the internal layers as reflectors of electromagnetic energy. All of these factors are influenced by the characteristics of the initial radar pulse and by the electromagnetic properties of sediment types.

The EM wave velocity in geological radar applications is the same as in TDR, $v = c / \sqrt{\varepsilon_r}$ (Annan & Davis 1976, Ulriksen 1982, Marttila 1982). The depth (D) of the layer surveyed is then $D = v / (2 * t)$. An electrical loss term, loss tangent (p_e; determines the attenuation of signal in earth materials) is defined as

$$p_e = \sigma_e / \omega\varepsilon_e = (\sigma' + \omega\varepsilon'') / (\omega\varepsilon' - \sigma'')$$

In the Debye-type water relaxation process the atomic or molecular dipoles fail to keep in phase with the impinging electromagnetic field, so they convert the electromagnetic energy to heat. The characteristic frequency at which this happens is known as relaxation frequency. For liquid water at 20 °C it is about 22 GHz and at 0 °C it is about 9 GHz, and for water in soils it is generally between 1 and 9 GHz (Hoekstra & Delaney 1974, Delaney & Arcone 1982, Arcone & Delaney 1984). Therefore the water relaxation processes happen at higher frequencies than those applied here. It has been shown (Von Hippel 1954) that ε_r is not strongly frequency-dependent in the range of 1 — 1000 MHz. Attenuation (A) is expressed (Marttila 1982) in a simplified form (assuming $\varepsilon'' = \sigma / \omega\varepsilon_o$ and $\varepsilon'' << \varepsilon'$) as follows:

$$1635 * \sigma / \sqrt{\varepsilon_r}\ \text{dB/m},\ [\sigma] = \text{S/m}$$

The signal attenuation applying the above formula for glacial materials of known dielectrics and conductivity is illustrated in Figure 7. The attenuation is insignificant in coarse-textured materials, such as gravel and sand, but increases significantly in conductive materials like silt and clay. The overall attenuation of the system used

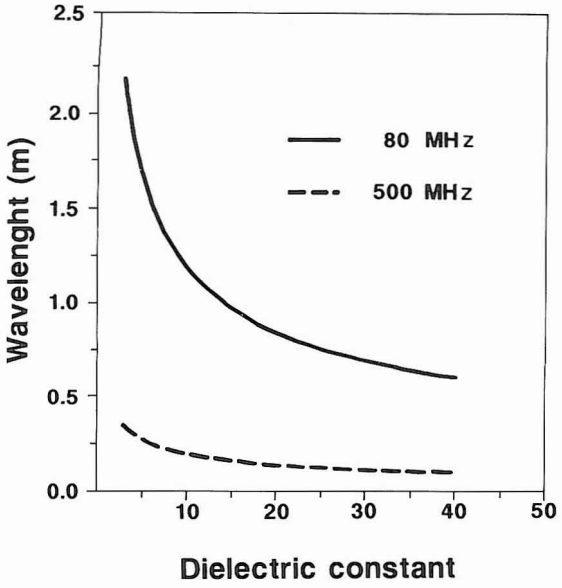

Fig. 9. Radar resolution for the antennas of center frequencies of 80 and 500 MHz as a function of dielectric properties of glacial materials.

here has to be less than 120 dB (GSSI, 1980), in which about 22 dB is caused by the antenna (Annan & Davis 1977b). Thus the attenuation resulted from the material (Fig. 7), the amount of interfaces and distance from the antenna can be no more than 100 dB.

When the transmitted pulse impinges the interface between materials with different dielectric properties, part of the wave energy reflects, and the reflection coefficient (R) and penetration coefficient (K) are defined as

$$R = (\sqrt{\varepsilon_1} - \sqrt{\varepsilon_2}) / (\sqrt{\varepsilon_1} + \sqrt{\varepsilon_2}) \text{ and}$$

$$K = 1 - R$$

Both the reflected and penetrated part of the pulse are attenuated (Fig. 8). Therefore materials containing many interfaces, like tills, attenuate the signal significantly.

The applied wavelength (λ) determines the radar resolution (see Saksa 1986) as follows:

$$\lambda = c / f * \sqrt{\varepsilon_r}$$

Figure 9 illustrates the resolution of 80 and 500 MHz antennas in the range of measured dielectrics.

Determination of electrical conductivity

The factors affecting conductivity (the reciprocal of resistivity) of geologic materials are texture, porosity, moisture content as well as concentration of electrolytes in the contained moisture. Conductivity of saturated materials is given according to Archie's law:

$$\sigma_a = \sigma_w n^m$$

where σ_a = bulk conductivity, σ_w = water conductivity, n = fractional porosity (0 to 1) and m = factor varying from 1.3 for spheres to 2.0 for plates.

The following techniques and instruments have been applied to determine electrical conductivity (resistivity) for the geologic materials: Galvanic DC resistivity soundings (Terrameter SAS system by ABEM), Mafrip resistivity meter (Puranen et al. 1983), 4-pin soil resistance meter (Model 400 by Nilsson Electrical Laboratory, Inc.), Electromagnetic terrain conductivity meter Geonics EM31 by Geonics Ltd.

Electrical resistivity soundings (totalling 78) were performed using the Schlumberger electrode configuration, and some of the sounding results and interpretation curve fittings have been presented. Resistivity measurements from samples were performed in the laboratory using the Mafrip instrument, originally designed for rock samples by Puranen et al. (1983). Continuous samples (sandy glaciofluvial deposits up to 20 — 30 m and tills 4 — 10 m) were drilled into 0.5 m long plastic tubes, 33 mm in diameter. The tubes were sealed in the field to prevent moisture evaporation. The sample tubes were opened in

Fig. 10. Equipment used in resistivity determination of Glacier Bay till near Burroughs Glacier, southeastern Alaska.

the laboratory by circular saw into halves and resistivity readings were taken every 2 cm intervals using a four electrode configuration with a = 2 cm spacing each. The following empirical half-Wenner resistivity transform was developed by E. Lanne for 3.3 cm diameter sample with a = 2 cm:

$$\rho_a = 15.8 * R^{1.31} \quad [R] = k\Omega.$$

A portable Nilsson resistance meter was used to measure conductivity in field (Fig. 10). Sample box 15*10*4.5 cm composes of 0.625 mm PVC-plastic with stainless steel electrode plates on the long sides of the box. Calibration of meter by using known solutions of known resistivities was made by R. Patenaude, Wisconsin Department of Transportation.

The electromagnetic terrain conductivity meter EM31 by Geonics Ltd. was used for detecting lateral conductivity variations over the landforms, e.g. locating gravel and sand deposits below till and silt. The EM31 measures the quadrature-phase component of the induced magnetic field, and this component of the magnetic field is linearly related to ground conductivity (McNeill 1980). The instrument has two coils, a transmitter and receiver, mounted 3.7 m apart in a rigid boom and the operating frequency is 39.2 kHz.

GLACIAL MATERIALS

Genetic classification

Till is more variable than any other sediment known by a single name. The term »till» was first introduced by Geikie (1863) as »a stiff clay full of stones varying in size up to boulders produced by abrasion carried on by the ice sheets as it moved over the land». A great number of studies has been done to describe and classify tills and till-like sediments (Hartshorn 1958, From 1965, Virkkala 1969, Lundqvist 1977, Boulton 1970, Lavrushin 1970, Marcussen 1973, Aario & Forström 1979, Dreimanis 1979, 1982, 1989, Lawson 1979, Shaw 1979, Gravenor et al. 1984). Flint et al. (1960) introduced a nongenetic term »diamicton» for nonsorted or poorly sorted nonlithified sediment that contains a wide variety of grain sizes. The term is favored in cases, when till might have been modified by postdepositional processes, such as solifluction or frost action. The term might be more practical when sections are observed visually, Figure 11 demonstrates one example.

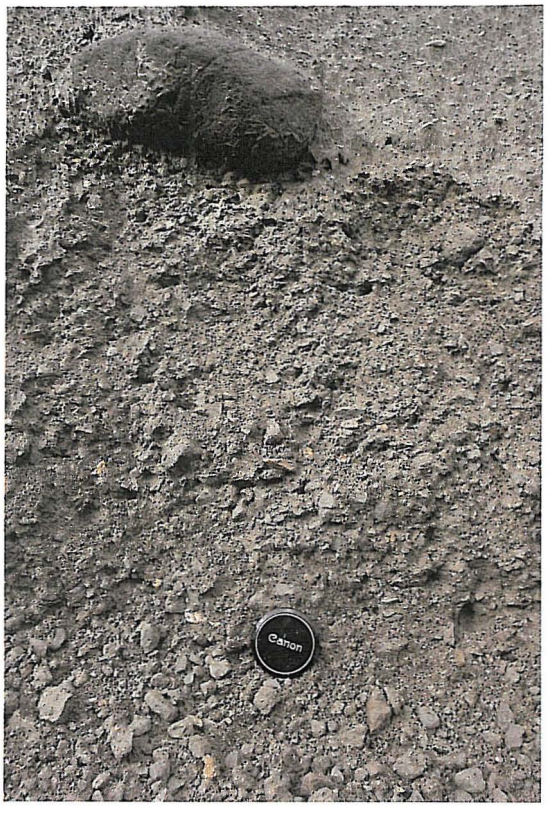

Fig. 11. Till? — no. Diamicton? — right. Figure shows an exposure of recent volcanic mudflow deposit from Mt. St. Helens, Washington. Photo R. Sutinen, 1988. Lens cap = 6 cm as a scale.

There is no till-nontill boundary that can be applied in genetical sense, and as a result of the lithological and textural variations, no single parameter unambiguously defines till. Since glacial deposition is always polygenetic, including direct glacial action, gravity action and meltwater action, sediment types tend to change gradationally from »true» tills to other sediment types. The INQUA (International Union of Quaternary Research) commission suggests a genetic classification of tills, divided into 1) primary tills and 2) secondary tills (Dreimanis 1989). Primary tills are formed mainly by direct release of debris from the glacier and deposited mainly by the primary glacial processes, such as melt-out, sublimation and lodgement with subsidiary participation of secondary processes. Secondary tills are products of resedimentation of glacial debris released by glacier ice, or an already deposited till in the glacial environment with little or no sorting by meltwater. The above classification has been argued by many geologists during the INQUA commission work and the most restrictive definition of till has been made by Lawson (1979) based upon the studies at the Matanuska Glacier, Alaska: »Till is defined as sediment deposited directly from the glacier that has not undergone subsequent disaggregation and resedimentation.» Consequently, sediments derived from secondary processes should not be called tills. His definition is agreed also in the following classification.

Fig. 12. Glacier Bay till, a layer-by-layer deposited sandy basal till one year after the retreat of the margin of the Burroughs Glacier, Alaska. Electrical characteristics; $\varepsilon_{till} = 17.8$ and $\sigma_{till} = 0.003$ S/m indicate strong oversaturation (clay content 10.5 %). Photo R. Sutinen, 1988. Lens cap (≈ 5 cm) as a scale.

Fig. 13. Basal melt-out till at Torassieppi, western Finnish Lapland. Note sand bands draping the stones. A pencil (15 cm) as a scale. Photo R. Sutinen, 1983.

Basal / subglacial till

Presumably the major part of transportation and deposition of glacial drift has been occurred basally or subglacially during the time the Scandinavian and Laurentide ice sheets occupied Finland and part of Wisconsin. Lodgement till is uniform, and the characteristics of the matrix depends on the source material. The long axes of clasts (fabric) parallel with the ice flow direction. It is deposited from the sliding base of the glacier presumably during both advance and retreat stages (Flint 1971). Pressure melting frees the debris, which is then plastered together particle by particle, sheet by sheet. Fissile structures in lodgement till is sometimes interpreted as a glaciodynamic feature. However, fissility sometimes cuts across primary sedimentary structures displaying evidence of post-depositional origin, quite obviously frost action (Aario & Forström 1979). An example of basal till, deposited layer-

by-layer rather than particle-by-particle, is shown in Figure 12 (see Mickelson 1971). After deposition the till stabilizes and becomes hard-packed as a result of the removal of the excess of water.

The distinction between lodgement till and melt-out till is difficult based on the external appearance as indicated by Dreimanis (1989, see From 1965, Lundqvist 1977). Sandy draping around stones and pebbles has been used as one of the criterion for (basal) melt-out till (Fig. 13). It may contain angular pebbles and is attributed more commonly to hummocky moraines. Shaw (1979) notes, that basal melt-out process is influenced by englacial structures and forms which are also largely responsible for the resultant landforms and deposits.

There is no practical way to apply that wide variety of genetical terms to glacial mapping. In the mapping routines by the Finnish Geological Survey till is classified into three textural categories; gravelly till, sandy till and silty till (see Virkkala 1969, Kauranne et al. 1972, Lindroos & Nieminen 1982). Genetic terms (lodgement, melt-out and flow till) have been introduced recently, but the use is still rare. In Wisconsin tills have been named according to the type localities and the tills are generally easy to differentiate by texture, and exhibit significant lateral extension (Schneider 1983, Mickelson et al. 1984).

Diamictons / flow sediments

Sediment flow processes are common near modern glaciers (Boulton 1972), but flow features has been described from the Pleistocene deposits, too (Marcussen 1973). In glacial environment any kind of gravitational or squeezing processes can produce sediment flow deposits, which are other than directly glacier derivated sediments (tills). Depending on the relationship to the position of debris (supraglacial, subglacial or even proglacial) within the glacier and adjacent lacus-

Fig. 14. An exposure showing vertical alteration from glacioflucial sand (at the bottom) to flow sediments and till (on the top) from Jumisko, northern Finland. A 35 cm high map case as a scale. Photo R. Sutinen, 1984.

Fig. 15. An exposure of flow sediments separated by sand stringers from Soukkavaara, Posio, northern Finland. A 12 cm long pipe as a scale. Photo R. Sutinen, 1984.

Fig. 16. A 5-meter-high exposure showing basal till mantled coarse-textured flow sediments interbedded with stringers of gravel and sand from Peuraselkä, 4 km west of Kemijärvi, northern Finland. Electrical parameters ($\varepsilon = 5.7$; $\sigma = 0.00003$ S/m) indicate significant water disaggregation during the deposition. Photo R. Sutinen, 1980.

trine/marine environment there have been proposed many different terms, such as supraglacial flowtill, ice-marginal waterlain flowtill, subglacial flowtill or subglacial waterlain flowtill (Dreimanis 1989). There is, however, growing reluctance to use the term flowtill (introduced by Hartshorn 1958) and terms like glacigenic sediment gravity flows (Gravenor et al. 1984) and watermorainic sediment (Morawski 1989) have been proposed.

The observations made near the Burroughs Glacier, Alaska and in northern Finland indicate that sediment flow deposits occupy the boundary area between till(s) and water deposited materials. No sharp limits, however, could be pointed out visually or texturally and sediment types may change gradationally from one type to another both laterally and vertically (Fig. 14). The term »flow sediment» (diamicton) is used here for all the materials other than basal till or glaciofluvial, glaciolacustrine/ glaciomarine deposits, and the term refers to gravity processes and also subglacial slurry flows of water-saturated material. The pebble fabric in sediment flow deposits do not indicate the ice flow directions, but only directions of the temporary mudflows or gravity flows. Because water (glaciofluvial activity) is present in temperate subglacial environment, mixed sedimentary sequences are formed exposing interbedded flow sediments and gravel, sand and silt (Fig. 15). Coarse-textured varieties of flow sediments (Fig. 16), appearing sometimes in large quantities, are important raw material potentials and substitutes for esker deposits.

Glaciofluvial and fluvial sediments

Material is defined to be glaciofluvial (or fluvioglacial, Price 1973) if it is fluvial of its origin and fluvial activity was ruled by the melting of the glacier ice (Lundqvist 1979). Debris, first carried by glacier is brought into action of glaciofluvial (secondary) processes, where significant disaggregation and stratification occurs.

Fig. 17. An exposure of the Salanki esker, western Finnish Lapland. Matrix supported stones and poor sorting indicate conduit infill deposition. Photo R. Sutinen, 1984.

Eskers are typical glaciofluvial landforms, and three different sedimentary facies has been separated: 1) Sliding-bed transportation and deposition in a tunnel filled with water-saturated slurry (Saunderson 1977, Sutinen 1977), 2) Open-channel transportation and deposition (Bannerjee & McDonald 1975) and 3) deltaic sedimentation. Sliding-bed facies is represented by poorly-sorted and coarse-textured material. Pebbles and stones are matrix-supported and the overall structure is massive (Fig. 17, see Sutinen 1985a). The material has been interpreted to be transported as a full-pipe flow, meaning that tunnel is full of slurry material. The term »conduit infill» is used further in the text for the full-pipe flow material. In the open-channel environment the meltwater channel is bordered laterally by the ice walls, and sedimentation occurs as a function of water velocity resulting in cross-bedding structures. Deltas and related terraces are gently sloping down ice and internal bottomset, foreset and topset sequences as well as different ripple marks are characteristic (Aario 1972). Those also are categorized as »open channel sediments».

The degree of stratification depends on the amount and velocity of water, sedimentary environment (type of channel) and the relation to the glacier. Ice-contact (sub- en-, supraglacial) gravel and sand are transported and deposited by high-energy meltwater released predominantly from retreating glacier ice. Meltwater tunnels (tunnel network) are suggested to be located predominantly beneath the glacier (From 1965, Kujansuu 1967, Saunderson 1977, Sutinen 1977, Lundqvist 1979, Gorrel & Shaw 1991). Drainage ends ice-marginally or proglacially into land (sandur and outwash deposits) or lacustrine/marine environment.

Fluvial sediments are deposited by rivers and are thus actually not related to glacial processes, but in some cases e.g. in the Kemijoki river valley, northern Finland fluvial sedimentation is closely related to the retreating ice margin and attributed marine/ice lake stages.

From the above standpoints unambiguous genetic classification of till and other glacigenic deposits is difficult and the terms vary from one geologist to another. Although the final report of the Commission on Genesis and Lithology of Glacial Quaternary Deposits of the International Union for Quaternary Research (INQUA) was published in 1989 (Goldthwait & Match 1989) still many interpretation differences prevail, and one might agree with the quotation »We are still confused — but on a higher level» (Schluchter 1979).

Textural classification

Besides genetic and stratigraphic classification, textural classification of materials is also required for mapping of glacial deposits. The texture usually is described as percentages of sand-, silt- and clay-size fractions. Hence, the particle size data do not refer to the entire composition of sediments, but mainly to the matrix. Grain size distribution of particles smaller than 20 mm is used in the mapping routines in Finland (Virkkala 1969). However, the amount of the matrix has a great influence on the specific surface area of the sediment (Nieminen 1985), and thus related to the moisture content and dielectric properties, as well (Dobson et al. 1985). In the following, the grain size statistics is applied for the different genetic classes of glacial materials.

The grain size statistics is based on 721 samples taken from exposures of different landform types in northern Finland (55 samples collected from Wisconsin and Alaska specifically for reference to the electrical classification). The samples represent six genetic categories: 1) basal / subglacial lodgement till (Late Weichselian), 2) basal / subglacial melt-out till, 3) flow sediments, 4) glaciofluvial conduit infills, 5) glaciofluvial open channel sediments and 6) fluvial (river)sediments.

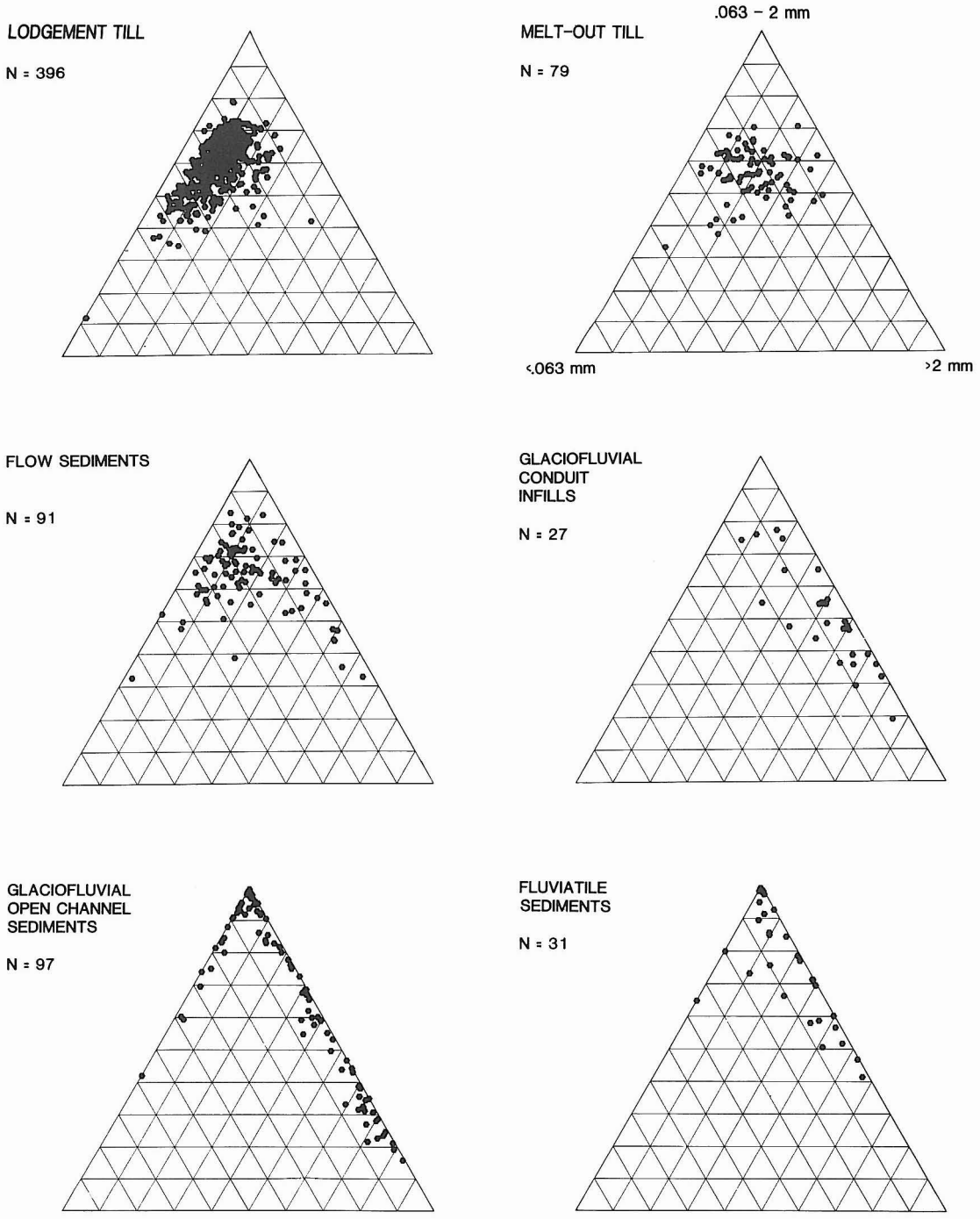

Fig. 18. A plot of ternary diagrams representing grain size distribution of different genetic sedimentary classes. Sampled material from northern Finland.

Grain size analysis involved dry-sieving for particles size d > 0.063 mm and a conventional areometer (hydrometer) analysis for particles d < 0.063 mm. Selected till samples were analyzed also by laser diffraction using Sympatec Helos analyzator. The graphic and moment grain size parameters (using phi-scale as introduced by Krumbein, 1934; $\Phi = -\log_2 d$, where d is the particle size in mm), are calculated by using formulas presented by Folk and Ward (1957), Folk (1966) and Friedman (1962) (summarized by McManus 1988).

Results of grain size distribution of the samples are illustrated as ternary diagrams in Figure 18. Lodgement till is uniformly clustered, but melt-out till indicates more wider variation, and clearly increased fractioning can be seen in the flow sediment group. Conduit infills indicate coarser texture, but also close relation to the flow sediments. Open channel sediments and fluvial sediments indicate clear stratification.

The average amount of the fines (d < 63 μm) in the sampled tills are significantly higher compared to the averages of the other sedimentary groups (28 % for lodgment till, 24.2 for melt-out till; 18.6 for flow sediments and 5 % for fluvial sediments). The removal of the fines is due to increased meltwater activity during the depositional cycle. If glaciolacustrine / marine deposits were included the fines-content would have increased again as a result of decreased velocity of the suspended water. Because the fines show significant differences between various sedimentary groups, the electrical characteristics should indicate a similar trend.

The graphic and moment parameters have been observed here to yield practically equal results in describing grain size distribution. The sorting parameters (inclusive graphic standard deviation (GDi) and moment standard deviation (MDi) are shown to be the statistically most significant in differentiating sedimentary categories (c.f. Landim & Frakes 1968). One might expect that tills are poorly sorted (indicated by higher sorting values) and glaciofluvial and fluvial sediments better sorted (lower values). A plot of sorting (GDi) and the variance of the mean grain size (GMz) for six sedimentary categories is illustrated in Figure 19. Now three pairs could be separated; tills with high sorting values (poorly sorted materials) and low mean grain size variation, conduit infills and flow sediments with moderate sorting and variance, and glaciofluvial and fluvial sediments with low sorting values and high variance of the mean grain size. Even though sorting indicates partial overlapping between the neighboring categories, it is shown to be a good indicator for different sedimentary facies. High mean grain size variation in the water-deposited sediments clearly shows stratification with relatively good sorting (cf. McManus, 1988).

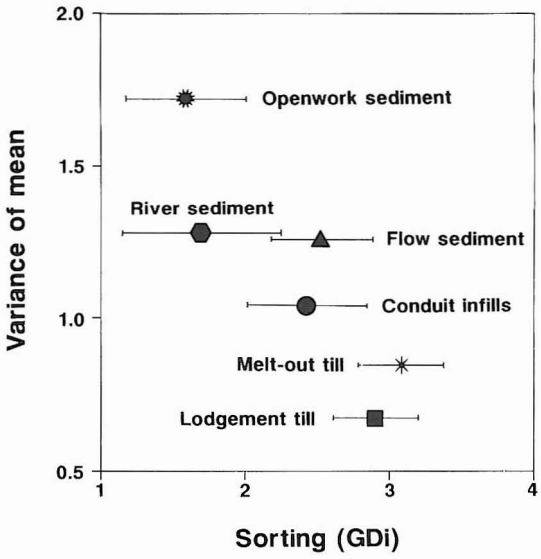

Fig. 19. A classification of sediment groups by means of variance of mean grain size (GMz) vs. graphic standard deviation (sorting, GDi).

The other way to differentiate the sediment types is to plot sorting against kurtosis (concentration of peakedness of the distribution). Figure 20 indicates that tills with low kurtosis and high sorting values could be clearly separated from other sediment types. Accordingly, the descriptive terms, such as »poorly sorted» , »uniform» and »non-stratified» are diagnostic for tills

(also for mudflow deposits, Fig. 11). Tills, at least in this case, could be separated from other sediments by means of sorting and kurtosis. However, the differentiation of the two genetical till types, lodgement and melt-out tills, is more difficult. A relatively clear clustering of flow sediments and conduit infills between tills and water-deposited sediments is shown. Therefore flow sediments are not here called tills and the term »flow till» is discouraged. The partial overlapping with GDi and Mkg indicates that sedimentation processes and the amount of water tend to change gradually. Sorted sediments show high but extremely large variation of kurtosis, meaning that materials are stratified and fractioned (due to water velocity), and exhibit very steep distribution curves.

The above plots could be interpreted to represent a glacial sedimentary cycle. Till as primary material has transported and deposited directly by glacier ice with no water disaggregation compose of mixture of all the source materials in the substratum, in this case precambrian metamorphic and plutonic rocks and »older» (pre-Late Weichselian) glacial deposits. When the amount of (subglacial) water increases due to melting of ice, till gradually begins to mobilize and move by gravity and hydrostatic pressure resulting in flow sediments and conduit infills.

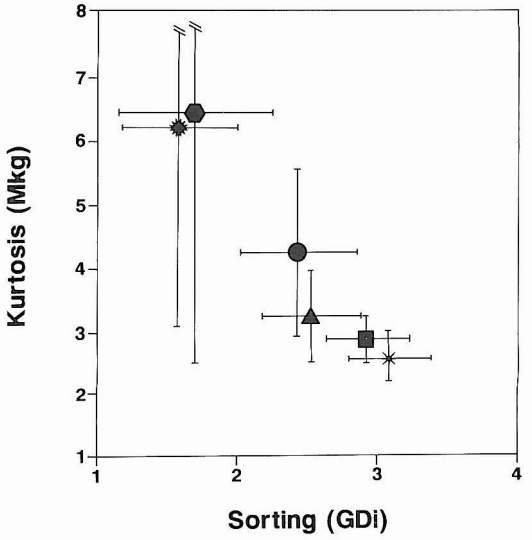

Fig. 20. A classification of sediment groups by means of graphic standard deviation (sorting) and moment kurtosis (Mkg). The symbols are the same as in Fig. 19.

Finally, when water is the main transporting agent in the esker tunnels and proglacial environment, stratification and fractioning is due to meltwater velocity. The cycle ends into the lake or sea, and silts and clays are deposited as a function of decreasing water velocity.

Texture and water content

Water in geologic materials is either bound or free. Bound water (or adhesive water) is attached to the surface of the grains through the influence of the forces of molecular attraction. These forces decrease with the distance of the water molecule to the grain. On the grain the first layer is the adsorbed layer, which is of the order of a few tens of molecules thick (about 0.1 μm; see de Marsily, 1986). Surrounding the adsorbed layer is a transition layer (between 0.1 and 0.5 μm) that contains water molecules that are still subjected to a nonneglible attraction and stay immobile. Beyond the transition zone the water is said to be free.

Water content generally increases downwards in the steady state moisture profile. In the uppermost region adhesive water surrounds particles and air-filled voids between grains and particles. Further down the profile the amount of free water increases until in the capillary stage all pore spaces are filled with liquid (free) water, although liquid pressure is less than total pressure caused by gravity since the capillary action within the fine pore spaces has caused the mois-

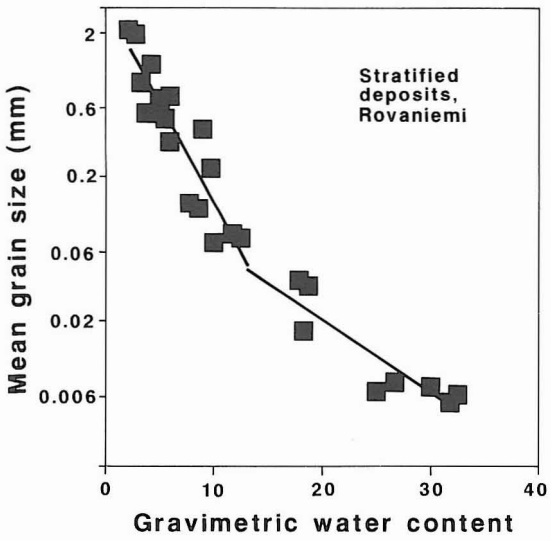

Fig. 21. A plot of mean particle size vs. gravimetric water content for glaciofluvial and fluvial sediments. Unsaturated samples near Rovaniemi, northern Finland.

ture to ascend to these pore spaces. Except in clays, capillary rise seldom exceeds several meters. In gravel capillary rise is less than 3 cm, in sand between 3 cm and 1 m and in silt from 1 m to 30 m, but in clay over 30 m (Andersson 1960). In the Finnish tills capillary rise ranges from 26 cm to ≥ 9 m as a result of variation in textural properties and the degree of weathering (Nieminen 1985). Below the ground water level (GWL) free water completely fills the pore spaces between grains. This zone below the ground water level is called the saturated zone; atmospheric pressure and hydrostatic pressure are in equilibrium.

Generally speaking, the soil surface area is related to particle size (Dobson et al. 1985). Because of the larger surface area, more water is adsorbed on fine-grained materials than on coarse-textured materials. The grain size distribution is not always a reliable criterion for judging the amount of bound water, however, because the shape of the grains varies with respect to mineralogical composition and the degree of weathering. The specific surface area is a more reliable criterion for determining the adsorption capacity of materials. The amount of adsorbed water in Finnish tills has been reported to average 21.5 g/kg and in clay 200 g/kg (Nieminen 1985).

As summarized by Schmugge at al. (1980), there are several methods for soil moisture determinations. The two terms commonly used to characterize the moisture content of soil sample are volumetric water content, Θ_v, and gravimetric water content, Θ_g.

$$\Theta_v = V_w / V_t$$

and

$$\Theta_g = W_w / W_{dry} * 100\ \%$$

where V_w is the water volume, V_t is the total volume of the sample; W_w and W_{dry} are the weights of the water in the sample and of the dry sample, respectively. In the following, the water content (on the gravimetric and volumetric basis) is determined for different glacial materials with varying in grain size. The effects of the amount of fines and mean grain size on water content is studied, and also the bulk water content is compared to the water adsorption capacity.

First, the relationship between gravimetric water content (Θ_g) was examined for stratified ($GD_i < 2.2$) sediments, such as openwork esker (glaciofluvial) and river (fluvial) deposit samples collected near Rovaniemi northern Finland. Dry weight was determined after drying 24 hours at 105 °C. A plot of mean grain size (Mz) against water content (Θ_g) (Fig. 21) indicates that water content increases slowly in materials from gravel size (d = 2 to 20 mm) to sand size (d = 0.06 to 2 mm). Rapid increase is seen for materials of silt size (d = 0.002 to 0.06 mm). Unsaturated esker gravel contains less than 3 % of water (Θ_g), sand from 5 — 15 % and silt 15 — 33 %. Accordingly, the water content is related to the coarseness of the stratified materials and could be predicted by mean grain size. Presumably this is the case also for tills.

Then, the fines was plotted against the volu-

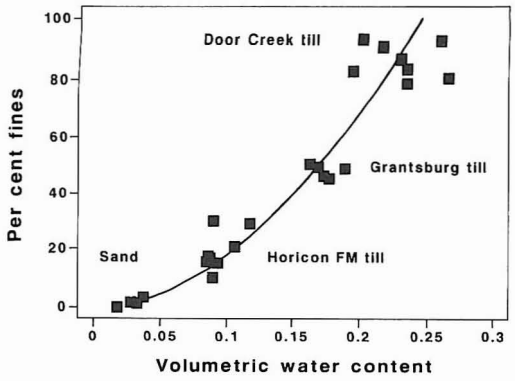

Fig. 22. A plot showing relationship between fines (d < 0.063 mm) and volumetric water content. Unsaturated samples from Wisconsin.

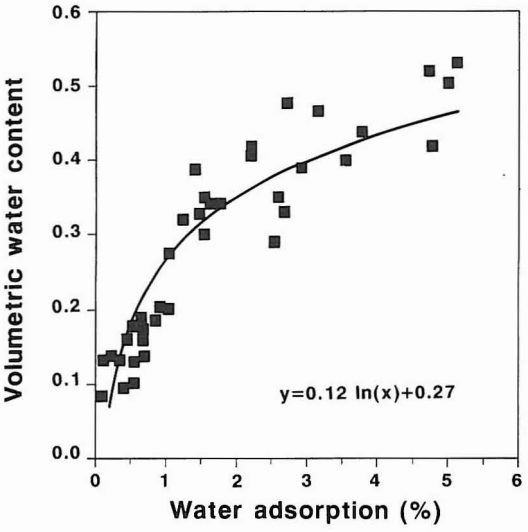

Fig. 23. A plot of the natural state volumetric water content against adsorption capacity of the selected materials from northern Finland. Adsorption determined according to procedure of Kellomäki and Nieminen (1986).

metric water content (Fig. 22). The unsaturated samples included; sand, Horicon Formation till (sand 80 %, silt 13 % and clay 7 %), Grantsburg till (52 %, 29 %, 19 %) and Door Creek till (10 %, 61 %, 29 %) from Wisconsin. Water content increases with increasing amount of fines in the same manner as was the case in the plot of mean grain size vs. Θ_g. Each sediment type is clearly clustered on the plot. It is evident that the amount of fines is a diagnostic factor for sediment classification and water content is greatly determined by the matrix.

Tills, glaciolacustrine / glaciomarine silt / clay, glaciofluvial and fluvial gravel / sand are expected to adsorb different amount of water on the particle surfaces. Because the dielectric constant of bound water and free water vary significantly, the crucial question is, what is the relationship between free and bound water in sediments. If the bulk water content predominantly is composed of bound water (low ε_r), the dielectric properties of sediment-water-air mixtures may be quite similar from one sediment type to the other and thus dielectrics is not relevant for sediment differentiation and classification. If there is free water ($\varepsilon_r \approx 80$) present, differences between mixture dielectrics of different sediment types may be big enough.

For that purpose adsorption water content (determined according to Nieminen 1985, Kellomäki & Nieminen 1986) was determined for gravel, sand, till and silt samples collected near Rovaniemi. The *in situ* volumetric water content was plotted against the adsorption water content (Fig. 23). As expected, water adsorption on fine-grained materials was greater due to larger surface area. After 7 days adsorption test finer than silt-size sediments contained over 1.5 %, till 0.5 — 1.5 % and sand less than 0.5 % of water. One can observe that the adsorbed water content is significantly lower compared to natural state bulk water content. Even the coarsest unsaturated materials contain significant amounts of free water, almost 20 times more than adsorbed water. The above simple tests evidently shows that free water ($\varepsilon_r \approx 80$) controls the dielectric properties of sediment mixtures. Since the amount of water is related to the texture the sediment differentiation is possible by dielectric properties.

ELECTRICAL PROPERTIES OF GLACIAL DEPOSITS

Dielectric properties

In the range of TDR and GPR frequencies (1 MHz to 1 GHz) the dielectric constant of soils (real part ε_{soil}) in which no liquid water is present varies between 2 and 4 (Ulaby et al. 1986) or more precisely $\varepsilon_{soil} = 3.5$ as given by Wobschall (1977). In that state ε_{soil} is independent of temperature and frequency. Practically all unconsolidated materials consist of a mixture of water, sediment particles and air. Because $\varepsilon_{air} = 1$ and $\varepsilon_{water} \approx 80$ ($\varepsilon_{water} = 87.8 - 0.37 * T$, where T is temperature °C; Wobschall 1977), it is the amount of water that determines the dielectric properties of earth materials and rocks, as well (Parkhomenko 1967, von Hippel 1954). In the earth materials water is regarded to have two dielectric phases: free and bound. The free water has a high dielectric constant, which is attributed to the fact that water molecule dipoles are free to rotate at radio frequencies. Bound water is regarded to have a lower dielectric constant resembling that of ice $\varepsilon = 3.5$ (Schmugge et al. 1980; bound water $\varepsilon = 20$ to 40 at the frequencies from 1.4 to 18 GHz; Dobson et al. 1985). These water molecules are tightly held by the particles and the dipoles are immobilized. However, the transition point between bound water and free water layers is somewhat arbitrary (Ulaby et al. 1986). Soil freezing decreases significantly dielectric properties (Delaney & Arcone 1982), but contrary to the electrical conductivity, dielectric properties are practically not dependent on salinity (Parkhomenko 1967, Topp et al. 1980, Jackson & O'Neill 1983).

The major part of the existing mixing formulas deal with the mixture of two constituents by implying direct dependence of the mixture dielectric constant on the dielectric constants (ε_1 and ε_2) and the volume fractions (V_1 and V_2) of the constituents. Wang and Schmugge (1980) summarized ten different mixing formulas and tested them for known soil data. Their results indicate that many of the formulas are not applicable to soil-water mixtures. The models that include dielectric components such as ε_{air}, ε_{water}, ε_{rock} and ε_{ice} give more reliable results. Because *in situ* characterization and differentiation of sediment types was the main purpose in this study, the application of mixing models was seen less appropriate. It was also evaluated if the dielectric properties constitute a useful parameter for glacial mapping.

The following approach is based on the fact that different types of deposits vary in water content as a consequence of their textural differences (Figs. 21 — 23). Because the dielectrics-water relation has been determined previously for soils containing varying amounts of organic material (e.g. 0 — 6 %; Topp et al. 1980), the relation for glacial sediments with no or insignificant amounts of organics (average = 0.186 %, 104 measurements) was determined here. The possible source of the organic material incorporated in the glacial drift is older interglacial / interstadial deposits. Dielectric properties, water content and texture of glacial deposits were determined in Wisconsin, northern Finland and near Burroughs Glacier in southeast Alaska. Several different tills of varying textures as well as glaciofluvial (esker/outwash gravel and sand) and glaciolacustrine/marine (silt and clay) deposits were studied. TDR was applied mostly for fine-grained and sandy materials, GPR-RSAD for coarse-textured materials.

Water content and texture effect

Dielectric properties of earth materials are dependent on the water content of the soil (Cihlar & Ulaby 1974, Hipp 1974, Hoekstra & Delaney 1974, Selig & Mansukhani 1975, Davies et al. 1977, Topp et al. 1980). The moisture content and consequently the dielectric constant of un-

saturated sediment mixtures primarily depend on soil texture and specific surface area (Dobson et al. 1985). It has been shown earlier (Fig. 23) that free water strongly dominates over adsorbed water in *in situ* earth materials allowing dielectric differentiation of sediments. However, the hydrogeological moisture profile in the ground is related to season and weather conditions, e.g., rains (de Marsily 1986), and thus affects dielectric properties (Davis 1975, Davis & Annan 1977). The moisture profile is changing also by evaporation, capillarity and even plant transpiration (Schmugge et al. 1980).

The relationship between soil moisture and dielectric properties is different if water content is expressed either on gravimetric (Θ_g) or volume basis (Θ_v) (Cihlar & Ulaby 1974, Hallikainen et al. 1985) and the laboratory determinations show differences in ε_r vs. Θ_v for different textures (Wang & Schmugge 1980, Hallikainen et al. 1985). Volumetric water content was preferred here. Based on the determinations of dielectric properties by TDR and GPR-RSAD

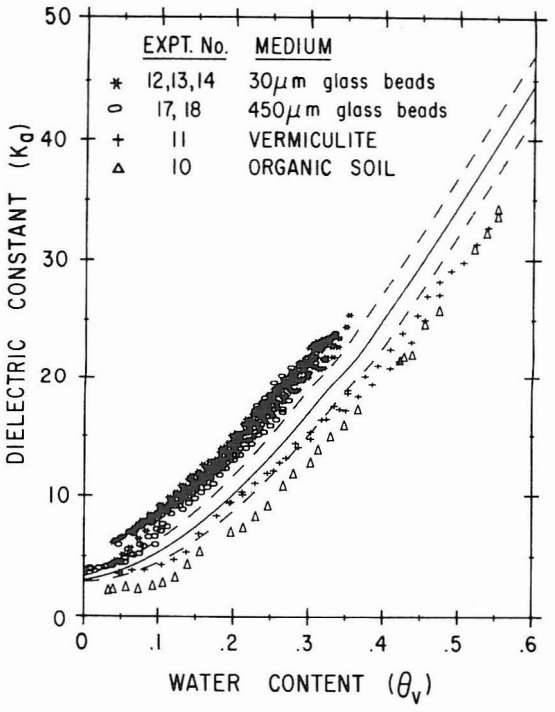

Fig. 25. A comparison of dielectric constant vs. volumetric water content for different types of materials according to Topp et al. (1980). Note the difference between the plots of organic samples and glass beads.

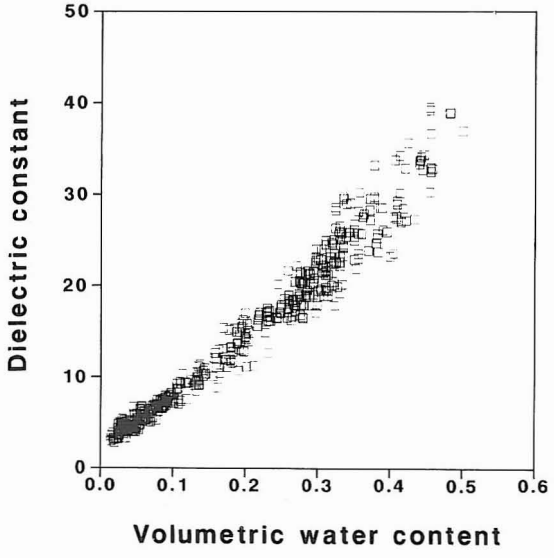

Fig. 24. A plot of dielectric constant vs volumetric water content. Dielectric properties determined *in situ* by TDR in Glacier Bay, southeast Alaska and Wisconsin, by TDR and GPR-RSAD in northern Finland and by TDR in laboratory.

the following relationship between dielectric constants and volumetric water content for glacial materials (ε_{gm}, results are plotted in Fig. 24) is given:

$$\varepsilon_{gm} = 3.2 + 35.4 * \Theta_v + 101.7 * \Theta_v^2 - 63\ \Theta_v^3$$

Some scattering of data were observed in the laboratory determinations, and it is presumably due to inhomogeneities resulting from mixing water into sediment samples. Also, the reference sampling for vertical TDR measurements might not always represent the bulk water content, which is indicated by TDR. The previously given relationship $\varepsilon_{soil} = 3.03 + 9.03 * \Theta_v + 146.0 * \Theta_v^2 - 76.7 * \Theta_v^3$ (Topp et al. 1980, Fig. 25) gives much lower values at water contents greater than 0.1 (as low as ε_{soil} about 10.1 at water content 0.2). The data presented by Hoekstra and Delaney (1974) at 500 MHz, however, has fairly

good agreement with the data shown here. At 250 MHz Alharthi and Lange (1987) found the average soil water content expression of Topp et al. (1980) was consistent with their results at low water contents but differed at high water contents for sandy soil. Also data and a model developed by Dobson et al. (1985) at 1.4 GHz indicate higher dielectric values (real part) for sandy loam soil compared to Topp et al. (op cit.).

One reason for the differences might be the presence of organic material up to 6 % in Topp et al.'s samples. The amount of humus was observed to significantly increase water adsorption when 0.7 to 6.0 % humus was added to sand (Andersson 1967). The effect is seen also in Figure 25 when organic soil is compared to glass beads. As Topp et al.'s data indicate, the amount of organic material in minerogenic sediments tends to bend the correlation curve while tests made by using glass beads indicate a straighter curve. In this study all materials were measured below the topsoil horizon, so a plot of the distribution of dielectric constant (ε_r) vs. volumetric water content (Θ_v) is expected to show more straighter curve.

An increase of clay-fraction content changes many of the geotechnical properties of glacial deposits. Moisture content and dielectric constant is expected to increase, too. A correlation between clay content and dielectric properties was determined by *in situ* TDR determination for following genetic types deposits: outwash sand, Horicon Formation till (sand 80 %, silt 13 %, clay 7 %), Grantsburg till (52 %, 29 %, 19 %) and Door Creek till (10 %, 61 %, 29 %). Results are plotted in Figure 26. Clay content is shown to be in good correlation to dielectric constant values (correlation coefficient = .976). Since tills are mixtures of many grain sizes, clay content is regarded to be a diagnostic parameter for tills. However, it is not a relevant criterion for all the sediment types. Lacustrine/marine silts may contain only a minor amount of clay fraction and still have a large moisture content and dielectric values.

Because the dielectric properties of glacial materials are determined by water content (Fig. 24), where free water strongly dominates over adsorbed water (Fig. 23) and since the water content is related to the texture (Figs. 21 — 22) and dielectrics is related to the matrix (Fig. 26), it is expected that classification of sediments is relevant by means of mean grain size (Mz, Folk & Ward 1957) and dielectric constant (ε_r). A plot

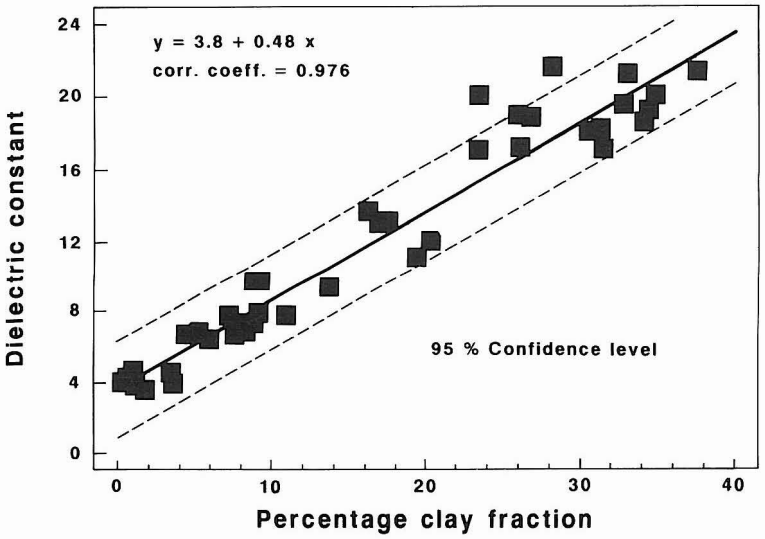

Fig. 26. A relationship between clay content and dielectric constant for different glacial materials. Data from Wisconsin.

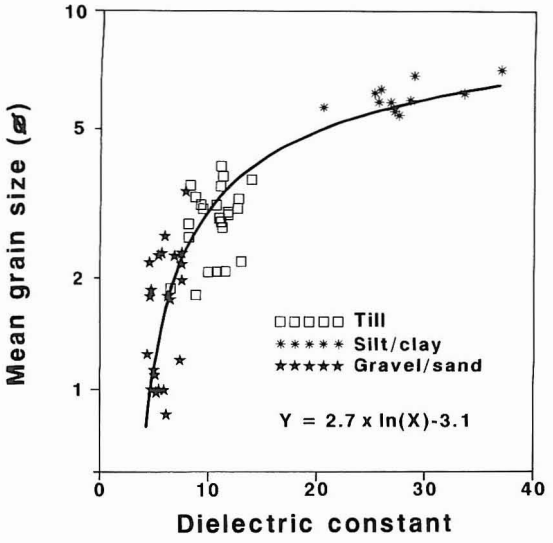

Fig. 27. A plot of mean grain size (Mz after Folk and Ward (1957) in phi scale) against dielectric constant for northern Finnish glacial sediments.

of Mz vs. ε_r is shown in Figure 27. Materials, such as glaciofluvial sand, tills from Rovaniemi — Kemijärvi (Rovaniemi till and Kemijoki till, see Fig. 91) area and glaciolacustrine silt are included. Dielectric constant changes are small in sandy materials (low moisture content) up to grain size 4 (in phi scale). Rapid ε_r increase is seen in silt-size materials due to increased moisture content as indicated in Figure 21. An empirical relationship $Mz = 2.7 * \ln(\varepsilon_r) - 3.1$ is given.

Unsaturated materials

In modern glacier environments, glacial tills, which have recently emerged from beneath the glacier contain an excess of water. The term »dry soil» or »dry sediment» seems inappropriate, when referring to these deposits. For the Pleistocene deposits the term »unsaturated» is preferred for the sediment (e.g. till) above ground water level and the term »saturated» or »wet» reserved for till below ground water.

Glacial tills contain different amounts of clay depending on the model of sedimentation and on the source material, as well. When the glacier advances over the older glaciolacustrine or marine clays, the clay is corporated into glacial drift. A typical example is Ozaukee till (averages sand 13 %, silt 47 % and clay 40 %) deposited by the Late Wisconsinan Lake Michigan Lobe. The type section is at the bluff of Lake Michigan at Port Washington, Wisconsin (Acomb et al. 1982, Schneider 1983, Mickelson et al. 1984), where the TDR measurements for this work were made. When the glacier advances over the Precambrian plutonic and metamorphic rocks as was the case in Finland and the Cambrian sandstone area in southern Wisconsin, predominantly sandy tills are deposited. Typical examples of sandy tills are Glacier Bay till (10.5 % clay) in southeast Alaska (Mickelson 1971), Horicon Formation till (7 % clay) of the Green Bay lobe in Wisconsin (Mickelson et al. 1984) as well as most of the tills in Finland (Virkkala 1969). In some cases clay content of Finnish tills exceeds 10 % (Nieminen 1985)

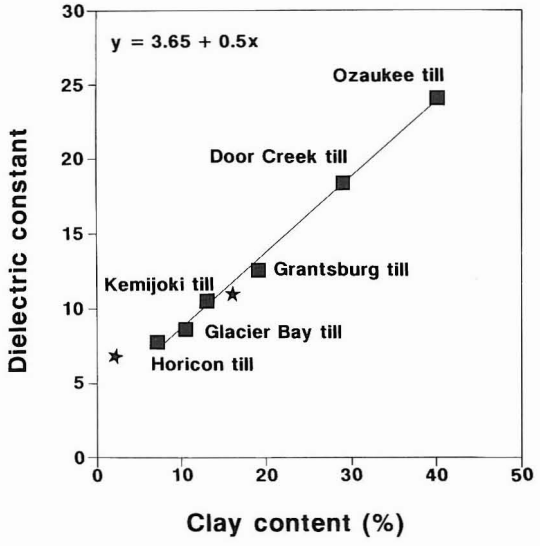

Fig. 28. A plot average of dielectric constant vs. average of clay content for different tills. Ozaukee (Michigan lobe), Horicon (Green Bay Lobe) and Grantsburg (Grantsburg lobe) tills represent Late Wisconsinan, Door Creek till pre Late Wisconsinan (Illinoian), Glacier Bay till Neoglacial, Kemijoki till Early Weichselian. Data from Morey and Harrington (1972) indicated by stars. Textural characteristics in the text.

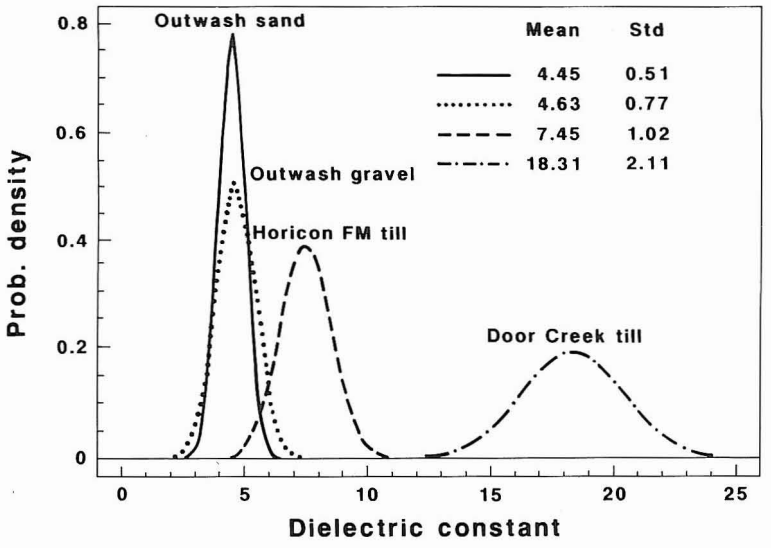

Fig. 29. Distribution of dielectric properties of unsaturated outwash materials and Horicon and Door Creek tills from Wisconsin, an *in situ* TDR determination.

but rarely 20 % (e.g. so called dark till, Rainio & Lahermo 1984).

Differentiation of six tills by means of the average dielectric properties and respective clay contents (Fig. 28) shows strong correlation. Data from Morey and Harrington (1972) on the dielectric properties, determined by GPR and TDR, and respective clay fraction contents for two tills (Billerica, MA: % clay = 16, ε_{till} = 11 and Groveland, MA: % clay 2, ε_{till} = 6.9) are in fairly good agreement with data shown here. As for different tills, dielectric properties of glaciofluvial deposits correlate with clay content and respective water content. However, both sand and gravel contain small amounts of clay due to transportation and sorting by water. Accordingly, dielectric constant values for unsaturated openwork gravel and sand are the lowest measured for glacial materials and they are difficult to be differentiated from each other, but easy to differentiate from tills and other diamictons as well as stratified fine-grained sediment types, such as silt and clay (Sutinen & Pekka Hänninen 1990). Figure 29 illustrates the similarity between glaciofluvial outwash gravel and sand as well as the difference between glaciofluvial deposits and tills as measured by TDR. Horicon FM till (sandy) and Door Creek till (silty) are shown as reference materials. Only small portions of the curves of sand and gravel overlap those of Horicon FM till. Accordingly, TDR is feasible for characterization of different glaciofluvi-

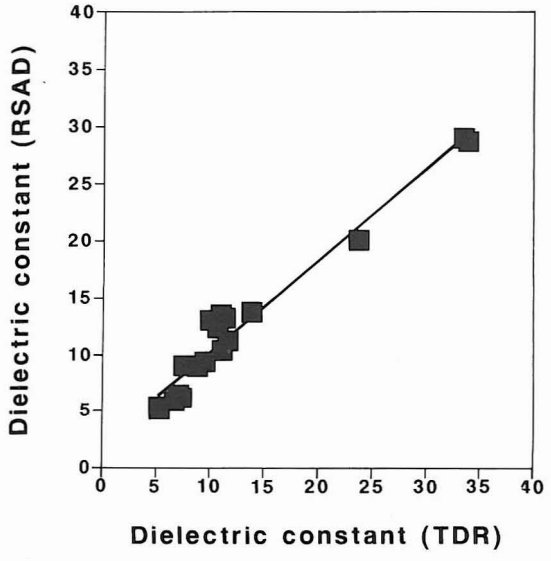

Fig. 30. A plot of comparison of *in situ* TDR and RSAD determination of dielectric properties of glacial materials. Adopted from Sutinen and Pekka Hänninen (1990).

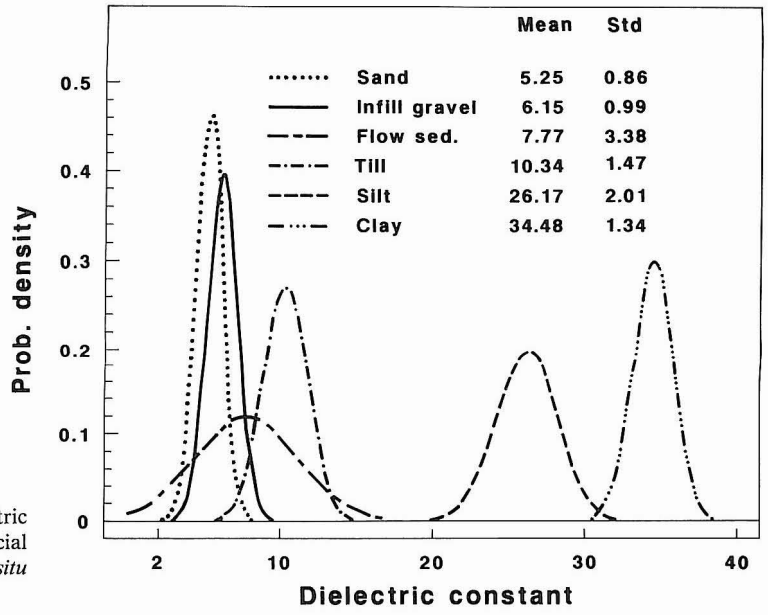

Fig. 31. A distribution plot of dielectric properties of northern Finnish glacial deposits. EM travel-time detection by *in situ* TDR and RSAD.

al materials as well as tills and therefore has potential for surface glacial mapping.

TDR is shown feasible for the sand-size and finer materials, whereas RSAD is more appropriate for the coarse-textured materials. In order to compare the methods, TDR (71 measurements) and RSAD (24 measurements) determinations of dielectrics were done for glacial deposits in the Rovaniemi — Kemijärvi area in northern Finland. The following sediment types were included: basal till (sandy), coarse-textured flow sediment in Kemijärvi (Sutinen 1985a; Fig. 16), glaciofluvial gravel, sand, silt and glaciolacustrine/marine silt/ clay. Dielectric values in Figure 30 (according to Sutinen & Pekka Hänninen 1990) show good correlation in linear fitting, but several points in the range of ε_r 10 to 13 (refers to till) show an irregular pattern. The macrostructure is thought to be reason for the difference, because parallel transmission line spacing of TDR was 5 cm, while radar antenna spacing was 2.5 — 4 m. Also, TDR gives slightly higher when, when $\varepsilon_r > 25$.

The TDR and RSAD determined dielectric properties of northern Finnish glacial deposit types are presented as distribution plot in Figure 31. Strong overlapping of the distribution curves is seen in the openwork (esker) sand and conduit infill (esker core) gravel as well as flow sediments categories. Also flow sediments overlap till. It is clear that fine-grained materials could be differentiated by the dielectric properties from other sediment types, but conductivity data is also needed for reliable separation of till, flow sediments and glaciofluvial materials.

Saturated materials

Texture and porosity highly determine the water content and consequently the dielectric properties of saturated materials. Because there are few occasions to determine *in situ* dielectric properties of saturated materials, the data for wet materials are obtained almost exclusively in laboratory. The use of TDR with parallel transmission line for *in situ* determinations of saturated materials is not without difficulties, especially when applied for layered earth. Always, when the transmission line is inserted vertically,

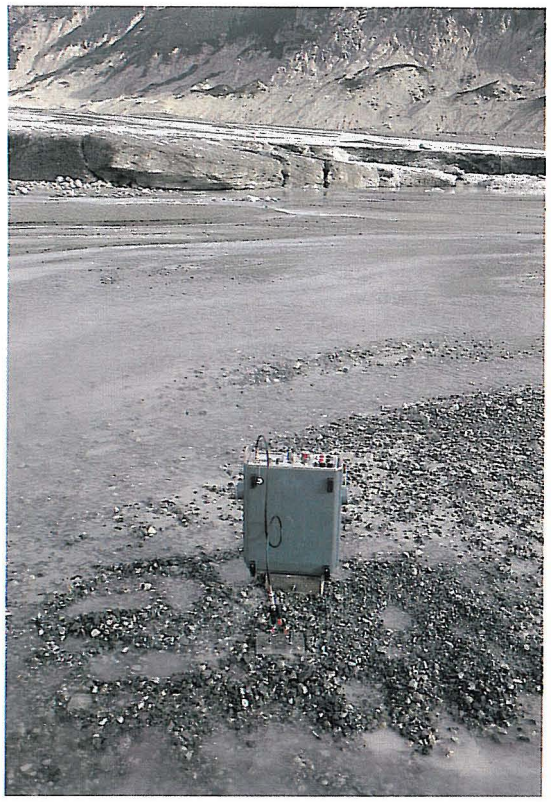

Fig. 32. An *in situ* TDR determination of saturated outwash deposits ($\varepsilon_r = 24.9$; $\sigma = 0.0028$ S/m; $\sigma_{water} = 0.0075$ S/m) close to the margin of the Burroughs Glacier, southeast Alaska. Photo R. Sutinen 1988.

the thicknesses of the layers has to be measured and test pits or borings are necessary.

TDR can be used on present outwash deposits (Fig. 32) and on the lake and river shorelines to measure saturated materials. A test was conducted in Picnic Point, near downtown Madison by inserting short probes (20 cm in length and 5 cm spacing) vertically at the edge of Lake Mendota to measure dielectric properties of beach sand and gravel (pebble diameter averages 1 cm). Results are presented in Figure 33. As a comparison, laboratory data obtained for outwash sand and fine gravel is shown, as well. The data indicate more variation between sand and gravel both in beach and outwash classes compared to unsaturated materials. Laboratory test was conducted also for two types (Horicon Formation till and Door Creek till) of tills. Figure 34 presents the results, where dielectric properties of natural dry and laboratory saturated tills are shown. As expected, also dielectric properties of saturated tills are significantly different from those in unsaturated condition.

One possibility for determination of ε_r of saturated glacial materials is to use TDR with long parallel transmission lines (several meters) inserted vertically below GWL. An experiment by using three-meter long steel probes, 25 mm in diameter, with 20 cm spacing was made on December 1989 for esker sand deposits. Percussion drilling was needed, because the surface was frozen to a depth of 0.7 m (based on the temperature logging). An example of the TDR trace obtained from Kolpene esker, near downtown Rovaniemi, is shown in Figure 35. The interval between the summits of the two leftmost peaks are interpreted to represent the frozen horizon (fh), giving $\varepsilon_{fh} = 3.0$ (cf. for frozen sand $\varepsilon = 4.2$ given by Baker et al., 1982). The value is smaller than that of any measured for dry sediments in this study. It was not possible to verify the microstructure of the frozen horizon, if there is any air ($\varepsilon_{air} = 1$) left between the particles or if ice (average $\varepsilon_{ice} = 3.18$; determined here in the laboratory by freezing brackish seawater, four ground water samples and distilled water; see Ulaby et al. 1986 Table E.1) fills the pore spaces. However, the initial amount of water before freezing does not have a significant effect on the dielectric constant value (Patterson & Smith 1981) of frozen soil. Layers in unfrozen and unsaturated sand is represented by the peaks below the frozen zone. The bulk $\varepsilon_{sand} = 6.1$ is given coinciding the results given in Figure 31. The GWL is clearly detectable from the TDR trace. Dielectric constant for saturated sand is given $\varepsilon_r = 31.6$. It is notable that the magnitude of the reflected wave (from open circuit) is still fairly strong meaning that even longer probes could be applied to sandy materials.

Another experiment was done during winter on

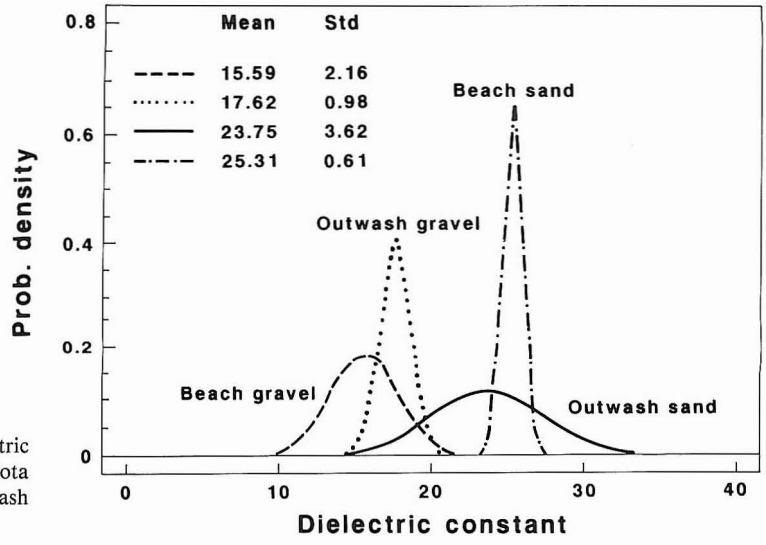

Fig. 33. A plot of the *in situ* dielectric properties of saturated Lake Mendota (Madison, WI) beach deposits and outwash deposits saturated in the laboratory.

Matkajänkä peat bog, 5 km from downtown Rovaniemi. Holes were handaugered through the ice cover. Steel probes, 16 mm in diameter with 20 cm spacing, was pushed into peat (3 meters thick) and through glaciolacustrine silt/clay deposits. A travel time detection was made at one-meter intervals down to 7 meters, where a hard-packed sediment surface was encountered. Figure 36 shows an example of three TDR traces indicating increasing probe lengths of 4 m, 5 m and 6 m. The bulk ε_{peat} = 69.4 is given for 3 meters of peat, while the top one-meter probe from the surface gave ε_{peat} = 57.4. Water content seems to increase downwards. The average ε_{peat} = 60 has been obtained by GPR from southern Finland (Marttila 1982). The silt/clay deposits below peat show increasing ε_r trend,

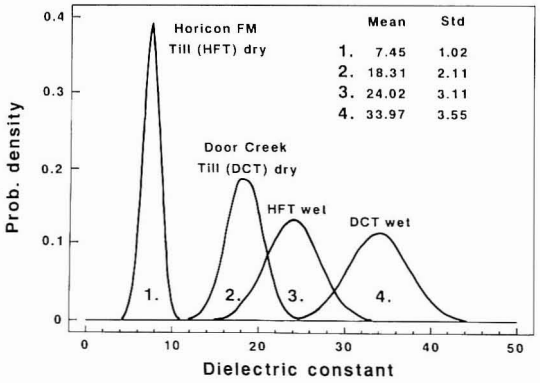

Fig. 34. A plot of dielectric properties of Horicon and Door Creek tills determined *in situ* (unsaturated) and in laboratory (saturated).

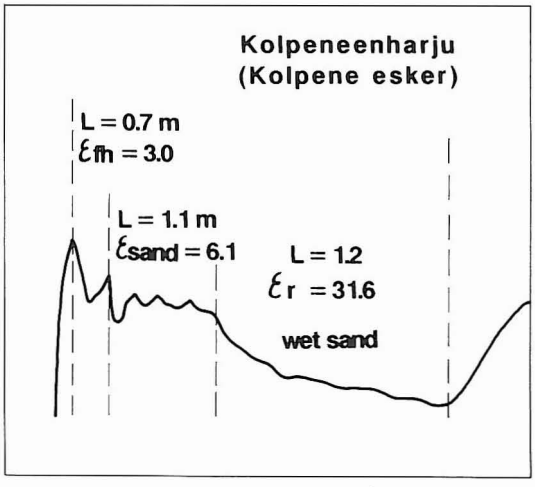

Fig. 35. A TDR trace representing frozen ground, unsaturated esker sand and saturated esker sand from Kolpene esker, near the city Rovaniemi, Finland. A parallel transmission line lenght 3 meters and spacing 20 cm.

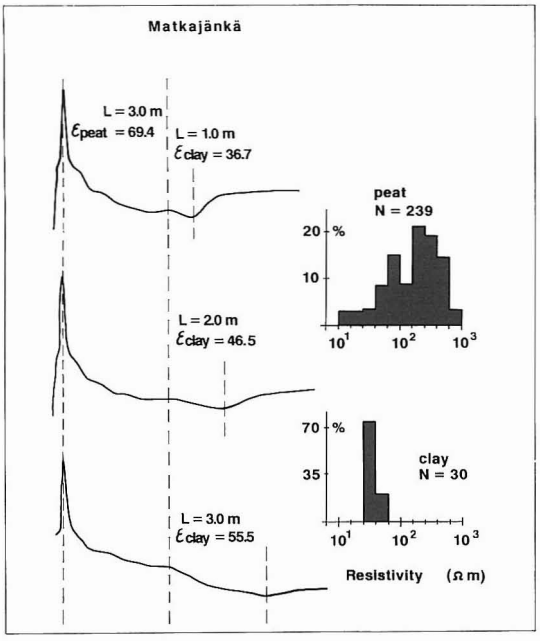

Fig. 36. Three TDR traces representing interface between peat and silt/clay from Matkajänkä peatbog, near Rovaniemi. The probe lenghts: 4, 5, and 6 meters.

too. When the probes were one meter in silt/clay ε_r = 36.7, two meters ε_r = 46.5 and three meters ε_r = 55.5, respectively. The results indicate that an impermeable layer separates the peat and minerogenic material and consequently the water in the Matkajänkä peatbog is perched. Below the impermeable layer the water profile is, again, increasing towards the saturation state. The saturation state for clay materials is observed to exceed over 50 % (volumetric water content) (Andersson & Wiklert 1972). The highest dielectric constant value may indicate too large of a water content. The explanation is the difficulty in determining the tangential point B (see Fig. 5) on the trace due to effective attenuation of signal, when probe length is 6 meters or more. The attenuation is due to electrical conductivity silt/clay material, measured to be between σ = 0.013 and σ = 0.025 S/m. Conductivity from σ = 0.003 to σ = 0.01 S/m is given for peat (Pernu 1979).

The above cases demonstrate that TDR with several-meters-long transmission lines will have applications in water profile studies as well as ground water and frost monitoring. Also, applications to peat investigations seem to be reasonable. TDR might be applied to predict landslide hazards, too.

Conductivity / resistivity

Conductivity (σ in S/m) is dependent on the texture, porosity, moisture content and particle shape of earth materials as well as the concentration of electrolytes in the water that is partially (unsaturated deposits) or totally (saturated deposits) filling the pore spaces between the grains (Smith-Rose 1933, Todd 1964, Hoekstra & McNeill 1973, McNeill 1990, Ward 1990) Conductivity has been shown to increase with finer texture (Culley et al. 1975, Jackson et al. 1978, Pernu 1979). It also is frequency dependent (Parkhomenko 1967, Hipp 1974), but in the frequencies lower than 1 MHz conductivity is relatively constant (King & Smith 1981). In general, conductivity is electrolytic and takes place through the moisture-filled pores and passages in the sediment. Unsaturated sediments, particularly gravel and sand, are resistive materials. The minerals in those materials are generally electrically neutral and thus are excellent insulators. By contrast, marine clay deposits contain clay minerals and relict electrolytes, which radically affect conductivity. Tills may occasionally contain conductive minerals such as magnetite in sufficient quantities to increase overall conductivity.

The following sections describes the conductivity properties of glacial deposits and the fac-

tors, such as moisture, temperature, salinity and mineralogy that determine the bulk conductivity of both unsaturated and saturated materials. Sediment classification is given by means of conductivity vs. dielectric properties. The combined application of electrical properties and SPOT HRV imagery (in Westport, WI, location in Fig. 2), airborne EM data (Oulunsalo, Finland) and high altitude IR photography (near Burroughs Glacier in southeastern Alaska, Fig. 1) to glacial mapping is also demonstrated.

Table 1. Bulk conductivity (σ) and water soluble potassium, sodium and magnesium contents of Littorina (L) and Ancylus (A) sediment samples from Oulu, Rovaniemi and Kemijärvi.

Reference area	σ S/m	K ppm	Na ppm	Mg ppm
Oulu (L)	0.360	70	800	27
Oulu (L)	0.490	100	1020	30
Oulu (L)	0.399	220	830	40
Rovaniemi (A)	0.021	50	60	20
Rovaniemi (A)	0.018	70	70	18
Kemijärvi (A)	0.032	13	40	6
Kemijärvi (A)	0.073	10	50	18

Moisture effect

Water content of unsaturated tills and glaciofluvial materials is related to the grain-size composition and particularly to the fine-grained matrix (Figs. 21 — 22). Conductivity of fine-grained marine/ lacustrine deposits is, however, strongly related to the depositional environment. Silt and clay deposited in a marine environment contain soluble ions, which have an increasing effect on the bulk conductivity. On the other hand, fresh water silts and clays are not strongly affected by relict salts (see Table 1). Because conductivity is related to the moisture content (Smith-Rose 1933, Parkhomenko 1967), which in turn is determined by the mean grain size and the amount of sediment matrix, it is useful in characterizing sediment types with various textural properties.

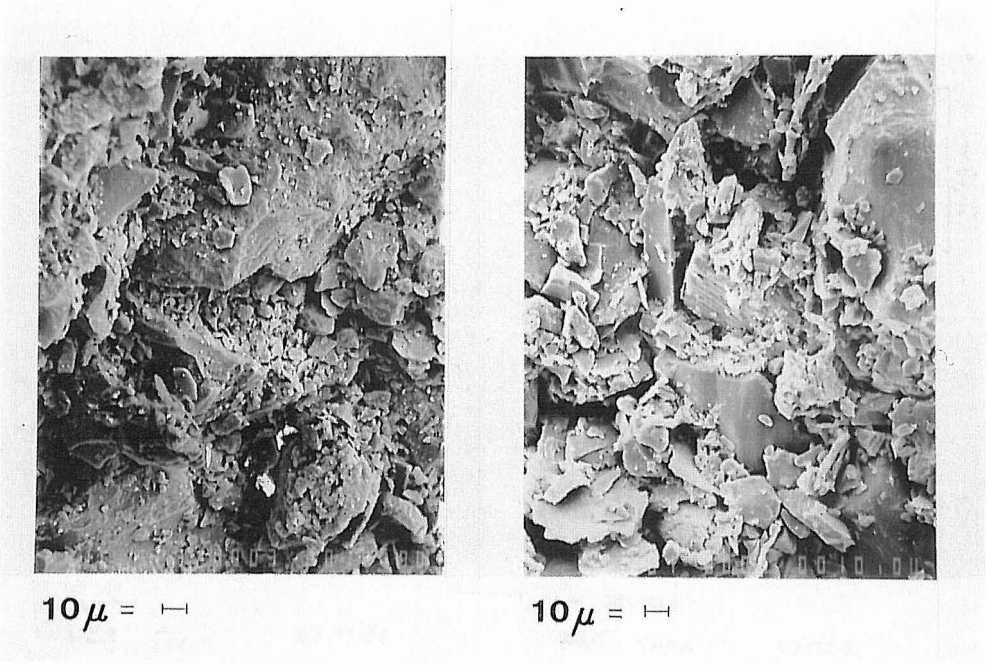

Fig. 37. A scanning electron micrograph of till (on the left; $\sigma = 0.0008$ S/m; $\Theta_v = 0.136$) and flow sediment ($\sigma = 0.00005$ S/m; $\Theta_v = 0.093$) matricies. Samples from Kemijärvi, northern Finland. Magnification * 500.

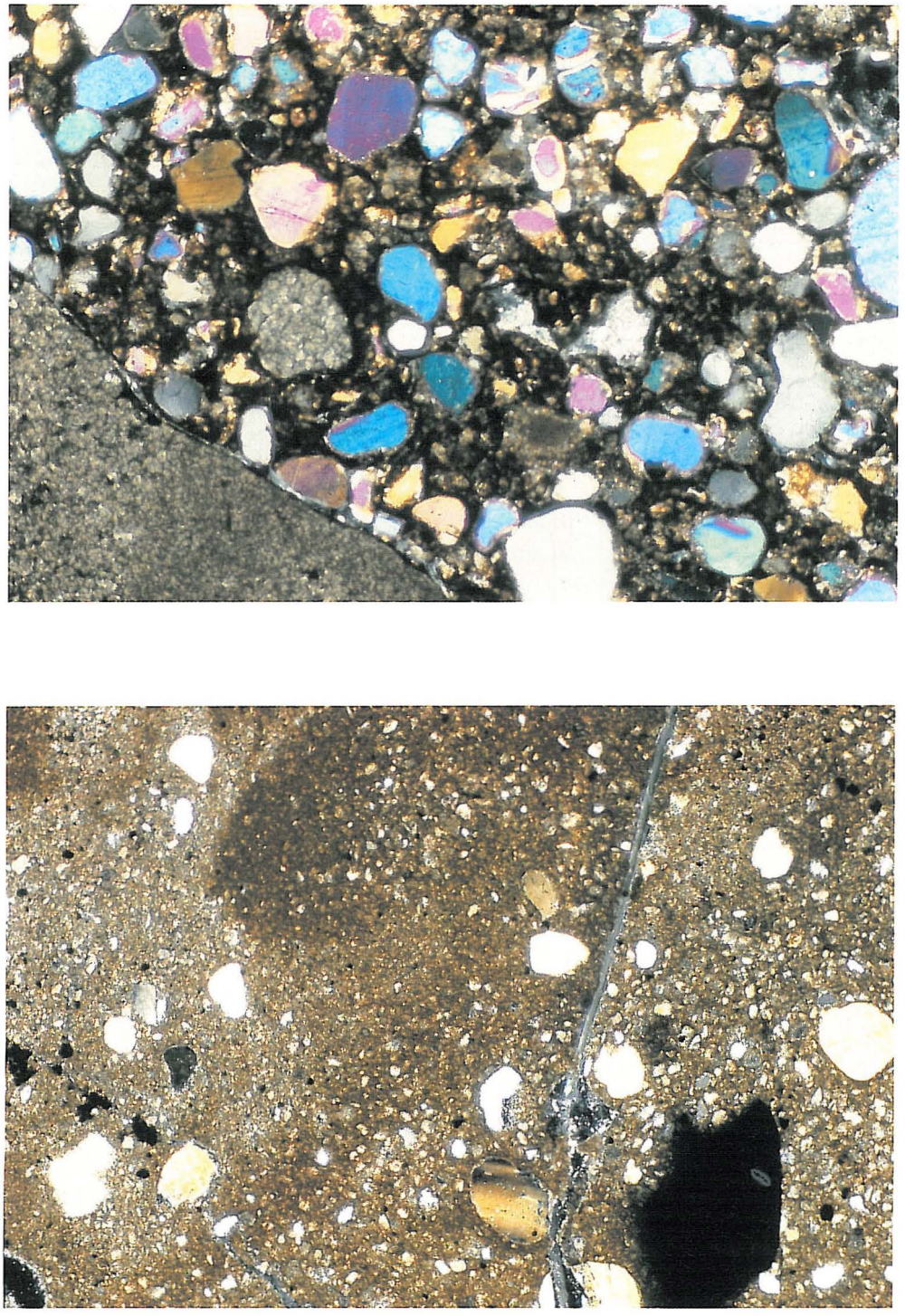

Fig. 38. Thin sections of matricies of the sandy Horicon Formation till (above) and silty Door Creek till (below) from Wisconsin. The electrical parameters ($\sigma_{HFT} = 0.0025$ S/m and $\varepsilon_{HFT} = 7.4$ and $\sigma_{DCT} = 0.01$ S/m and $\varepsilon_{DCT} = 21.1$) are dependent on the respective water contents (0.091 and 0.274). Magnification * 50.

Two examples help to illustrate the effect of water content and matrix (microstructure) on conductivity. Scanning electron micrographs (Fig. 37) of matrices of till and sediment flow diamicton (see Fig. 16) from Kemijärvi area show distinctly different microstructures in the SEM specimens. A Jeol JSM3 SEM instrument was applied and SEM specimens were silver coated using the method of Lynn and Grossman (1970). Sand grains in till are clasts supported in a matrix of closely spaced silt- and clay-size particles. These particles are randomly scattered around the sand grains in the diamicton specimen leaving abundant pore spaces in between the grains. The volumetric water content measured were 0.136 and 0.096, and (unsaturated) conductivies σ = 0.0008 S/m and σ = 0.00005 S/m, respectively.

Thin sections, shown in Figure 38, of sandy Horicon Formation till (HFT) and silty Door Creek till (DCT) from Wisconsin show a similar trend. Higher conductivity is due to a finer matrix and greater moisture content. For unsaturated HFT the proportion of d < 0.063 mm is 18.96 % and Θ_v = 0.091. For unsaturated DCT d < 0.063 mm = 89.37 % and Θ_v = 0.274. Respectively σ_{HFT} = 0.0025 S/m and ε_{HFT} = 7.4 as well as σ_{DCT} = 0.01 S/m and ε_{DCT} = 21.1 has been determined.

In unsaturated glacial materials with mean grain size less than 0.06 mm in diameter the water content increases significantly (Fig. 21), conductivity changes are expected to show a similar trend. Figure 39 is a plot of electrical conductivity (σ) vs. gravimetric water content (Θ_g) for stratified (GDi < 2.2) esker (glaciofluvial) and river (fluvial) sediment samples collected near Rovaniemi, North Finland. Conductivity changes approximately one order of magnitude, when water content (Θ_g) increases from 3.5 to 10 %. However, a more minor effect on conductivity is seen when Θ_g increases from about 15 to 25 %. Since the stratified materials with Θ_g < 10 % are gravel to sand size materials and Θ_g > 10 % silt or finer, therefore conductivity seems to in-

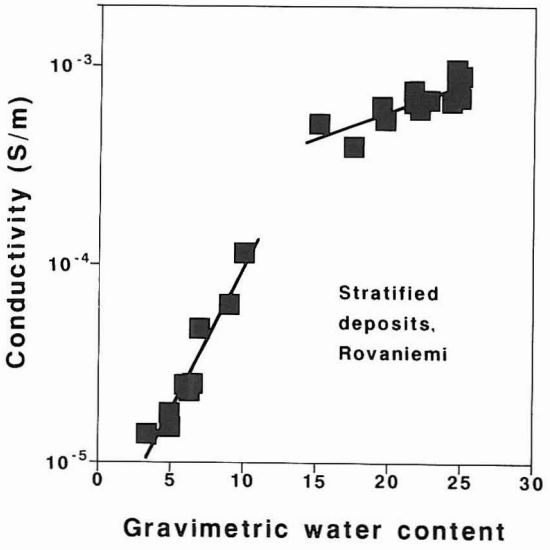

Fig. 39. A plot of electrical conductivity (σ) vs. gravimetric water content (Θ_g) for stratified (GDi<2.2) esker (glaciofluvial) and river (fluvial) sediments. Best fits for observed data. Samples collected near Rovaniemi, northern Finland. Conductivity measured in the laboratory with the Mafrip resistivity meter.

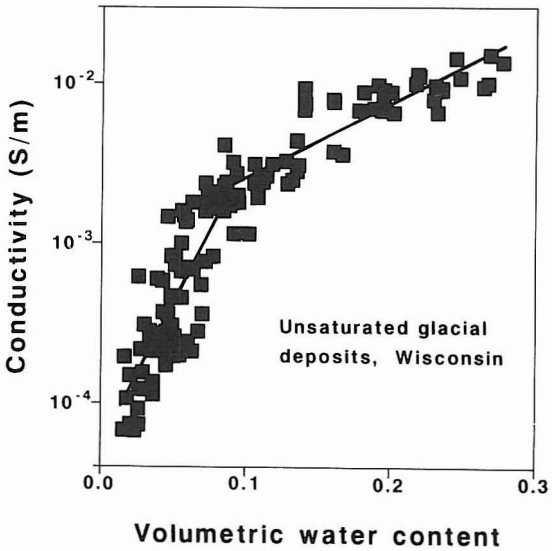

Fig. 40. A plot electrical conductivity vs. volumetric water content for unsaturated glacial deposits in Wisconsin. Best fits for observed data. Conductivity (DC) measured in the field using instrumentation shown in Fig. 10.

crease with finer grain size, which also is characterized by larger water content.

Unsaturated tills (Horicon, Grantsburg and Door Creek tills) and stratified outwash deposits in Wisconsin show a trend similar to those of Finland when DC conductivity is plotted against volumetric water content (Θ_v). Significant increase in conductivity, more than ten times, between the range of $0.02 < \Theta_v < 0.1$ is observed (Fig. 40). When $\Theta_v > 0.1$, conductivity tends to increase more gently. The data indicate a weak tendency toward clustering, probably due to many different material types. Clustering, however, can be seen more distinctly in the classification plot of conductivity and dielectric constant (Fig. 47).

The fractional porosity of sedimentary materials varies from 55 % (maximum value for clays) to 20 % (minimum value for gravel, Todd 1964). It is expected that full saturation of materials takes place at different water contents. Since conductivity changes are due to water content and porosity, saturated materials should indicate the texture dependent trend similar to that of unsaturated materials (assuming that water conductivity is constant). This was tested in laboratory by determining water saturation and respective conductivity for sieved fractions of 20 mm < d < 2 mm (esker gravel), 2 mm < d < 0.2 mm (esker sand) and d < 0.06 mm (esker silt). Spring water, sampled next to esker, was added gradually to oven dry (24 h in 105°C) materials up to saturation point. Results are presented in Figure 41. A rise of water content in the range of 3 % $< \Theta_g <$ 10 — 15 % radically affected the conductivity in all the tested size fractions. The conductivity change is about ten times from $\sigma = 10^{-5}$ S/m to $\sigma = 10^{-4}$ S/m, the lower boundary referring to oven dry state. The full saturation of a gravel sample was observed to be at $m_g \approx 20$ % with $\sigma \approx 8 * 10^{-4}$. Respectively, full saturation state for sand is $m_g \approx 30$ %; $\sigma \approx 2 * 10^{-3}$ S/m and for silt $m_g \approx 35$ %; $\sigma \approx 1.3 * 10^{-2}$ S/m. The experimental conductivity data obtained here are in fairly good agreement with Pernu's (1979) data (see Table 2).

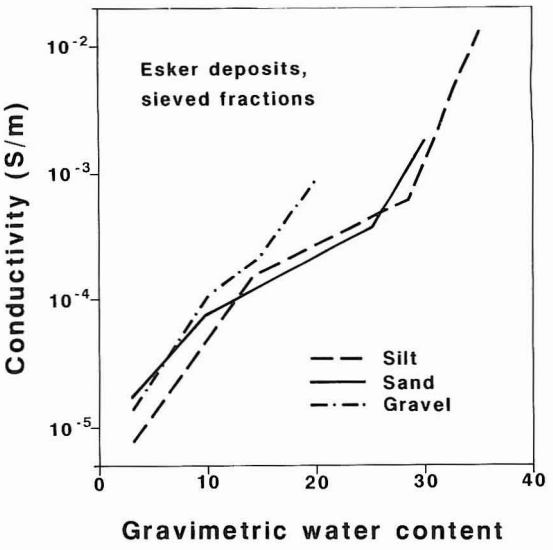

Fig. 41. A diagram of electrical conductivity vs. gravimetric water content indicating the full saturation points for gravel, sand and silt fractions of glaciofluvial material. A laboratory determination using Mafrip resistivity instrument.

The experimental data from both Finland and Wisconsin indicate that the conductivity of both unsaturated and saturated deposits is highly related to the moisture content. Since variations in

Table 2. Electrical conductivity of Finnish Quaternary deposits. Data obtained by galvanic earth resistivity measurements (Pernu 1979).

Material type	Conductivity (S/m) Saturated	Unsaturated
Lake or stream water	0.002 —0.01	—
Sea water	0.2 —1	—
Coarse sand and gravel	0.0007—0.001	0.0000125—0.00005
Sand	0.001 —0.002	0.00005 —0.0002
Silt	0.005 —0.012	0.0005 —0.0025
Clay	0.015 —0.03	—
Till	0.002 —0.005	0.0002 —0.001
Peat	0.003 —0.01	—
Mud, gyttja	0.007 —0.012	—
Saline or graphitic clay	0.02 —0.5	—

water content are due to varying amounts of fine-grained matrix in different sediment types, glacial materials can be characterized effectively on the basis on electrical conductivity. The water conductivity on saturated materials, however, is of great importance.

Temperature effect

In unfrozen sediments resistivity (or conductivity) is in practice not temperature dependent (Hoekstra & McNeill 1973). But, resistivity rises when interstitial water in between the grains begins to freeze. Frost phenomena in most cases are due to freezing of free water, because the adsorbed water has a very low freezing point (-78 °C, Parkhomenko 1967). Since the frozen sediment is a mixture of minerogenic particles, ice and air, the resistivity of ice ($4.7 * 10^5$ at -12 °C, von Hippel 1954) has significant importance.

A laboratory test was conducted for determining the electrical resistivity for both unfrozen and frozen saturated till as well as fine sand (from Oulu area). Figure 42 indicates that the resistivity of both materials tends to be approximately one order of magnitude higher in the frozen state, i.e. for till ρ_{wet} = 80 — 800 Ωm and ρ_{frozen} = 600 — 2000 Ωm, for fine sand ρ_{wet} = 400 — 6000 Ωm and ρ_{frozen} = 2000 — 80 000 Ωm are determined. The experimental data shown here point out a similar trend reported by Hoekstra and McNeill (1973) and Sellman et al. (1976).

The difference in electrical properties between frozen and unfrozen ground is sufficient enough

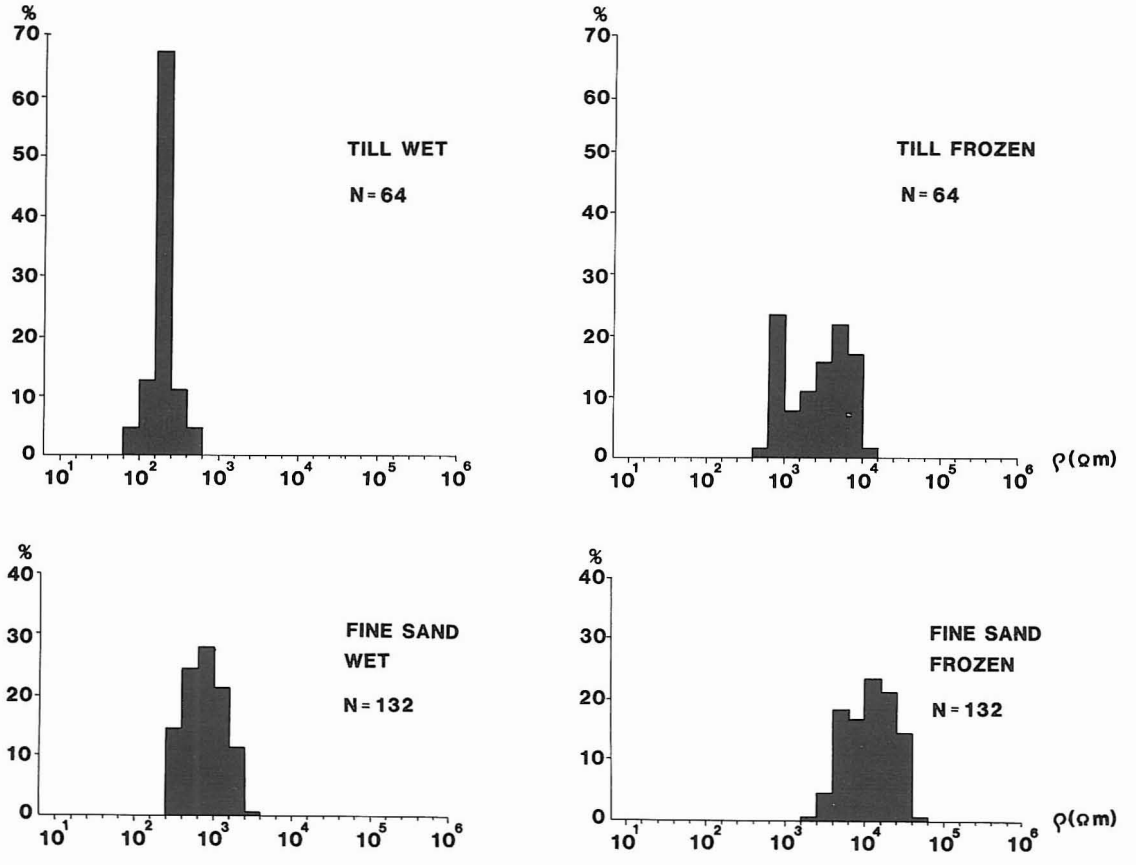

Fig. 42. Frequency histograms showing resistivity ranges for saturated unfrozen and frozen till and fine sand. Samples from the Oulu area, northern Finland.

to be detected by TDR and GPR. This could be utilized in geotechnical applications, e.g. in monitoring the thickness of the frozen layer. On the other hand, radar profiling is technically more simple to perform during winter time, when the ground, lakes and rivers are frozen.

Salinity effect

Generally, ionic concentration variations in ground water are due to the bedrock type, the mineral composition of unconsolidated materials and the degree of weathering. Since the dissolved solids are linearly related to the bulk conductivity of ground water (Day & Nightingale 1984), conductivity changes of ground water in different parts of northern Finland are expected to be substantial enough to significantly affect the overall conductivity of materials.

Of special importance when dealing with sediments around the Baltic coastal area is the relation of sediments to the marine stages of the ancient Baltic Sea. The shoreline displacement due to the sea level changes controlled by the isostatic fluctuations in the area is well known (Donner 1980, Eronen 1983). Today the maximum glacial rebound/ land uplift is about 1 cm/yr. The salinity of the ancient Baltic Sea undergone considerable variation during the Quaternary period as a result of fluctuations in sea level of the Atlantic Ocean. In the study area lake / marine sedimentation occurred during the Ancylus Lake about 9000 B.P. and Littorina Sea about 7000 — 7500 B.P. (Eronen 1983). Diatom and shell data indicate that during the Ancylus stage fresh water covered areas from the Bothnian Bay north to Kemijärvi and Kittilä. At the Littorina stage saline water (about 8 ‰, From 1965) covered the Baltic coastal areas as far north as the Oulu — Kemi region.

The salinity changes are indicated by the content of water soluble ionic components in marine / lacustrine clays and silts deposited during different Baltic Sea stages. The salinity effect was tested by a simple laboratory procedure for clay/silt samples collected from Oulu, Rovaniemi and Kemijärvi areas. Samples from Oulu represent the Littorina from Rovaniemi and Kemijärvi Ancylus stages, respectively. Ten milligrams of each sample material was dissolved in 100 ml distilled water, and conductivity was determined using a WTW LF 90 conductivity meter and water soluble components of K, Na and Mg were determined using a Perkin-Elmer Modell 306 atomic adsorption spectrophotometer (AAS). The results, presented in Table 1, clearly indicate that conductivity of the Littorina clays around Oulu (commonly known as sulphide clays) is about one order of magnitude higher than is the conductivity of the Ancylus clays. This is especially affected by the content of soluble K and Na concentration. Mg seems to only have a minor effect. It is suspected that the relict Baltic Sea salt concentration affects the ground water conductivity and bulk conductivity of saturated coarser materials, too.

The ground water and stream water data provided by Geological Survey of Finland (Lahermo et al. 1990, Nordkalottproject 1986a) indicate significant ground water conductivity variations in different parts of northern Finland. The highest conductivities are recorded in the areas of schistous rocks and in areas covered by the Littorina Sea. The effect of ground water salinity to bulk conductivity of saturated materials has been examined by applying Archie's law. Figure 43 shows a plot of bulk conductivity for gravel and sand size materials of varying (measured) fractional porosities against average water conductivity of four areas (Oulu, Kittilä, Rovaniemi and Kemijärvi). A bulk conductivity (determined by TDR) for medium esker sand saturated with different ground water samples collected around Oulu is plotted, too.

The plot indicates that also bulk conductivities of natural state saturated materials in Oulu area (covered by Littorina Sea ca. 7000 — 7500 B.P.) might be considerably lower compared to other tested areas (covered by Ancylus Lake ca. 9000 B.P.). Theoretically, there is almost a difference of one order of magnitude in bulk conduc-

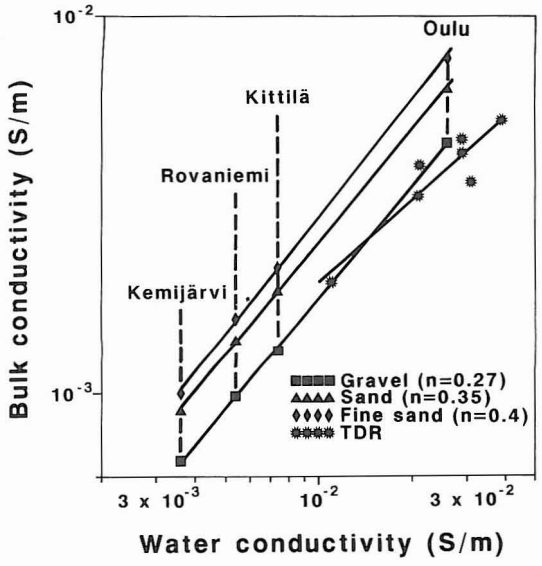

Fig. 43. A plot of bulk conductivity (determined applying the Archie's law) against ground water conductivity for three glaciofluvial materials. Fractional porosity measured, grains assumed to be spherical (m = 1.3). A plot of TDR determined bulk conductivity for sand (saturated with ground water samples) also shown.

tivity of saturated gravel and sand between Oulu and Kemijärvi. Therefore characteristic conductivities of saturated glacial materials are due to genetic type of material, fractional porosity and ground water conductivity σ_{GW}, which significantly affects bulk conductivity. The changes in σ_{GW} are at least partially explained by the stages of the ancient Baltic Sea.

Mineralogical effect

Glacial tills are composed of many different rock types. Mineralogic material is entrained and comminuted at the base of the glacier to produce drift with many different grain sizes. Although generally the effect of mineralogy on conductivity is far less significant than that of the water contents, there are some rock types that contain sufficient amounts of conductive minerals (e.g. magnetite, graphite and sulfides) to increase the overall bulk conductivity of till. Magnetic susceptibility is strongly correlated with the magnetite content in rocks (Puranen 1989), and it is indicative of the magnetite content of tills, as well (Pulkkinen et al. 1980).

Short-transported till (Figs. 105 — 106), derived from magnetite-bearing norite and greenstone rocks from Jaurakkajärvi, Pudasjärvi (Meriläinen 1977, location in Fig. 89) was sampled to evaluate mineralogical effect on conductivity. Bulk conductivity was measured in the laboratory using a Mafrip instrument by saturating the till samples with distilled water at room temperature. Magnetic mass susceptibility K($10^{-8}m^3/kg$) was determined by TH-1s susceptibility meter (by Geoinstruments ky, Finland) according to the procedures of Pulkkinen et al. (1980).

The pneumatic borehole logs (example in Fig 44A) indicated that magnetic susceptibility and conductivity peaks are correlated with the peaks of the percentages of magnetic grains in each measured fractional classes. One should note that percentage of magnetic grains increase with increasing particle size. Therefore, coarse till fractions presumably are more indicative of local glaciomorphic dispersion than the fine-grained matrix (see Figs. 105 — 106). A plot of conductivity against magnetic susceptibility (Fig. 44B) shows a clear trend of increasing conductivity with increasing magnetic susceptibility. Because the test material was saturated with distilled water, the obtained conductivities (in the range of 8 * 10^{-4} to 2 * 10^{-2} S/m) are different from the *in situ* conductivities. However, the trend is correct, and conductivity variations of about one order of magnitude are expected in some local tills as a result of high magnetite content.

It has been demonstrated above that conductivity (inverse of resistivity) is related to the moisture content rather than the mineralogic composition of glacial deposits. Although, mineralogic affect on conductivity of local tills might be significant, conductivity of glaciofluvial and fluvial materials likely are governed by moisture content and ground water properties. Moisture content, on the other hand, is directly related to

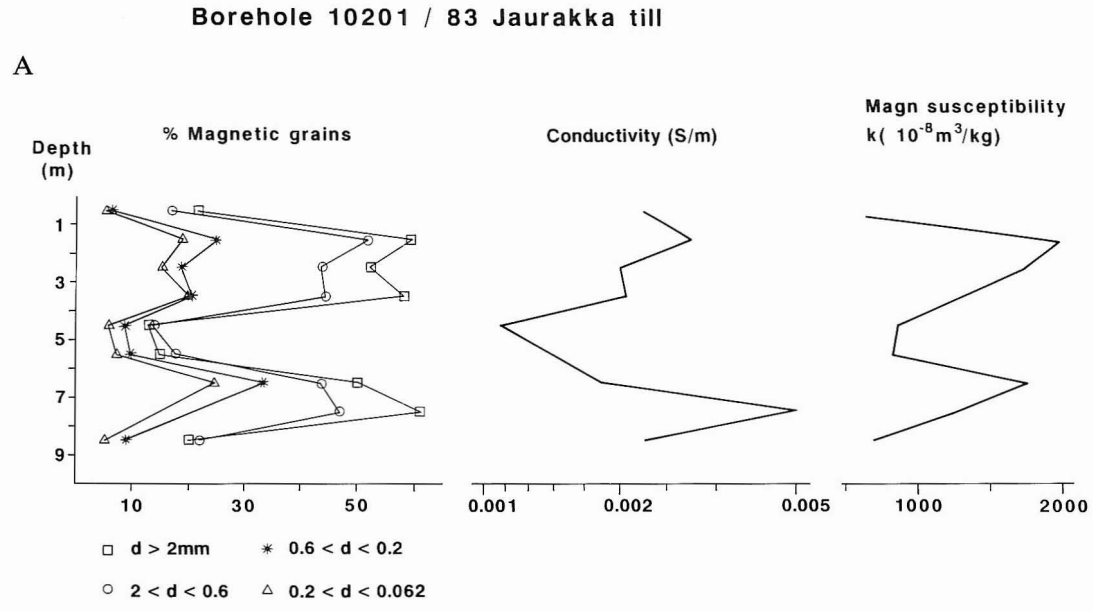

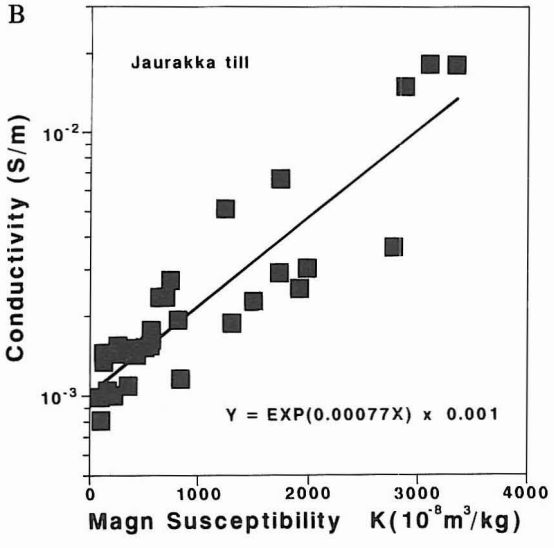

Fig. 44. A borehole profile showing variation of percentage of magnetic grains, conductivity and magnetic mass susceptibility in the Jaurakka till, near Pudasjärvi northern Finland. A plot of conductivity against magnetic susceptibility for saturated Jaurakka till is shown below. Susceptibility determined by TH-1s susceptibility meter, conductivity by Mafrip resistivity meter.

textural composition and porosity of the materials. From these standpoints unsaturated materials can be classified by means of conductivity, but the ground water conductivity is of significant importance for saturated materials, and the bulk conductivities tend to vary from one place to another.

Glacial deposits in northern Finland

The average conductivities of both saturated and unsaturated Finnish Quaternary deposits are listed in Table 2. Data is obtained by means of galvanic earth resistivity soundings by Pernu (1979). Conductivity of unsaturated materials generally is one order of magnitude lower than those of saturated materials. The salinity of ground water (relict marine electrolytes in the Littorina sediments) has a strong effect to bulk conductivity.

Galvanic resistivity soundings and data interpretations are feasible for the surveying of coarse-textured glacial materials in cases where they exist in large quantities (thick layers). However, due to rapid changes in meltwater flow velocities, sedimentary structures in glaciofluvial deposits (of sand size or finer) are often only a few centimeters thick. In order to get accurate

textural control, 4725 resistivity measurements were performed by Mafrip resistivity meter in the laboratory. Percussion drill samples collected from three areas; Oulu, Rovaniemi and Kittilä — Kemijärvi. Frequency histogram plots of the results are presented in Figure 45.

All the sedimentary groups: till, gravel, sand and silt, indicate tendency of a bimodal resistivity distribution in all three test areas. The lower resistivity mode refers to a saturated sediments (with original water), the upper mode to an unsaturated sediments. Resistivities of unsaturated deposits are roughly one order of magnitude higher than those of saturated materials in each sedimentary group. Saturated till in the Oulu area seems to be slightly less resistive than that in the other two areas, and the differences seem to be attributed to the ground water salinity effect (see Fig. 43). Significant areal resistivity differences were not apparent in the other sediment classes. The measured resistivities of the unsaturated flow sediments (see Figs. 14 — 16), typical to hummocky moraines e.g. in Kemijärvi and Posio areas, are closely related to gravel and sand. The values measured here are slightly higher than those obtained by Pernu (1979). It is suspected that the differences are due to laboratory test arrangement; when inserting electrodes into sample material placed into a half of plastic tube, the original structure may be disturbed and small voids created in the sediment. This is especially true for gravel- and sand-size samples. Also, when opening a sample tube, moisture evaporation begins immediately.

Electrical classification

Dielectric properties and electrical conductivity of glacial materials are shown to be strongly dependent on water content which is governed by texture and porosity. Therefore those two elec-

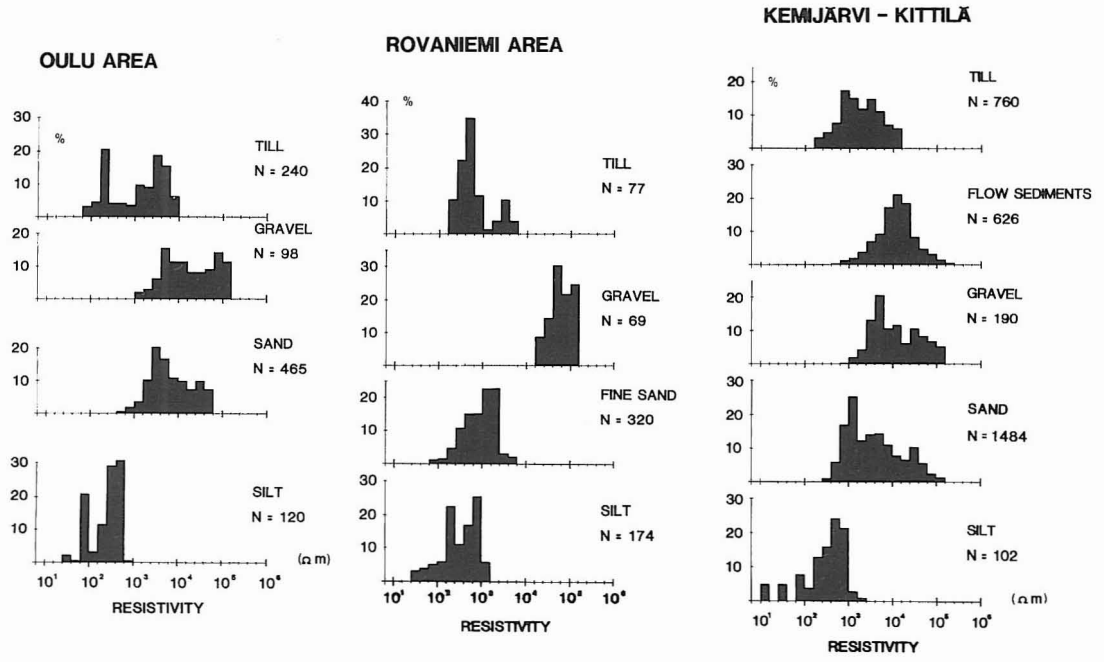

Fig. 45. Frequency histograms of laboratory resistivity data for different Quaternary deposits in Oulu, Rovaniemi and Kittilä — Kemijärvi areas. Original water content in the saturated materials, sampling technique described in the text.

trical parameters constitute a reliable basis for characterization of both unsaturated and saturated glacial materials. The following presentation summarizes the electrical parameters of glacial deposits from northern Finland, Wisconsin and Glacier Bay, Alaska. Classification by means conductivity and dielectric properties is presented for unsaturated and saturated materials.

The classification of five types of unsaturated northern Finnish glacial deposits (Fig. 46) are based on the conductivity data from Rovaniemi and Kittilä — Kemijärvi areas (see Fig. 45) and the dielectric data are for the most part the same as those in Figures 27 and 31. The diagram indicates clearly that various sedimentary groups can be differentiated by those two electrical properties. Glaciofluvial deposits (gravel and sand) typically have the lowest and glaciolacustrine deposits (silt and clay) have the highest dielectric and conductivity values. For gravel is given $7 * 10^{-6} < \sigma < 6 * 10^{-5}$ and $3.5 < \varepsilon_r < 6.5$; for sand $1.1 * 10^{-5} < \sigma < 10^{-4}$ S/m and $4 < \varepsilon_r < 7.5$; for till $1.8 * 10^{-4} < \sigma < 7 * 10^{-4}$ S/m and $7 < \varepsilon_r < 13$; for silt $1.3 * 10^{-3} < \sigma < 1.5 * 10^{-2}$ S/m and $22 < \varepsilon_r < 28$ as well as for clay $2 * 10^{-2} < \sigma < 3.3 * 10^{-2}$ and $32 < \varepsilon_r < 37$.

Due to low clay content (< 1 %) and contents of fines, the electrical value ranges of openwork sand and gravel are overlapping. Also, some coarse-textured flow sediment types tend to have similar electrical properties. Therefore, recognition of those materials by radar is based on the different reflection characters from various sediment structures. For example, laminar, sinusoidal and foreset-type sedimentary structures typical for sandy deposits are indicated by repeated reflections with varying intensities on GPR profiles (e.g. Figs. 86, 92, 94). Gravel deposits generally are massive (several meters thick) with abundance of stones and boulders, which are depicted by hyperbolic reflections on the profile (Fig. 93). Sometimes massive and homogenous sandy deposits occur in glaciofluvial formations, and those deposits have no electrical interfaces and reflections are absent (Fig. 97).

Till in the Rovaniemi — Kemijärvi area is typically sandy with the average clay content of 3.7 %. Electrically it is separated clearly from sand and silt deposits. In GPR profiles it can be recognized by closely spaced high-intensity interfaces (Morey & Harrington 1972, e.g. Fig. 76). Glaciolacustrine silt and clay are clearly clustered and separated by electrical properties from other sediment groups. Glaciomarine deposits tend to have larger electrical values, but the relationship is presumably similar to glaciolacustrine materials. Due to strong attenuation of the signals radar profiling is not particularly feasible for silt and especially for clay deposits (see Fig. 54). Therefore shallow reflection seismology is preferred for those deposits.

Similar trend of the electrical characteristics are recorded from Wisconsin. The electrical properties of two types of tills (Horicon Formation till and Door Creek till; inside the Late-Wisconsinan glacial margin near Madison, Wisconsin) and outwash sand and gravel, and also properties of till at Brooklyn (outside of Late-Wisconsinan end moraine) are plotted in Figure 47. A plot shows

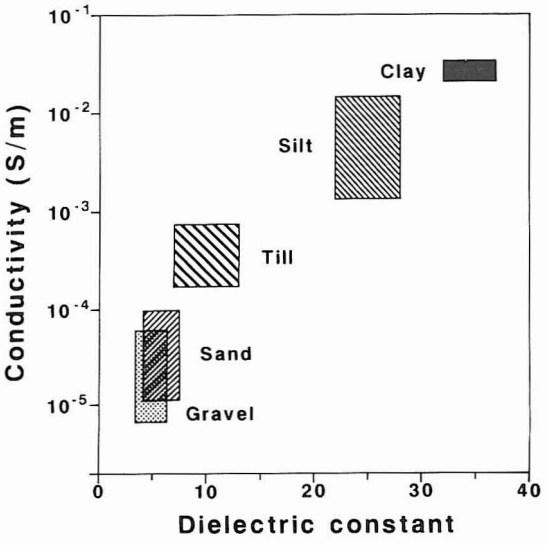

Fig. 46. Electrical classification of five northern Finnish glacial deposit types. Adopted from Sutinen and Pekka Hänninen (1990).

clearly that sediment types of different textural properties can be separated by electrical properties, and the trend is consistent with the results from Finland. The electrical properties of Brooklyn till strongly resemble those of Door Creek till. Stratigraphically, Door Creek till is located below Late-Wisconsinan Horicon Formation till and likely represents an older ice advance. Based on the electrical similarities of Door Creek till and Brooklyn till, those tills may represent the same glacial advance, which presumably is older than Late Wisconsinan.

Classification of saturated glacial deposits by electrical parameters is not so unambiguous, since conductivity is highly related to ground water conductivity (Fig 43). Therefore, bulk conductivity values of sediments are area specific. Dielectric properties, on the other hand, are not salinity dependent (Parkhomenko 1967, Topp et al. 1980, Jackson & O'Neill 1983). Figure 48 shows a plot of conductivity against dielectric constant for four different sediment types: *in situ* determined properties of Lake Mendota beach deposits (gravel and sand) and Glacier Bay till, laboratory determined properties of Horicon till and Door Creek till. Also, the best fit for unsaturated glacial materials is shown for comparison.

As illustrated in Figure 33, the dielectric properties of saturated beach deposits are texture dependent. Also conductivity behaves in a similar manner. The best fit for saturated beach deposits indicates strong correlation between conductivity and dielectric constant. It is probably coincidental that other plotted sediment types are consistent with the fit for beach deposits, especially, because Door Creek till and Horicon Formation till have been saturated in laboratory with distilled water. However, those two tills are clustered as would be expected based on their textural properties. On the other hand, Glacier Bay till shows irregular scatter plot. Some points are located near the unsaturated curve while others indicate an increased moisture content. Moisture variations are related to the deposition processes and the time during which the till emerged from beneath of glacier. A more detailed description of the sedimentation and stabilization of till is presented in the next section.

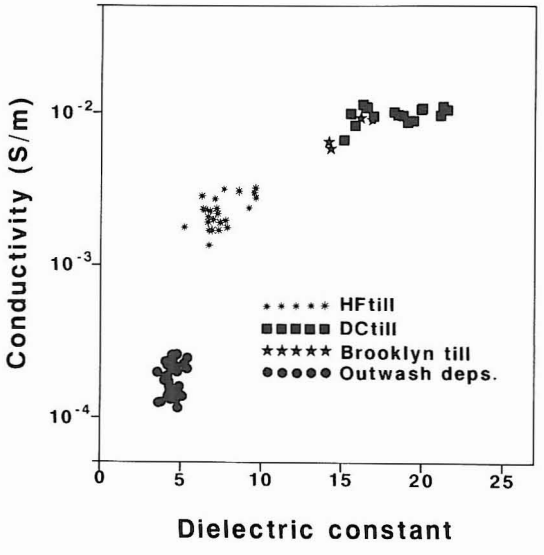

Fig. 47. Electrical classification of four glacial deposit types in Wisconsin. Determinations of dielectric properties *in situ* by TDR, conductivity as shown in Fig. 10.

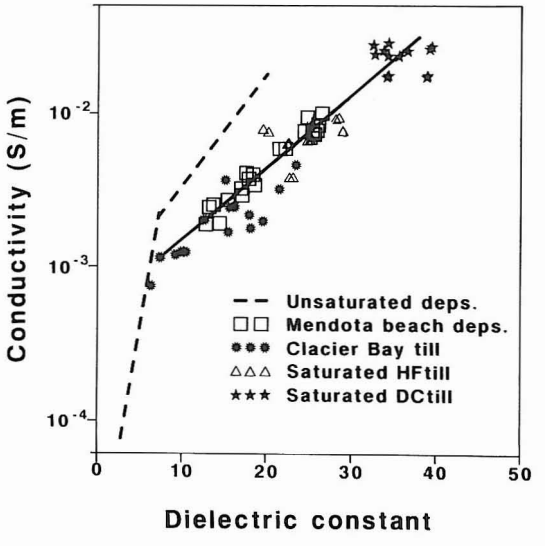

Fig. 48. A plot of conductivity against dielectric constant for saturated glacial deposits from Wisconsin and Glacier Bay, Alaska. Best fits for Lake Mendota beach deposits and for unsaturated deposits.

As a conclusion, conductivity and dielectric properties unambiguously characterize both unsaturated and saturated glacial deposit types. However, ground water salinity effect has to be taken into account in conductivity (resistivity) surveys, and absolute values are site specific. Even though survey depth of TDR technique is limited due to transmission line design it is seen feasible tool for surface mapping of soils and glacial deposits. Particularly in northern Finland, where topsoil cover usually is only a few centimeters thick, transmission line could be inserted into unaltered glacial materials. TDR is seen extremely valuable tool for providing reference data for interpretation of remotely sensed data.

Electrical classification and image interpretation

Water content of surface materials is the link between texture and electrical properties. It also largely determines (in different climates) the vegetation types and drougthness within species of the plants and trees. Classification of glacial materials by electrical parameters is unquestionable in cases, where measurements are done on fresh exposures. As a result of the layered structure of the earth, lateral mapping of surface materials by EM techniques, however, is more complicated. The surveyed depth depends on the applied instrumentation, and the obtained data indicate bulk properties of materials. The effective penetration of the conductivity meter EM 31 is either 3 or 6 meters (McNeill 1980, Geonics 1982) and the GPR penetration is largely determined by the applied frequency, the electrical properties and the amount of layers in the surveyed materials (see Figs. 7 — 8). The surveyed TDR data depends on the applied probe length. Different remotely sensed data also vary in terms of penetration: APs and satellite data (SPOT and Landsat TM) give information only from the ground surface, vegetation canopies, and droughtness variations, the airborne gamma ray data from near surface (approximately from a half meter or less, Burson 1973, Grasty 1977, Lanne 1986) and electromagnetic data from several tens of meters (Peltoniemi 1982). Therefore, a combination of different terrain data sets and remotely sensed data sets is not always straightforward. For example indirect information sources, such as vegetation variations and droughtness might indicate reliably the underlying soils types in uncultivated regions, but those features are not relevant criterion for soils on cultural areas. This section describes different airborne and space borne data as surface materials indicators, and their feasibility has been evaluated using terrain geophysics methods. Example of the use of SPOT HRV data is presented from Wisconsin, airborne geophysics from Finland and digital AP from Alaska.

SPOT HRV data

Recent development of high-resolution satellite imaging, in particular SPOT HRV, provides an useful tool for environmental monitoring. The advantage of SPOT is large, 60 * 60 km, land coverage and still 10-meter spatial resolution in panchromatic mode and 20-meter resolution in multispectral mode. SPOT also yields stereoscopic viewing and interpretation. The spectral reflectance is, however, resulted rather from the canopy variations than actual soil characteristics. But, vegetation canopy variations and droughtness indirectly indicate soil types.

SPOT HRV data and EM terrain surveys were tried out to outline sand and gravel reserves in an end moraine complex in Westport, Wisconsin (location in Fig. 2). The EM field reconnaissance surveys included: measurements of dielectric properties by TDR (f = 200 — 750 MHz, a parallel transmission line of 20 cm inserted vertically into the ground, 245 waveforms record-

Fig. 49. An exposure showing glacially tectonized glaciofluvial sands covered by soil and the Late Wisconsinan Horicon till in the Westport End Moraine, Wisconsin. Photo R. Sutinen 1988.

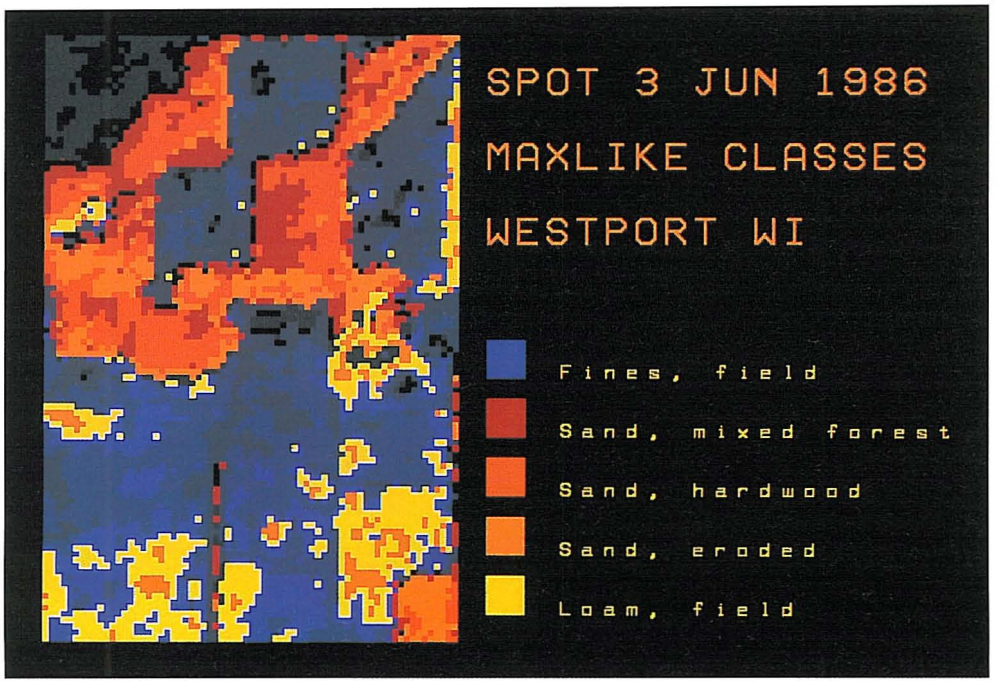

Fig. 50. A maximum likelihood classified image of the SPOT HRV data indicating (pseudocolored) surface texture variations on the Westport end moraine, (690 × 1020 m) Wisconsin.

ed), ground conductivity measurements (Geonics EM 31 electromagnetic conductivity meter with l = 3.66 m and f = 39.2 kHz, 1200 measuring points), and GPR survey with SIR-8 (antenna c.f. = 500 MHz).

The Westport end moraine covers 68 hectares and is located about eight kilometers northwest from downtown Madison. The end moraine rises about 30 meters from the surrounding terrain, and it is 50 meters above the lake level of the nearby Lake Mendota. It is composed of sand and gravel that are superimposed by sandy till, and silty and loamy soils (Fig. 49). The sand core shows strong glaciodynamic folding and the top of the moraine is clearly drumlinized. The drumlin topography and the overlying sandy till (Horicon Formation) are attributed to the Late Wisconsinan, and those featured terminate at the Johnstown moraine, ten kilometers southwest from Westport.

Madison scene Spot-1 image from June 3, 1986 shows different types of farmlands at the beginning of growing season, and therefore bare soil is common. Different soils indicate significant variations in texture and consequently in surface moisture content, too. Forest canopies compose of mixed hardwood with tiny patches of red pine. Subset (69 * 102 pixels) of merged 10-meter resolution panchromatic band and 20-meter resolution multicolor bands were geometrically corrected using cubic convolution. Based on the spectral information a linear stretch from each three

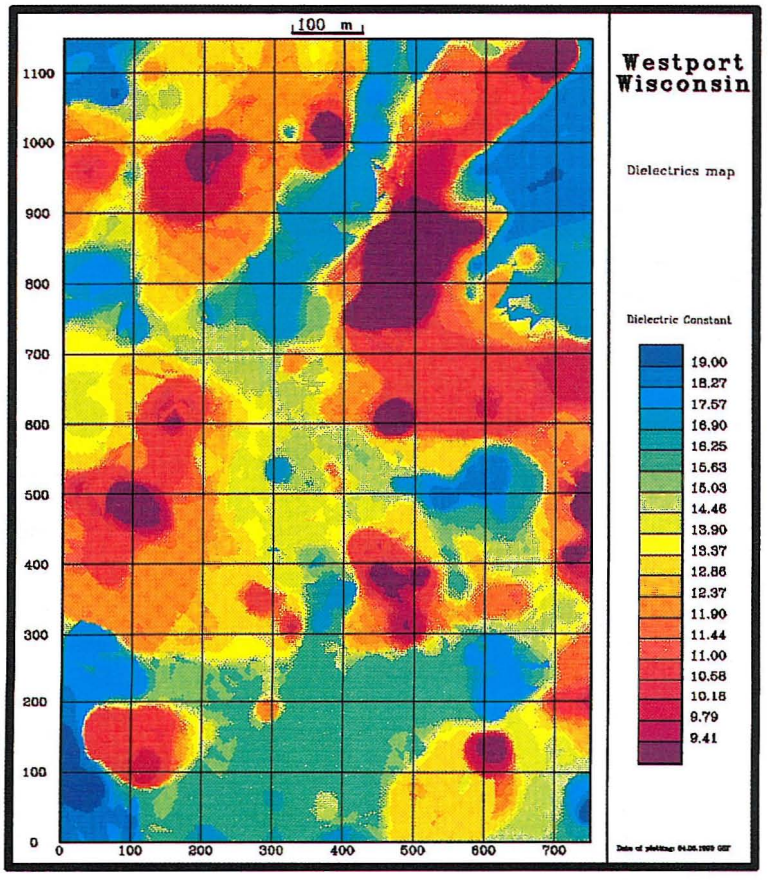

Fig. 51. The moving median of the surface dielectric properties obtained by TDR on the Westport end moraine.

bands (two visible and one near-IR) created for training set procedures and classification. A maximum likelihood classification was partially based on the soils map and partially on the field observations. A classified image indicate both fine-grained and sandy soils (Fig. 50).

The dielectric records (Fig. 51) indicate that the high dielectric anomalies correlate fairly well with the fine-grained soil-type coverages on the classified SPOT data (shown by dark blue color code). Also, major sand coverages are consistent with the low dielectric anomalies. Because the TDR survey was performed two years after the SPOT recording, weather conditions presumably have been different during those times, and explains some of the differences between the classified SPOT image and the dielectric records.

The resistivity data indicate bulk resistivity roughly to a depth of 6 meters (Fig. 52). The high resistivity anomalies correspond extremely well to the sandy coverages in the classified SPOT image. Those anomalies are located in the areas of forest canopies, but also in the (corn) field areas. The classified SPOT information therefore indicates surface soil types and moisture variations. The fact, that the ground water level is far deeper than the effective penetration of the EM 31 (verified by the DC resistivity soundings with ABEM Terrameter SAS 300 B instrument), suggests that the high resistivities are rather due to the subsurface materials than indicate only near-surface conditions.

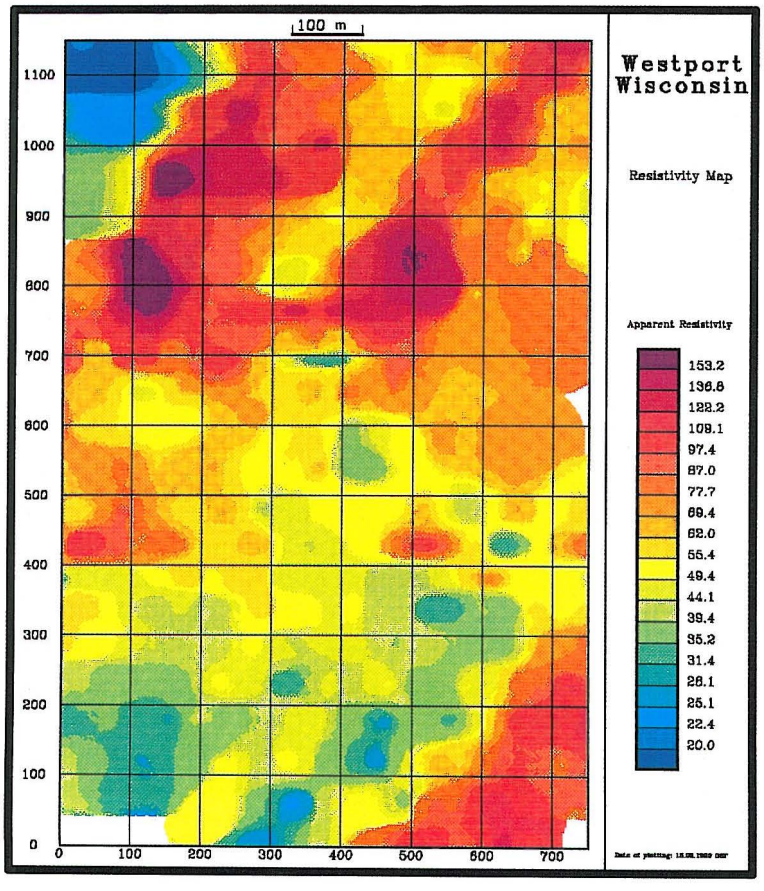

Fig. 52. The moving median of the resistivity data obtained by the EM 31 on the Westport end moraine.

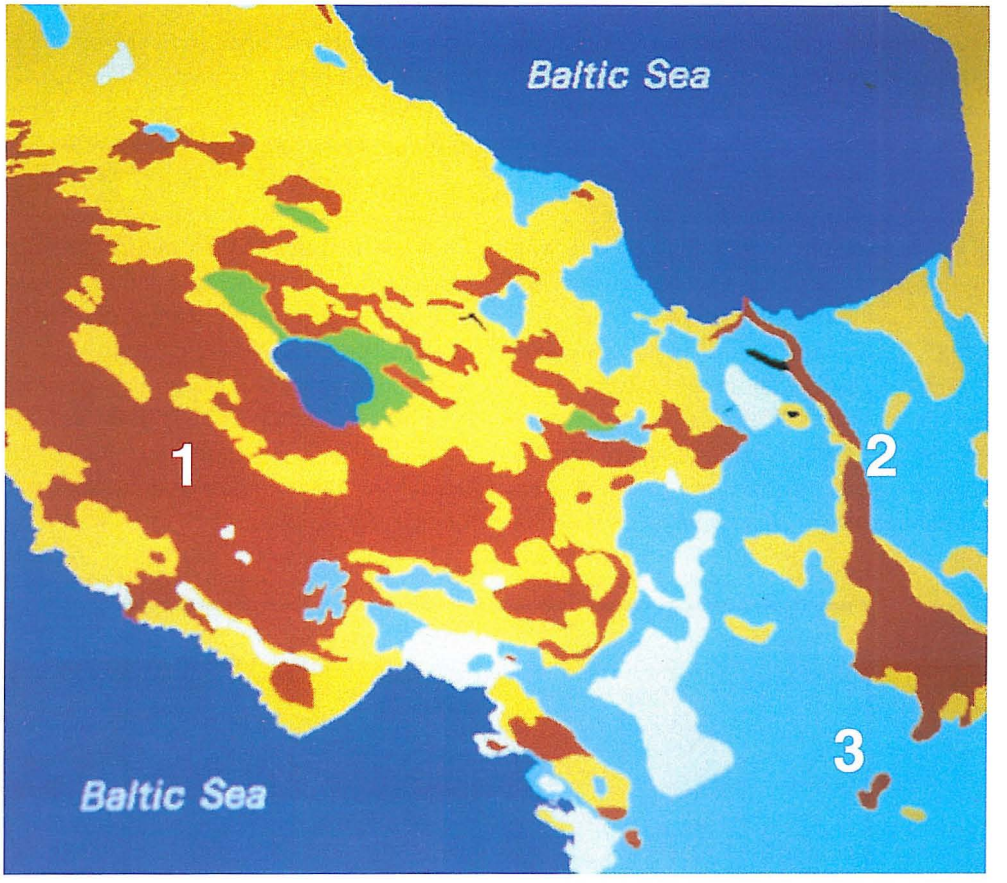

Fig. 53. Surface materials of the Oulunsalo basic map sheet area. Redbrown color code indicates sand, yellow fine sand, light blue silt, white fine silt and green indicates peat. Vertical scale is 10 km. Sites mentioned in the text: 1. Salonselkä esker, 2. Kempele esker, 3. Niittyranta.

In order to verify the subsurface sand and gravel deposits, a GPR survey was conducted at the sites with high resistivities, also indicated in the classified SPOT image. At those sites GPR indicated systematically cross-bedded glaciofluvial material (7 — 8 meters; $\varepsilon_{sand} = 5$), also the overlying soil and the till were at the thinnest. Therefore surface moisture variations result both from surface soils materials, and also from the subsurface glaciofluvial sandy materials, that allow effective surface water percolation. The other important feature was that at the sites with bulk resistivities less than 100 ohm-m, GPR penetration was less than 0.3 m ($\varepsilon = 18$ for silty loam) and sites with the bulk resistivity about 200 ohm-m, GPR penetration of 8 m ($\varepsilon_{sand} = 5$) was obtained.

The Westport study site indicated that SPOT-imagery combined with the EM terrain methods could be applied to outline sand and gravel reserves. For this purpose the SPOT- imagery might be best if recorded before the growing season. It was also shown that EM ground conductivity surveys could be utilized in planning and directing of the GPR surveys. In the Westport site glaciofluvial material was exploited for concrete production and the silt-size materials for the landfill site lining.

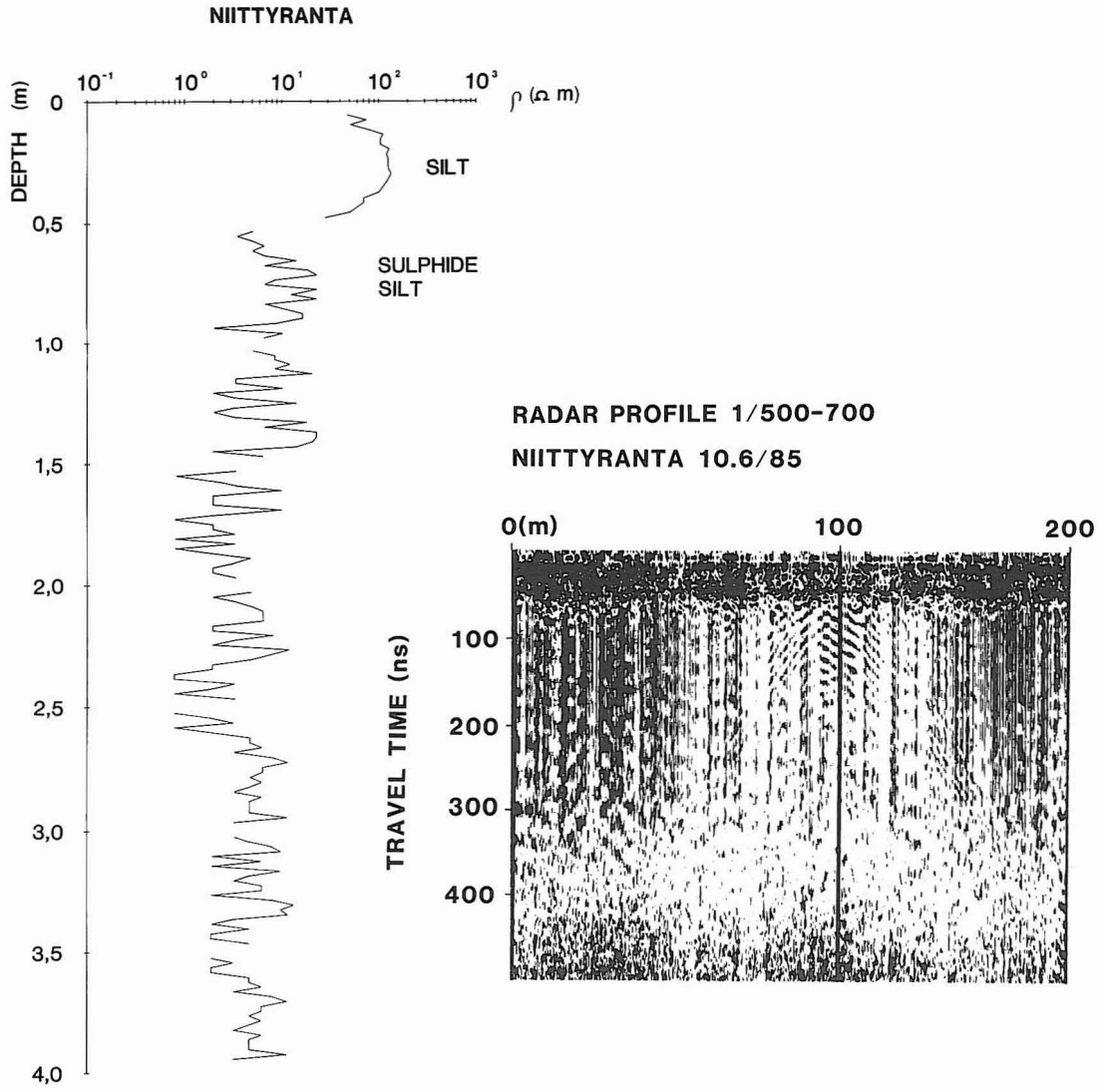

Fig. 54. A resistivity log and radar profile from Littorina silt, Oulunsalo, Finland. Note poor radar penetration. The hyperbola reflection is due to the electrical power line crossing perpendicularly the profile line.

Airborne EM and gamma radiation data

Feasibility of airborne gamma radiation (potassium window) and electromagnetic (quadrature component) data, gridded into 50-meter pixels, were applied to mapping of glacial materials in the Oulunsalo area, northern Finland (basic map sheet area 2444 08, Oulunsalo). The »ground truth» data were collected by GPR (SIR-8 with antenna c.f. = 80 MHz) and TDR (f = 130—500 MHz, vertically inserted parallel transmission line of 30 cm and 5 cm spacing). The terrain conductivity survey (Geonics EM 31 electromagnetic conductivity meter, l = 3.66 m and f = 39.2 kHz) data were used to locate buried esker deposits.

The 25 — 50 meters thick Quaternary deposits,

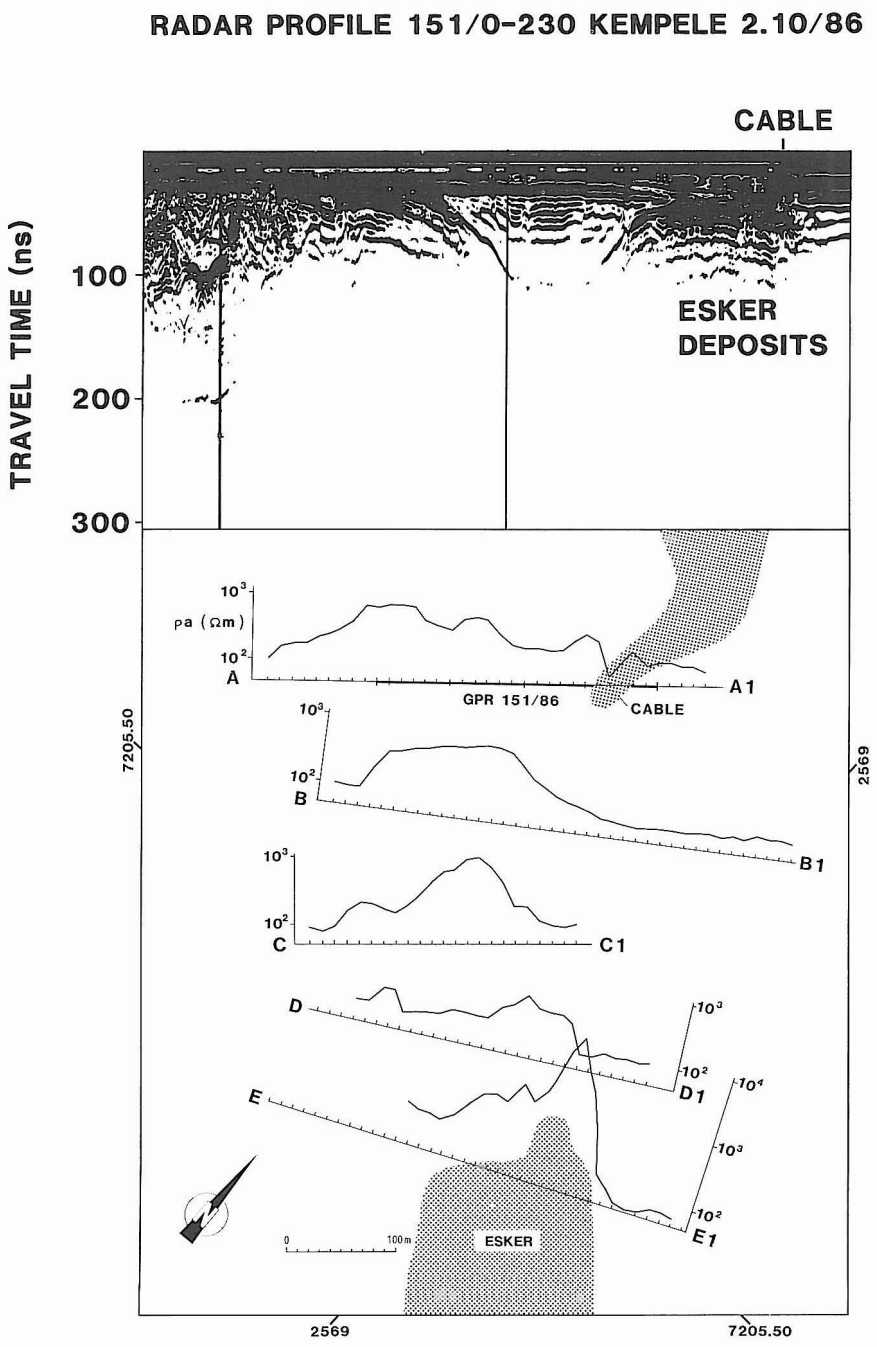

Fig. 55. A radar (c.f. = 80 MHz) profile and EM-31 resistivity profiles showing continuation of esker deposits beneath finegrained materials. Kempele esker, Oulunsalo, Finland.

overlying the Jothnian sedimentary Muhos formation in the Oulunsalo, compose of till, glaciofluvial gravel and sand, littoral sand and silt, and marine silt and clay (Fig. 53). The two

(Late Weichselian) eskers, Salonselkä esker and Kempele esker, are trending NW — SE and have been modified and reworked by the littoral activity. Till is rare at the surface, but is superimposed by the beach sand deposits.

The marine silt and clay, deposited in the Littorina Sea water about 7500 — 7000 yr B.P. (Eronen 1983) contain significant amounts of soluble electrolytes (Table 1), and therefore those sediments are electrically most conductive met in northern Finland (see Pernu 1979, Table 2). The EM conductivity field survey, and resistivity log data indicate resistivity less than 20 ohm-m (Fig. 54), and ε_{silt} ranges from 32 to 43. The vertical resistivity variations (in the range from 1 to 10 ohm-m) are interpreted to indicate seasonal salinity variations in the Littorina Sea. Due to effective signal attenuation in the Littorina silt GPR shows only the (c.f. = 80 MHz) near-surface ($d < 1$ m) reflections. Instead, esker deposits are good targets for GPR due to low conductivity, but in the Oulunsalo test area some parts of esker ridges are buried beneath marine silt layer and are not detectable well by GPR. In those sites EM 31 conductivity surveys are capable to locate the esker sands and gravel deposits by resistivity anomalies, one example is presented in Figure 55.

The ratio-image of gamma radiation and EM quadrature component data (Fig. 56) clearly indicate the above features as surface moisture variations and as conductivity changes. The surface depressions and small basins are wet as a result from silt/ clay lining and a moss vegetation. Those are classified by the light grey code. Water is coded as white. Dry sand is coded as black, intermediate codes refer to fine sand. The field dielectric data were compared to the smoothed airborne gamma radiation data (Fig. 58), indicates that water and peat are gaining highest dielectric and lowest K-equivalent values. Unsaturated sand shows an opposite trend. The correlation between the airborne and field data is fairly good, even if the data were obtained in different years and the weather conditions are suspected to have been different.

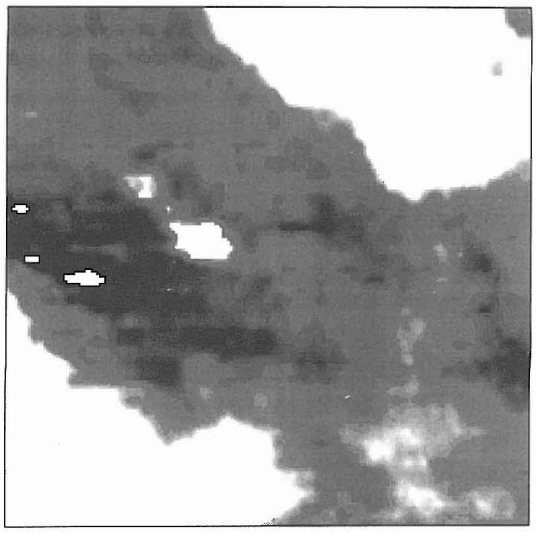

Fig. 56. The Im/K ratioimage from Oulunsalo (10 × 10 km) area, northern Finland. Sand as black coded. Adopted from Hyvönen et al. (1991).

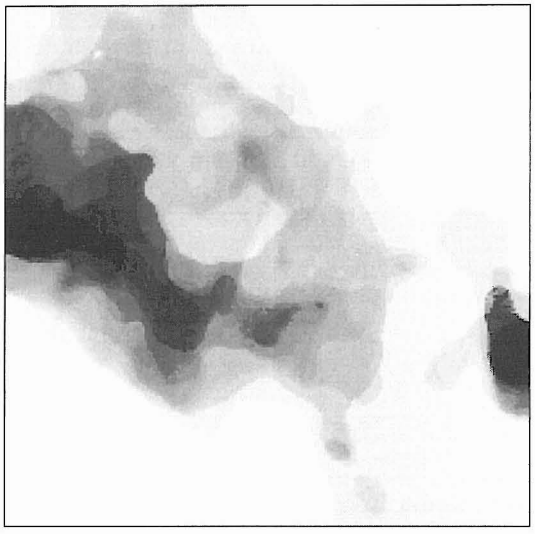

Fig. 57. The maximum radar TWT/ dielectrics ratioimage (sand/gravel coded as black) from Oulunsalo (10 × 10 km) area. Adopted from Hyvönen et al. (1991).

GPR profile data (about 130 km) and TDR dielectric data were used to verify the Im/ K ratio raw materials anomalies. Maximum twt (two way time) radar travel time and dielectric proper-

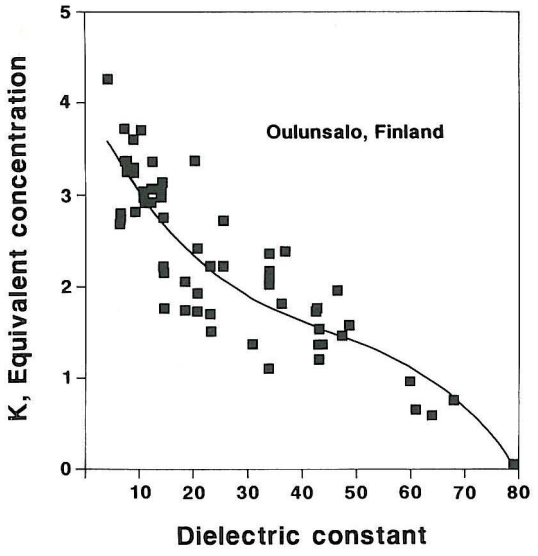

Fig. 58. A relationship between *in situ* dielectric properties (TDR recorded in 1990) and smoothed airborne K-equivalent concentration (flight in 1980) from Oulunsalo area.

ties were utilized. Long delay times were typical for thick unsaturated sands (ε_{sand} = 6 — 7, σ = 0.0001 S/m) and saturated sand deposits, but those sediments could be separated based on dielectric data (253 waveforms recorded). Short delay times were typical for marine deposits (ε_{silt} = 32 — 43, σ = 0.5 S/m). In the ratio-image of maximum twt / ε glaciofluvial sand and gravel reserves are shown (Fig. 57) consistently with the Im / K ratio-image. All the sand and gravel pits are located in the areas indicated by the both ratio-images.

The airborne electromagnetic data, normally used for the exploration purposes, is capable of detecting conductive silts / clays in sufficient large volumes, and therefore can be used in the outlining the conductive areas not feasible for radar surveys. The Oulunsalo experiment data show that the airborne Im/K ratio is feasible for detecting sand and gravel potentials, and silt / clay deposits in the areas of significant thickness of unconsolidated materials.

Digital API of Glacier Bay till

Rapid retreat of the terminus of Burroughs Glacier and the glacial processes in Glacier Bay, southeastern Alaska (Fig. 1) are well documented (Reid 1896, Taylor 1962, Mickelson 1971, 1986, Goldthwait 1986). Land uplift in Glacier Bay, resulted from tectonic processes and postglacial rebound is recorded as much as 4 cm/yr (Barnes 1990). Therefore earthquakes are common, and the precise seismic monitoring started in 1978 by the Geological Survey of Canada, B.C. (Horner 1990).

This section describes the textural and electrical characteristics Glacier Bay till. Also till slides near the SE-margin of the Burroughs Glacier are desribed and attribution to the seismic activity is discussed. The till slide morphology and the

Fig. 59. Streamlined features (drumlins) in the north side of the West Arm, Glacier Bay, Alaska. Photo R. Sutinen 1988.

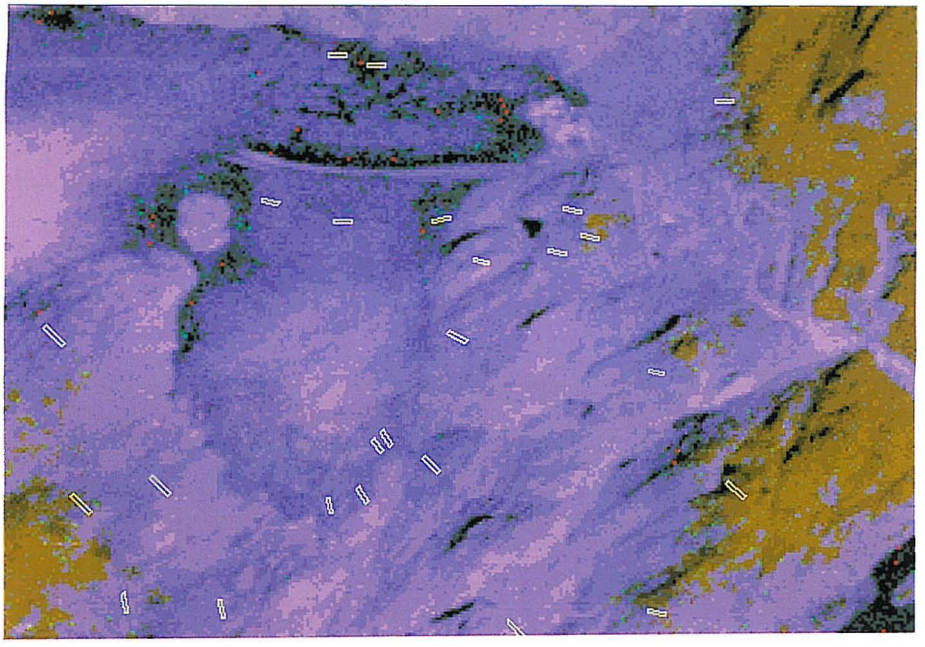

Fig. 60. A digitally processed portion of the high-altitude colorIR-AP Jul. 1979 from the SE-end of the Burrougs Glacier, SE Alaska. The blue color coding indicates ice-cover approximately in 1940 and green coding the ice-free terrain and nunataks. Crag-and-tail forms plotted based on the data presented by Mickelson (1971) and this study.

water content variations on the till surface were studied. Air photos and digital image processing was used to determine the deglaciation time frame, particularly between 1979 and 1988. High altitude color IR stereo photos from 1979 were available from the area as well as oblique B/W APs from 1961, 1963, 1964, 1969. Oblique B/W low altitude APs, Sept. 12, 1986 and Aug. 24, 1987, were purchased. Color oblique photos were taken in Aug. 25, 1987 and Sept 18. 1988 during the field surveys, Aug. 19 — 24, 1987 and Sept. 12 — 18, 1988.

Drumlins in the Glacier Bay area (Fig. 59) have formed during the Neoglacial time period and those have consistent orientation from west to east near Burroughs Glacier and Washusett Inlet (Goldthwait 1986). Drumlins in the area are only blanketed by thin Glacier Bay till. The cores compose of gravel and sand deposited prior to the drumlin shaping (Goldthwait 1974). Although the ice flow in the southeastern end of the Burroughs Glacier since 1960 has been very slow, about 1 m / yr (Taylor 1962), it has been still active enough to create crag-and-tail forms (Mickelson, 1971) on the drumlins. Crag-and-tails, typically 0.25 m high and 2 m long, but extend up to 1 m high and 15 m long, are plotted on the digitally classified colorIR-AP from 1979 (Fig. 60). The classification, depicting the ice-cover in late 1930's and early 1940's (compared to the APs), is based on the variations of the vegetation (alder) cover. The oldest alder canopy has been developed on the tops former nunataks emerged first from beneath the ice. It is clear that crack-and-tail forms are deposited after drumlinization, because the orientation is significantly different from the trend of the drumlins. Since the deposition rate of the Glacier Bay till has been

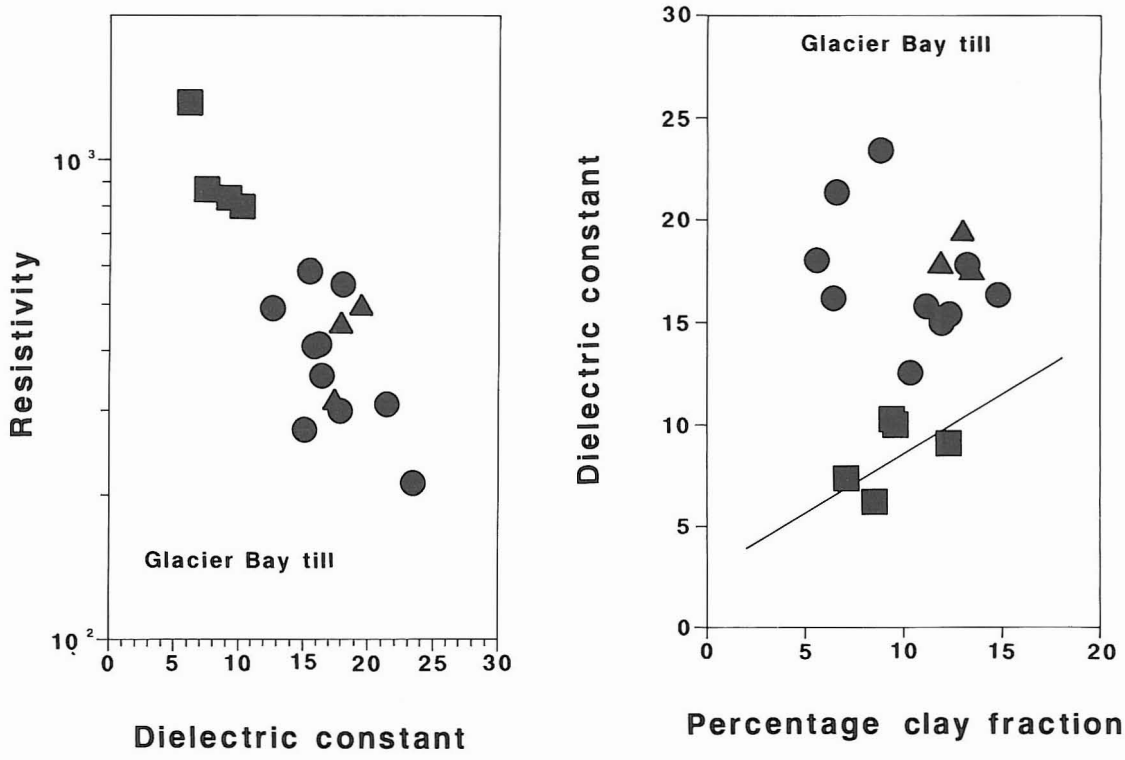

Fig. 61. The electrical properties of the Glacier Bay till. Triangles = till beneath the ice; dots = till 2-3 years after and squares = till 8—18 years after emerged from beneath the ice. Best fit of dielectric sonstant vs. clay content for glacial deposits from Wisconsin also shown.

approximately 2.5 cm/ yr (Mickelson 1971), and the typical till thickness in the area averages 1 to 2 meters that would accumulate in less than 100 years, only a few tens of years is required for the accumulation of the crack-and-tails. The above example shows that topographically controlled near-marginal ice-flow might be very different from the trend of the drumlin-facies ice-flow, and therefore must consider in terms of boulder tracing in high-relief terrain (see Fig. 82).

The Glacier bay till is typically sandy. Sand percentages range from 32 to 81, silt from 16 to 62, and clay from 3 to 15 percent, with a mean of 57 percent sand, 36 percent silt, and 7 percent clay (Mickelson 1971). The data collected here shows averages (18 samples) of sand 60 %, silt 30 and clay 10 %. The electrical properties (Fig. 61) of the till show significant variations depending on the time, when the till has been emerged from beneath the ice. Higher resistivity (800 — 1200 ohm-m; sample based DC-determination) and low dielectrics (ε_{till} = 6 — 10; *in situ* TDR determination) are typical for till 8 — 18 years after the retreat of the ice (ice-margin positions based on APs and the data by Mickelson 1971). As compared to the Wisconsinan deposits (the best fit of ε_r vs. clay content from Fig. 26), the 8 — 18 years old till seems to be stabilized and do not contain excess of water. The till, less than two years after been exposed, seems to be unstabilized and shows an opposite trend within the electrical properties: resistivity ranges from 200 to 600 ohm-m and dielectrics from 12 to 24, respectively. Also the »fresh» till beneath the ice show correlative properties. Since the electrical properties are strongly dependent on the

A

B

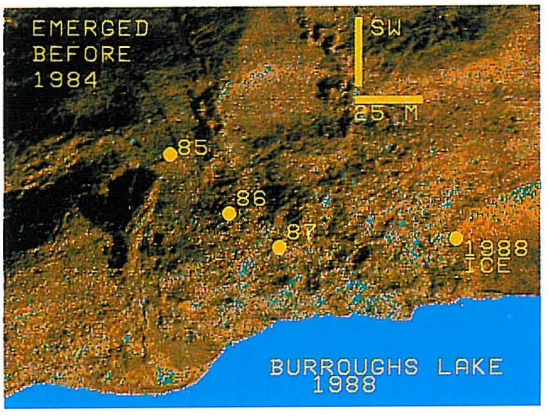

C

Fig. 62. A seismics-induced landslide near the margin of Burroughs Glacier Alaska. (A) overview of the SE end of the glacier, (B) close-up of the slide scar and (C) digitally classified AP showing oversaturated till near the ice margin.

water content (Figs. 24, 40 and 48) the unstabilized till contains 2 to 3 times more water compared to the stabilized till, 8 — 18 years after retreat of the ice margin. The result suggests that the oversaturated till is susceptible for sliding triggered either by rainfall or earthquake. The till beneath the ice (when unfrozen) is presumably mobile enough to squeeze and even flow subglacially and create ridges and hummocks into the shape of the base of the ice.

Three types of slides are met near the Burroughs Glacier. Gullies, subparallel V-shaped erosion forms, and normally less than 1.5 m deep (Mickelson 1971) are common on steep slopes (25 — 35°). Those are created shortly after the ice retreat and maintained by rainwater runoff. Ice-marginal mudflows along the margin of Burroughs Glacier are created annually and have been observed to be triggered by rainstorms. For example, between the night of August 13 and the morning of Aug. 15, 1969, 36 mm of rain fell (Mickelson 1971).

Rotational till slides scars are observed in several localities, one of the most significant between Nunatak B (Mickelson, 1971) and the Burroughs Lake (Fig. 62A). The shape of this slide scar resembles that of small amphitheater (Fig. 62B). The size of the scar is 20 by 25 meters, and the back wall is four meters high. It has been occurred near the ice margin, between Jun 16. 1986 (the INQUA excursion; see Goldthwait 1986) and Aug. 19, 1987 based on the field observations. The slide presumably occurred abruptly. The slow-motion creep is denied, because the till on the walls of the scar has a fabric with an azimuth of 310° parallelling to the striation 15 meters upslope. The electrical characteristics indicated that till less than two years after being exposed is still

strongly oversaturated. That feature can be clearly seen on the digitally classified image (Fig. 62C) created from the low-altitude low-angle AP. The till surface being emerged before 1984 is stabilized and does not show excess of water. Instead, the till surface emerged between 1986 and 1988 is clearly oversaturated. Consequently, the till surface at the site of the slide scar was with high water content at the time the slide occurred. Because the till was strongly oversaturated, a seismic shock or heavy rainfall (or both) triggered the slide. Unfortunately, relevant precipitation data lacks, but 8 km northeast from the slide an earthquake of magnitude of 3.6 were recorded on Aug. 8, 1987. In the area also other major rotational landslides may be also seismic-induced. Based on the APs and field observations the landslide scars on the SE side of the Burroughs Glacier must have occurred after 1980, because the site was ice-covered in 1979. An earthquake of magnitude of 4.4 was recorded in the area on Jun. 22, 1981. Even if strong evidence of the rain-induced landslides have been presented from the Yukon territory and British Columbia (Evans & Clague 1989), the slides near the Burroughs Glacier are suggested to be seismic-induced.

GLACIAL LANDFORMS

Geomorphology and genesis has been used as criteria in mapping and classification of glacial landforms, and two broad categories have been proposed, 1) direct glacial landforms and 2) indirect glacially induced landforms (Goldthwait 1989). Subglacial morainic landforms are oriented either parallel to ice flow, like drumlins, drumloids and flutes or transverse to the ice flow, like Rogen moraines (Lundqvist 1989), also called as ribbed moraines (Bouchard 1980, 1989). Rogen moraines have been suggested to grade laterally into drumlins and flutings (Aario 1977, Lundqvist 1989), and no sharp definitions can be applied to parallelly oriented landforms, although the ice flow direction could be precisely determined by the landscape streamlining. Ice-marginal forms, such as end moraines (Figs. 89, 92 — 94, 103) have been classified as direct glacial landforms.

Morphogenetic classification of glaciofluvial landforms is based on the relation of the landform to the former glacier ice margin. Woodworth (1899) classified water-laid drift into intraglacial and extraglacial groups; eskers and kames belong to the first group, and outwash deposits, fans, terraces and lacustrine/marine deposits to the other. Lundqvist (1979) grouped glaciofluvial deposits into 1) inframarginal (formed behind ice margin), 2) marginal (formed at the ice margin) and 3) extramarginal or proglacial (formed outside ice margin). Basically the same type of classification is presented in the final INQUA report (Goldthwait 1989).

Below, morphological features, internal structures and composition of drumlins, Rogen moraines and associated subglacial bedforms as well as eskers (glaciofluvial sheetwash and tunnel deposits) has been described. Since end moraines are specifically related to the glacial stratigraphy those are described in detail in the chapter: Glacial stratigraphy in North Finland.

Weak glacial erosion — preglacial weathering

Erosional features, such as striations, roché moutonnees, large scale crescentic troughs, U-valleys and depositional features like drumlins, Rogen moraines and related subglacial landforms

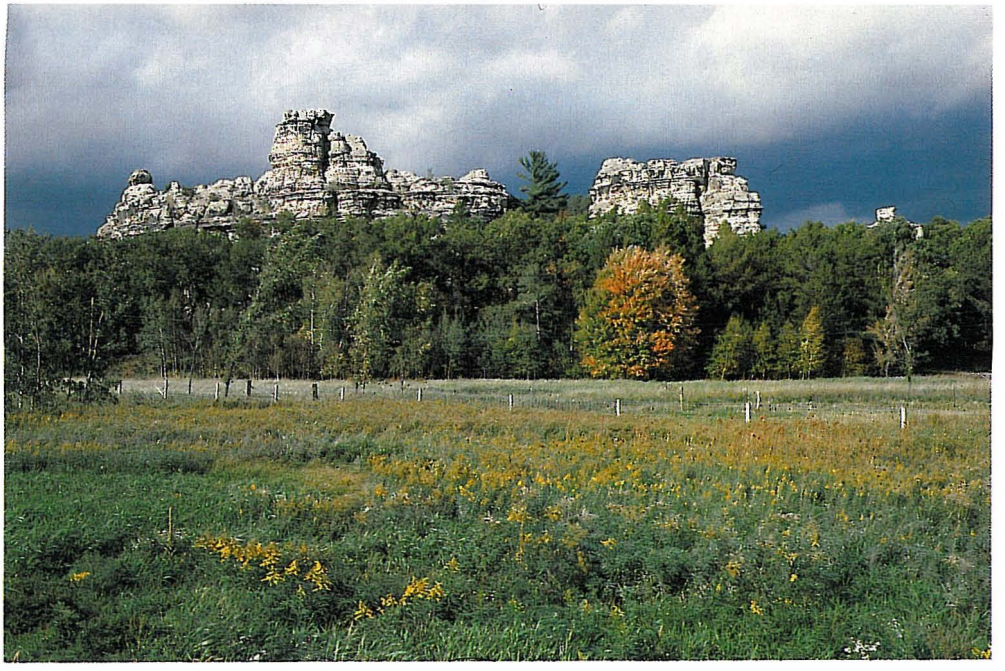

Fig. 63. Sandstone pinnacles along the interstate highway I-94 between Wisconsin Dells and Eau Claire. Pinnacles are typical to so called driftless area (see Fig. 2) where no evidence of glacial advance is met. Proglacial lake sediments are surrounding the pinnacles. Photo R. Sutinen, 1988.

Fig. 64. An exposure of grussificated granitoid rock superimposed by the Late Weichselian sandy till near the Vuotso airfield, Finnish Lapland. Finnish base map co-ordinates x = 7555 82; y = 505 60. Photo R. Sutinen, 1985.

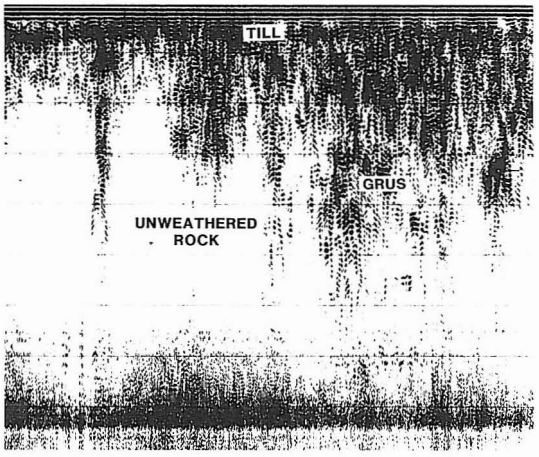

Fig. 65. A 150 m long portion of the radar (c.f. = 120 MHz, max. twt = 460 ns) record cross one of the grussificated fracture zones at the Vuotso airfield.

display evidence of strong glacial erosion and accumulation. Due to glacial quarrying, plucking and abrasion preglacial landscape has been smoothened, and preglacial weathered bedrock features seldom are preserved. Pinnacle shaped rock formations (Fig. 63) are common in unglaciated terrains (see Fig. 2), but seldom met in the glaciated terrains.

The tor features (built up from the Nattanen granite), somewhat similar to sandstone pinnacles in Wisconsin, appear on the tops of the fells (mountains) around Vuotso, Central Lapland. Because the Vuotso area has been consecutively glaciated, the age of the tors is problematic; those are either result from preglacial weathering processes (preferred here) or those are of postglacial origin. Except the tors, also weathered bedrock (Fig. 64) is common in the area (Hyyppä 1983). Instead, the lack of active-ice landforms (streamlining) indicate low glacial erosion and accumulation rate. The top of the granite / granite gneiss rock in Vuotso is weathered by grussification (Isherwood & Street 1976, Mutanen 1979), which is caused by the expansion of biotite that converts coherent rock into loose grains. The gruss, generally a few meters thick (Sutinen 1985b), is soft like sand and is easy to spade. It is overlain by the Late Weichselian sandy till, composing of local lithologies, still some non-local amfibolite clasts. The bulk density of the solid rock varies between 2.5 and 2.7 g/cm^3, of grus between 1.6 and 2.0 g/cm^3 and of till between 1.4 and 1.8 g/cm^3 (Hyyppä 1983).

Grussification has been intruded along the rock fractures and joints, extending down to tens of meters. One of the grussificated fractures was outlined by GPR (c.f. = 120 MHz, max. twt = 460 ns) at the Vuotso airfield. The zone, 20 to 200 meters wide, is trending NW-SE. Several GPR profiles were carried out across the zone and one example is presented in Figure 65. The 1.0 to 4.5 m thick till ($\varepsilon_{till} \approx 7.8$, determined by TDR from the section shown in Fig. 64; $\sigma \approx 0.12$ mS/m, based on conductivity logs; the clay content 3.5 %, silt 16.5 % and sand 80 %) is displayed by intensive, dark-toned and partially overlapping ($\lambda = 0.94$ m) refections on the top of the graph. The grussification ($\varepsilon = 5.3$; $\sigma = 0.17$ mS/m; clay fraction content 2 — 4 %) intrusions are displayed clearly. The lower boundary of the grus, however, is not sharp, and the reflection intensities are fainting downward. According to the DC resistivity and seismic refraction soundings the grussificated zone have a maximum thickness of about 20 meters. The experiment shows that due to relatively low dielectrics and conductivity, the till could be easily penetrated by radar and detect the lower boundary of the grussificated rock.

The only evidence of glacial activity at the site is the low-density sandy till. The till is practically lacking on the tops of the fells suggesting that the ice flow and deposition of till has been occurred only in the valleys. The area has been ice-covered during the Late Weichselian and presumably during the Early Weichselian (see Figs. 107 — 108). The nearest locality of multiple till sequence (stratigraphic units till II and till III; Hirvas et al. 1977) is 15 km southwest from Vuotso. The lack of surface streamlining suggests weak basal erosion during the Weichselian, and the tors and grussification in the Vuotso area might be pre-Weichselian.

Strong glacial erosion/ accumulation — drumlins

Drumlins in Wisconsin, particularly in the southeastern part of the state (Waukesha drumlin field; Whittecar & Mickelson 1979) are of high economic significance due to extensive volumes of exploitable gravel in their cores. Drumlins in northern Finland, however, are predominantly built up of sandy tills (Aario et al. 1974, Aario & Pernu 1990), and therefore have minor economic significance. Drumlins display similar morphological characteristics: elongated and inverted spoon-shaped ridges, throughout the glaciated terrains. They always appear in diverging fields (down ice) heading towards the end moraines and/or interlobate moraines (Upham 1896, Alden 1918, Aario & Forsström 1979, Boulton 1987, Piotrowski & Smalley 1987, Attig et al. 1989, Figs. 2 and 89 in this paper). Length of the drumlin fields are ranging from tens of kilometers to more than 200 km (Aario & Forsström 1979, Punkari 1985). Because of the morphogical conformity, the drumlin shaping presumably has been resulted from the same mechanisms from one area to another.

However, high spatial variability of materials in drumlins has generated argumentation of mechanisms and formation of drumlins, and there is no consensus about their genesis. Basically two categories of mechanisms, erosional and depositional, in drumlin shaping have been suggested. Direct erosion by glacier ice (Whitte-

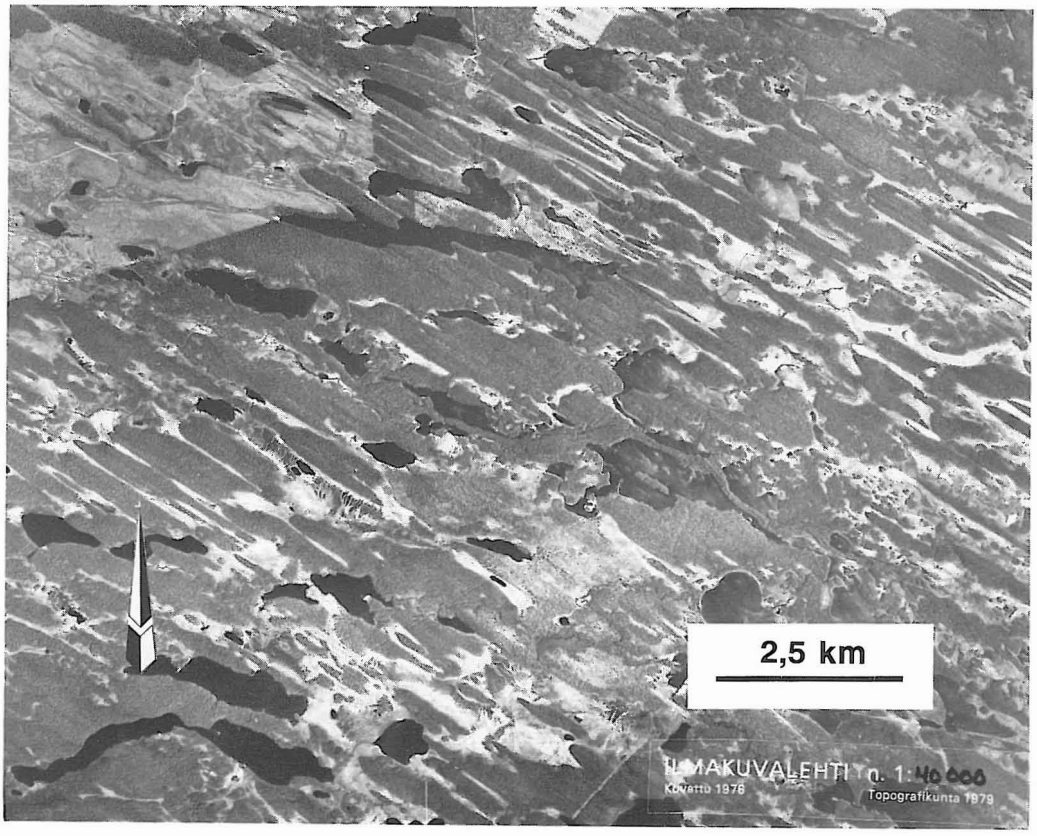

Fig. 66. A portion of the AP 7609/28 showing the W—E trending drumlins superimposed by the NW—SE trending Late Weichselian drumlins in Kuusamo, Finland. AP by permission of Topografikunta (The Army Map Service).

car & Mickelson 1979) and erosion by subglacial meltwater (Shaw & Kvill 1984) or by large-scale catastrophic subglacial floods (Shaw et al. 1989) have been proposed. Depositional characteristics are considered due to subglacial lodgement (Boulton 1982) or melt-out of subglacial debris (Shaw 1980) or subglacial deformation (Smalley & Unvin 1968, Evenson 1971, Boulton 1982, 1989) or glaciofluvial infilling of subglacial cavities (Shaw 1983, Dardis & McCabe 1983, Hanvey 1989, Shaw et al. 1989). Erosion or deposition or combination of those mechanisms has been suggested by Aario (1987).

Drumlin morphology

Streamlined morainic landforms were mapped in northern Finland by the author for the Nordkalottproject (1986b and 1986c) down to 66° N lat. For this thesis those features were mapped further south, down to about 65° N lat. (Fig. 3). The large-scale streamlined features, called rock-drumlins or drumlinoids, are generally several kilometers long and bedrock is often exposed at the proximal sides and steeper stoss slope points up-ice.

The large-scale features are partially eroded and superimposed by the younger drumlins, drumloids and flutes (Figs. 66 — 67). Their origin suggests pre-Late Weichselian based on the till stratigraphy and buried organic deposits (Nordkalottproject 1986b, Lagerbäck 1988, Lagerbäck & Robertsson 1988). The large-scale forms, located in the south-southeastern part of the study area, are trending roughly west-east and are slightly fanning out in the east (Fig. 66). This

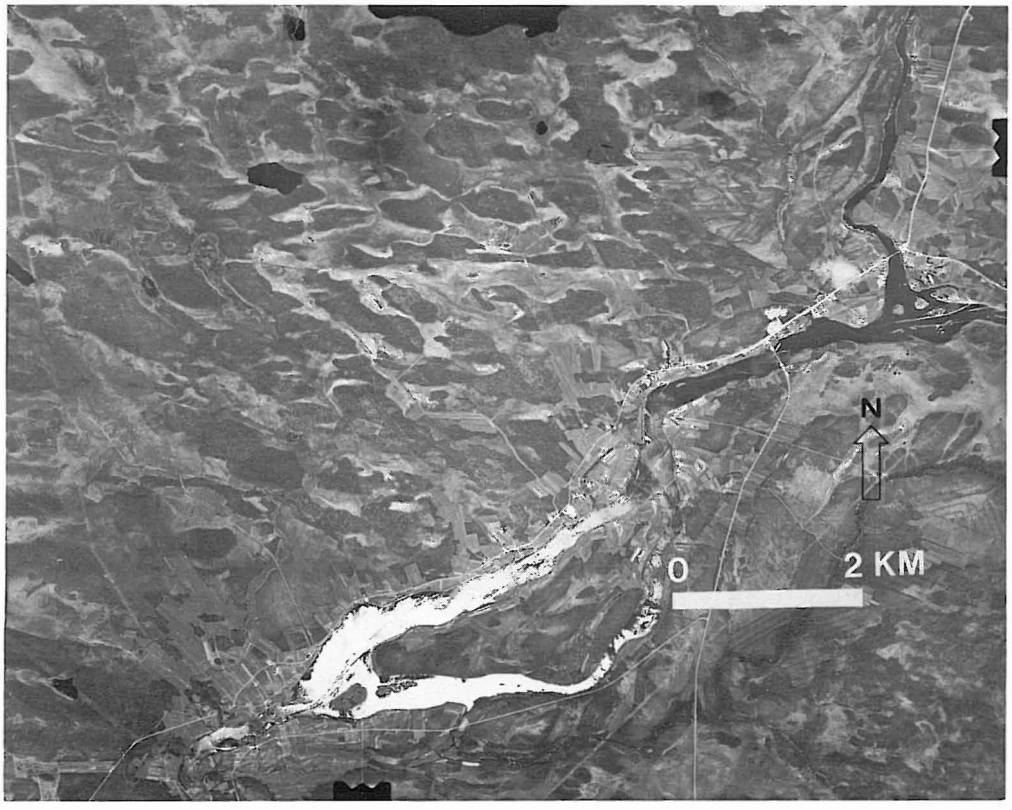

Fig. 67. A portion of the AP 6331/137 showing NW—SE trending Early Weichselian drumlins superimposed by the W—E trending streamlining near Oulu, Finland. AP by permission of Topografikunta.

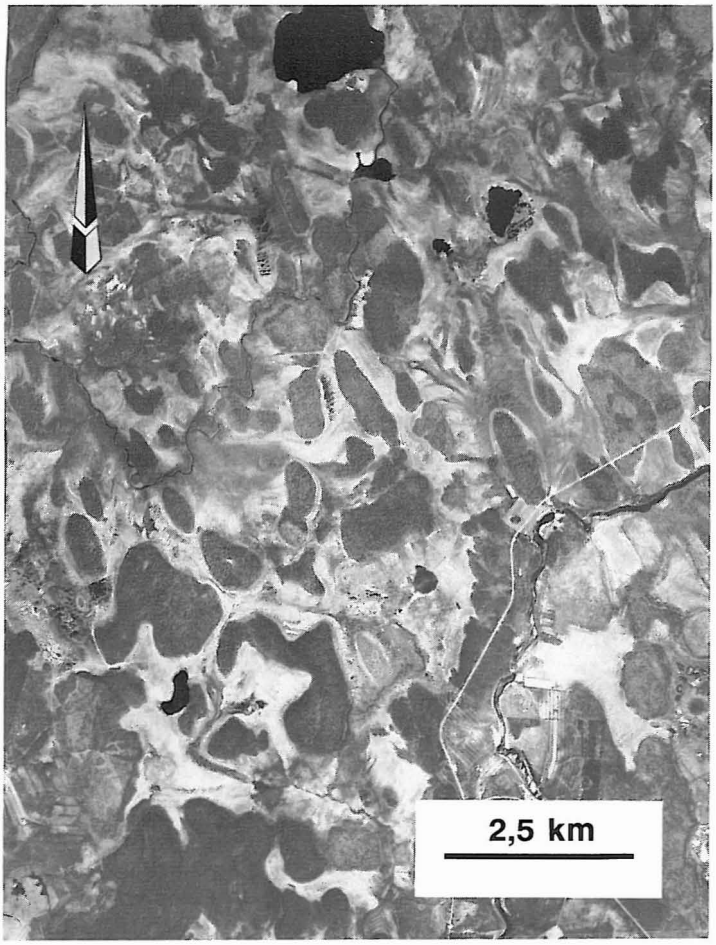

Fig. 68. A portion of the AP 7608/211 showing the Early Weichselian drumlins near Ranua, Finland. AP by permission of Topografikunta.

pattern is strongly reworked and superimposed by the spectacular Kuusamo drumlin field (Aario et al. 1974), which is bounded by the end moraine near the lake Pyaozero (Pääjärvi) in Soviet Karelia (Aario & Forsström 1979, Punkari 1985).

The other large-scale streamlined features in northern Finland are generally trending NW-SE (Nordkalottproject 1986b) fanning out in the southeast and south. Near Ranua (see Fig. 89) these features have practically no morphological signs of the younger (Late Weichselian) glacial activity (Fig. 68), whereas in Yli-Ii, near Pudasjärvi, a younger streamlining is strongly visible (Fig. 67). These large-scale forms disappear down at 65° N lat. and no more such forms could be found further south suggesting termination of the drumlinization in a similar way as Late Wisconsinan Green Bay lobe drumlin field in Wisconsin (Fig. 2).

Utsjoki drumlin field in northermost Finnish Lapland (Nordkalottproject 1986b, 1986c) is fanning out in the north and northeast and is bounded by the Tromsö-Lyngen End Moraine in Norway (11,000 — 10,000 B.P. yr., Marthinussen 1961). Tromsö-Lyngen is correlative with the Salpausselkä-Middle-Swedish-Ra moraines in south-

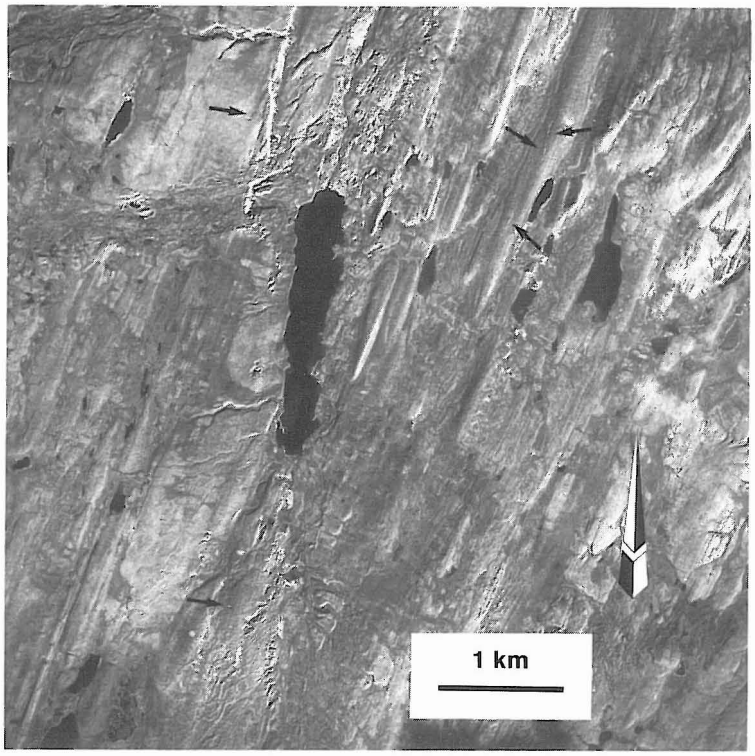

Fig. 69. An AP 61182/176 showing a portion of Utsjoki drumlin field, Finnish Lapland. Note the kettle holes on the drumlins. AP by permission of Topografikunta.

ern Fennoscandia. The Utsjoki drumlin field presumably is created at the same time with the Kuusamo drumlin field in eastern Finland. Drumlins in Puolbmakkeäsjavri (javri = lake) area (Fig. 69, a portion of AP 61182 / 176)) are varying in length from 600 m to 3.5 km and L/W ranges from 1 : 7 to 1 : 11. Those drumlins exhibit numerous kettle holes on their surfaces. Kettle holes, common features on glaciofluvial landforms, are arranged in the lines along the crests of the drumlins. It is very likely that iceblocks were buried in the cores of the drumlins at the time of the streamlining. After the drumlin shaping the iceblocks melted and kettles were formed. Kettles indicate that the drumlins are built up, at least partially, of glaciofluvial deposits or flow sediments. Stratified materials were verified by GPR on the drumlins, but those are absent in the valleys between the drumlins. In this case deposition is regarded to be more probable shaping factor than erosion, either by water (Shaw 1983, Shaw & Kwill 1983, Shaw et al. 1989) or glacier.

Drumlins sometimes appear in narrow valleys. An example of an extremely narrow, only 3 — 5 drumlins wide, and 10 km long drumlin field is presented (Fig. 70; APs 61186/236 and 61196/279) from Pajib Haltejavri (lake) area. This narrow field is in the valley, topographically isolated by the fells (mountains) on both sides. Evidently the fell topography has been controlled the orientation of the ice flow during the drumlin shaping. The catastrophic flood theory is argued here, because if large volumes of water had eroded drumlins, one would expect also significant large areas of bedrock exposed. Glaciofluvial erosion channels are present, though, but those are related to the sheetwash esker generation after the drumlin shaping.

Fig. 70. An AP-mosaic showing very narrow drumlin field in Utsjoki, Finnish Lapland. Note the Pulju moraines and attributed small esker ridges pointed by the N-arrow. APs 61186/297 and 61186/236 by permission of Topografikunta.

Composition of drumlins

The structures of drumlins in Livonniska, Posio in northern Finland was studied by using the ground-penetrating radar with an antenna center frequency of 80 MHz. GPR traverses were done at 50 m intervals across the drumlins and 3D-plots of structures were created. Continuous drill core samples were taken for textural analysis, and for the determination of electrical conductivity. Due to relatively low conductivity and dielectric properties of the materials, radar penetration extended to a depth of 10 — 15 m, where the bedrock surface was encountered.

It is found that some of the drumlins are composed of two different till units, but some of them

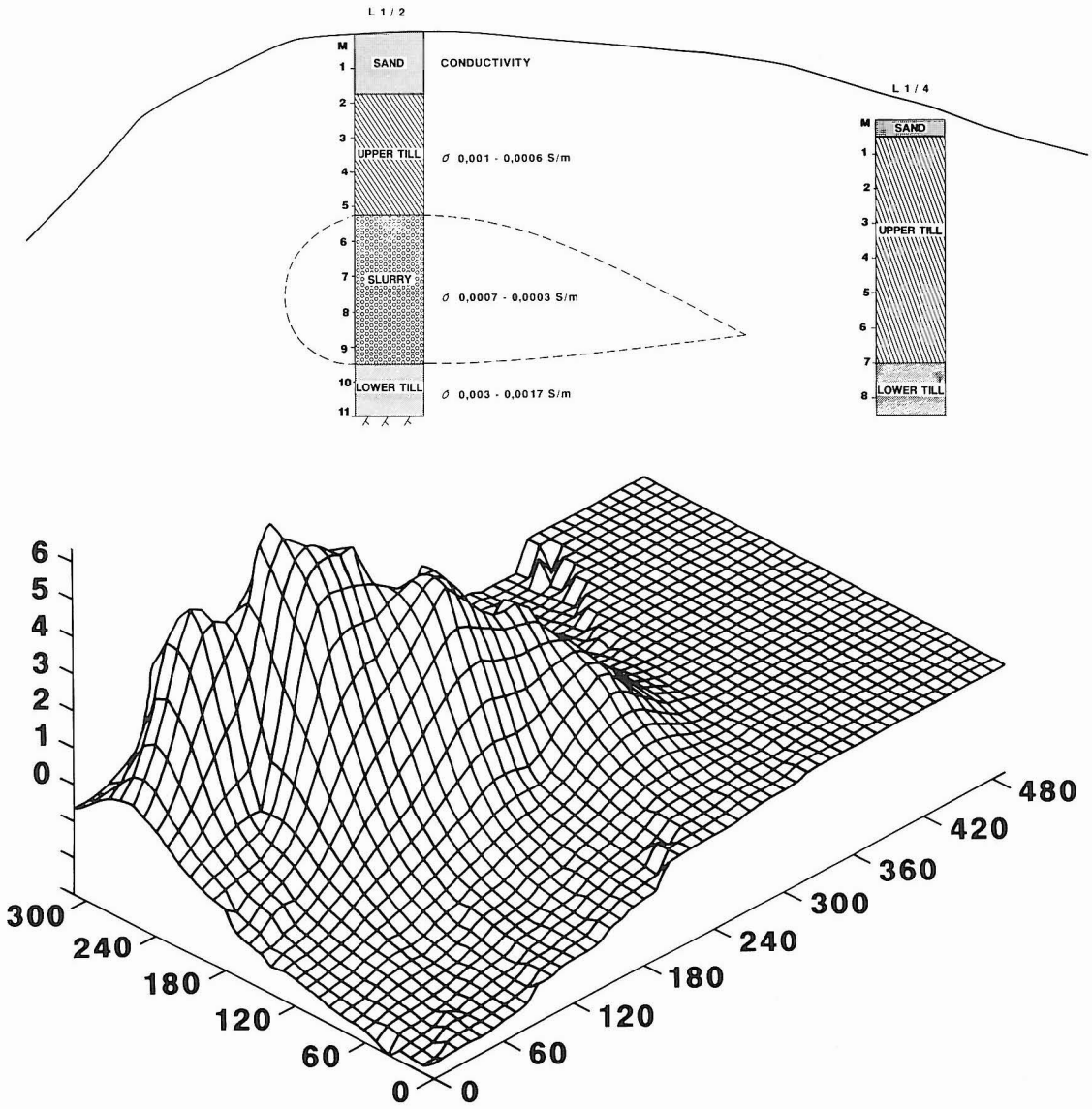

Fig. 71. An example of the stratigraphy of one of the drumlins near Posio, Finland. Lower till is correlative to the Early Weichselian, upper till to the Late Weichselian. The thickness of the sandy slurry diamicton in the core is presented by the 3-D plot based on the GPR (c.f. = 80 MHz) records.

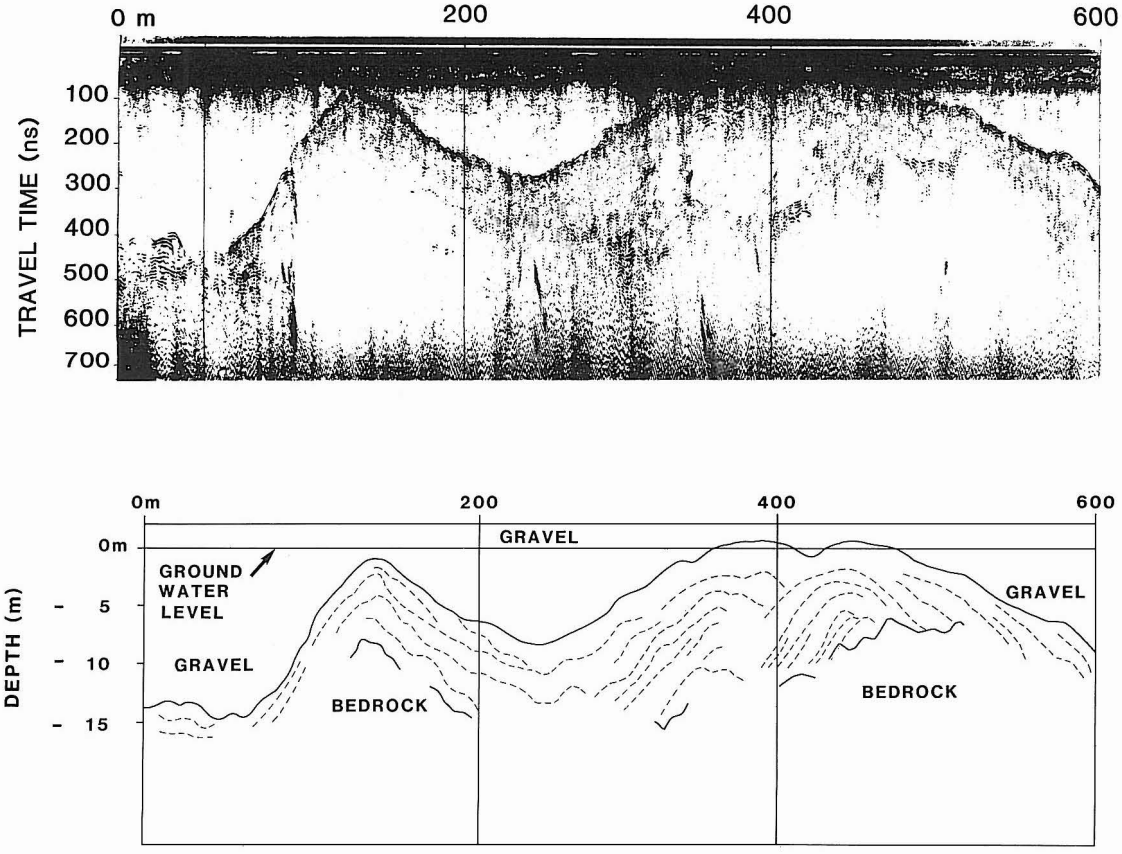

Fig. 72. Radar (c.f. = 80 MHz) profile across two drumlin ridges (below GWL) near Posio, north Finland. The onion-shaped structures (radar resolution $\lambda = 0.75$ m; $\varepsilon_r = 25$ for saturated diamicton) indicate glacial deposition, away from the observer. Bedrock topography controls partially the forms of drumlins, superimposed by glaciofluvial gravel ($\varepsilon_r = 4$; $\varepsilon_r = 16$ saturated). Antenna pulled by car (10 km/h) on a logging road.

show interlayered sandy diamictons and sand between the tills (Fig. 71). The cross-sectional radar profiles of some of the drumlins depict onion-type structures, one of the transect is shown in Figure 72. The electrical conductivity of the grey lower till (see Fig. 71) in the cores of the drumlins were found to be $0.003 < \sigma < 0.0017$ S/m (saturated). This till is discontinuously superimposed by several meters thick lenses of mixed glaciofluvial and flow sediments with $0.0007 < \sigma < 0.0003$ S/m (saturated). The drumlins are mantled by grey-brown till with $0.001 < \sigma < 0.0006$ S/m (saturated). Although there is no age control, the conductivity differences and the stratigraphic position suggest that the lower till represents an older (Early Weichselian) ice advance and it therefore represents an erosional part of the drumlin. Sandy diamicton and interbedded with sands are presumably deposited subglacially by (squeezed) slurry flows and deformed by active ice (Late Weichselian), which also deposited the upper till during the final shaping of the drumlins.

Altough the size and volume of drumlins tend to increase toward the end moraines, those are lacking in the narrow zone near the end moraines (Attig et al. 1989, Fig. 2). In Wisconsin, the Madison drumlin field (Upham, 1896) is bound-

Fig. 73. A longitudinal section of the Door Creek drumlin near Madison, Wisconsin. Note the weathered Cambrian sandstone blocks draped by the silty Door Creek till. Photo R. Sutinen, 1988.

ed by the Johnstown moraine on the west and south and by the Kettle Interlobate Moraine on the east. The Door Creek drumlin (Mickelson & Sutinen 1989, Sutinen 1989), 6 — 8 meters high, displays evidence of two generations of litho- and chronostratigraphic units (Fig. 73). The top 2 — 4 meters are composed of sandy till of Horicon Formation (HFT) (according to the Pleistocene stratigraphic units in Mickelson et al. 1984). The color of the HFT changes from brown to red as resulted from color variations in the source rock, Cambrian sandstone. The brown and red till units were discontinuously separated by sand lences. HFT is superimposing sand and gravel outwash deposits, the foresets indicating paleoflow from the east. The pit was dug to exploit this outwash unit. The lowermost part of the drumlin is composed of silty till deposited on Cambrian sandstone. Because no other observations of the fine-grained till have been made below FHT in this area, the silty till is called here as the Door Creek till (DCT) according to the type locality.

The two till units in the drumlin show significantly different electrical properties (Fig. 74, see also Figs. 29, 34, 38), and therefore those likely are deposited during different ice flow stages/phases. The sandy HF till unit is deposited by the Late Wisconsinan Green Bay lobe (Mickelson et al. 1984) and has correlative electrical properties with the same lithostratigraphic unit at the top of the Westport end moraine, west side of Madison (see Fig. 49). The surface of the Door Creek till provide evidence of the earlier ice flow based on the radar (c.f = 500 MHz; max. twt 70 ns) records. The GPR survey was conducted by handpulling the antenna on the top of the pit, and a grid of six 19-meters long profiles, one meter apart, was created. Figure 75A shows one of the transects. The strongest reflections (R = -0.33; ε_{gravel} = 5, ε_{DCT} = 20) on the profile are resulted from the top of the DCT, and the depth of this reflection interface was determined from each profile and plotted as 3-D (Fig. 75B). The DCT surface is not even, but displays a form of

crag-and-tail feature. A sandstone block on the proximal end indicates the ice flow from east-northeast.

The Door Creek drumlin sequence evidently shows an older core of silty Door Creek till incorporated with Cambrian sandstone blocks. The outwash gravel is suggested to be deposited in front of the retreating ice margin. Although there is no age control of the Door Creek till, its stratigraphic position suggests at least pre-Late Wisconsinan. Since the electrical properties are quite similar to those of Brooklyn till (Figs. 2 and 47) outside Johnstown Moraine, the maximum of the Late Wisconsinan Glaciation, Door Creek till is correlated with the Brooklyn till. Bleuer (1971) assigned the tills west of the Rock River (located east of Brooklyn site) to the Illinoian Stage, and recently Curry (1989) concluded that Altonian Glaciation did not reach Illoinois. Therefore Brooklyn and Door Creek tills might represent Illinoian, and consequently the Altonian ice margin position is north from these sites. Assuming that the global climate changes controlled the Laurentide and Scandinavian ice sheets in a similar way, the stratigraphy suggested above resembles that of northern Finland (Sutinen 1984, Figs. 107 — 108), where the Early Weichselian ice advance did not extend as far as the Late Weich-

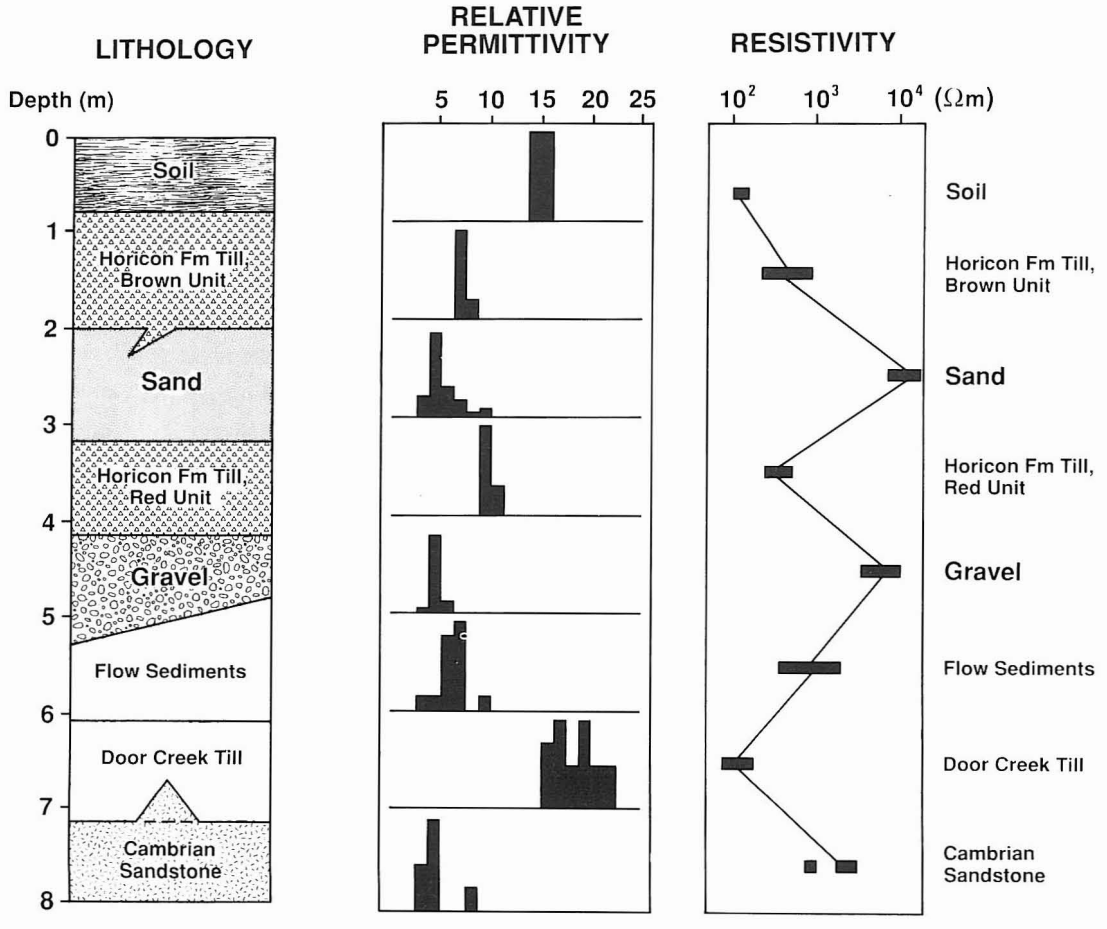

Fig. 74. The electrical properties of the sediments in the Door Creek Drumlin measured from the exposure shown in Fig. 73.

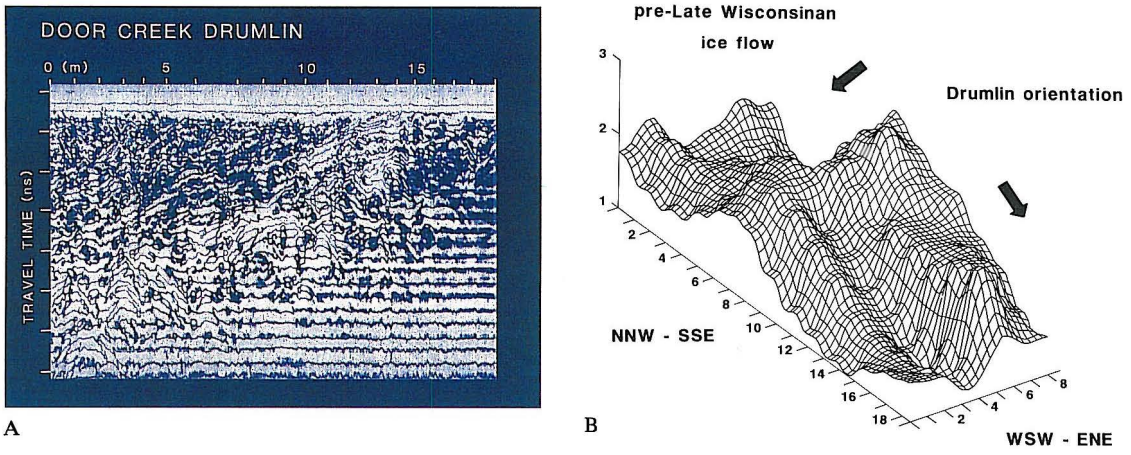

Fig. 75. An example of radar (c.f. = 500 MHz) profile (A) showing the Door Creek till superimposed by the outwash deposits. A 3-D plot (B) showing the surface topography of the Door Creek till based on the GPR data.

selian.

The DCT and the outwash deposits were eroded on both sides of the drumlin during the Late Wisconsinan ice advance, but were preserved in the core of the drumlin. The Horicon formation till draped the drumlin by the Green Bay Lobe Ice and the drumlin got its shape seen today. The ice becan to retreat from the Johnstown moraine about 12,500 B.P. yr (Maher 1981).

The examples presented above indicate that drumlins are subglacially eroded and deposited landforms, and reveal stratigraphic units from different glaciations. In Finland, contrary to Wisconsin, they generally do not have significant economic value, because of the lack of outwash deposition prior to drumlinization. However, a systematic airborne geophysics and GPR tracing might reveal significant sand and gravel reserves in the drumlins shaped on previously deposited end moraines.

Rogen moraines

Rogen moraines (also called ribbed moraines) are transveral elongated ridges composing predominantly of basal till (Lundqvist 1969, Aario 1977, 1987, Shaw 1979), although lences of stratified sediments occur (Bouchard 1980) and the surface may be washed. The term Rogen moraine is a morphologic term, and has been used for a long time to describe particular type of morainic landscape according to the type locality in Sweden (Lundqvist 1969). These ridges, being transversally oriented, show transition to drumlins (Aario 1977), and several genetical interpretations have been proposed as rewieved by Lundqvist (1989). This section descibes a radar reconnaissance of sediments in the Rogen moraines and those landforms are evaluated as reserves of raw materials. An example of a single Rogen ridge is presented from Iso Latvasuo area, near Ranua and an example of ridge complex from Peuraselkä site, near Kemijärvi, Finland.

The Iso Latvasuo (suo = peat bog) area, near Ranua (Fig. 89), exhibit well developed transversal ridges, similar to the Rogen moraines. The ridges are gently undulating, 250 — 1500 meters long and 50 — 200 meters wide. The internal

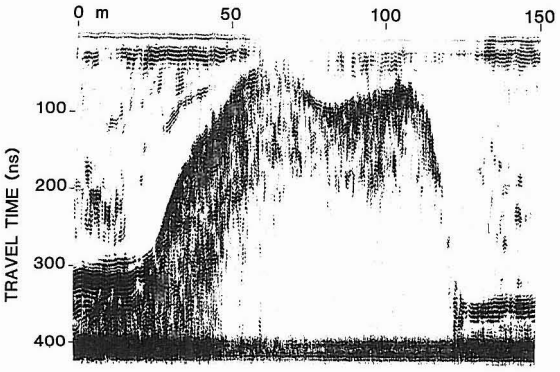

Fig. 76. Radar (c.f. = 120 MHz) profile cross the Rogen moraine ridge near Ranua, Finland. The antenna drawn by snow vehicle on a frozen peat bog. Ice flow from right to left. Adopted from Sutinen (1985b).

structure was studied by GPR (c.f. = 120 MHz) by pulling the antenna by snow vehicle on a frozen peat bog. An example of radar transects cross one of the ridges is shown in Figure 76. On both sides of the ridge glaciolacustrine / marine silt is indicated by the smooth and dark reflections. The ridge is composed of till, displayed by numerous, partially superimposing radar interfaces. Those are resulted from closely-spaced shearing structures, typical to basal tills. That kind of confused radar reflection characteristics can be used as a identification basis for tills (see Morey & Harrington 1972). Percussion drilling record indicated the till thickness of 3 — 4 meters, yielding saturated ε_{till} = 19. The resistivity ranges from 200 to 1000 ohm-m, which is correlative to the resistivity range given (Fig. 45) for saturated basal till.

The top of the ridge is covered by numerous stones and blocks as indicated by the tail-shaped hyperbolic reflections. The rough surface is presumably a result from strong glacial plucking, and the till deposition occurred at the top and the distal part of the ridge, from right to left on the profile. Bedrock topography primarily seems to have controlled the form of the ridge and is displayed blank beneath the till reflections. The strong compressive plucking and the lack of stratified sediments indicate grounded ice. The radar records are consistent with the observations from the exposures in the area.

Another example is presented from Kemijärvi, about 80 km NE from Rovaniemi. Peurasel-

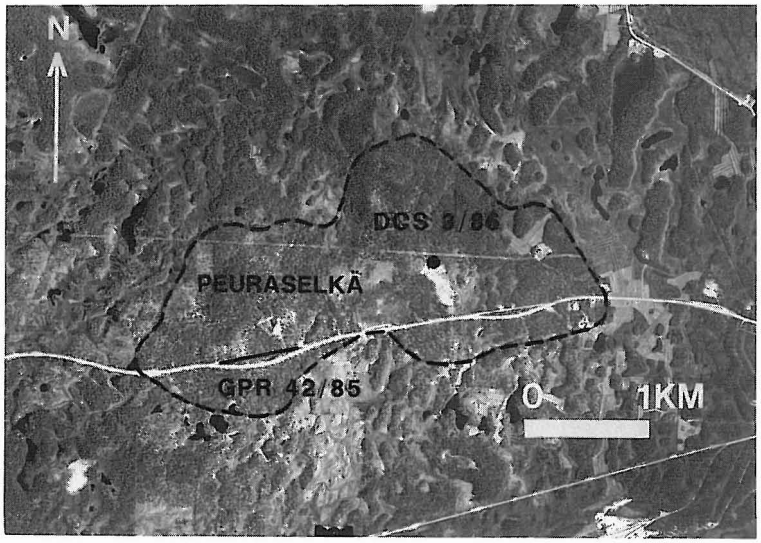

Fig. 77. A portion of AP 721/83 showing the Peuraselkä moraine complex surrounded by Rogen ridges. Ice flow from west to east. GPR and DCS survey sites also shown. AP by permission of Topografikunta.

Table 3. Interpretation of DC resistivity sounding (DCS 3/86) survey by means of a multilayer model from Peuraselkä site, Kemijärvi area. Thickness of layer = d, resistivity = ρ_a (ohm-m).

Layer	d m	ρ ohm-m	Type of layer
1	1	30 000	Gravelly sand
2	2	50 000	Flow sediment
3	4	100 000	Stony flow sediment
4	8	1 500	Till (wet)
5	—	20 000	Bedrock

kä is a large (2 km^2) irregular morainic landform (Fig 77; AP 721/83), five kilometers west from the city of Kemijärvi. It is surrounded by the well-developed Rogen ridges. The surface is covered by stones and blocks decreasing in amount distally to the southeast. A steep proximal contact demarcates the complex in the west. Several meters thick layers of extremely coarse-textured flow sediments are exposed (Fig. 16) in the core. The flow sediments are sandwiched between the two basal till units (correlative to the Late Weichselian) with till fabric trending roughly to the west. GPR (c.f. = 80 MHz; 3.5 kilometers of profiles) and refraction seismic surveys (800 meters of profile) and DC resistivity soundings (9 soundings with a Schlumberger configuration) were performed to outline the extension and continuation of the flow sediments within the moraine. The DC resistivity sounding (3/86; Table 3) data at the top of the exposure (Fig. 16) indicate significant resistivity variations between

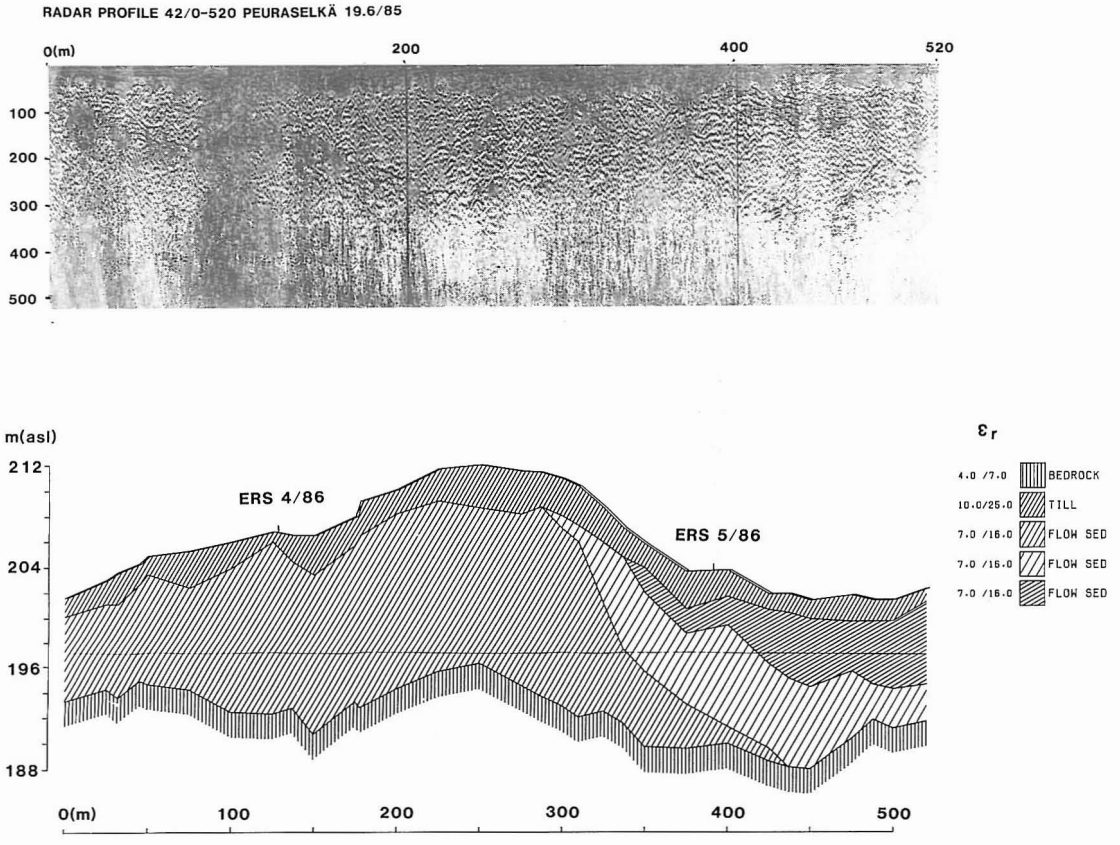

Fig. 78. A portion of radar (c.f. = 80 MHz) profile along the Peuraselkä moraine. Antenna drawn by car along the gravel road. Some of the flow sediment beds interpreted to show sediment flow direction, which also parallels to the ice flow direction (from left to right).

Table 4. Interpretation and comparison of GPR and DC resistivity sounding data from Peuraselkä moraine, Kemijärvi. Thickness of layer = d, dielectric constant = ε_r, resistivity = ρ_a.

Layer	Point 4/86		Point 5/86	
	d(m)/ε_r	d(m)/ρ_a (ohm-m)	d(m)/ε_r	d(m)/ρ_a (ohm-m)
1	1.2/10	—	2.4/10	1/4500
2	8.7/7	9.5/30 000	4.4/7	5/22 000
3	5.0/16	7/5000	7.5/16	7/2500
4	—/7	—/15 000	—	2/200
5	—	—	—/7	—/15 000

the sedimentary units. The highest resistivity of 100 000 ohm-m for matrix supported stony flow sediment unit is consistent with the log-based resistivity data (Fig. 45).

In the GPR profiles the coarse-textured flow sediments are indicated by numerous superimposing hyperbolic reflections. An example of a portion of the GPR profile and schematic interpretation of the survey data (Fig. 78) is presented 1.5 kilometres south-west from the pit. The dark interfaces on the top indicate the basal till (verified also by three test pits). Some flow structures are indicated by reflections sloping to the west (left to right on the profile). Ground water level can be detected clearly, but as a result of signal attenuation in the saturated material, only part of the bedrock surface can be observed.

The results of the DC resistivity surveys (DCS 4/86 and DCS 5/86) on the example GPR profile (Fig. 79, interpretation of the survey data listed in Table 4) reveal subtill flow sediments with slighly sandier matrix compared to the material exposed in the pit. At the point 5/86 a low resistive layer at the bottom represents saturated till. The thicknesses obtained with the two methods are consistent. Also, the refraction seismic sounding records from the same points indicated similar trend. In point 4/86 total thicknesses are interpreted to be as follows: 15 m (GPR), 16.5 m (DCS) and 13 m (SS). Correspondingly in the point 5/86: 14 m (GPR), 15 m (DCS) and 15 m (SS).

The geophysics records, sedimentary structures at the exposure and the test pits indicate that the

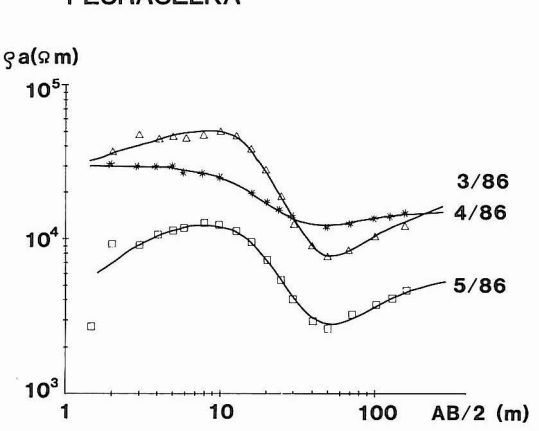

Fig. 79. Examples of the DC resistivity sounding results from Peuraselkä moraine. Half value of current electrode separation = AB/2, Schlumberger electrode configuration. Discrete points refer to survey data, curves denote the theoretical model results with the parameters as listed in Tables 3 and 4.

Peuraselkä moraine complex is composed of extensive masses of coarse-textured flow sediments. Angular bebbles and stones representing local granitoid litologies and sandy / gravelly matrix suggest rapid and short-lived deposition (slurry flows) under subglacial conditions.

The rock material has been plucked from the base prior to slurry flows and the »Rogenized» surface was shaped after the flows. Since the sandy till units at the top and also beneath the flow sediments have the fabric trending W — E, those both are correlated to the Late Weichselian. The morphologic pattern of the Rogen ridges around the Peuraselkä indicate slighly convergent

ice flow towards the Peuraselkä and thus explains the subglacial water seepage. The Peuraselkä moraine complex is not morphologically the type of »real» Rogen moraine, but genetically it is closely related to the procesesses (eroding substratum and stacking/ piling till units) forming the large Rogen moraine field in the Kemijärvi area. Moraine complexes, similar to Peuraselkä, may contain significant raw materials reserves. Those are easy to detect by APs, Landsat TM and SPOT data. In the materials surveys a combined use of GPR and earth resistivity soundings are recommended for detecting the volumes and coarseness of the materials. Particularly in northern Finland radar penetration is sufficient for that purpose.

Eskers

Sinous, continuous, steep-sided and narrow ridges of cobbles, gravel, sand and silt are called eskers. The term esker originates from the Irish word »eiscir» or Welsh word »escair» meaning crooked or winding. Long esker (ås in Swedish; harju in Finnish) chains and network patterns are typical in Fennoscandia (occupied by the Scandinavian ice sheet; e.g. Tanner 1915, Nordkalott-project 1986b) and in Canada (occupied by Laurentide Ice Sheet; see e.g. Fig. 3. in Aylsworth & Shilts 1989). The Munro esker in Canada, for example, can be traced for 400 km (Lee 1965). In the area occupied by the Late Wisconsinan Superior Lobe, Minnesota, eskers tend to be located on the bottoms of tunnel valleys, which are interpreted to be catastrophically eroded channels (Wright 1973). Long esker chains are not so common in the outer part of former Laurentide Ice Sheet in Wisconsin. Eskers near the modern glaciers generally are small, only a few meters high and tens or a few hundreds of meters long. Eskers are significant raw materials reserves, and are exellent ground water sources, as well.

Several eskers in northern Sweden and Finland have been reported (From 1965, Kujansuu 1967, Sutinen 1977) to be composed of poorly sorted, matrix supported material (conduit infill; see Fig. 17). Kujansuu (1967) used the term 'embryonic esker' for such small esker ridges and suggested partial transition between moraine hummocks and esker-like sequences in the western Finnish Lapland. Sutinen (1977) observed that many of the small supra-aquatic eskers are built only of the conduit infill core, but the infill cores are superimposed by the openwork sediments in large subaquatic eskers. Carey and Ahmad (1961) suggested that the water seepage pressure gradient in the saturated till at the base of glacier may be sufficient to open a conduit by piping. Once formed, this conduit would be maintained by erosion and could form a subglacial tunnel and localize the esker formation.

Below, morphology and sedimentation of eskers as well as material supply are discussed. Since textural and electrical properties show clear transition from tills and flow sediments to glaciofluvial conduit infills and openwork sediments (Figs. 19 — 20, 31, 45), the morphological transition from morainic landforms, flutes and ribbed moraines, to eskers is descibed in this section. Due to very low permittivity and conductivity of glaciofluvial sand and gravel materials (Figs. 46 — 47), radar is particularly feasible for surveying esker materials (Bjelm et al. 1982, Sutinen 1985a).

Sheetwash and conduits

In the Utsjoki area, northernmost Finnish Lapland, small parallel or subparallel esker ridges appear in networks, oriented diagonally crossover the drumlins (Fig. 80; AP61182/ 174). The esker pattern is not controlled by the underlying bedrock topography, but the debris seems to have been subglacially forced downice (toward northeast) as a mobile sheet of watersaturated slurry.

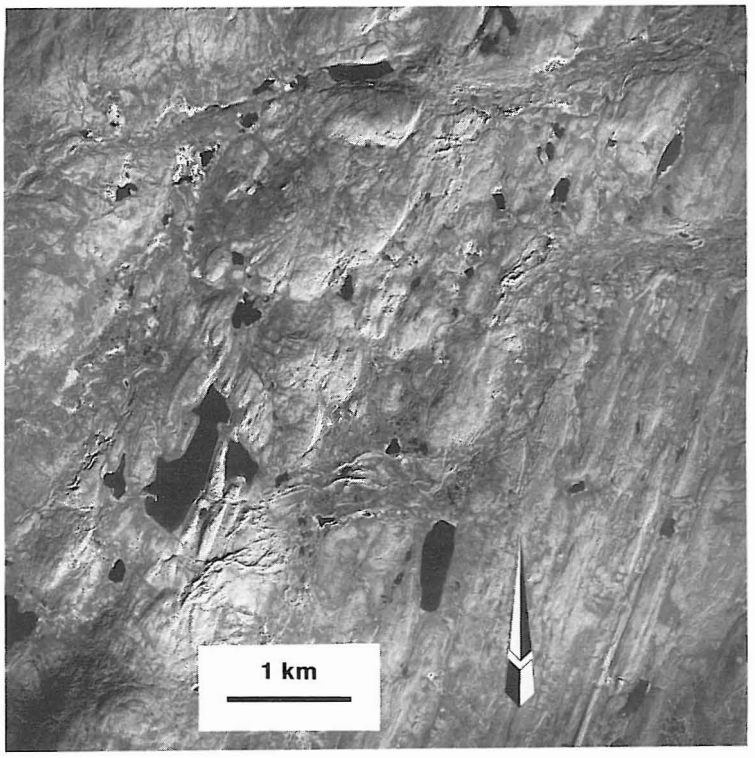

Fig. 80. A sheetwash type esker network oriented diagonally crossover the drumlins in Utsjoki, northermost Finnish Lapland. A portion of AP 61182/174 by permission of the Topografikunta.

Some of the esker ridges are typically sinuous, but some of them have a form of flutes. Those features evidently indicate subglacial drainage of meltwater (as heavily loaded slurry) beneath still actively overriding ice. If the water would have drained without debris load, one would expect to see extensive polished outcrops of bedrock as a result of glaciofluvial erosion.

An example of the transition from flutes to tiny, straight and discontinuous esker ridges is also presented from Utsjoki (Fig. 81; AP 61182/202). Transversely oriented, poorly developed ribbed moraines also seem to be associated to the transition being partially superimposed by the eskers. Sinuosity of the eskers increase downice, toward NNE and also the rate of glaciofluvial erosion increases as indicated by small channels. The transition is regarded to be attributed to the processes before the ice stagnates and terminates the glaciofluvial conduit drainage.

In high-relief areas in Finnish Lapland the stagnation of ice generates patchy fields of irregular mounds and ring ridges, often associated with discontinuous »embryonic» esker ridges (shown in Figure 70, west side of the drumlins). This kind of moraines are called the Pulju moraines according to the type locality in Kittilä (Kujansuu 1967). Even though they are composed of diamicton, texturally similar to basal till, the orientation of the clasts is not resulted from the ice flow. Either the ring ridges cannot be glaciodynamically controlled: if the ice was in motion, flutes would have been formed. Another way to explain the origin of the Pulju moraines is to apply the concept of deformable bed beneath the ice (see Hansel et al. 1985, Clark & Hansel 1989, Alley 1991).

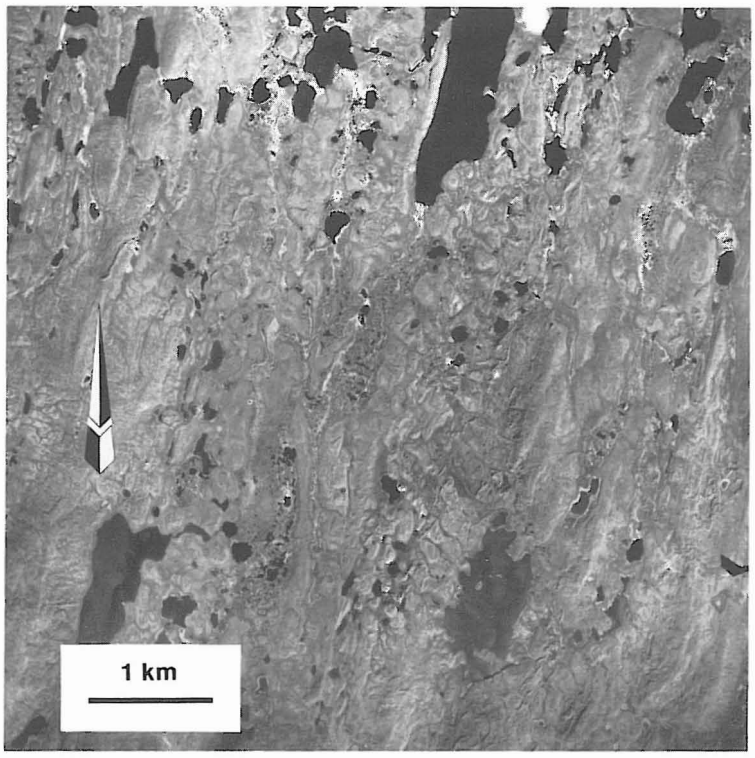

Fig. 81. A transition of flutes and ribbed morainic ridges to conduit infill eskers in Utsjoki. A portion of AP 61182/202 by permission of Topografikunta.

The dielectric properties of the Glacier Bay till beneath the margin of the Burroughs Glacier, Alaska indicated strong oversaturation. The excess of water allows the slurry diamicton easily deform to any shape of cavities or holes at the base of the ice (see Kujansuu 1967). When the stagnated ice loads the saturated base, a »glacierprint» is created in a similar way as the fingerprint into a soft clay. The excess of water intrudes downslope and creates small eskers. After stabilization the diamicton is texturally similar to the basal till.

Debris supply and maintenance of esker tunnel

The lithologies of the esker materials generally indicate longer transport distance than the surrounding till. Eskers are supplied by the material brought convergently from the sides of the esker systems. The convergent ice flow toward the interlobate eskers and complexes (Kettle Moraine, Fig. 2; Pudasjärvi-Hossa interlobate complex, Fig. 89) could be clearly seen by the orientation of streamlined morainic features and till fabric, as well. I suggest this is the case for all the eskers. An example is presented from Sivakkaharju esker, Kuusamo (Fig. 82).

Within the exploration of gold and uranium (Vanhanen 1989), Au- and U-bearing boulders were found on the south side of the W — E trending Sivakkaharju esker. The esker ridge is diagonally oriented with respect to the landscape dominating drumlins, trending NW — SE. The boulder fan is almost at the right angle to the drumlins. The AP interpretation revealed faint streamlining next to esker, and those features were the clue to trace the source at the SW side of the esker. By using the tractor mounted excavator the Au/U bedrock source was located. The

boulder fan clearly shows the convergent mechanism for the material supply toward the esker. It appears to me that the hydrostatic pressure maintains and erodes the esker tunnel at the same time when material is brought into the system. Therefore esker ridges are higher than the surrounding terrain. Later U-bearing boulders were found in the esker pit several kilometers east from the study site.

The convergent ice flow pattern is also demonstrated by the lateral landform transitions on the APs, and an example is presented from the NE-side of the lake Iijärvi, Inari, Finnish Lapland. The Ordavääri esker (Fig. 83, AP 61170/ 358) is trending SW — NE and exhibits several parallel ridges with numerous kettle holes on the surface. Northwest side of the esker a transition of flutes to ribbed ridges and mounds is spectacularly demonstrated. The flute field, crossover the drumlins, turns slightly toward the esker. The

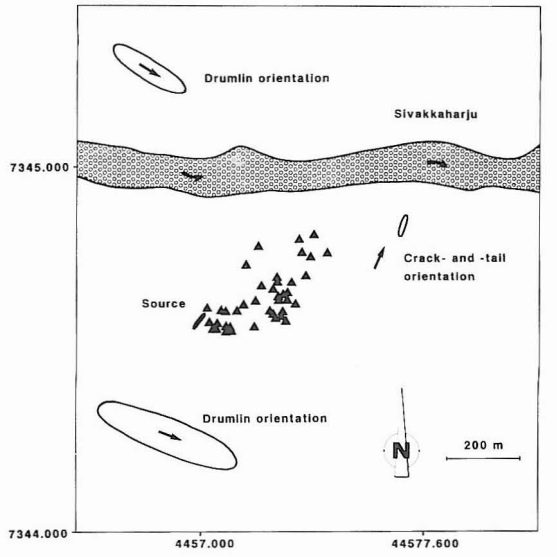

Fig. 82. An example of material supply of the Sivakkaharju esker near Kuusamo, Finland. The Au/ U-bearing surface boulders clearly indicate convergent ice flow toward the esker ridge.

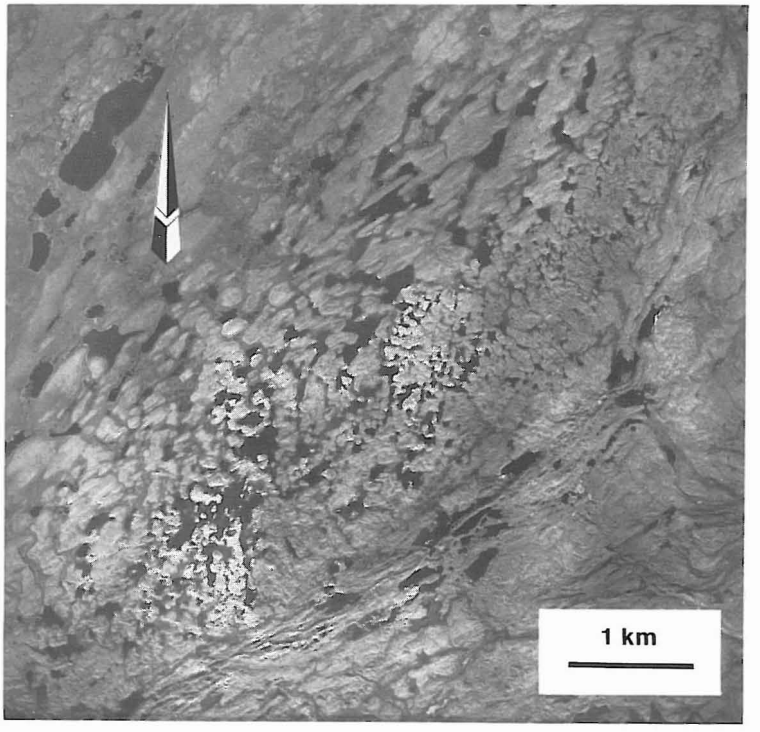

Fig. 83. A convergent ice flow toward the Ordavääri esker indicated by the transition of flutes to ribbed ridges/ mounds and tributary esker ridges. A portion of AP 61170/358 from Inari, Finnish Lapland by permission of Topografikunta.

ribbed ridges and mounds show a transition to tiny tributary esker ridges, which almost perpendicularly fed the main esker. Evidently the amount of subglacial water increased towards the Ordavääri esker.

Esker composition — radar detection

The Pudasjärvi-Hossa interlobate complex (Figs. 84 — 86, 89) is the largest glaciofluvial system (also one of the largest sand and gravel reserves) in northern Finland, and it continuously crosses the Finnish territory (Sutinen & Pollari 1979, Sutinen 1985c); the term was introduced by Aario and Forsström (1979). The esker system was deposited during the Late Weichselian and it crosses at two sites the Early Weichselian end moraines. It appears as a single ridge in the west (up-ice), whereas in the east (down-ice) the interlobate complexity is characterized by the large parallel ridges and tributary eskers (Fig. 84; AP 7609/ 100). Two examples of GPR profiles are presented, the first one illustrates the transect of the esker ridge at Vuornosoja and the other a longitudinal profile near the village of Pudasjärvi (locations shown in Fig. 89).

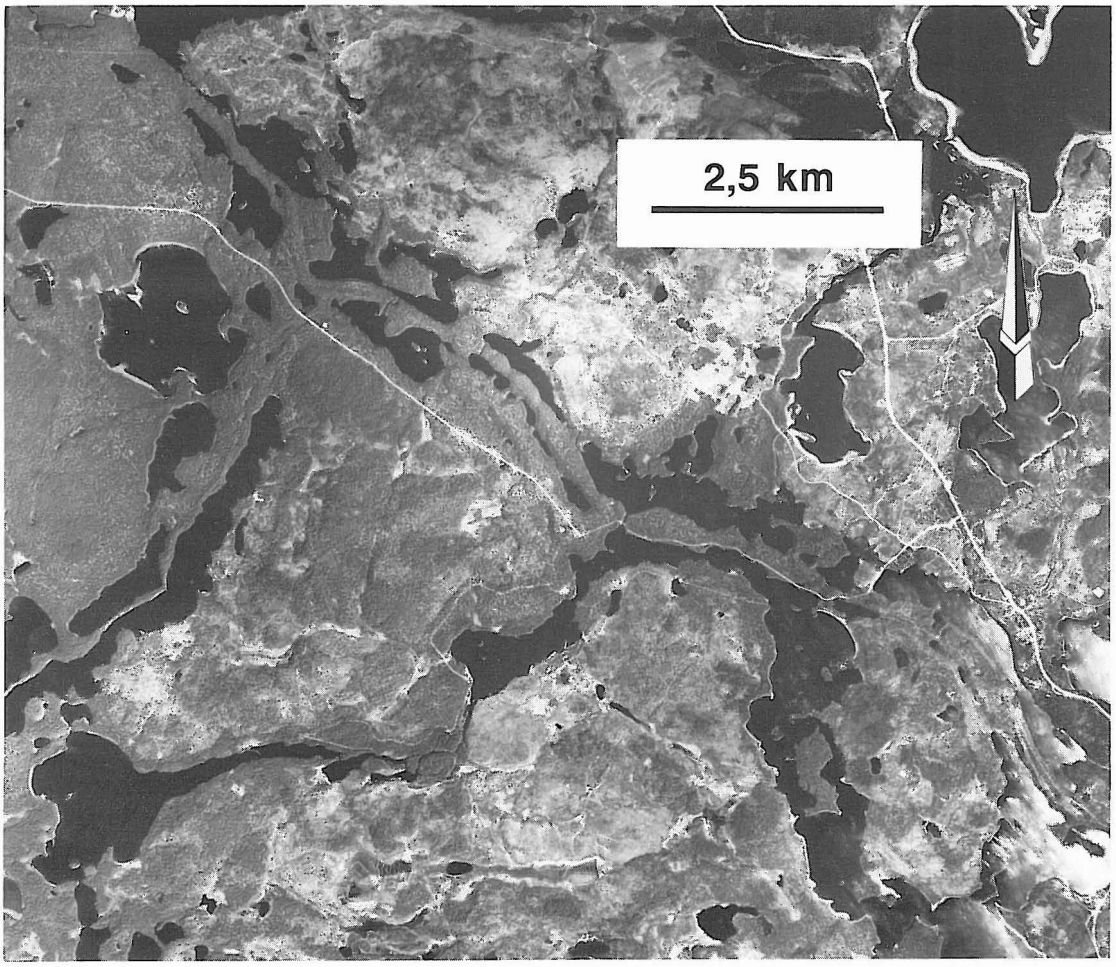

Fig. 84. A portion of AP 7609/100 showing the interlobate complex near Hossa, Finland (see the Quaternary map by Sutinen and Pollari, 1979), AP by permission of Topografikunta.

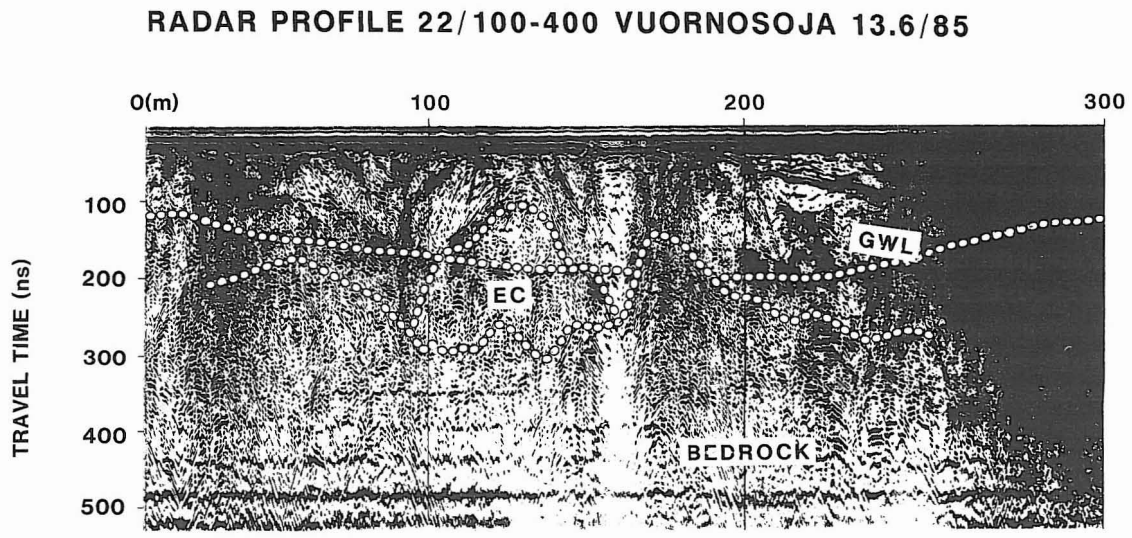

Fig. 85. Radar (c.f. = 80 MHz) transect of the Vuornosoja esker, Pudasjärvi. Esker core (EC) composing of coarse-textured conduit infill gravel, ground water level (GWL) and the bedrock surface shown. Meltwater paleoflow toward the observer.

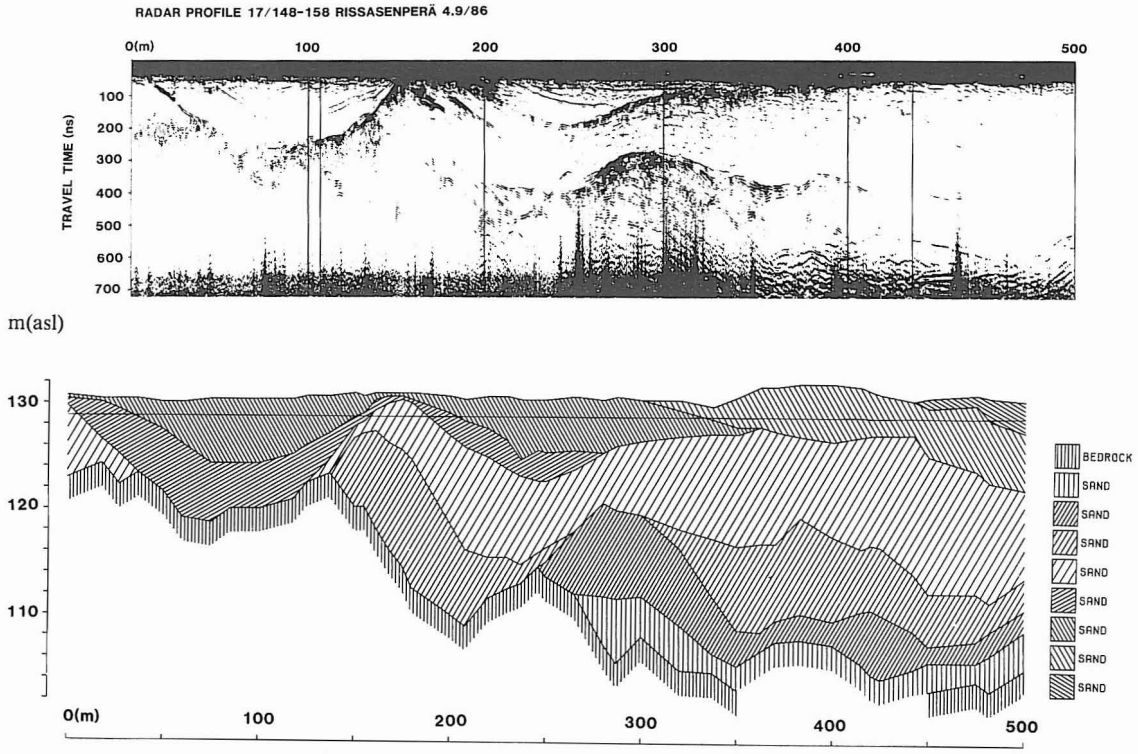

Fig. 86. Radar (c.f. = 80 MHz) profile along interlobate esker near Pudasjärvi, Finland. Gravel/ sand antidune structures are controlled by underlying bedrock topography. Meltwater paleoflow from left to right.

At the Vuornosoja site the esker is sinuous and gently sloping ridge, whose surface is covered by well-rounded cobbles and stones. Due to good hydraulic conductivity the surface is dry as indicated by the Scotch pine stands. The transect radar (c.f. = 80 MHz, max twt = 520 ns) profile (Fig. 85) shows the ground water level (GWL) as a continuous reflection line that crosses sand and gravel interfaces. The GWL, as indicating reversely the esker ridge topography, is at its maximum depth of 18 meters (ε_{gravel} = 4) below the crest of the esker. The esker core (EC) is composed of coarse-textured conduit infill deposits and is displayed by the dome-like structures. It seems very likely that the conduit has been opened in a bedrock depression. When the conduit was opened, the hydrostatic pressure kept the channel open and the convergent ice flow brought more saturated debris to system. The EC was then superimposed by the openwork gravels and sands. Postdepositonally the esker sand and gravel were deformed by the littoral action. As a result a beach sand was deposited, and it could be seen above the silt reflection on the right portion of the profile; the maximum beach sand thickness is about 5.5 m (ε_{sand} = 5).

A longitudinal radar section of the interlobate system (Fig. 86) is presented from Rissasenperä site near the village of Pudasjärvi. The structures are very different from the above transect. This profile does not show the center core, but the large-scale antidunes indicated by the dark interface (sand / gravel) boundaries. Paleoflow of water has been from west to east (left to right on the graph). On the proximal side of antidune crests bedrock knobs seem initially to have been controlled the formation of the antidunes. These structures indicate large amounts of free water in the channel.

Valley fillings

The river valleys in the northern Finland are filled with late- and postglacial fluvial sand and gravel, often superimposed by the windblown sand. Those are simple to map by APs and also by satellite images. Due to low dielectrics and conductivity of the materials, excellent radar sections can be obtained. An example is presented from the Jatuninkangas site in Kittilä, western Finnish Lapland (Fig. 87). Radar (c.f. = 80 MHz) profile cross the sand plain in the river Ounasjoki valley demonstrates a variety of sediment types. Ground water level is near the surface and is therefore displayed by consistent straight line on the top of the profile. The deepest interface is interpreted to represent solid rock surface. The till with darktoned and numerous closely-spaced interfaces is excellently visible on the

Table 5. GPR (C.F. = 80 MHz) and earth resistivity survey records on valley filling from Jatunikangas site, Kittilä.

Layer	GPR 20/100/85 d(m)/ε_r	DCS 2/85 d(m)/ρ(ohm-m)	
1	.9/4	1/800	Sand dry
2	3/25	3/400	Sand wet
3	2.8/30	3/250	Fine sand wet
4	2.2/16	2/100	Till wet
5	8.9/14	9/400	Weathered rock
6	—	—/800	Bedrock

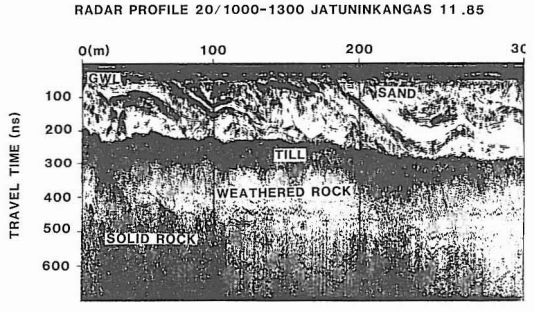

Fig. 87. A portion of radar (c.f. = 80 MHz) profile along the river Ounasjoki valley filling north from Kittilä, Finnish Lapland.

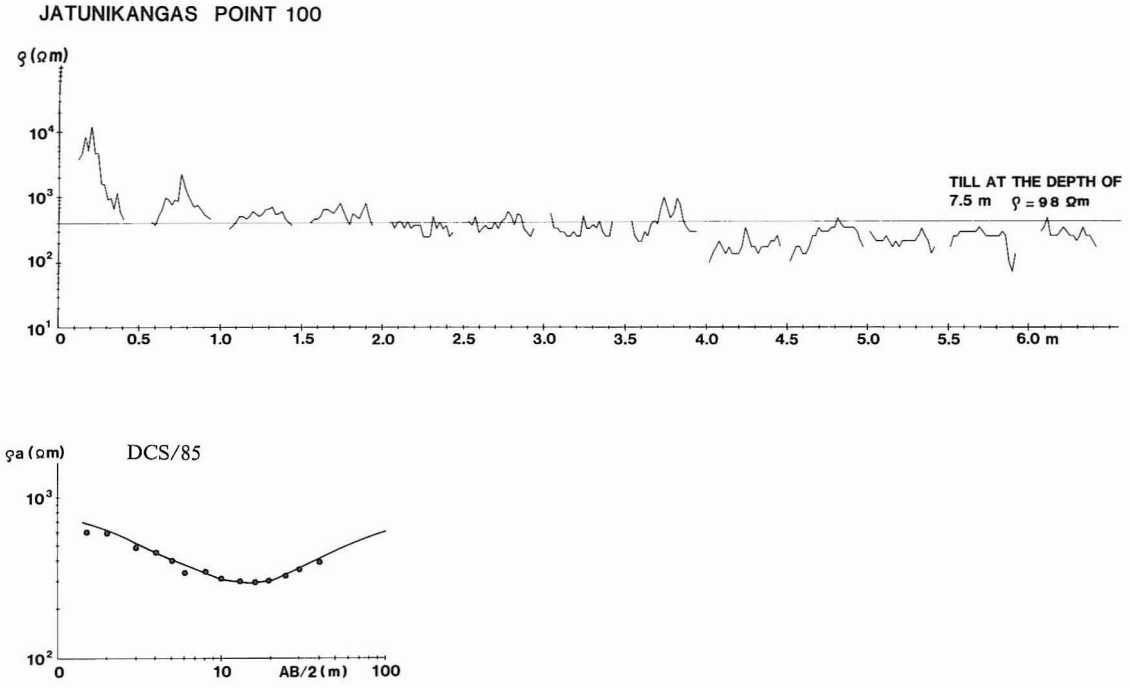

Fig. 88. Drillcore resistivity log and DC earth resistivity sounding results at point 100 in the GPR profile 20/85 (shown in Fig. 87). Half-value of the current electrode separation = AB/2, Schlumberger electrode configuration. Discrete points refer to survey data, curve denote the theoretical model result with the parameters of the model as listed in Table 5.

graph. Between the till and solid rock a weathered bedrock horizon is encountered. It seems to be fractured and blocky as indicated by the hyperbolic reflections. The till is overlain by saturated fluvial sands and the reflection interface is clear (R = 0.16; saturated ε_{till} = 16; ε_{sand} = 30).

The above sequence was also verified by the DC resistivity sounding (2/85) and drillcore resistivity logging (point 100 on the radar profile 20/85). The resistivity log and resistivity sounding results are presented in Figure 88 and interpretation of DCS data and GPR profile data in Table 5.

GPR and DCS data show similar trend in differentiating of the sediments. High resistivities at the top of the log are due to dry weather during the sampling, whereas DCS survey was undertaken after rainfall to get current enough into the ground. High-resolution GPR is shown to be excellent method for subsurface profiling of the sediments, but the above example demonstrates the necessity of additional data e.g. DCS data.

GLACIAL STRATIGRAPHY IN NORTH FINLAND

The Quaternary sequences in North Finland reveal a wide variety of interbedded materials. These interbedded sequences result both from facies changes among subglacial sediments deposited during single glacial cycle and multiple glacial — interglacial / interstadial cycles (Kujan-

suu 1967, Korpela 1969, Aario et al. 1974, Hirvas et al. 1977, also Hirvas 1991, Aario & Forström 1979, Punkari 1984, Aario 1984, Sutinen 1984, Tervo 1986, Nordkalottproject 1986b, 1986c). The majority of the glacial stratigraphic studies in North Finland have addressed the Weichselian Glacial Episode, and the stratigraphy is based primarily on glacial morphology, differentiation of till sequences (till beds), lithological, textural, and geochemical properties of tills, and clast fabric. In the Nordkalottproject (1986b) glaciofluvial deposits in the northern Fennoscandia were classified either Late Weichselian or pre-Late Weichselian. Descriptions and correlations between vegetation associations during interglacial/ interstadial periods are based on the palynological studies and diatom stratigraphy (e.g. Eriksson 1982, Grönlund 1991).

The main impetus in this study has been on radar applications, and the highest priority has been given to locating »old» (the pre-Late Weichselian) gravel and sand potentials concealed beneath the »youngest» (Late Weichselian) till cover, and thus provide information relevant for hydrogeological and geotechnical studies. The advantage of GPR is to obtain rapidly extensive amounts of continuous stratigraphic data from Quaternary sequences. GPR also allows reliable determination of meltwater paleoflow directions, which helps reconstruction of the deglaciation patterns of different ice flow stages. The chronostratigraphy has been given the lowest priority, probably because the age estimates, based on the conventional ^{14}C method, are not relevant for the Early Weichselian interstadial(s) (see Donner et al. 1979), and only limited amount of thermoluminescence (TL) age estimates (e.g. Punning & Raukas 1983, Jungner 1987, Peltoniemi et al. 1989) are available. Also, the palynological evidence of the subtill organic deposits may be in some cases disputable because of the possibility of redeposition (see Forsström 1989).

Lithostratigraphic units (till units / beds) and Late Quaternary (primarily Weichselian) chronology in Peräpohjola and Lapland were studied during the construction of hydroelectric power plants on the Kemijoki (Korpela 1969) as well as during the till stratigraphical project for ore prospecting purposes in the 1970's in Lapland (Hirvas et al. 1977, also Hirvas 1991). It was concluded that after the Eemian interglacial two Weichselian (equivalent to Wisconsinan) glacial periods and only one Weichselian interstadial, the Peräpohjola interstadial (introduced by Korpela 1969) existed. Only limited information on the tills attributed to the Saalian or older stages is available in Lapland and there is no age control, either (Hirvas et al. 1977, also Hirvas 1991). However, a peat layer reported (Hirvas & Eriksson, 1988, also Hirvas 1991) below till units (correlated to Weichselian and Saalian) in Naakenavaara, western Finnish Lapland (location in Fig. 99) has been interpreted to represent Holsteinian interglacial based on macrofossils of Aracites johnstrupii (Aracites interglacialis). A major chrono- and lithostratigraphic correlation discrepancy exists with the glacial stratigraphy in Sweden and Norway (Larsen et al. 1987, Lagerbäck & Robertsson 1988, Andersen & Mangerud 1989, Olsen 1988), where evidence for two Weichselian interstadials has been presented.

Glacial landforms and Quaternary sequences in the Pudasjärvi and Kuusamo areas reveal several ice-flow phases / stages (Aario & Forsström 1979, Sutinen 1984, 1985c, Forsström 1988, see also Punkari 1984). Aario and Forsström interpret the streamlined ice-flow features in the area to indicate different Late Weichselian deglaciation phases. The earliest ice-flow phase, Tuoppajärvi, is manifested by the large-scale (several kilometers long) streamlined features trending WNW — ESE and slightly fanning out in the east (Figs. 3, 66). Those features are superimposed by the Kuusamo drumlin field in the Kuusamo area, but are uncovered in the Tuoppajärvi area, outside the Pääjärvi — Kuittijärvi marginal complex (Aario & Forsström 1979, see also Punkari 1985). That marginal complex is correlative with the Salpausselkä end moraine and presumably also with the Tromsö — Lyn-

gen end moraine in the northern Norway (see Marthinussen 1961, Nordkalottproject 1986b). Soivio till was deposited during that time. The Tuoppajärvi phase was interpreted to have followed by the generation of more stationary ice lobe structures. No morphological features related to the west — east trending ice flow (Tuoppajärvi) could be observed in Peräpohjola and Lapland (Nordkalottproject 1986b). Those were either eroded during the later ice flow stages or they never formed there (preferred here). After the Tuoppajärvi phase an interlobate complex was interpreted to have been deposited and mantled by (basal) till at the southwest side of the village Pudasjärvi (Aario & Forsström 1979 Fig. 20). During the final flow stage, rearrangement of the ice sheet created the Ranua, Oulu and Kuusamo ice lobes; the Ranua, Jaalanka and Kuusamo tills and the Pudasjärvi — Hossa interlobate complex were deposited.

Sutinen (1984), however, has argued against the interpretation of the arc-shaped till-covered glaciofluvial landforms as Late Weichselian interlobate systems and instead suggests that those features are end moraines and relate to glacial events older than Late Weichselian. The subtill organic material (Fig. 98), on one of the feeding eskers (Katosharju esker, location in Fig. 89) indicate an Early-Weichselian rather than a Late-weichselian age for the eskers. However, the glaciofluvial landform patterns in the Pudasjärvi area (Sutinen 1985c) are very complicated allowing different chronostratigraphic interpretations.

Because of the unresolved stratigraphical discrepancies and correlation problems in relation to the other Scandinavian countries, more study is needed for good understanding of the glacial episodes. I have applied radar to provide sedimentological evidence for the extension of the pre-Late Weichselian ice advances in northern Finland. Numerous end moraines and associated till covered eskers have been profiled. In order to classify a glaciofluvial complex to be an end moraine following criteria had to be met: 1) The overall height of the formation rises significantly above the surrounding landscape and the formation is independent of bedrock topography. 2.) Meltwater paleoflow directions are roughly perpendicular to the orientation of the formation, which is transverse to the large-scale streamlined features up-ice. To verify the above criteria extensive GPR profiling (totalling about 500 km) was performed. Refraction seismic sounding (profiles totalling 18 km) and DC resistivity sounding (soundings totalling 74) surveys were used in determining the total thicknesses of glacial deposits on selected sites. Also, test pits (totalling 422, usually extended to a depth of four meters) were excavated for till stratigraphic verification. In the following, glacial and interglacial/interstadial stages and examples of attributed deposits have been presented at the chronological basis. The features attributed (tentatively) to Eemian and Early Weichselian have been described from the Pudasjärvi region (Fig. 89) and Rovaniemi. The evidence for features attributed to the Early / Mid Weichselian ice advance have been presented from the Kittilä (Fig. 99) and Savukoski areas (Fig. 101) .

Interglacial deposits

Puhosjärvi interglacial

The key evidence for a Saalian-Eemian-Weichselian record in the Pudasjärvi area is the subtill organic deposit found at the Puhosjärvi site (Fig. 89; the Finnish base map co-ordinates: x = 7241.07 and y = 3552.45, see Sutinen 1984), located outside the southernmost till-covered (Early Weichselian) end moraine. The 1.7 meters thick gyttja, which slightly glacially tectonized, lies between two till units. The clast fabric of the up-

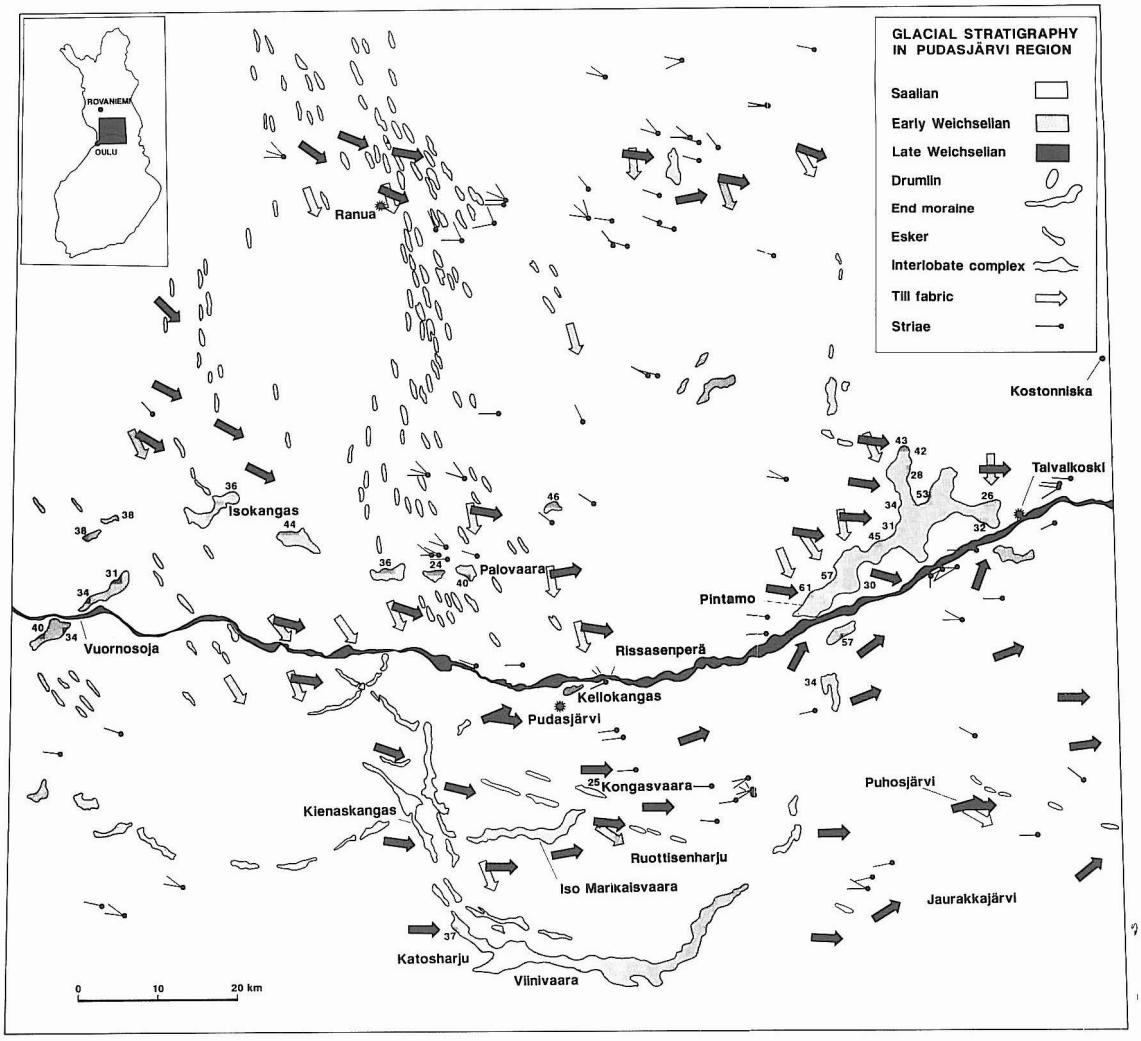

Fig. 89. The glacial stratigraphy in the Pudasjärvi region. Numeric symbols refer to thickness of glacial deposits determined by refraction seismics surveys. (Modified from Sutinen 1985c).

per till at Puhosjävi parallels the small-scale (correlative to Late Weichselian) streamlined features. The upper till unit has azimuth of 270° at the bottom of the till bed and 250° at the top of the bed suggesting converging flow towards the Pudasjärvi — Hossa interlobate complex at the final stage of deglaciation (cf. Figs. 82 — 83). The lower till unit, underlying the gyttja, has an azimuth of 300° and is called as Puhosjärvi till. Texturally the two tills do not vary significantly, clay content of the younger till is about 4 % and older till about 6 %. The lithologic composition shows more significant variation, the granitoid contents are 86 % and 56 % and the mafic rock contents 5 % and 30 %, respectively. The upper till is correlated to the Jaalanka till of Aario and Forsström (1979) but for the Puhosjärvi till there is no reliable correlation basis to any of the till units described by Aario and Forsström (1979). Several sites from the village of

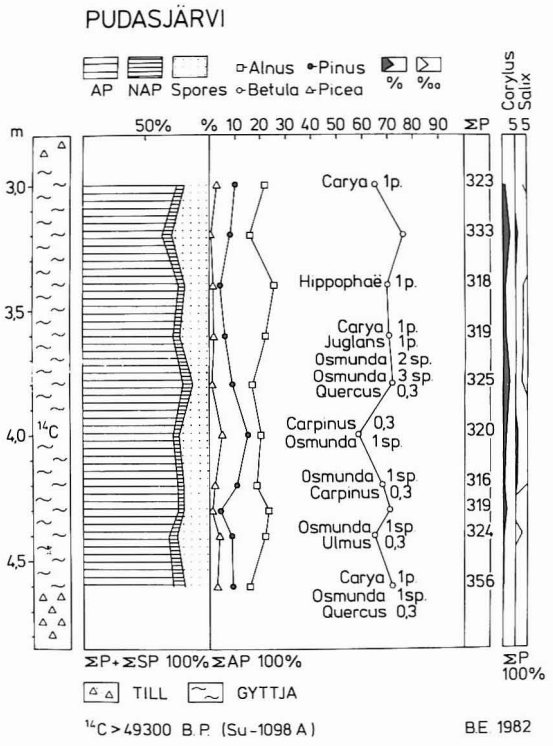

Fig. 90. The pollen spectra of the Puhosjärvi gyttja indicating both interglacial (Eemian) and interstadial (Peräpohjolan) features. Analyzed by B. Eriksson.

Ranua down to Viinivaara end moraine revealed grey till similar to Pudasjärvi till of Aario and Forsström (1979), but was not found at the Puhosjärvi. At the Kellokangas type section (op. cit.) dielectric properties were determined by TDR as follows: Ranua till (correlative to Jaalanka till) $\varepsilon_r = 6 - 8$ and Pudasjärvi till $\varepsilon_r = 8 - 10$.

The Puhosjärvi gyttja yielded ^{14}C- age estimates of >49,300 B.P. (Su-1098A) and >52,000 B.P. (Su-1098B). The organic sediment, at the depth of 3 — 4.7 meters, was sampled at 20 cm intervals for pollen (anal by B. Eriksson) and diatom (anal. by T. Grönlund) analysis. No succession was indicated either in the pollen (Fig. 90) or diatom spectra. The AP pollen content shows 58 — 76 % of *Betula*, 16 — 26 % of *Alnus*, 4 — 15 % of *Pinus* and less than 4 % of *Picea*. Also, far transported species, such as *Carya* and *Juglans* are present. Although the percentage of *Corylus* pollen is low, it is consistent throughout the profile. The spores are predominantly represented by *Sphagnum* and *Polypodiaceae*. The most indicative for Eemian Stage is the small but consistent representation of *Osmunda Regale* in the profile.

Although *Betula* dominated, the pollen record of the Puhosjärvi organic sequence is interpreted to represent the Eemian interglacial due to the presence of *Alnus*, *Corylus* and particularly thermophilus *Osmunda*, which indicate a climate warmer than present. *Osmunda* is found in some other Eemian deposits in Finland, but not in modern deposits (see Eriksson 1982). The far-transported exotic species, on the other hand, have been found within modern deposits.

Diatom flora composed for the most part of species indicative of fresh water, *Melosira distans var. lirata, M. undulata var. Normanni* and *M. italica var. lirata* as well as *Pinnularia* and *Eunotia* species. However, some of the diatoms are typical of salt water, *Grammatophora oceanica, Melosira sulcata* and some brackish water, *Campylodiscus echeneis, Diploneis smithi* and *Nitzschia punctata*.

I interpret the diatom and pollen flora in the organic sequence at Puhosjärvi record both interglacial and interstadial conditions, although the flora mixed probably as a result of glacitectonic deformation. The occurrence of the two flora spectras (interglacial and interstadial) in the same stratigraphic position indicates that sedimentation at that site was not interrupted by an Early Weichselian glacial advance i.e., that the Early Weichselian ice margin was north of the Puhosjärvi area and (before deformed) recorded a transition from interglacial to interstadial conditions. Consequently, south of the Pudasjärvi region the organic deposits correlated with the Eemian interglacial and Weichselian interstadial (Peräpohjola) occur between Saalian and Late Weichselian lithostratigraphic units (tills).

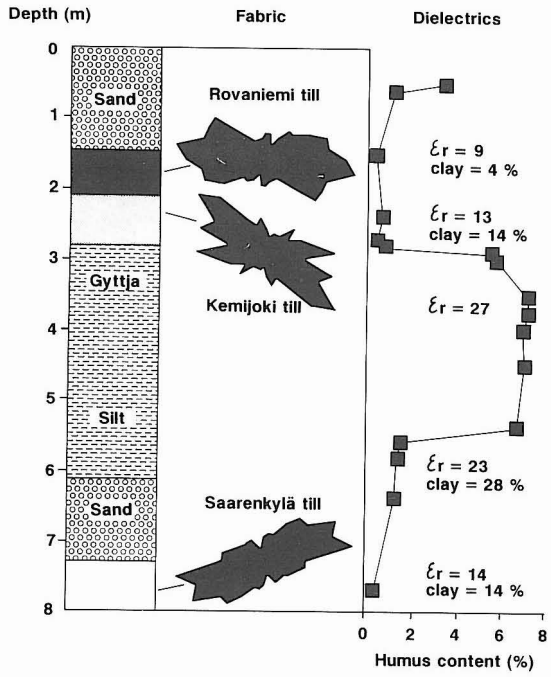

Fig. 91. Stratigraphic units of the Saarenkylä Interglacial type section. Differentiation of the Late Weichselian Rovaniemi till, Early Weichselian Kemijoki till and Saalian Saarenkylä till based on the till fabric, texture and dielectric properties (measured by TDR from the exposure).

Saarenkylä interglacial

During road construction operations, a subtill gyttja was exposed in Saarenkylä (Finnish base map co-ordinates x = 7382 540; y = 444 760; z = 72.5 a.s.l.) in the Kemijoki river valley, 2 km north from downtown Rovaniemi. Lithostratigraphically the 3-meters thick gyttja and silt was above one till unit and superimposed by two till units (Fig. 91). The topmost unit, called here the Rovaniemi till is greyish brown and uniform with a clast fabric with an azimuth of 260° at the depth of 1.5 m and 280° at the depth of 2 m. The portion of the fine fraction $d < 2.2$ µm is 4 — 5 % (measured by Sympatec Helos laser particle size analyzator using dry dispersion), and $\varepsilon_{till} = 9$ (unsaturated; determined by TDR). This unit displays similar characteristics through Rovaniemi to Kemijärvi and is correlative to the upper till (Late Weichselian) of Korpela (1969).

The Rovaniemi till is underlain by a grey, compact and uniform till unit with a clast fabric with an azimuth of 310°. The portion of $d < 2.2$ µm was analyzed to be 13.9 %, and $\varepsilon_{till} = 13.4$ (unsaturated). Similar dielectric properties (ε_{till} between 13 and 14) have been measured from the same litho-stratigraphic unit elsewhere around the city of Rovaniemi and also 40 km upstream in the Kemijoki river valley. Therefore this unit is called here the Kemijoki till (see Fig. 28). Because the dielectric properties, fine fraction content and fabric of Rovaniemi and Kemijoki tills vary significantly, those are interpreted here to represent different ice flow stages. Since the fabric of the Kemijoki till is consistent with the with the lower till of Korpela (1969) it might be correlated with the Early Weichselian. No organic material (should be at Peräpohjolan stratigraphic position as described by Korpela, 1969) was found in the contact between the Rovaniemi till and the Kemijoki till.

The lowest till unit (underlying the gyttja and silt) in the exposure (80 by 235 meters) is extremely compact, grey and uniform with a fabric with an azimuth of 250°. The portion of $d < 2.2$ µm is 14.2 and $\varepsilon_{till} = 13.9$ (unsaturated). It is called here the Saarenkylä till, and its stratigraphic position suggests Saalian based on the interglacial organic material described below.

Between the Kemijoki and Saarenkylä tills a 3-meter thick organic gyttja ($\varepsilon_r = 27.2$) was exposed continuously 150 meters . The gyttja is *in situ*, and only slightly glacially tectonized at the top and it grades downward into minerogenic silt ($\varepsilon_r = 23.3$). The humus content varies between 5.5 and 7.5 per cent, but it is less than 1 % in all the three tills and varies between 1 and 2 per cent in silt (Fig. 91). The organic material contains macroscopic remains of cones and twigs and the pollen content (to date only one sample analyzed; by B. Eriksson) is interglacial. The AP flora compose 97 % of total with a predominance of *Pinus*, 51.6 %, *Betula* content is 33.7 % and *Alnus* 9.9 %. The small but consistent represen-

tation of *Larix* 0.9 % and *Osmunda* 0.3 % also indicate period warmer than today. The gyttja is correlated with the Eemian interglacial and is called here the Saarenkylä interglacial. At the time of writing of this thesis no ^{14}C, TL or photolumunescence (PL) age estimates were available.

Lithostratigraphy and palynology at the Puhosjärvi and Saarenkylä localities provide the key evidence for outlining the maximum position of the Early Weichselian glaciation. If the interpretations presented here (i.e. W1 litho-stratigraphic unit (Pudasjärvi till) absent in Puhosjärvi, but is superimposing the Eemian organic deposits in Saarenkylä) are correct, the maximum ice margin position of the Early Weichselian advance should be in between these two type localities. However, the lack of till do not necessarily prove the absence of glacial advance because of the possible erosion resulted from later (Late Weichselian) ice advance(s). Morphological and GPR evidence suggesting an Early Weichselian esker and end moraine complex in the Pudasjärvi area is presented below.

Weichselian ice flow stages

Pudasjärvi stage

Large till-covered and arc-shaped landforms are common in the Pudasjärvi area (Aario & Forsström 1979, Sutinen 1984, 1985c, Fig. 89). Those have been interpreted to be end moraines by Sutinen (1984), but Aario and Forström (1979), and Forsström (1988) interpreted those as interlobate eskers attributed to the Late Weichselian. According to the interpretations of the refraction seismic soundings the thicknesses of the those glaciofluvial landforms range from 27 to 54 meters. The seismic velocities are generally on the order of v = 450 — 800 m/s (unsaturated sandy material) and v = 1300 — 1650 m/s (saturated material). Till is common on the tops of the formations, but is difficult to differentiate on seismic records. Some of the end moraines also contain compact material (presumably till or very coarse-textured conduit infill material) in their core, as indicated by the high seismic wave velocities, on the order of v = 2000 — 2300 m/s (cf. Kauranne et al. 1972, Taanila 1976). The end moraine arches have been cut by the Late Weichselian Pudasjärvi — Taivalkoski — Hossa interlobate esker complex at two sites: Vuornosoja and Pintamo (locations in Fig. 89). In this study no evidence of ice advance over the interlobate complex (see Figs. 84 — 86), glaciotectonic structures and till-cover, has been found. I therefore disagree with Aario and Forsström's (1979) and Forsström's (1988) interpretation that the Kellokangas till-covered ridge belongs to the interlobate complex. I regard Kellokangas a part the Early Weichselian recessional moraine arches in the area (see Fig. 89).

The glaciofluvial landform zone extending from Viinivaara to the village Taivalkoski (Fig. 89; MZ1 in Sutinen 1984) is classified as end moraine and is interpreted to mark the maximum ice margin position during the Early Weichselian glaciation. It is called the Pudasjärvi end moraine, and correspondingly the ice flow stage is called the Pudasjärvi stage. Systematic GPR surveying of this end moraine (covered by the Late Weichselian till) indicated deltaic deposition with foreset slopes from 25° to 40° down-ice. Several other end moraines occur north of the W1 maximum (Sutinen 1984). Those end moraines are presumably formed at the glacier margin during temporary standstills of the Early Weichselian deglaciation, and thus should properly be called recessional moraines. Generally the end moraines consist of large hills (1 to 2 km by 2 to 3 km), that are 2 to 20 kilometers apart from each other. They are composed predominantly of glaciofluvial gravel and sand.

All the end moraines are covered by the lithostratigraphic unit (till) correlated with the Late Weichselian. The till cover tends to increase in thickness downslope. Three GPR case studies (Iso Marikaisvaara, Isokangas and Palovaara, locations in Fig. 89) are discussed below.

Iso Marikaisvaara end moraine

The Iso Marikaisvaara end moraine reveals three sedimentary facies; a glaciofluvial core, a till, and a beach deposit at the top. The GPR profiling (c.f. = 80 MHz; max. twt = 720 ns) was performed by towing the antenna by car on a logging road between two hills that rose 20 — 25 meters above the surrounding terrain. Figure 92 shows a 600-m long portion of the unprocessed GPR profile and a schematic presentation of the data interpretation.

Glaciofluvial gravels deposited on the bedrock are seen as dark dome-like reflections at the bottom of the graph. Faint indications of infill cores could be seen (x = 100 — 150 m; y = 200 — 400 ns) suggesting deposition perpendicular to the moraine ridge. The gravelly unit is covered by till that is similar to the Jaalanka till (Aario & Fors-

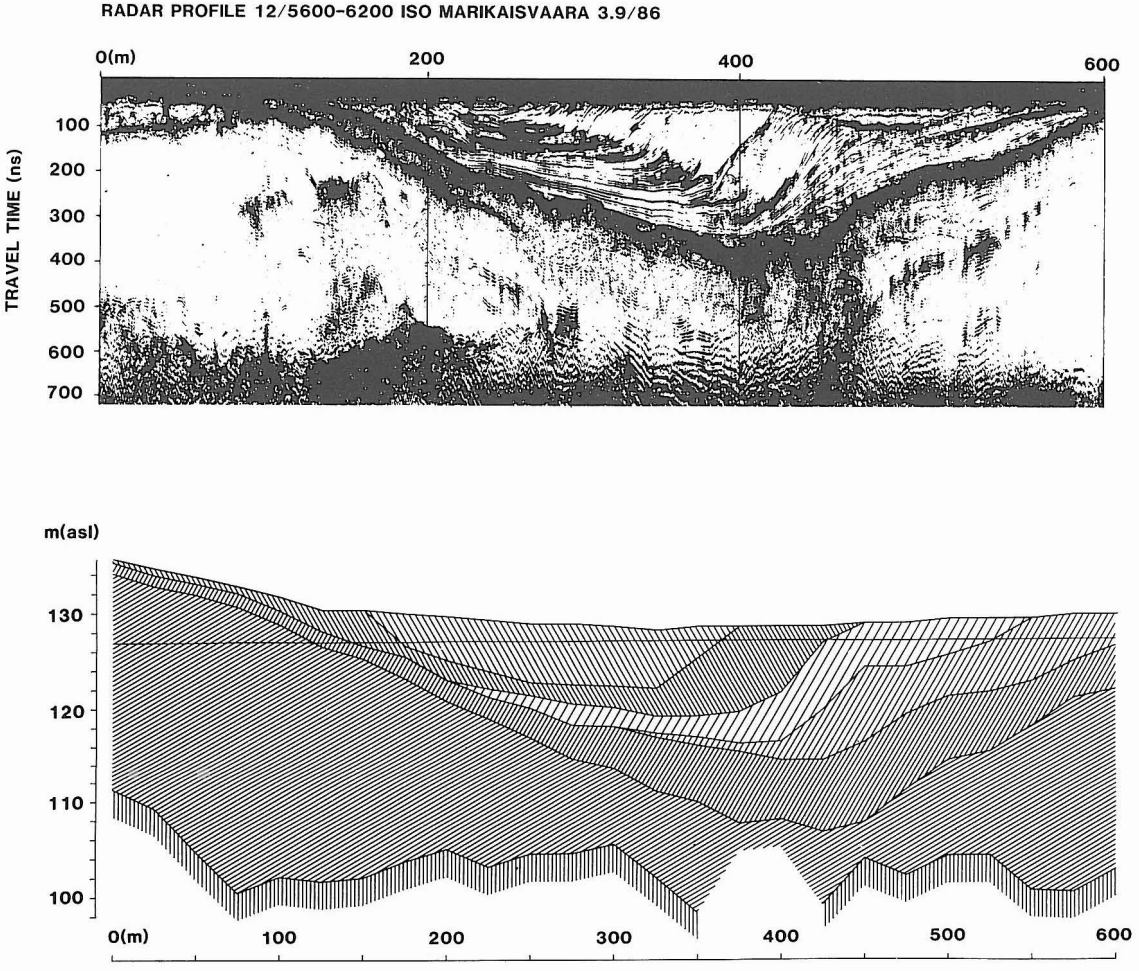

Fig. 92. Portion of radar (c.f. = 80 MHz; max. twt = 720 ns) profile along the Early Weichselian Iso Marikaisvaara endmoraine, Pudasjärvi. Antenna pulled by car on the logging road.

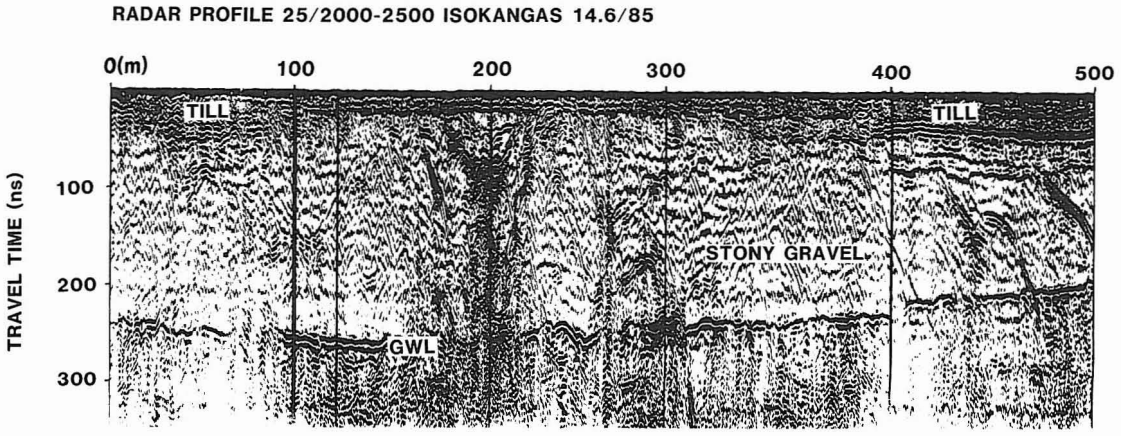

Fig. 93. A portion of radar (c.f. = 80 MHz; max. twt = 330 ns) profile along Isokangas, the Early Weichselian end moraine in Pudasjärvi.

ström, 1979) in that it has a clast fabric with an azimuth of 270°, which parallels the latest ice movement over the area. Till cover is thickest in the depression exceeding 5 — 7 m.

The till is overlain by beach sand and gravel, seen as superimposed reflection interfaces on the radargraph. Some of the gravelly sand beds are shown; for unsaturated $\varepsilon_{sand} = 6$ and saturated coarse sand $\varepsilon_{sand} = 25$ as well as for unsaturated $\varepsilon_{gravel} = 4$ and saturated $\varepsilon_{gravel} = 16$ are given. Beach deposits are interpreted to reworked from the till unit. Ground water level (GWL) is depicted by the straight line crossing the sediment structures.

Isokangas end moraine

The Isokangas end moraine ridge (location in Fig. 89) was profiled by GPR (c.f = 80 MHz, max. twt = 330 ns) by pulling the antenna on the logging road along the ridge crest. The hill rises about 20 — 30 m above the surrounding area, and the maximum thickness of glaciofluvial deposits is 36 m according to seismic surveys. The gravel and sand core is blanketed by basal till. A 500-meter long portion of the GPR profile (Fig. 93) shows GWL clearly as a continuous interface between twt = 200 and 300 ns cutting gravel/sand interfaces. The form of the GWL reflection interface is the reverse of the surface topography of the formation ($\varepsilon_{gravel} = 4$ and $\varepsilon_{till} = 7$), which is relatively flat presumably due to Late Weichselian glacial erosion. The maximum thickness of unsaturated gravel deposits is 18 meters. The interior of the Isokangas end moraine is built up of conduit domes, interbedded gravel and sand units. These structures indicate meltwater discharge from north (towards the observer in the profile). The discharge must have been controlled by ice tunnel(s) that were gradually widened by the glaciofluvial erosion as the bedload increased. The substantial amounts of stones present resulted from rapid bedload sedimentation. Single stones are indicated by tail-shaped hyperbola reflections superimposed on reflections from lower interfaces. The sedimentary strata are similar to those in the GPR cross sections of the esker infill of the Vuornosoja esker (Fig. 85).

Till cover is depicted by strong, dark, closely-spaced and partially overlapping reflections (λ = 1.4; c.f = 80 MHz and $\varepsilon_{till} = 7$) at the top of the profile. Till thickness ranges from 1.5 to 3 meters as indicated by GPR data as well as by percussion drillings and test pits. On the right portion of the graph, between x ≈ 400 and 500 m, a dark reflection boundary is seen at the con-

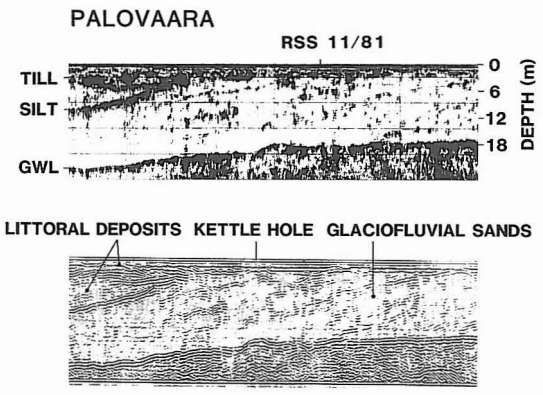

Fig. 94. A portion of radar (c.f. = 120 MHz; max. twt = 450 ns) profile across Palovaara, the Early Weichselian end moraine in Pudasjärvi, North Finland. Depth scale for unsaturated sand ($\varepsilon = 5$).

tact between till and glaciofluvial sediments. The high-intensity reflection is due to higher dielectric and lower conductivity properties indicating this internal layer to be fine-grained (silty) material.

The till unit is sandy, uniform, compact and brown; it shows slight fissility due to frost activity. Substantial amounts of well-rounded pebbles and stones are present in the till, which is classified as basal meltout type. The preferred orientation of pebbles indicates ice flow from 300°, parallel to the small-scale streamlined features in the area (Fig. 3). The silt layer between the till and glaciofluvial deposits may be attributed to basal melting during the sliding of ice over the formation. Basal sliding probably tended to decrease the glacial erosion rate, thereby protecting the major part the older (presumably Early Weichselian) glaciofluvial material. Alternatively, the silt layer may represent lacustrine sediment from interstadial period, similar to those on the Kienaskangas and Katosharju eskers as discussed below.

The Isokangas end moraine complex was fed from the north by an esker (Sutinen, 1985c; Fig. 89), the surface of which appears to be greatly smoothened by glacial erosion. The esker is covered by the Late Weichselian till (clay content = 7 %) with clast fabric with an azimuth of 300°. The underlying sand is extremely hard-packed. Both the conduit structures observed in the GPR profile and the presence of a feeding esker suggest the Isokangas end moraine is sedimentologically an esker delta complex.

Palovaara end moraine

The Palovaara end moraine (Sutinen 1984, Fig. 89), is a rounded hill, 2.2 km long and 1.5 km wide, rising 20 — 35 meters above the surrounding area. It is composed of sand and overlain by till and late glacial beach gravel and sand deposits. A refraction seismic sounding survey shows the maximum thickness of the formation to be 40 meters, seismic velocities of v = 750 — 900 m/s were measured for unsaturated sand and v = 1600 — 1650 m/s for saturated sand. A bedrock velocity of v = 4700 m/s indicates a granite gneiss basement (see Parasnis 1974).

Several GPR (c.f 120 MHz, max. twt = 450 ns) transects (down-ice) were performed across the formation, by pulling the antenna by snow scooter. A 200 meters long portion of GPR profile, transverse to the Palovaara ridge, is shown in Figure 94. The upper unprocessed graph shows +/- polarities while lower graph displays only + polarity. The GWL is seen as a smoothly undulating interface in the lower part. The bump in GWL indicates the inverse of a kettle hole at the surface of the formation. Maximum thickness of unsaturated sand varies between 16 and 20 m ($\varepsilon_{sand} = 5$), matching well with the seismic records. The foreset beds show a meltwater paleoflow direction from NNE (from right to left on the graph). The low angles of the foreset beds, varying between 10° and 20°, indicate quite calm delta sedimentation.

Palovaara is covered by the Baltic ice lake beach ridges, which have been utilized by TVL (Public Roads and Waterways) for road construction and maintenance. Beach gravel is seen on the top left in the graph. A basal till layer is

seen distinctly below the gravel due to the finer matrix. Near the surface in some places till is exposed, too. Below the till another sand sequence is detected. That has also been interpreted to be a littoral deposit, because a strong reflection interface is encountered further down. The intensity of the reflection indicates higher ε_r and σ values and is attributed to a fine-grained layer, presumably silt, which also commonly is found at the base of late glacial beach sequences.

The Palovaara foreset beds clearly indicate glaciofluvial delta sedimentation from north-northwest, presumably during the Early Weichselian. The lower beach sequence is interpreted to have deposited during the deglaciation of that stage. The basal till is a typical Late Weichselian till with a fabric parallelling the small-scale streamlined features in the area. The small Late Weichselian eskers pass through this end moraine zone (MZ2 in Sutinen 1984) without interruption and join the Pudasjärvi — Hossa interlobate esker complex 10 — 15 kilometers southward.

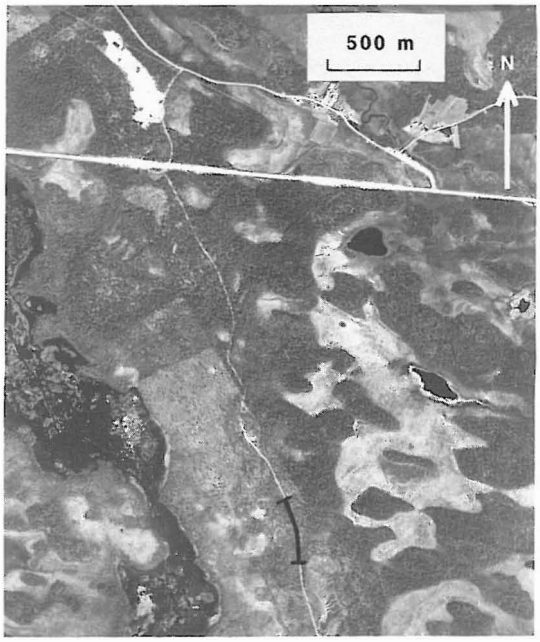

Fig. 95. Kienaskangas, the Early Weichselian esker superimposed by the Late Weichselian streamlined morainic features. A Portion of the AP 61152/294 by permission of Topografikunta (The Army Map Service).

Eskers attributed to the Pudasjärvi stage / Kienaskangas esker

Some of the till covered eskers parallel the orientation of the WNW-ESE trending large-scale streamlined forms in the southern part of the study area. However, the majority of the eskers shown as the pre-Late Weichselian eskers in Nordkalottproject (1986b) map north of lat 66° parallel roughly the NW — SE trend. Eskers with that trend are common as far as the Pudasjärvi end moraine. Two GPR case studies near the Pudasjärvi end moraine are presented below. Also, relevant stratigraphical observations are described.

The Kienaskangas (Fig 95; location in Fig. 89) is a large NNW-SSE oriented till-covered glaciofluvial ridge. Based on orientation parallel to the large-scale streamlined forms in the area, it has been interpreted to be an esker. The morphology of Kienaskangas is smooth and gently sloping probably as a result of glacial advance diagonally over the formation. It is easy to detect on air photos even though the vegetation on the esker is similar to that of the moraine terrain surrounding it.

The overlying lithostratigraphic unit is an uniform brownish and compact basal till with clay content of 2 %. It grades downwards into a flow-type slurry diamicton. The clast fabric of the till indicates ice flow from 280° parallelling the orientation of the small-scale drumloid features. The structures of the esker and the till thickness were determined by GPR (c.f = 80 MHz, ε_{till} = 7, λ = 1.4 m) profiling, ground conductivity measurements (Geonics EM 31; f = 39.2 kHz) and refraction seismic survey. Till thickness varies between 1.5 and 4 meters and is shown by the dark overlapping reflections at the top of the GPR profile. Coarse-textured glaciofluvial deposits are identified by irregular dome structures with numerous hyperbolas indicating single stones. Only the upper part (12 m; ε_{gravel} =

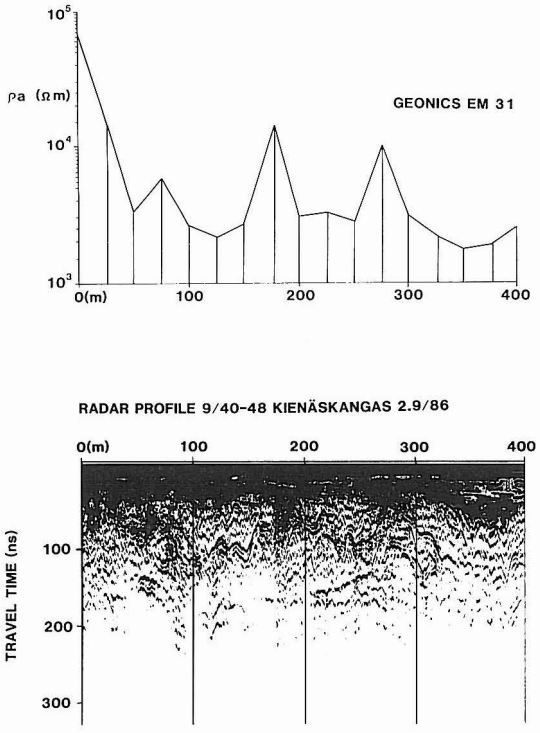

Fig. 96. An example of ground conductivity survey (Geonics EM 31; f = 39.2 kHz) and radar (c.f. = 80 MHz; max. twt = 330 ns) profile along the Kienaskangas esker showing Early Weichselian gravel domes superimposed by the Late Weichselian Jaalanka till and flow sediments.

5) of the esker can be seen on the graph due to attenuation of radar signals at the surface of the logging road and in the fissile till and slurry diamicton. Between the till unit and gravel, flow-type slurry diamicton is present. The ground conductivity survey reveals gravel domes by distinct apparent resistivity anomalies, but care must be taken in the interpretation of such features because the instrument is designed for materials with relatively low resistivity (generally less than 1000 ohm-m). However, the trend is correct (i.e. consistent with the GPR survey data), and the low resistivity anomalies are interpreted to represent thicker till cover and underlying diamicton. The surface topography of the esker ridge material is regarded to result from glacial erosion rather than melt-water activity. The section exposes glacially eroded grooves that parallel the Late Weichselian ice flow over the esker ridge. The grooves likely were filled with the saturated slurry diamicton during the streamlining of the landscape, and later basal (melt-out) till was draped over the top of the sequence.

As glacial erosion removed part of the esker sediments also the interstadial deposits were transported away. However, some remains have been preserved in kettle holes on the esker. A half kilometer south of the GPR site in the wall of the exposure reddish clay pockets were observed between the till unit and glaciofluvial deposits. The majority of diatom species from the clay indicate a fresh water environment with a predominance (95 %) of *Melosira islandica ssp. helvetica*. Only 2 % indicate salt water. Therefore the lacustrine clay represents an (Early Weichselian) interstadial rather than the Eemian interglacial. The esker sand and gravel were deposited during the Early Weichselian and the slurry diamicton and basal (melt-out) till during the Late Weichselian.

Katosharju esker

Katosharju esker (locality shown in Fig. 89) is similar to Kienaskangas and it fed the Pudasjär-

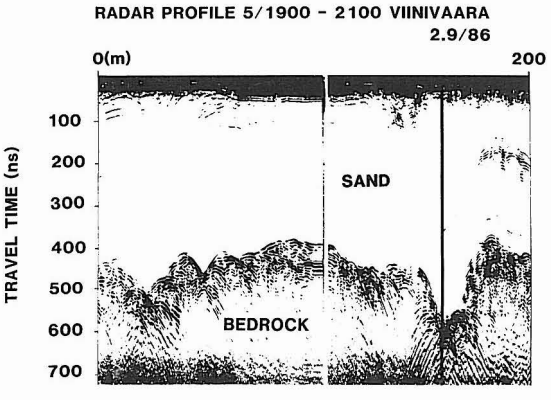

Fig. 97. A portion of the radar (c.f = 80 MHz; max. twt = 720 ns) profile along Katosharju, the Early Weichselian esker. Early Weichselian saturated esker sand on the granitoid rock ($\varepsilon_{sand} = 30$, $\varepsilon_{rock} = 8 \rightarrow R = 0.32$) and late Weichselian till cover at the top ($\lambda = 1.4$ m; $\varepsilon_{till} = 7$) are shown.

Fig. 98. An exposure showing the Betula dominated interstadial (Peräpohjolan) Katosharju gyttja with $^{14}C \approx 49{,}200\ ^{+3200}/_{-2300}$ B.P. yr covered by the Late Weichselian Jaalanka till in Pudasjärvi.

vi end moraine complex 20 kilometers south from the study site. Figure 97 presents a part of GPR profile along the esker showing homogenous sand on the bedrock, which was geologically mapped (Enkovaara et al. 1952) as a granite gneiss complex and verified also by seismic survey (v = 4750 — 5000 m/s). The GWL is seen on the top of the graph partially superimposed by till reflections. Seismic velocity of the saturated sand (v = 1500 m/s) was also measured. The reflection at the saturated sand and bedrock interface is clear because of high contrast in dielectric properties; $\varepsilon_{sand} = 30$ $\varepsilon_{rock} = 8$; → reflection coefficient R = 0.32. The bedrock surface at twt = 400 — 600 ns is 11 — 16 meters deep. Strong hyperbolas at the bottom indicate blocks and partially splittered bedrock surface. Glaciofluvial erosion apparently removed the older sediment, presumably till(s).

An exposure in the esker, 0.5 km north of the GPR profile site, revealed a sequence of organic deposits (Fig. 98; see Sutinen, 1984) overlain by a Late Weichselian till with a clast fabric indicating ice flow from 260° — 270°. The till, with clay content of 2 — 4 %, has a sharp lower contact with the underlying sandy esker material and it appears to be similar to Jaalanka till (Aario & Forsström 1979). The gyttja yielded radiocarbon age estimates of 49,200 $^{+3200}/_{-2300}$ BP (Su-1159A) and 44,900 $^{+2600}/_{-2000}$ B.P. (Su-1159B), and is characterized by *Betula* -dominated (98 %) AP flora. Minor amounts of *Pinus, Salix* and *Corylus* are present suggesting cool interstadial.

The esker chain, however, is not continuous (Fig. 89) and a dislocation gap exists between Kienaskangas and Katosharju. A similar system to the east contains a similar gap. There are two explanations for the discontinuity. It may have generated during a temporary standstill of the retreating glacier margin as indicated by recessional moraines in the area (Fig. 89). Alter-

natively, the esker chains may have been offset by faulting. A major tectonic fault line trending WSW — ENE is indicated on high altitude magnetic data, but the magnitude of displacement (several kilometers) is presumably too great to be neotectonic.

The esker complex (Kienaskangas and Katosharju as examples; Fig. 89), on the other hand, resembles the Kettle Moraine complex in Wisconsin (Fig. 2), where also two parallel ridges, several kilometers apart, demarcate the moraine. Therefore I agree with the interpretation by Aario and Forsström (1979) that the esker complex is an interlobate complex, but based on the palynological and till stratigraphic evidence it is Early Weichselian and is bounded by the Pudasjärvi end moraine (Viinivaara) in the south. The presence of both the glacial erosion features on the esker ridge and the subtill gyttja and clay overlying the esker sediments is clear evidence for a cool Viinivaara interstadial (correlative to the Peräpohjola interstadial of Korpela, 1969).

Problematic glaciofluvial deposits

Probably the most problematic features in the Pudasjärvi area are the WNW — ESE trending till covered and straight glaciofluvial ridges (e.g. Kongasvaara and Ruottisenharju, locations shown in Fig. 89). Those are oriented uniformly in a 290° to 110° trend. During the early radar experiments of the Geological Survey of Finland (Lappalainen et al. 1984), Kongasvaara was chosen as one of the experimental sites. Morphologically the ridge (0.5 * 3 km) is smoothened by glacial erosion and draped by till. I interpreted it to be an esker based on the internal structures seen on radar (c.f. = 120 MHz, max. twt = 310 ns) transects. A center conduit was clearly detectable to a depth of 17 meters, even where 2 — 4 meters of till (ε_{till} = 7, clay content = 4 %) covers the esker. Seismic wave propagation velocities of 2150 — 2300 m/s were measured for the saturated conduit infill gravel. Openwork glaciofluvial sediment (unsaturated sand) overlying the conduit core is gently sloping sideways and the seismic wave velocities of 700 — 1250 m/s were recorded. The Kongasvaara esker exceeds a maximum thickness of 24 meters. The longitudinal GPR profiles show the foreset sand beds sloping 15° — 25° in the downice direction to the east-southeast. It is evident that also ice flow was one time to the same direction. Only one till unit, similar to Jaalanka till by Aario and Forström (1979), was found on the top, and has a clast fabric from 260° — 280° parallelling the orientation of small-scale drumloid forms (Late Weichselian, see Fig. 3) in the area.

Kongasvaara and Ruottisenharju eskers, not necessarily belonging to the same system, presumably are correlative based on the parallel orientation. Ruottisenharju sand and gravel contain fragments of organic material in a secondary position, and the ^{14}C age estimate of > 52.000 BP (CrN-7651) has been given (Aario & Forsström 1979). The palynological evidence suggests either interstadial (Pudasjärvi interstadial) or even interglacial. Recently, PL- (photoluminescence) age estimate of about 90 ka (Kujansuu oral comm.) from silty material beneath the till at Ruottisenharju section has been determined. Therefore it seems evident that Kongasvaara and Ruottisenharju eskers (and their correlatives) are not attributed to the Late Weichselian post-Tuoppajärvi phase as interpreted by Aario and Forsström (1979), but are possibly Early Weichselian, as suggested by Forsström (1988).

However, the esker core might be still older. The sedimentological evidence (the ESE-sloping foresets) at Kongasvaara suggests that ice one time must have flown also to that direction. On the other hand, there is no morphological indication that Kongasvaara and Ruottisenharju esker systems erosionally cut any of the other glacifluvial landform systems in the area. However, similar ridges are present on the southeast side the Pudasjärvi end moraine, the Early Weichselian maximum ice margin position. Although only one till unit was found on the top of the eskers, probably due to erosion, Kongas-

vaara and Ruottisenharju esker systems likely are Pre-Weichselian and may be related to the Saalian.

Although the meltwater paleoflow suggested ice flow to ESE it might be too hazard to make correlation between the eskers and the large-scale streamlined morainic features (drumlins) in the Kuusamo area (Figs. 3, 66). A Saalian origin is controversial, because the drumlin field extends further east to the Tuoppajärvi area, outside the Pääjärvi — Kuittijärvi marginal complex. Beyond the marginal complex the Tuoppajärvi drumlins are fresh suggesting Late Weichselian origin (Aario & Forsström 1979, Punkari 1985). Another alternative is that two parallel generations of drumlins (Saalian and Late Weichselian) are superimposed in the Tuoppajärvi area, and therefore morphological differentiation is difficult.

Lapland stage

Although evidence exist for another Weichselian interstadial in Sweden and Norway (Lagerbäck & Robertsson 1988, Larsen et al. 1987, Olsen 1989, see also Andersen & Mangerud 1989), heretofore none has been presented in Finland. This interstadial has been named according to the type localities as the Tärendö interstadial (Lagerbäck & Robertsson 1988) in Norrbotten, northern Sweden and the Sargejåk interstadial (Olsen 1988) in Finnmarksvidda, northern Norway (Figs. 107 — 108). Since part of Finland is between those two localities it is logical that also part of Finland has been ice-free during that period.

The Viinivaara interstadial sediments (and its correlatives) are overlain only by one till unit (Late Weichselian) through Pudasjärvi region to Central Lapland; Jaalanka till in Pudasjärvi, Rovaniemi till (correlative to upper till of Korpela 1969) in Rovaniemi and Peräpohjola region. Since only one post-Peräpohjolan ice advance has been identified in the Central Lapland, the maximum ice margin position of the second Weichselian glacial stage must be located further north in Lapland. Below, morphological and sedimentological data are presented as possible evidence for an Early/Mid Weichselian ice advance and deglaciation. Two case studies are presented: Kittilä in western Finnish Lapland and Savukoski in eastern Finnish Lapland.

Kittilä, western Finnish Lapland

Glacial morphologic and stratigraphic information, collected within GSF's mapping program between 1980 and 1984, indicates three different ice flow patterns (Fig. 99) in the Kittilä region. The ice flow trending NW — SE is indicated by large-scale rock drumlins, striation, and some till fabric observations (see Nordkalottproject 1986b, 1986c). The ice flow trending N — S is indicated by small-scale streamlined landforms (slightly fanning in the south), striation, till fabric as well as esker morphology and an arc-shaped end-moraine. The ice flow pattern trending roughly SW — NE is indicated only by the till fabric and striation (c.f. Hirvas 1991, Salonen 1986).

Those three ice flow stages / facies were verified by determining the glacial dispersal of magnetite-bearing surface stones at Suasselkä (location in Fig. 99). Because the thickness of Quaternary deposits in the Suasselkä area is generally less three meters, according to refraction seismic survey and test pits, it was assumed that all the three glacial dispersal patterns could be detected. Based on the high-altitude airborne magnetic data, a source of magnetic rock was located by magnetometric measurements, and the magnetic susceptibility of the surface stones and boulders were measured using a susceptibility meter JH-8 by Geoinstruments. Measurements, totalling 8300, were done using 40 by 40-meter grid-cells, 50 measurements per cell. The measured data is plotted (Fig. 100) as smoothed percentages of high-magnetic rocks. The plot clearly indicate three different dispersal patterns consistent with the till stratigraphic data: the oldest trending NW — SE, the second oldest trending N — S and the youngest trending SW — NE.

The above morphologic / stratigraphic outline is correlative to the stratigraphy reported by

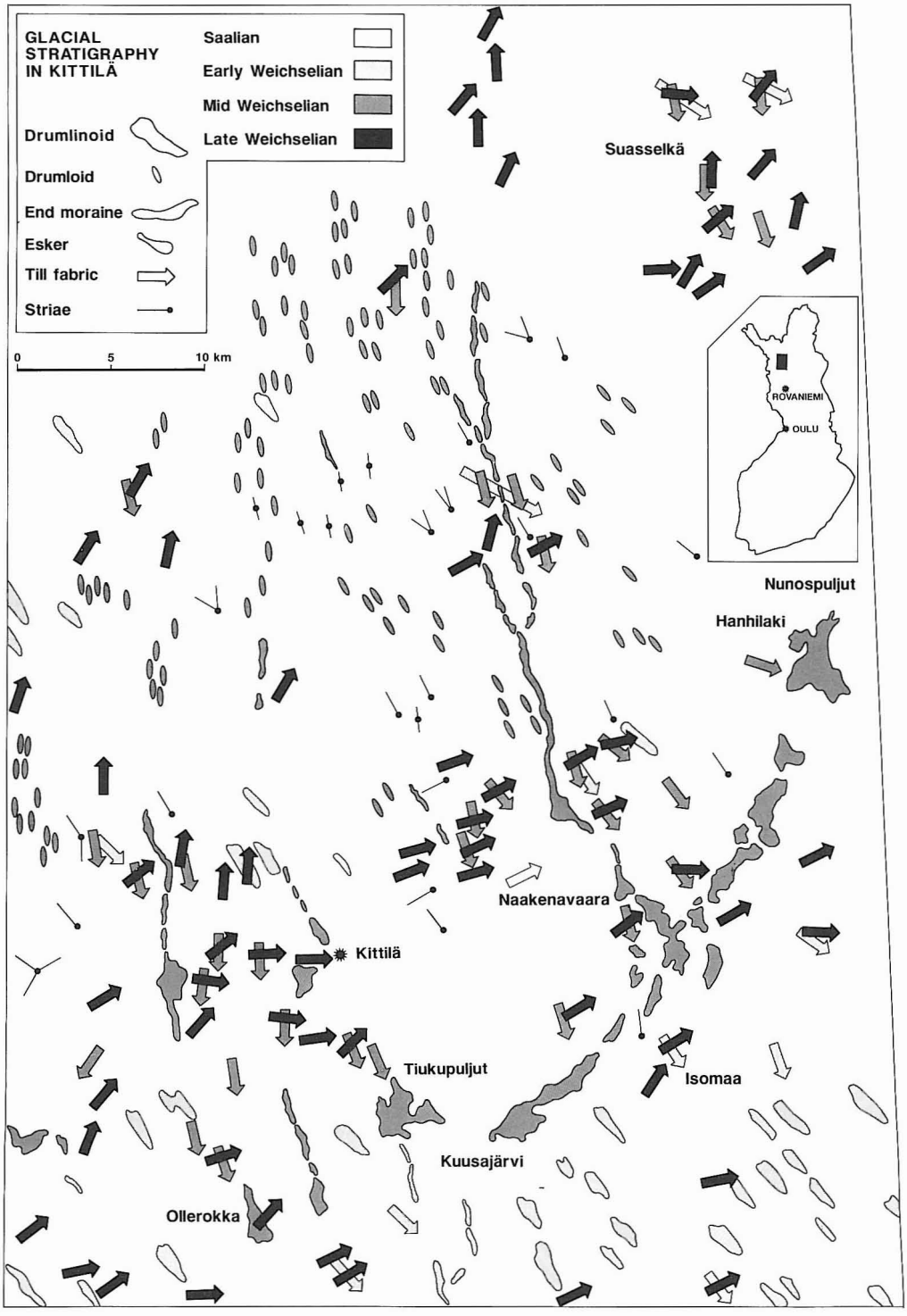

Fig. 99. Glacial stratigraphy in the Kittilä area. Additional information from Aario (1984), Tervo (1986), Hirvas (1991, Naakenvaara), Johansson and Keinänen (1988) included.

Aario (1984) and Tervo (1986) in the nearby areas. They named the oldest till trending NW — SE as the Silas till, the till trending N — S as the Suas till and the youngest till trending SW — NE as the Rova till. They regarded all the three tills to be resulted from the Weichselian ice advances. Also, recent mineral exploration investigations north of Suasselkä (Härkönen oral comm.) has confirmed the N — S trending ice flow (till unit) below the unit trending S — N.

Subtill organic deposits have been found within geochemical survey (Äyräs & Koivisto 1984) at two sites about 10 km northeast of Suasselkä. At the Jalkajoki site an organic deposit was identified to be overlain by two till units (presumably Suas and Rova tills) and indicate Peräpohjola-interstadial pollen flora with 70 — 90 % of *Betula* and 10 — 20 % of *Pinus* (analyzed by B.Eriksson). At the Sammalselkä site, organic material was covered only by one till unit (correlative to till I by Hirvas et al. 1977 and presumably Rova till by Aario 1984 and Tervo 1986). Unfortunately, no palynologic information is available from the this material, but its stratigraphic position may indicate presence of the Early/Mid Weichselian interstadial in western Finnish Lapland. Johansson and Keinänen (1988) reported organic material at Isomaa, outside the Kuusajärvi — Nunospuljut end moraine (location in Fig. 99). The organic layer was found between the SW — NW trending till (Late Weichselian) and the NW — SE trending till (Early Weichselian) and it was correlated to the Peräpohjola based on the *Betula* dominated (94 %) flora and ^{14}C age estimate 40 000 $^{+2100}/_{-1700}$ yr B.P.

Even though the palynologic evidence lacks and there is no age control of the Early/Mid Weichselian interstadial (Sammalselkä), strong morphologic and stratigraphic evidences presume independent ice-advance, which is represented by the Suas till and its correlatives. Therefore the terminal ice margin position of this advance has to be somewhere between Suasselkä and Isomaa. The Kuusajärvi — Nunospuljut endmoraine is proposed to be the Early/Mid Weichselian maximum ice margin position in western Finnish Lapland. The sedimentological evidence is presented below.

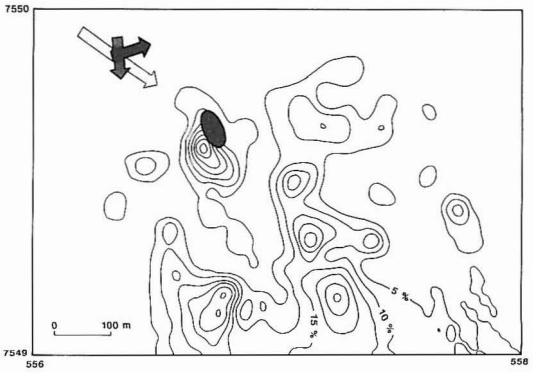

Fig. 100. Glacial dispersal of the magnetite-bearing surface stones in the Suasselkä. The Early Weichselian dispersal trending NW—SE, Mid-Weichselian N—S and Late Weichselian SW—NE. Source indicated as black.

Kuusajärvi delta complex

Near the village Kittilä an arc-shaped belt of till (Late Weichselian) covered complex of ridges, hummocks and delta plateaus, identified by Kujansuu (1967), has been re-examined here. Kuusajärvi ice-marginal delta complex (1 by 5 km; Fig. 99) with steep ice-contact slope on the NW-side (up-ice) is trending SW — NE. The GPR survey (c.f = 80 MHz; max. twt = 560 ns) shows paleoflow direction to southeast by gently sloping foresets. The delta complex is overlain by 2 — 3-meters thick sandy till (ε_{till} = 7), which is correlated to Rova till. The glaciofluvial (gravelly)sand exhibited glaciotectonic deformation structures in the test pits, and the overall thickness is ranging from 16 to more than 25 meters according to GPR profiles (ε_{sand} = 5, unsaturated; ε_{sand} = 25, saturated). A DC resistivity sounding at the top of the delta shows σ_{till} = 0.00029 S/m, (d = 3 m); σ_{sand} = 0.000045 S/m (unsaturated, d = 5 m) and σ_{sand} = 0.00025 S/m (saturated, d = 15 m). A refraction seismic survey indicated quite similar stratigraphy: un-

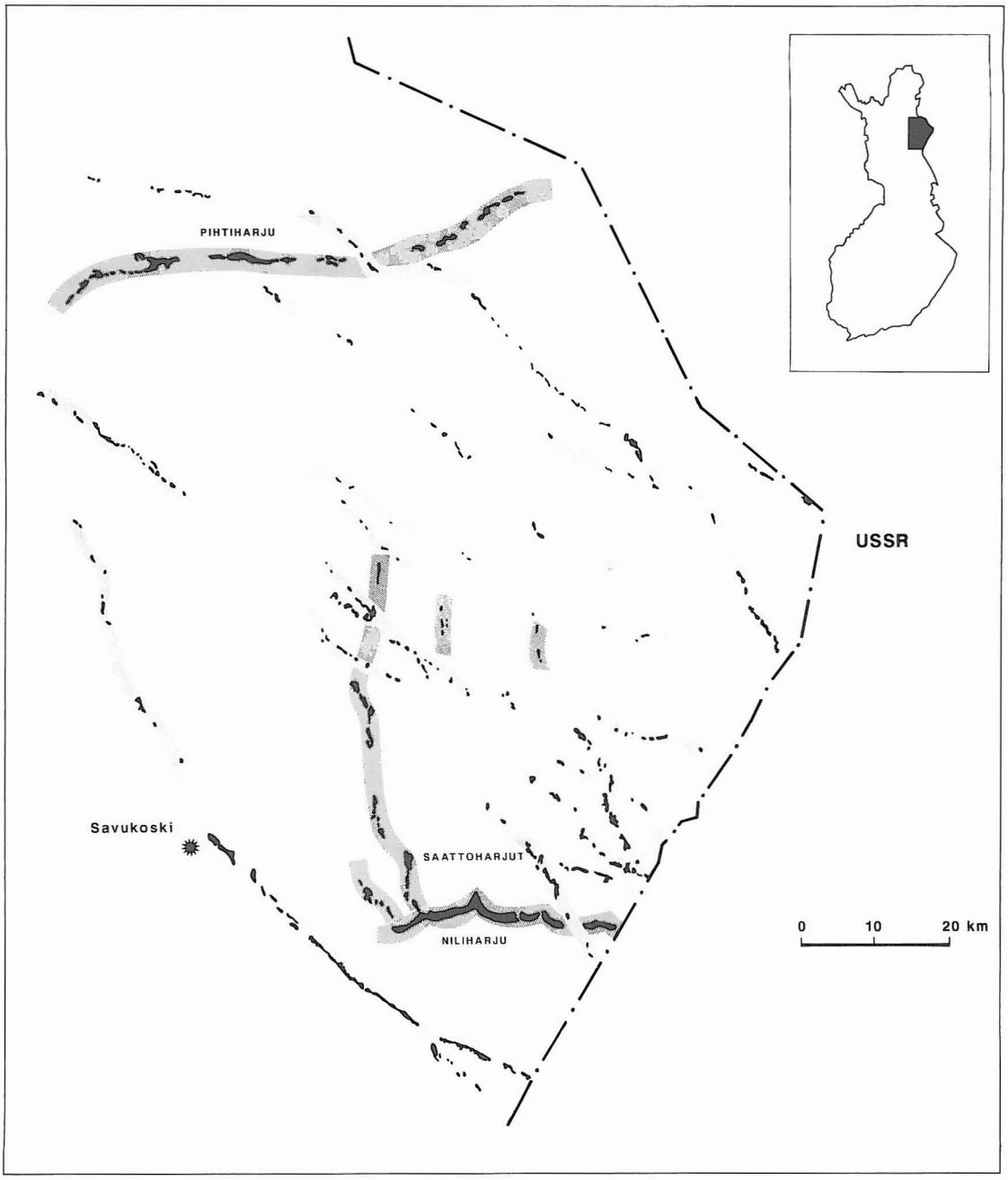

Fig. 101. Esker patterns in the Savukoski area. The Mid-Weichselian Pihtiharju esker deposited from east to west, Saattoharjut from north to south. The Mid-Weichselian ice advance demarcated by the Niliharju endmoraine. The Late Weichselian eskers shown by light shading.

saturated sandy materials with v = 650 — 800 m/s (d = 6 — 8 m) underlain by saturated sandy materials with v = 1400 — 1500 m/s (d = 15 — 13 m).

Kuusajärvi with several other similar landforms, such as Tiukupuljut, Lopsuntievat and Nunospuljut in the Kittilä area clearly indicate an arc-shaped ice margin position. This ice-marginal belt is interpreted to be an end moraine by Kujansuu (1967), and is confirmed here. But he considers the end moraine to be Late Weichselian and resulted from a slight re-advance of the ice margin. However, the general trend of the retreat of the Late Weichselian ice margin was to southwest (Kujansuu 1967 Fig. 51), while the delta foresets and proximal ice-contact slope indicate ice margin retreat to north-northwest. The other argument against the Late Weichselian origin is that all the end moraine ridges and delta plateaus are glacially tectonized and draped by the till trending roughly SW — NE i.e. the latest ice flow direction in the area.

Also, the eskers north from Kuusajärvi — Nunospuljut line seem to have fed the end moraine and are covered by one till unit, as well. The Ollerokka esker delta (Fig. 99) is fanning out in the south, and has a till cover (1 — 2 -meters thick) indicating a trend of SW — NE ice flow (Late Weichselian). According to GPR and seismic survey sandy esker deposits are 10 — 18 meters thick. Seismic wave velocities range from 450 m/s to 650 m/s. Sand is underlain by 18 — 25-meters thick gravel deposits with v = 950 — 1300 m/s. The GWL is near the bedrock surface. The esker materials, as being deposited from north and later draped by till indicate rather older (Early/ Mid Weichselian) than Late Weichselian origin.

Based on the morphologic, stratigraphic, glacial dispersal and sedimentological evidence the Kuusajärvi — Nunospuljut end moraine in western Finnish Lapland represents the terminal ice margin position of an independent stage. Chronostratigraphically it is between the Early Weichselian (pre-Peräpohjolan) and Late Weichselian ice advances. For the Early/ Mid Weichselian age control, palynologic verification, and correlation to the Tärendö and Sargejåk interstadials, the Sammalselkä organics is recommended to be re-examined.

Savukoski, eastern Finnish Lapland

The continuation of the (proposed Early / Mid Weichselian) end moraine in the western Lapland to the eastern Lapland is highly tentative, although there are some significant glaciofluvial complexes (end moraines) and eskers that might be related to the Kuusajärvi — Nunospuljut system and attributed eskers.

In the Savukoski area esker patterns exhibit different orientations (Fig. 101). The Pihtiharju is a large till-covered esker, whose material has been deposited roughly from east to west as indicated on the sedimentological GPR (c.f = 80 MHz, max. twt = 760 ns) survey along the esker (Fig. 102). The 10 — 30 -meters thick foreset sequences slope to the west at an angle from 15° to 35°. The maximum thickness above bedrock based on the last radar arrivals is about 38 meters (assumed unsaturated ε_{gravel} = 5, saturated ε_{gravel} = 16). Only one till unit (Late Weichselian) has been observed to cover the esker material, and the Late Weichselian esker pattern oriented from NW to SE is cross-cutting the Pihtiharju system.

Although no glacial advance(s) from the east have been previously reported the presence of the

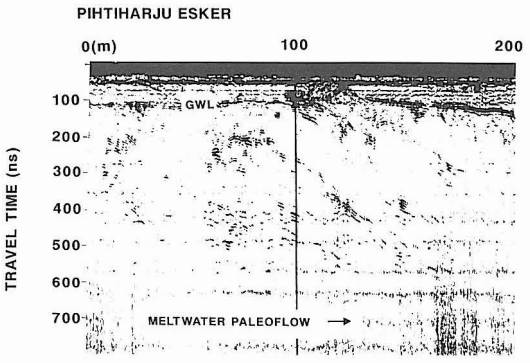

Fig. 102. A 200-meter long portion of radar (c.f. = 80 MHz, max. twt = 760 ns) profile along the Mid-Weichselian Pihtiharju esker. Paleoflow from east to west (left to right in the graph).

Fig. 103. A stretched geometrically corrected (cubic convolution) subimage of Landsat TM-5, 840604, Ch. 7 showing the Niliharju end moraine in Savukoski, North Finland.

esker foresets sloping to the west indicate that at one time ice must have flowed in that direction. Besides the sedimentological evidence, also other features (till cover and crossing esker pattern) are suggesting ice advance after Peräpohjola interstadial, but before the Late Weichselian stage.

Saattoharjut — Niliharju system (Figs. 101 and 103) is another example of till covered glaciofluvial landforms that are cut by the Late Weichselian eskers. The N — S trending Saattoharjut esker fed the W — E -oriented arch-shaped Niliharju glaciofluvial system that is interpreted to be an end moraine. Niliharju can be traced to the east across the Finnish-Soviet border. A GPR survey (c.f = 80 MHz, max. twt from 300 to 450 ns) along the Saattoharjut esker, shows 10 — 20 -meter thick (ε_{sand} = 5, unsaturated and ε_{sand} = 25, saturated) foresets sloping 25° — 30° to the south. The cross-section is similar to that of Vuornosoja esker (Fig. 85). The Saattoharjut-Niliharju system must be older than the cutting Late Weichselian eskers, and it is regarded to be correlative with the Pihtiharju system. Those are tentatively correlated to the Early / Mid Weichselian glaciation in the eastern Finnish Lapland, and the Niliharju end moraine demarcates the maximum extent of that glaciation.

Late Weichselian ice flow pattern

The Late Weichselian landforms and deglaciation are well known in northern Finland (e.g. Kujansuu 1967, Aario 1977, Aario et al. 1974, Aario & Forsström 1979, Nordkalottproject 1986b, 1986c; section glacial landforms in this presentation). Schematic ice flow-line pattern of

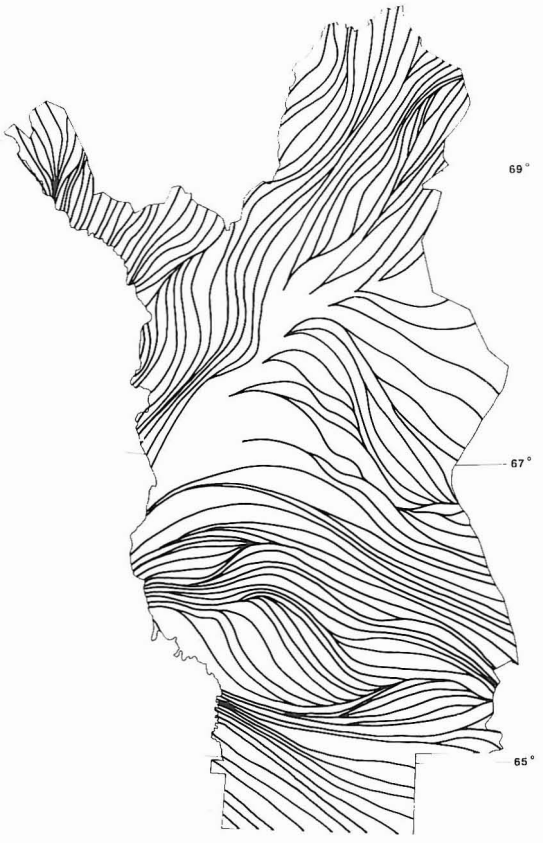

Fig. 104. A schematic Late Weichselian ice flow-line pattern from North Finland. Partially cubic spline fitted with input parameters: orientation and center points of the streamlined morainic features (see Fig. 3).

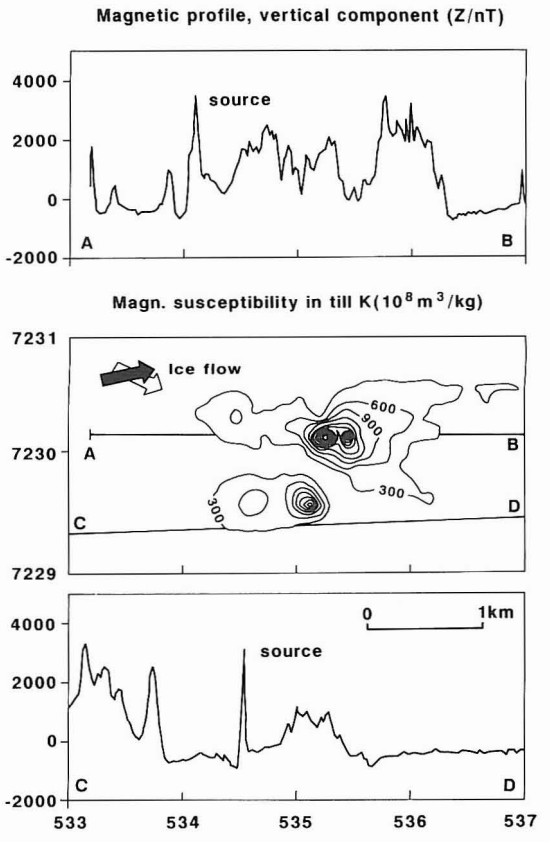

Fig. 105. Glacial dispersal of till expressed by the magnetic mass susceptibility in Jaurakkajärvi, Pudasjärvi.

this phase is presented in Figure 104.

The Late Weichselian glacial erosion and deposition has been weak in the Central Lapland (grussification at Vuotso, Figs. 64 — 65). On the other hand, the drumlins in the Utsjoki and Kuusamo areas, 100 — 200 km away from the center of the Scandinavian ice dome, indicated strong glacial erosion and accumulation. One might consider the glacier transport distance to increase correspondingly, but it is not necessarily the case. An example of glacial dispersal is presented from Jaurakkajärvi, outside the Early Weichselian maximum ice margin position. In the area gently undulating morainic hummocks and ridges superimpose the bedrock, varying in thickness from eight to twenty meters based on the GPR and refraction seismics surveys (Sutinen 1985b). High-altitude airborne magnetic anomalies, suitable for testing the glacial dispersal pattern, were located by the magnetometric profiles (Fig. 105). The magnetic mass susceptibility of till was measured (500 samples) using a TH-1s susceptibility meter by Geoinstruments from the dry-sieved 0.06 — 0.5 mm fraction according to procedures presented by Pulkkinen et al. (1980). Till indicated two susceptibility dispersal fans likely representing a complex transport of the Pre-Weichselian (Saalian) and Late Weichselian ice flows. The surface anomaly is met about one kilometer from the source.

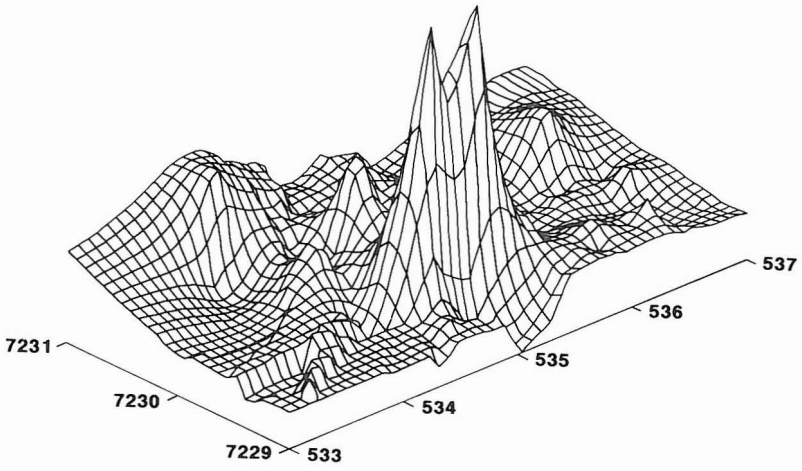

Fig. 106. Glacial dispersal of magnetite-bearing boulders in Jaurakkajärvi, Pudasjärvi.

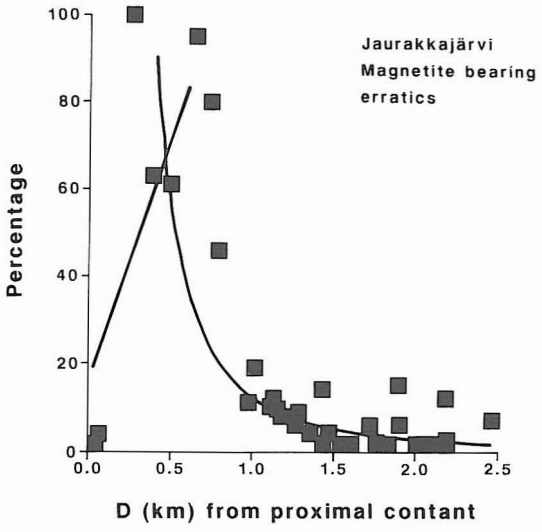

Magnetite bearing surface blocks indicate much shorter transport distance. The magnetic susceptibility of about 5000 stones and blocks were measured (JH-8 by Geoinstruments) at 84 sites. The results, plotted in Figure 106, show the Late Weichselian dispersal of the blocks with the transport distance of less than a half kilometer.

Correlation

One of the main problems in the Eemian-Weichselian chronostratigraphy is the validity of the ^{14}C age estimates reported for interglacial and interstadial intervals. For example, a peat layer at Sokli in North Finland is considered to be Eemian age yielded ^{14}C ages of 46,100 $^{+9,000}/_{-4,000}$ B.P. yr (upper part) and >45,000 B.P. yr (lower part) (Ilvonen 1973). Most of the over one hundred pre-Holocene organic deposits found in North Finland are correlated with the Eemian interglacial on the basis of infinite ^{14}C age estimates and flora characteristics of a climate warmer than present (Hirvas et al. 1977, also Hirvas 1991, Kankainen & Huhta 1984). The Peräpohjola interstadial (Korpela 1969, radiocarbon ages range from about 42,000 to 48,000 B.P. yr) is correlated with the Jämtland interstadial in Sweden and also with the Brörup interstadial in Denmark (see Andersen & Mangerud 1989). However, sediments interpreted as Peräpohjolan has not been found *in situ* at the same stratigraphic section with the Ee-

mian sediments. One possibility is that the Peräpohjolan sediments actually are redeposited Eemian sediments, as proposed by Forsström (1989).

On the basis of microfossil and ^{14}C age estimates Kankainen and Huhta (1984) concluded that 47 % of the subtill organic deposits originated from the Early Weichselian or Eemian period (over 40,000 and over 52,000 B.P. yr) and one third from the Middle Weichselian period (<40,000 B.P. or 40,000 — 50,000 B.P yr). In addition, 16 % of the subtill organic deposits indicate a cool (interstadial) climate, yet yield infinite ^{14}C ages (over 40,000 ... over 52,000 B.P. yr) suggesting Eemian interglacial. The validity of the radiocarbon method for the material of this age range is therefore disputable. Donner et al. (1979), based on the Finnish ^{14}C ages, concluded that Peräpohjola interstadial cannot be dated accurately by the standard ^{14}C-method. Therefore the ^{14}C-age estimates for the Peräpohjola interstadial, 45,400 +/- 2000 B.P. at Kostonniska (Korpela 1969) and its correlatives the Viinivaara interstadial, 49,200 $^{+3200}/_{-2300}$ B.P. and 44,900 $^{+2600}/_{-2000}$ B.P., Isomaa (Johansson & Keinänen 1988), 40,000 $^{+2100}/_{-1700}$ B.P. might be disputable.

I interpret the glacial morphology, till stratigraphy, radar determinations of meltwater paleoflow and the organic deposits (Puhosjärvi, Katosharju and Saarenkylä) as evidence for multiple glacial advances in northern Finland (Figs 107 — 108). The termination of the Early Weichselian Pudasjärvi ice flow stage is marked by the large arc-shaped Pudasjärvi end moraine (proposed by Sutinen 1984). This stage is manifested by the NW — SE trending large-scale drumlins and drumlinoids extending from Kittilä region down to Pudasjärvi and also by several recessional moraines (Sutinen 1984; Nordkalottproject, 1986b; Figs. 89, 99). During this stage the Kemijoki till was deposited, and it may be correlated to the lower till of Korpela (1969), till 3 of Hirvas et al. (1977), also Hirvas (1991), Silas till by Aario (1984) and Tervo (1986) and presumably also to till 3 of Lagerbäck and Robertsson (1988) and till FGI of Olsen (1988).

The Kemijoki till is superimposing the Saarenkylä interglacial organic gyttja at the Saarenkylä type section. Based on the pine dominated pollen flora it suggests the Eemian interglacial. The pollen and diatom flora in the organic Puhosjärvi sequence, stratigraphically located between the Puhosjärvi till (tentatively Saalian) and Jaalanka till (Late Weichselian), clearly records both interglacial and interstadial conditions.

Because the Pudasjärvi end moraine demarcates the Early Weichselian maximum (Sutinen 1984), the Eemian interglacial and Weichselian interstadial deposits are superposed in areas south of Pudasjärvi rendering palynological and chrono-statigraphical interpretation problematic. Oulainen organic deposit, covered by one till unit was, for example, originally interpreted (Forsström 1982) to be interglacial (Eemian) but later correlated with the Early Weichselian Brörup Interstadial (Forsström 1988). The thermoluminescence (TL) dates have been determined for the Oulainen interstadial 94 ka and 121 ka (Jungner 1987). Similarly, the Vimpeli organic sediment initially correlated with the Eemian, but later reinterpreted as Weichselian (Brörup) interstadial (Aalto et al. 1989). The Marjamurto organic sequence in Ostrobothnia, yielding TL-age estimate of 107 +/- 15 ka (Peltoniemi et al. 1989) is described between esker sediments (interpreted as Saalian) and one till unit, and it is correlated with the Oulainen interstadial.

Recent photoluminescence-age estimates of 80 to 140 ka from above and below soil(s) buried beneath one till unit in Ostrobothnia (Kujansuu oral comn.) suggest that the Eemian and Weichselian interstadial (Brörup / Jämtland / Peräpohjola and Odderade / Tärendö) deposits are located at the same stratigraphic position. Consequently the ice advanced over Ostrobothnia and South Finland only once during the Weichselian (see Bouchard et al. 1990), and the period between the isotope stages 5a and 5e of Andersen

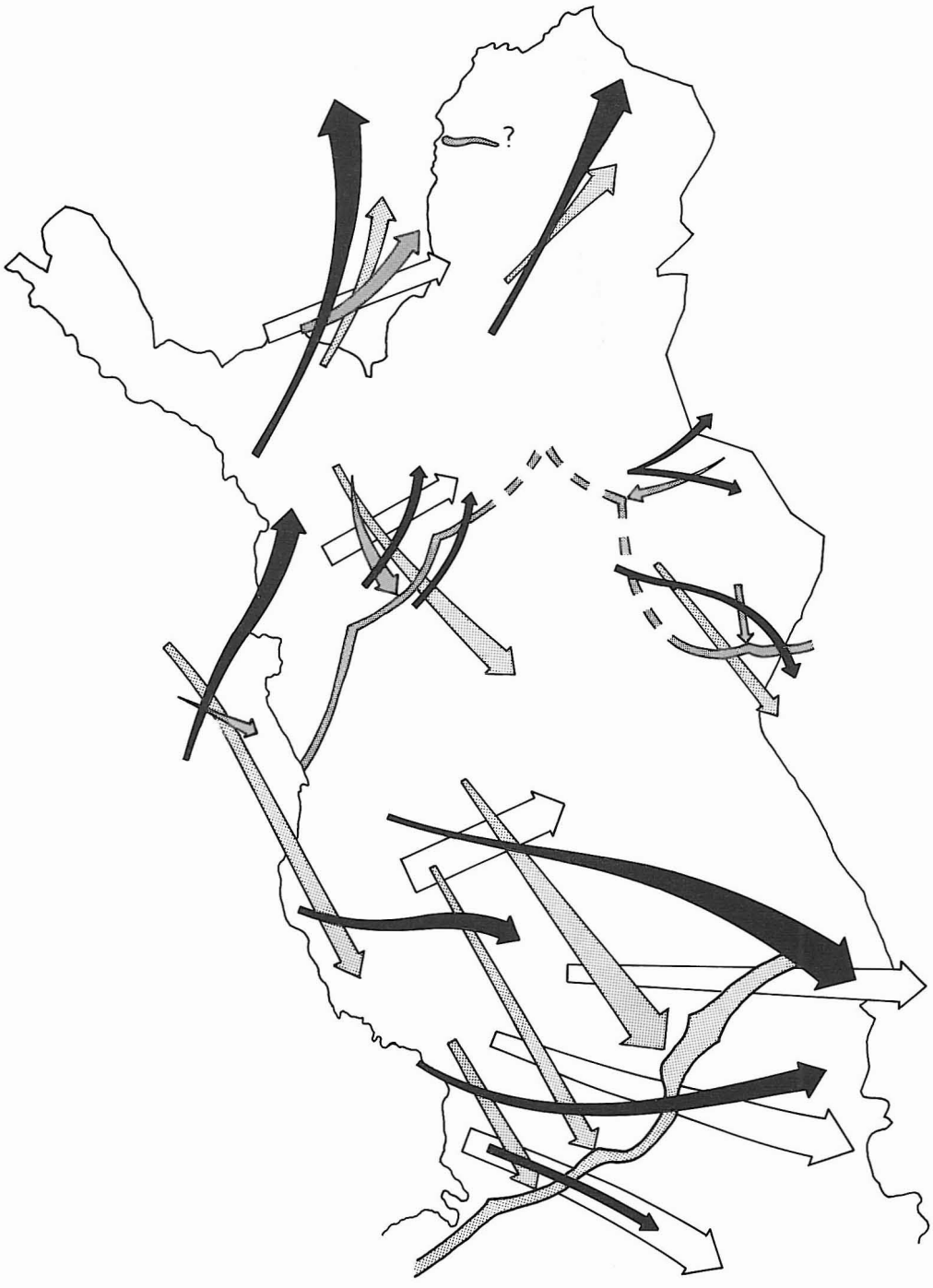

Fig. 107. A schematic presentation of the ice flow stages in northern Finland and adjacent areas in Norrbotten, Sweden and Finnmark, Norway. Partially modified from Aario (1984), Nordkalottproject (1986c), Tervo (1986), Hirvas and Eriksson (1988), Lagerbäck and Robertsson (1988), Olsen (1988). Shading codes same as in Fig. 99.

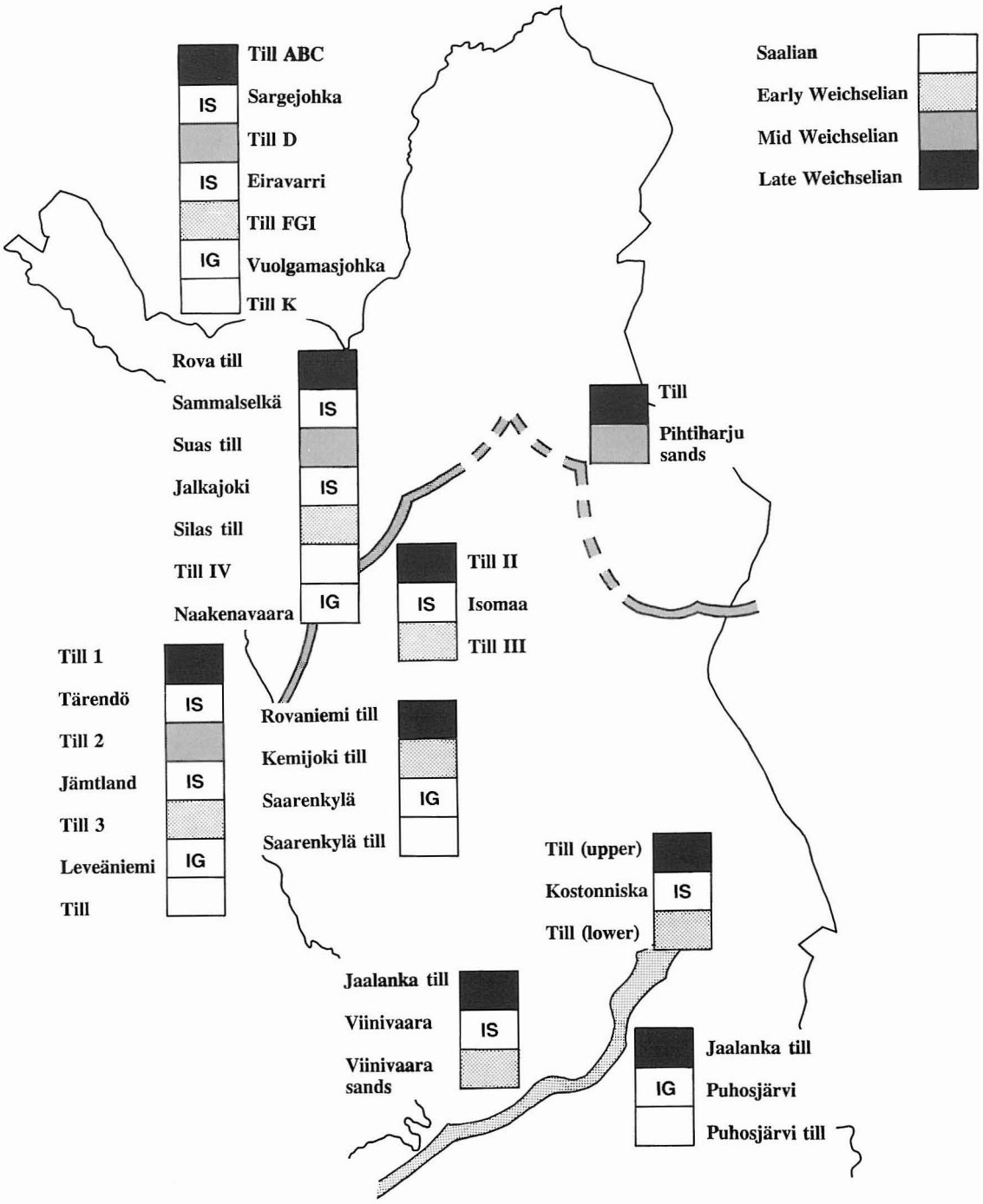

Fig. 108. A schematic correlation of till stratigraphic units in northern Finland and adjacent areas in Norrbotten Sweden and Finnmark, Norway. IS = interstadial, IG = interglacial. Sources: this study, Korpela (1969), Lundqvist (1971), Aario and Forström (1979), Aario (1984), Sutinen (1984), Äyräs and Koivisto (1984), Tervo (1986), Hirvas and Eriksson (1988), Lagerbäck and Robertsson (1988), Johansson and Keinänen (1988), Olsen (1988).

and Mangerud (1989) was ice free south of Pudasjärvi end moraine. Forsström's (1989) conclusion that the Early Weichselian maximum ice margin position was located further south in Estonia is therefore contradictory to the outline presented here, but is supported by the marine stratigraphy by Lykke-Andersen (1987) from Denmark.

Morphologic, stratigraphic, glacial dispersal and radar evidences presume the existence of the previously unrecognized ice flow stage in Lapland (Figs. 107 — 108). This stage, the Lapland ice flow stage, is represented by the Suas till of Aario (1984) and Tervo (1986) in the western Lapland and might be correlative with the isotope stage 5b of Andersen and Mangerud (1989). I propose the Kuusajärvi — Nunospuljut end moraine in Kittilä demarcates that stage, and the Niliharju end moraine in Savukoski is regarded to be a correlative maximum ice margin position in the eastern Finnish Lapland.

Even though the palynologic evidence lacks and there is no age control, the stratigraphic position of the Sammalselkä organic deposit (Äyräs & Koivisto 1984) suggests interstadial younger than Peräpohjola interstadial in Lapland. The stratigraphy is regarded to be correlative to the ones in northern Sweden and Norway, where evidence for two Weichselian interstadials has been presented (Lagerbäck & Robertsson 1988, Olsen 1988). The Sammalselkä site is recommended to be re-examined to verify the suggested correlation to the Tärendö and Sargejåk interstadials.

SUMMARY AND CONCLUSIONS

This presentation summarizes genetic, textural and electrical characteristics of a wide variety of glacial deposits in northern Finland, Wisconsin and Glacier Bay, Alaska. Dielectric properties, measured *in situ* by TDR and GPR techniques in the frequency range from 1 MHz to 1 GHz, and conductivity have been demonstrated to be related to the textural characteristics of glacial materials, thus providing an effective tool for numeric classification and mapping. The electrical terrain data have been applied to digital classification and interpretation of remotely sensed data, particularly airborne gamma radiation and EM data. Since the EM wave propagation is governed by dielectric properties and conductivity, performance and feasibility of GPR have been evaluated for a variety of glacial deposits. Continuous GPR data provide an excellent sedimentological information, which has been used to evaluate raw materials potential of different types of landforms, and those data also were applied to outline and interpret the Pleistocene stratigraphy.

Genetic classification: basal lodgement till, basal melt-out till, flow sediments, (esker) conduit infills, (esker) openwork sediments and fluvial sediments, indicate sedimentary transition, where direct glacial activity gradually changes to secondary processes such as pressure flow, gravity flow and glaciofluvial and fluvial processes. Therefore field recognition of different genetic types of tills is sometimes difficult. Instead, the textural classification and grain size parametristics are shown to be consistent with the above genetic classification as determined by means of graphic sorting and moment kurtosis.

Electrical characteristics of glacial materials are governed by the contained volumetric water content. The *in situ* volumetric water content, demonstrated to be ten to twenty times greater than respective bound water content, is highly determined by the textural characteristics of sediments, particularly the fines and clay content. Since free water dielectrics ($\varepsilon_r = 80$) strongly dominates over bound water dielectrics (similar to that of ice, $\varepsilon_{ice} = 3.5$), in the sediment mix-

tures of water, air (ε_r = 1) and mineral particles (ε_r from 2 to 4), the dielectric differentiation is diagnostic for both unsaturated and saturated glacial materials. Contrary to conductivity, dielectric properties are not salinity dependent. Conductivity of unsaturated materials is demonstrated to be strongly dependent on moisture content, texture and porosity, but the bulk conductivity of saturated materials is strongly dependent on the ground water conductivity. Occasionally local tills may contain conductive minerals such as magnetite in sufficient quantities to increase overall conductivity. Because of the drastic change in the electrical properties below free water freezing point, monitoring of the frozen/ unfrozen interface in glacial materials is possible by TDR and GPR.

Soil moisture content determines indirectly the spectral signatures of the optical airborne and space borne data. Those are indicated in the SPOT and Landsat TM data by vegetation canopy and droughtness variations. However, classification of those data are problematic due to dense variation of different surface patterns, such as culture, farmlands and forests of different ages. The airborne gamma radiation data, particularly potassium window, is directly related to the near-surface (a half meter or less) water content. Since water content is sediment specific, gamma radiation data provide a good basis for mapping of surface materials. The airborne EM data (by the Geological Survey of Finland) indicate directly subsurface conductivity variations. But those data can be effectively applied to mapping of conductive deposits (marine clays/silts) with significant volumes, because the instrumentation (low frequency) is designed mainly for exploration purposes.

Grussificated rock and pinnacle-shaped tor formations, commonly met in unglaciated terrains, presumably have preserved in Central Finnish Lapland at least through the latest glaciation as a result of extremely weak glacial erosion. Glacial erosion and deposition rate increase away from the centers of ice domes. Air photo interpretation and GPR sedimentological data indicate that drumlin patterns have been shaped during several glaciations. For example, drumlins in Wisconsin may compose of large amounts of exploitable sand and gravel as a result of significant large-scale outwash deposition prior to the drumlin shaping. In southern Wisconsin, the drumlin stratigraphy, based on the electrical classification of tills indicates that the Late Wisconsinan (equivalent to Late Weichselian in Fennoscandia) sandy till unit superimpose outwash deposits and silty till unit. Electrically similar silty till has been met outside the maximum Late Wisconsinan ice-margin position suggesting that the core of the drumlin is erosional, and those deposits may date back to Illinoian (equivalent to Saalian). Outwash deposits lack in Finland presumably due to higher-relief topography, and therefore drumlins are composed predominantly of tills. Minor portions of sandy flow deposits occur. But because the cores of drumlins are erosional, glaciofluvial materials, eskers and end moraines, deposited prior to the drumlinization presumably are preserved in some of the drumlins. Those deposits are possible to outline by systematic airborne EM and terrain geophysics surveys, such as GPR and DC resistivity.

Rogen moraines and related subglacial landforms are depositional active-ice forms and are built up of basal till. Bedrock topography seem to have controlled the grounded ice flow and till deposition. Inside the Rogen moraine fields, larger moraine complexes have been shown to contain significant amounts of coarse-textured flow sediments, suitable for construction materials. Flow sediments are deposited by short-lived subglacial slurry flows. This kind landforms contain substitute raw materials reserves for esker deposits.

API reveals morphological transition from streamlined morainic features to eskers in high-relief areas in northern Finland. Esker structures and composition indicate three transitional sedimentation facies, too. Conduit infill core, deposited as a full-pipe slurry flow, is represented by the coarse-textured poorly sorted sedi-

ments. Those are superimposed by the openwork gravels and sands typically showing cross-bedding structures. Deltaic facies terminates the esker sedimentation. Esker materials and other glaciofluvial deposits are excellent GPR targets due to low dielectric properties and conductivity.

GPR investigations of end moraines and till-covered eskers, till stratigraphy and glacial morphology in northern Finland revealed following glacial stages: The Pudasjärvi ice flow stage is manifested by NW — SE trending large-scale streamlined features and very large end moraines, which terminate at Pudasjärvi, and it is correlated with the Early Weichselian. The end moraines contain significant amounts of exploitable gravel and sand and are important ground water sources. The till stratigraphical and palynological evidences consistently show that southern Finland was ice-covered only once during the Weichselian, and the Eemian interglacial and Weichselian interstadial deposits are superposed south from Pudasjärvi. The other (Early or Mid) Weichselian stage, the Lapland stage, is represented by eskers and end moraines in Kittilä and Savukoski areas. The Kuusanjärvi — Nunospuljut end moraine in the western Finnsh Lapland and the Niliharjut end moraine in the eastern Finnish Lapland mark the maximum ice margin position of the Lapland ice flow stage. North Finland was entirely covered by ice during the Late Weichselian.

The EM field techniques applied in this study have many advantages compared to the conventional mapping routines. The portable TDR has been demonstrated to be an accurate technique to determine dielectric properties and water content of surface glacial materials. Dielectric field data are relevant basis for classification of e.g. airborne gamma radiation data. The TDR might be also useful in reforestation planning and in detection of frozen/ unfrozen interface, and monitoring of water content changes in slopes to predict landslide hazards. The EM ground conductivity surveys are shown to be feasible to detect sand and gravel deposits, which are buried by till or silt/ clay sediments.

The GPR is extremely fast and versatile technique to produce continuous subsurface data. The GPR with lower frequencies (c.f. = 80 — 120 MHz) is reliable for materials surveys, detection of ground water level, thickness of peat, determining fresh water depth and monitoring the thickness of frost. Higher frequencies (c.f. = 500 — 1000 MHz) are feasible for many kinds of geotechnical applications and e.g. for testing of quality of building and dimension stones. The disadvantage of GPR, however, is its poor penetration into electrically conductive materials, such as marine silt/ clay deposits and wind-blown loess. Radar signal processing and digital image shape detection will help to interpret data and recognize different types of glacial materials.

None of the presented techniques can alone solve the problems in the Quaternary studies, but the combination of digital processing and interpretation of remotely sensed data and EM terrain data provide a good basis for lateral mapping of surface materials, outlining of raw materials potentials and environmental monitoring.

REFERENCES

Aalto M., Donner J., Hirvas H. & Niemelä J. 1989. An interglacial beaver dam deposit at Vimpeli, Ostrobothnia, Finland. Geol. Surv. Finland, Bull. 348, 34 p.

Aario R. 1972. Associations of bed forms of palaeocurrent patterns in an esker delta, Haapajärvi, Finland. Ann. Acad. Sci. Fenn. Ser. A, 111, 55 p.

Aario R. 1977. Classification and terminology of morainic landforms in Finland. Boreas 6, 87—100.

Aario R. 1984. Jäätikkösyntyisten maaperämuodostumien koostumus, ominaisuudet ja käyttösoveltuvuus. Määräaikainen loppuraportti Suomen Akatemian tutkimusprojektista 04—114.

Aario R. 1987. Drumlins of Kuusamo and Rogen-ridges of Ranua, northeast Finland. *In* J. Menzies and J. Rose (eds.), Drumlin Symposium. Balkema, Rotterdam, 87 — 102.

Aario R. & Forsström L. 1979. Glacial stratigraphy of Koillismaa and North Kainuu, Finland. Fennia 157 (2), 1 — 49.

Aario R., Forsström L. & Lahermo P. 1974. Glacial landforms with special reference to drumlins and fluting in Koillismaa, Finland. Geol. Surv. Finland, Bull. 273, 30 p.

Aario R. & Pernu T. 1990. The Säynäjäluoma drumlin. Excursion quide. III Intl. drumlin symposium. Nordia Ser A. 1. 38 — 42.

Aarnisalo J. 1984. Image processing and integration of geophysical, Landsat and other data as a tool for mineral exploration in glaciated Precambrian terrain. *In* ERIM Proceedings of International Symposium on Remote Sensing for Exploration Geology 1. Colorado Springs, 107 — 128.

Acomb L.J., Mickelson D.M. & Evenson E.B. 1982. Till stratigraphy and late glacial events in the Lake Michigan Lobe of eastern Wisconsin. Geol. Soc. Am. Bull. 83, 289 — 296.

Ahokas H. 1984. Maaperätutkan ja suosondin soveltuvuus polttoturve-tutkimuksiin. IVO R-tutkimukset R-84-2. IVO, Helsinki, 28 p.

Alden W.C. 1918. The Quaternary geology of southeastern Wisconsin, with a chapter on the older rock formations. U.S. Geol. Survey Prof. Paper 106, 356 p.

Alharthi A. & Lange J. 1987. Soil Water Saturation: Dielectric Determination. Water Resources Research 23 (4), 591 — 595.

Alley R.B. 1991. Deforming-bed origin for southern Laurentide till sheets. Journal of Glaciology 37 (125), 67 — 76.

Andersen B.G. & Mangerud J. 1989. The last interglacial-glacial cycle in Fennoscandia. Quaternary International 3/4, 21 — 29.

Andersson S. 1960. Kapillaritet. Uppsala.

Andersson S. 1967. Den organiska substansen i våra jordar och vattenbindningen. Uppsala.

Andersson S. & Wiklert P. 1972. Om de vattenhållande egenskaperna hos svenska jordarter. Grundförbättring 2 (3). Uppsala.

Annan A.P. & Davis J.L. 1976. Impulse radar sounding in permafrost. Radio Science 11 (4), 383—394.

Annan A.P. & Davis J.L. 1977. Impulse radar applied to ice thickness measurements and freshwater bathymetry. Geol. Surv. Can. Paper 77—1B, 63 — 65.

Annan A.P. & Davis J.L. 1977b. Radar range analysis for geological materials. Geol. Surv. Can. Paper 77—1B, 117 — 124.

Arcone A. 1984. Pulse transmission through frozen silt. U.S.Army CRREL Report 84 — 17, 10 p.

Arcone S.A. 1990. UHF model simulation of detecting voids in a dielectric medium using HF-VHF airborne short-pulse radar. U.S.Army CRREL Rept. 90 — 11, 12 p.

Arcone A. & Delaney A.J. 1984. Radar investigations above the trans-Alaska pipeline near Fairbanks. U.S.Army CRREL Report 84 — 27, 15 p.

Attig J.W., Mickelson D.M. & Clayton L. 1989. Late Wisconsin landform distribution and glacier-bed conditions in Wisconsin. Sedimentary Geology 62 (2/4), 399 — 406.

Aylsworth J.M. & Shilts W.W. 1989. Bedforms of the Keewatin Ice Sheet, Canada. Sedimentary Geology 62 (2/4), 407 — 428.

Äyräs M. & Koivisto T. 1984. Pokan karttalehtialueen geokemiallisen kartoituksen tulokset. Geol. Surv. Finland, Explanatory notes to geochemical maps, Sheets 2744 and 3722. Summary: The results of the geochemical survey in the areas of the Pokka map-sheets. 35 p.

Baker J.M. & Allmaras R.R. 1990. System for automating and multiplexing soil moisture measurement by time-domain reflectometry. Soil. Sci. Soc. Am. Journal 54 (1), 1 — 6.

Baker T.H.W, Davis J.L., Hayhoe H.N., & Topp G.C. 1982. Locating the frozen-unfrozen interface in soils using time-domain reflectometry. Can. Geotech. Jour. 19, 511 — 517.

Banerjee I. & McDonald B.C. 1975. Nature of esker sedimentation. *In* Glaciofluvial and Glaciolacustrine Sedimentation, ed. by A. V. Jopling and B. C. McDonald. Spec. Publs. Soc. Econ. Paleont. Miner., Tulsa 23, 132 — 154.

Barnes D.F. 1990. Gravity, gravity-change and other geophysical measurements in Glacier Bay National Park and Preserve. Proc. 2nd Glacier Bay Science Symposium 1988. Gustavus, Alaska. 12 — 18.

Berg F., Andreasen F. & Ahrentzen P. 1983. Georadar till, sand- og gruskortlegning. Et samarbejdsprojekt mellem fredningstyrelsen, Danmarks Geologiske Undersfogelse og Statens Veijlaboratorium. Statens Veijlaboratorium. Interne notater 147, Vedirektoratet. Kobenhavn. 44 p.

Bjelm L., Follin S. & Svensson C. 1982. Georadar som undersökningsmetod. BFR project No. 800141—9, Coden: LUTVDG/(TVTG-3002)/1—71.

Bleuer N.K. 1971. Glacial stratigraphy of south-central Wisconsin. Unpubl. Ph.D. Thesis, Univ. of Wisconsin-Madison, 173 p.

Bogorodsky V.V., Bentley C.R. & Gudmansen P.E. 1985. Radioglaciology. D. Reidel Publ. Co. Dordrecht, Holland. 251 p.

Bouchard M.A. 1980. Late Quaternary geology of the Temiscamie area, central Quebec. Unpubl. Ph.D. thesis, McGill University, 284 p.

Bouchard M.A. 1989. Subglacial landforms and deposits in central and northern Quebec, Canada, with emphasis on Rogen moraines. Sedimentary Geology 62 (2/4), 293 — 308.

Bouchard M.A., Gibbard P & Salonen V.P. 1990. Lithostratotypes for Weichselian and Pre-Weichselian sediments in southern and western Finland. Bull. Soc. Geol. Finland 62 (1), 79 — 95.

Boulton G.S. 1970. On the origin and transport of englacial debris in Svalbard glaciers. Journal of Glaciology 9 (56), 213—229.

Boulton G.S. 1972. Modern arctic glaciers and depositional models for former ice sheets. J. Geol. Soc. 128, 361 — 393.

Boulton G.S. 1982. Subglacial processes and the development of glacial bedforms. *In* Research in glacial Glaciofluvial and Glaciolacustrine Systems. 6th Guelph Symp. on Geomorph, ed. by R. Davidson — Arnott, W. Nickling and B.D. Fahey. Geo Books, Norwich. 1 — 31.

Boulton G.S. 1987. A theory of drumlin formation by subglacial sediment deformation. *In* Drumlin symposium, ed. by J. Menzies & J. Rose. Balkema, Rotterdam. 25 — 80.

Burson Z.G. 1973. Airborne surveys of terrestrial gamma radiation in environmental research. IEEE Nuclear Science Symposium 558 — 571.

Carey S.W. & Ahmad N. 1961. Glacial marine sedimentation. First Internat. Symposium of Geology of Arctic, Proc. 2, 865 — 894.

Cihlar J & Ulaby F.T. 1974. Dielectric Properties as a Function of Moisture Content. RSL Tech. Rep. 177—47. Remote Sensing Laboratory. The University of Kansas Center for Research, Inc. 47 p.

Clark P.U. & Hansel A.K. 1989. Clast ploughing, lodgement and glacier sliding over a soft glacier bed. Boreas 18, 210 — 207.

Culley R.W., Jagodits F.L. & Middleton R.S. 1975. E-phase system for detection of buried granular deposits. Symposium on modern innovations in subsurface exploration. 54th Annual Meeting of Transportation Research.

Curry B.B. 1989. Absence of Altonian Glaciation in Illinois. Quaternary Research 31, 1 — 13.

Dalton F.N., Herkelraht W.N., Rawlins D.S., & Rhoades J.D. 1984. Time-Domain Reflectometry: Simultaneous Measurement of Soil Water Content and Electrical Conductivity with a Single Probe. Science 224, 898 — 990.

Daniels J.J. 1989. Fundamentals of ground penetrating radar. Proc. Symposium on the application of geophysics to engineering and environmental problems (SAGEEP'89) Golden Co. 62 — 142.

Dardis G.F. & McCabe A.M. 1983. Facies of subglacial channel sedimentation in late-Pleistocene drumlins, Northern Ireland. Boreas 12, 263 — 278.

Dasberg S. & Dalton F.N. 1985. Time domain reflectometry field measurements of soil water content and electrical conductivity. Soil Sci. Soc. Am. J. 49, 293 — 297.

Davies J.L., Topp G.C. & Annan A.P. 1977. Measuring Soil Water Content In Situ Using Time-Domain Reflectometry Techniques. Geol. Surv. Can. Paper 77—1B, 33 — 36.

Davis J.L. 1975. Relative Permittivity Measurements of a Sand and Clay Soil In Situ. Geol. Surv. Can. Paper 75—1 (C), 361 — 365.

Davis J.L. & Chudobiak W.J. 1975. In Situ Meter for Measuring Relative Permittivity of Soils. Geol. Surv. Can. Paper 75—1 (A), 75 — 79.

Davis J.L. & Annan A.P. 1977. Electromagnetic Detection of Soil Moisture: Pregress Report. Can. Jour. of Remote Sensing 3 (1), 76 — 86.

Day B.A. & Nightingale H.I. 1984. Relationship between ground-water silica, total dissolved solids, and specific electrical conductivity. Groundwater 22 (1), 80 — 85.

De Loor G.P. 1983. The Dielectric Properties of Wet Materials. IEEE Transactions on Geoscience and Remote Sensing, GE-21 (3), 364 — 369.

Delaney A.J. & Arcone A. 1982. Laboratory measurements of soil electric properties between 0.1 an 5 GHz. U.S.Army CRREL Report 82—10. 7 p.

Denny J.E., Yarger H.L., Macfarlane P.A., Knapp R.W., Sophocleus M.A., Lucas J.R. & Steeples D.W. 1984. Remote sensing and geophysical investigations of glacial buried valleys in northeastern Kansas. Groundwater 22 (1), 56 — 65.

Dobson M.C., Ulaby F.T., Hallikainen M.T. & El-Rayes M.A. 1985. Microwave Dielectric Behaviour of Wet Soil-Part II: Dielectric Mixing Models. IEEE Transaction on Geoscience and Remote Sensing GE-23 (1), 35 — 46.

Donner J., Jungner H. & Kurtén B. 1979. Radiocarbon dates of mammoth finds in Finland compared with radiocarbon dates of Weichselian and Eemian deposits. Bull. Geol. Soc. Finland 51, 45 — 54.

Donner J. 1980. The determination and dating of synchronous Late Quaternary shorelines in Fennoscandia. *In* Earth Rheology, Isostasy and Eustasy, ed. by N. Mörner. John Wiley & Sons Ltd. 285 — 293.

Dreimanis A. 1979. The problems of waterlain tills. *In* Moraines and Varves, ed. by Ch. Schlucter. Rotterdam, A.A. Balkema, 167—177.

Dreimanis A. 1982. Work group (1) — Genetic classification of tills and criteria for their differentiation: Progress report on activities 1977—1982, and definitions of glacigenic terms. *In* INQUA Commission on genesis and lithology of Quaternary deposits, ed. by Ch. Schluhter. Report on activities 1977—1982, ETH, Zurich, 12 — 31.

Dreimanis A. 1989. Tills: Their genetic terminology and classification. *In* Genetic Classification of Glacigenic Deposits, ed. by R.P. Goldthwait and C.L. Matsch. A.A. Balkema, Rotterdam, 17 — 83.

Edwards W.A.D. & Richardson R.J.H. 1989. Remote sensing techniques for sand and gravel exploration by the Al-

berta Geological Survey. Proc. 7th Thematic Conference on Remote Sensing for Exploration Geology. 151 — 165.

Enkovaara A., Härme M. & Väyrynen H. 1952. General geological map of Finland, 1 : 400 000. Pre-Quaternary rocks. Sheet C5 and B5, Oulu and Tornio. Geological Survey of Finland, Helsinki.

Eriksson B. 1982. Piirteitä interglasiaalikerrostumien siitepölyfloorista. Geologi 34 (9 — 10), 179 — 180.

Eronen M. 1983. Late Weichselian and Holocene shore displacement in Finland. *In* Shoreline and Isostasy, ed. by D.E. Smith & A.G. Dawson. Institute of British Geographers, Spec. Publ. 16. Academic Press. 183 — 205.

Evans S.G. & Clague J.J. 1989. Rain-induced landslides in the Canadian Cordilliera, July 1988. Geoscience Canada 16 (3), 193 — 200.

Evenson E.B. 1971. The relationship of macro- and microfabric of till and the genesis of landforms in Jefferson County, Wisconsin. *In* Till — A Symposium, ed. by R.P. Goldwaith. Ohio State University Press, 345 — 346.

Fellner-Feldegg H. 1969. The Measurement of Dielectrics in the Time Domain. The Journal of Physical Chemistry 73 (3), 616 — 623.

Flint R.F. 1971. Glacial and Quaternary Geology, John Wiley & Sons, New York. 892 p.

Flint R.F., Sanders J & Rodgers J. 1960. Diamictite, a substitute term for symmictite. Geol Soc. Am. Bull. 71, 1809 p.

Folk R.L. 1966. A review of grain size parameters. Sedimentology 6 (2), 73 — 93.

Folk R.L. & Ward W.C. 1957. Brazos River bar, a study in the significance of grain size parameters. Jour. Sed. Petr. 27, 3 — 27.

Forsström L. 1982. The Oulainen interglacial in Ostrobothnia, western Finland. Acta Univ.. Ouluensis A, 136. Geol. 4, 123 p.

Forsström L. 1988. The northern limit of pine forest in Finland during the Weichselian interstadials. Ann. Acad. Sci. Fennicae A III, 147, 24 p.

Forsström L. 1989. The Fennoscandian ice sheet in the last half a million years. Nordia 32 (2), 91 — 103.

Friedman G.M. 1962. Comparison of moment measures for sieving and thin-section data in sedimentary petrological studies. Jour. Sed. Petr. 32 (1), 15 — 25.

From E. 1965. Beskrivning till jordartskarta över Norrbottens län nedanför Lappmarksgränsen. Sver. Geol. Unders. Ser. Ca. 39, 236 p.

Gaál G. (ed.) 1988. Exploration target selection by integration of geodata using statistical and image processing techniques: an example from Central Finland. Geol. Surv. Finland, Rept. Invest. 80. 156 p.

Geikie A. 1863. On the phenomena of the glacial drift in Scotland. Geol. Soc. Glasgow, Trans. 1, 190 p.

Geonics 1982. Operating manual for EM31 non-contacting terrain conductivity meter. Geonics limited, Ontario, Canada, 58 p.

Geophysical Survey Systems, Inc. 1980. Operation manual Subsurface Interface Radar, SIR system 8. 81 p.

Goldthwait R.P. 1974. Rates of formation of glacial features in Glacier Bay, Alaska. *In* Glacial Geomorphology, Binghampton NY, ed. by D.R. Coates, Publications in Geomorphology, SUNY-Binghampton, 165 — 185.

Goldthwait R.P. 1986. Glacial history of Glacier Bay park area. *In* Observed processes of glacial deposition ion Glacier Bay, Alaska. ed. by P.J. Anderson, R.P. Goldthwait & G.D. Mckenzie Misc. Publ. Byrd Polar Research Center, 236, 5 — 16.

Goldthwait R.P. 1989. Classification of glacial morphologic features. *In* Genetic Classification of glacigenic deposits, ed. by R.P. Goldthwait & C.L. Matsch. A.A. Balkema, Rotterdam, 267 — 278.

Goldthwait R.P. & Matsch C.L. (eds.) 1989. Genetic Classification of glacigenic deposits. A.A. Balkema, Rotterdam, 294 p.

Gonzales R.C. & Wintz P. 1987. Digital Image Processing. Second Edition. Addison-Wesley Publishing Company. 503 p.

Gorecki R.C., Schmidt B.J. & Smith D.G. 1989. The application of satellite remote sensing to aggregate exploration in northwestern Alberta. Proc. 7th Thematic Conference on Remote Sensing for Exploration Geology. 701 — 712.

Gorrell G. & Shaw J. 1991. Deposition in an esker, bead and fan complex, Lanark, Ontario, Canada. Sedimentary Geology 72, 285 — 314.

Grasty R.L. 1977. Applications of gamma radiation in remote sensing. *In* Remote sensing for environmental sciences, ed. by Shanda. Springer-Verlag, New York, 257 — 276.

Gravenor C. G., von Brunn V. & Dreimanis A. 1984. Nature an classification of waterlain glaciogen sediments, exemplefied by Pleistocene, Late Paleozoic and Late Precambrian deposits. Earth-Science Reviews 20 (2), 105 — 166.

Grönlund T. 1991. The diaton stratigraphy of the Eemian Baltic Sea on the basis of sediment discoveries in Ostrobothnia, Finland. Geol. Surv. Finland, Rept. Invest. 102, 26 p.

Hadley D.W. & Pelham J.H. 1976. Glacial deposits of Wisconsin. Map 10. Cartographic lab., Univ. of Wisconsin-Madison.

Hallikainen M.T., Ulaby F.T., Dobson M.C., El-Rayes M.A. & Wu L-K. 1985. Microwave Dielectric Behavior od Wet Soil-Part I: Empirical Models and Experimental Observations. IEEE Transactions on Geoscience and Remote Sensing GE-23 (1), 25 — 34.

Hänninen, Pekka 1991. Maatutkaluotaus maaperägeologisissa tutkimuksissa. Summary: Ground penetrating radar in Quaternary geological studies. Geol. Surv. Finland, Rept. Invest. 103, 33 p.

Hansel A.K., Johnson W.H. & Socha B.J: 1987. Sedimentological characteristics and genesis of basal tills at Wedron, Illinois. Geol. Surv. Finland, Spec. Paper 3, 11 — 22.

Hanvey P.M. 1989. Stratified flow deposits in a Late Pleistocene drumlin in northwest Ireland. Sedimentary Geology 62 (2/4), 211 — 222.

Hartshorn J.H. 1958. Flowtill in southeastern Massachusetts. Geol. Soc. Am. Bull. 69, 477 — 482.

Hayhoe H.N., Topp G.C. & Bailey W.G. 1983. Measurements of soil water contents and frozen soil depth during a thaw using time domain reflectometry. Atmos.

Ocean 21 (3), 299 — 310.

Hipp J.E. 1974. Soil Electromagnetic Parameters as Functions of Frequency, Soil Density, and Soil Moisture. Proc. IEEE 62 (1), 98 — 103 .

Hirvas H. 1991. Pleistocene stratigraphy of Finnish Lapland. Geol. Surv. Finland, Bull. 354. 123 p.

Hirvas H. & Eriksson B. 1988. Naakenavaara-Interglacialen — en Pre-Eemisk torvförekomst i Kittilä i norra Finland. Abstracts. 18 Nordiske Geologiske Vintermöde. Kobenhavn, p. 164.

Hirvas H., Alfthan A., Pulkkinen E., Puranen R. & Tynni R. 1977. Raportti malminetsintää palvelevasta maaperätutkimuksesta Pohjois-Suomessa vuosina 1972 — 1976. Summary: A report on glacial drift investigations for ore prospecting purposes in northern Finland 1972 — 1976. Geol. Surv. Finland, Rep. Invest. 19, 54 p.

Hoekstra P. & McNeill J.D. 1973. Electromagnetic probing of permafrost. Proc. Second Intl. Conference on Permafrost. Yakutsk, USSR, 517 — 526.

Hoekstra P. & Delaney A. 1974. Dielectric Properties of Soils at UHF and Microwave Frequencies. Jour. Geophys. Res. 79 (11), 1699 — 1708.

Holloway A.L., Soonawala N.M. & Collett L.S. 1986. Three-dimensional fracture mapping in granite excavations using ground-penetrating radar: CIM Bull. 79 (896), 54 — 59.

Horner R. 1990. Seismicity in the Glacier Bay region on southeast Alaska and adjacent areas of British Columbia. Proc. 2nd Glacier Bay Science Symposium 1988. Gustavus, Alaska. 6 — 11.

Hyvönen E., Sutinen R. & Kairakari H. 1991. Application of airborne geophysics to soils mapping. 11th Annual IGARSS'91, Espoo, 3, 1683 — 1686.

Hyyppä J. 1983. Suomen kallioperän preglasiaalisesta rapautumisesta. Rapautuminen kallioperässä, Symposium 9.11.1983. Rakennusgeologinen Yhdistys — Byggnadgeologiska föreningen. Julkaisuja 15, II/1—8. 17 p.

Ignatius H., Korpela K. & Kujansuu R. 1980. The deglaciation of Finland after 10,000 B.P. Boreas 9, 217 — 228.

Ilvonen E. 1973. Eem-kerrostuma Savukosken Soklilla. Summary: An Eemian Interglacial deposit at Sokli in Savukoski. Geologi 25, 81 — 84.

Inkster D.R., Rossiter J.R., Goodman R., Galbrait M. & Davis J.L. 1989. Ground penetrating radar for subsurface environmental applications. Proc. 7th Thematic Conference on Remote Sensing for Exploration Geology. 127 — 140.

Isherwood D. & Street A. 1976. Biotite-induced grussification of the Boulder Creek Granodiorite, Boulder County, Colorado. Geol. Soc. Am. Bull., 87, 366 — 370.

Jackson T.J. & O'Neill P.E. 1983. Salinity Effects on the Microwave Emission of Soils. IEEE Transactions on Geoscience and Remote Sensing GE-25 (2), 214 — 220.

Jackson P.D., Smith D.T. & Standford P.N. 1978. Resistivity-porosity-particle shape relationships for marine sands. Geophysics 43 (6), 1250 — 1268.

Jezek K.C., Clough J.W., Bentley C.R. & Shabtaie S. 1978. Dielectric permittivity of glacier ice measured *in situ* by radar wide-angle reflection. J. Glaciol. 21 (85), 315 — 329.

Johansson P. & Keinänen V. 1988. Raportti malminetsinnällisistä maaperätutkimuksista Kittilän Hormakummussa vuosina 1987 ja 1988 sekä Isomaasta löydetystä interstadiaalikerrostumasta. Geol. Surv. Finland, Rep. P.2.23.4.003. 5 p.

Jungner H. 1987. Thermoluminescence dating of sediments from Oulainen and Vimpeli, Ostrobothnia, Finland. Boreas 16, 231 — 235.

Kankainen T. & Huhta P. 1984. Problems in dating the Weichselian in northern Fennoscandia. AMS'84. Proc. 3th Intl. Symp. on Accelerator Mass Spectrometry, Zurich p. 63.

Kauranne L.K., Gardemeister R., Korpela K. & Mälkki E. 1972. Rakennusgeologia II. TKY/ Otapaino, Espoo. 528 p.

Keller G.V. & Frischknecht F.C. 1965. Electrical methods in geophysical prospecting. Pergamon Press, Oxford, 517 p.

Kellomäki A. & Nieminen P. 1986. Adsorption of water on the fine fractions of Finnish tills. Bull. Geol. Soc. Finland 58 (2), 13 — 19.

Kihlblom U. 1970. Flygbildstolkning för jordartsbestämning. Stockholm, Svenska Utbildningsförlaget. 189 p.

King R.W. & Smith G.S. 1981. Antennas in Matter. MIT Press, 868 p.

Korpela K. 1969. Die Weichsel-Eiszeit und ihr Interstadial in Peräpohjola (Nördliches Nordfinnland) im Licht von Submoränen Sedimenten. Ann. Acad. Sci. Fenn. Ser. A III, 99. 108 p.

Kovacs A. 1990. Investigation of the LIZ-3 dew line station water supply lake. U.S.Army CRREL Spec. Rept. 90—11, 10 p.

Kovacs A. & Gow A.J. 1977. Dielectric constant and reflection coefficient of the near-surface internal layers in the McMurdo Ice Shelf. Antarctic J. of the U.S. 12, 137 — 138.

Kovacs A. & Morey R.M. 1983. Detection of cavities under concrete pavement. U.S. Army CRREL Report 83—18. 41 p.

Kovacs A., Gow A.J., Cragin J.H. & Morey R.M. 1982. The brine zone in the McMurdo Ice Shelf: Antarctica. U.S. Army CRREL Report 82—39, 28 p.

Krumbein, W. C. 1934. Size frequency distributions of sediments. Jour. Sed. Petr. 4, 65 — 77.

Kuittinen R. & Vironmäki J. 1980. Aircraft gamma-ray spectrometry in Snow water equivalent measurements. Hydrogeological Sciences Bulletin 25 (3), 63 — 75.

Kujansuu R. 1967. On the deglaciation of western Finnish Lapland. Bull. Comm. géol. Finlande 232, 98 p.

Kujansuu R. 1972. On landslides in Finnish Lapland. Geol. Surv. Finland, Bull. 256. 22 p.

Lagerbäck R. 1988. The Veiki moraines in northern Sweden-widespread evidence of an Early Weichselian deglaciation. Boreas 17, 469 — 486.

Lagerbäck R. 1990. Late Quaternary faulting and paleoseismicity in northern Fennoscandia, with particular reference to the Landsjärv area, norhern Sweden. Geol. Fören. Stockh. Förh. 112. 333 — 354.

Lagerbäck R. & Robertsson A.-M. 1988. Kettle holes-stratigraphical archives for Weichselian geology and paleoenvironment in northernmost Sweden. Boreas 17, 439 — 468.

Lahermo P., Ilmasti M., Juntunen R. & Taka M. 1990. The

geochemical atlas of Finland, part 1: The hydrogeochemical mapping of Finnish groundwater. Geol. Surv. Finland, Espoo. 66 p.

Landim P.M.B & Frakes L.A. 1968. Distinction between tills and other diamictons based on textural characteristics. Jour. Sed. Petr. 38 (4), 1213 — 1223.

Lanne E. 1986. Statistical multivariate analysis of airborne geophysical data on the SE border of the Central Lapland greestone complex. Geophysical Prospecting 34, 1111 — 1128.

Lappalainen E., Hänninen Pauli, Hänninen Pekka, Koponen L., Leino J., Rainio H. & Sutinen R. 1984. Geofysikaalisten mittausmenetelmien soveltuvuus maaperätutkimuksiin. Interim Report P 13.4/84/157. Geol. Surv. Finland, Espoo.

Larsen E., Gulliksen S., Lauritzen S-E., Lie R., Lovlie R. & Mangerud J. 1987. Cave stratigraphy in western Norway; multiple Weichselian glaciations and interstadial vertebrate fauna. Boreas 16, 276 — 292.

Larson G. J. 1978. Meltwater storage in a temperate glacier, Burroughs Glacier, souteast Alaska. The Ohio State Univ. Inst. of Polar Stud. Rept. 66, 56 p.

Lawrushin Yu. A. 1970. Recognition of facies and subfacies in ground moraine of continental glaciations. Lithology and economic deposits 6, 684 — 692.

Lawson D. E. 1979. Sedimentological analysis of the western terminus region of the Matanuska Glacier, Alaska. U.S.Army CRREL Rep. 79—9, 122 p.

Lee H.A. 1965. Investigations of eskers for mineral exploration. Geol. Surv. Can. Paper 65—14, 17 p.

Leschanskii Yu. I, Lebedeva G. N. & Schumilin F.D. 1971. Electrical parameters of sandy and loamy soils in the range of centimeter, decimeter and meter wavelengths. Izvest. Vuz. Ucheb. Zaved. Radiophyhyz. 14, 562 — 569.

Lillesand T.M. & Kiefer R.W. 1987. Remote sensing and image processing. John Wiley & Sons, Inc. 721 p.

Lindroos P. & Nieminen P. 1982. Maaperäkartoituksen uusi moreeniluokitus. Geologi 4, 65 — 67.

Lundqvist J. 1969. Problems of the so-called Rogen moraine. Sveriges Geol. Unders. Ser C 648, 32 p.

Lundqvist J. 1971. The Interglacial deposit at the Leveäniemi mine, Svappavaara, Swedish Lapland. Sver. Geol. Unders. Ser. C 658, 163 p.

Lundqvist J. 1977. Till in Sweden. Boreas 6, 73 — 85.

Lundqvist J. 1979. Morphogenetic classification of glaciofluvial deposits. Sver. Geol. Unders. Ser. C 767, 72 p.

Lundqvist J. 1989. Rogen (ribbed) moraine-identification and possible origin. Sedimentary Geology 62 (2/4), 281 — 292.

Lykke-Andersen A.-L. 1987. A Late Saalian, Eemian and Weichselian marine sequence at Norre Lyngby, Vendsyssel, Denmark. Boreas 16, 345 — 357.

Lynn W. C. & Grossman R. B. 1970. Observations of certain soil fabrics with the scanning electron microscope. Proc. Soil Sci. Soc. Amer. 34 (4), 645 — 648.

Maher L.J. Jr. 1981. The Green Bay Lobe began to retreat 12,500 BP: Total pollen flux during the early Greatlakean Substage (11,900 to 10,900 BP) was but half the influx during the Twocreekan. Geol. Soc. Am. Abstracts with Programs 13, p. 288.

Maijala P. 1991. Maatutkaluotausaineisto ja sen käsittely. Unpubl. M.S. thesis. University of Oulu. 113 p.

Marcussen I. 1973. Studies of flow till in Denmark. Boreas 2, 213 — 231.

Marsily C. de 1986. Quantitative Hydrogeology. Academic Press, San Diego. 440 p.

Marthinussen M. 1961. Brerandstadier og avsmeltningsforhold i Repparfjord-Stabbarsdal-området, Finnmark. NGU 213, 118 — 169.

Marttila I. 1982. Maaperätutkan tutkiminen ja kehittäminen polttoturve-soiden mittauksiin. Unpubl. Thesis, Helsinki University of Technology. 56 p.

McNeill J.D. 1980. Electromagnetic terrain conductivity measurement at low induction numbers. Technical note TN-6. Geonics Ltd., Ontario, Canada 15 p.

McNeill J.D. 1990. Use of electromagnetic methods for groundwater studies. *In* Investigations in geophysics 5: Geotecnical and environmental geophysics, ed. by S.H Ward. Soc. Expl. Geoph., Tulsa, 191 — 218.

McManus J. 1988. Grain size determination and interpretation. *In* Techniques in sedimentology, ed. by M. Tucker. Blackwell Scientific Publications. 63 — 85.

Meriläinen K. 1977. Geological Map of Finland 1 : 100 000, Pre-Quaternary Deposits, Sheet 3531, Jonku.

Mickelson D.M. 1971. Glacial Geology of the Burroughs Glacier, southeastern Alaska. The Ohio State Univ. Inst. of Polar Stud., Rep. 40, 149 p.

Mickelson D.M. & Sutinen R. 1989. The Use of Groundpenetrating Radar for D.O.T. Materials Studies. Rept. Univ. of Wisconsin-Madison. 49 p.

Mickelson D.M., Clayton L., Baker R.W., Mode W.N & Schneider A.F. 1984. Pleistocene Stratigraphic Units of Wisconsin Geol. and Nat. History Survey. Univ. of Wisconsin-Extension, Misc. Paper 84—1, 15 p.

Morawski W. 1989. Watermorainic sediments: Origin and classification. *In* Genetic Classification of Glacigenic Deposits, ed. by R.P. Goldthwait & C.L. Match. A.A. Balkema. Rotterdam. 143 — 144.

Morey R.M. & Harrington W.S. Jr. 1972. Feasibility Study of Electromagnetic Subsurface Profiling. EPA-R2—72-082, 71 p.

Mutanen T. 1979. Sääksjärvi on sittenkin astrobleemi. Geologi 31 (9 — 10), 125 — 130.

Nieminen P. 1985. Moreenin hienoaineksen laatu ja sen vaikutus routimisherkkyyteen. Abstract: The quality of the fine fractions of till and its influence on frost susceptibility. Tampere University of Technology. Publ. 34, 81 p.

Nordkalottproject 1986a. Geochemical Atlas of Northern Fennoscandia, 1 : 4 million. Geological Surveys of Finland, Norway and Sweden, in cooperation with Swedish Geological Co. and Geological Survey of Greenland.

Nordkalottproject 1986b. Map of Quaternary geology, sheet 2: Glacial geomorphology and paleohydrography, Northern Fennoscandia, 1 : 1 million. Geological Surveys of Finland, Norway and Sweden.

Nordkalottproject 1986c. Map of Quaternary geology, sheet 3: Ice flow indicators, Northern Fennoscandia 1 : 1 million. Geological Surveys of Finland, Norway and Sweden.

Olhoeft G.R. 1986. Direct detection of hydrocarbon and organic chemicals with ground penetrating radar and complex resistivity. Proc. of the National Water Well Assoc.

Conf. on Petroleum Hydrocarbons and Organic Chemicals in Ground Water, Nov. 12 — 14, Houston.

Olhoeft G.R. 1988. Selected bibliography on ground penetrating radar: Proc. of the Symposium on the Appl. of Geoph. to Engr. and Environ. Problems, Soc. of Engr. and Mineral Explor. Geoph., 462 — 520.

Olsen L. 1988. Stadials and interstadials during the Weichsel glaciation on Finnmarksvidda, northern Norway. Boreas 17, 517 — 539.

Patterson D.E. & Smith M.W. 1980. The Use of Time Domain Reflectometry for the Measurement of Unfrozen Water Content on Frozen Soils. Cold Regions Science and Technology 3, 205 — 210.

Patterson D.E. & Smith M.W. 1981. The measurement of unfrozen water content by time domain reflectometry: results from laboratory tests. Can. Geotech. J. 18, 131 — 144.

Parasnis D.S. 1971. Physical property quide for rocks and minerals. Abem, Geophysical memorandum 4/71, 12 p.

Parkhomenko E.I. 1967. Electrical Properties of rocks. Transl. and Ed. by G.V. Keller. Plenum Press, New York. 314 p.

Peltoniemi M. 1982. Characteristics and results of an airborne electromagnetic method of geophysical surveying. Geol. Surv. Finland, Bull. 321, 229 p.

Peltoniemi H., Eriksson B., Grönlund T. & Saarnisto M. 1989. Marjamurto, an interstadial site in a till-covered esker area of Central Ostrobothnia, western Finland. Bull. Geol. Soc. Finland 61 (2), 209 — 237.

Pernu T. 1979. Maa- ja kallioperän tutkiminen tasavirtamittauksilla, erityisesti Suomen oloissa. Unpubl. thesis. University of Oulu. 99 p.

Pernu T. 1991. Model and field studies of direct current resistivity measurements with the combined (half-Schlumberger) array $A\overline{MN}$, $\overline{MN}B$. Acta Universitatis Ouluensis. Ser A, Sci. Rev. Nat. 221, 71 p.

Pilon J. 1983. General state-of-the-art review of ground probing radar. A-Cubed Inc. Missauga, Ontario, Canada. 89 p.

Piotrowski J. & Smalley I.J. 1987. The Woodstock drumlin field, southern Ontario, Canada. *In* Drumlin Symposium, ed. by J. Menzies & J. Rose. Balkema, Rotterdam, 309 — 321.

Prest V.K. 1968. Nomenclature of moraines and ice-flow features as applied to the glacial map of Canada. Geol Surv. Canada, Paper 67 — 57.

Price R.J. 1973. Glacial and fluvioglacial landforms. Oliver & Boyd, Edinburgh. 242 p.

Pulkkinen E., Puranen R. & Lehmuspelto P. 1980. Interpretation of geochemical anomalies in glacial drift of Finnish Lapland with the aid of magnetic susceptibitlity data. Geol. Surv. Finland, Rep. Invest. 47, 39 p.

Punkari M. 1982. Glacial geomorphology and dynamics in the eastern parts of the Baltic Shield interpreted using Landsat imagery. The Photogrammetric Journal of Finland 9, 77 — 93.

Punkari M. 1984. The Relations between Glacial Dynamics and Tills in the Eastern Part of the Baltic Shield. *In* Ten Years of Nordic Till Research, ed. by L-K. Königsson. Striae 20, 49 — 54.

Punkari M. 1985. Glacial geomorphology and dynamics in Soviet Karelia interpreted by means of satellite imagery. Fennia 163, 113 — 153.

Punning J.M. & Raukas A. 1983. The age of tills: Problems and methods. *In* Tills and related deposits, ed. by E. Evenson, Ch Schlucter & J. Rabassa. Balkema, Rotterdam. 357 — 364.

Puranen R. 1989. Susceptibility, iron and magnetite content of Precambrian rocks in Finland. Geol. Surv. Finland, Rep. of Invest. 90. 45 p.

Puranen R., Sulkanen K. & Jäppinen T. 1983. Kivinäytteiden (ominais)vastusmääritykset Mafrip-mittarilla. Laiteseloste. Rep. Q15/83/1. Geol. Surv. Finland, Espoo. 6 p.

Rainio H. & Lahermo P. 1984. New Aspects on the Distribution and Origin of the So-Called Dark Till. *In* Ten Years of Nordic Till Research, ed. by L-K Königsson. Striae 20, 45 — 47.

Reid H.F. 1896. Glacier Bay and its glaciers. U.S. Geol. Surv. 16th Ann. Rept. [for the year] 1894 — 95, Pt.1, 415 — 461.

Sakayama T., Hara T. & Imai T. 1983. Study of the combined use of ground probing radar and electric profiling in soil exploration. Bull. Int. Ass. Eng. Geol. 26 — 27, 309 — 313.

Saksa P. 1986. Tutkamittaukset kallion rakennetutkimuksissa. Valtion teknillinen tutkimuskeskus. Geotekniikan laboratorio. Espoo. Tiedotteita 634, 48 p.

Salonen V-P. 1986. Glacial transport distance distributions of surface boulders in Finland. Geol. Surv. Finland, Bull. 338, 57 p.

Saunderson H. C. 1977. The sliding bed facies in esker sands and gravels: a criterion for full-pipe (tunnel) flow? Sedimentology 24, 623 — 638.

Scarpace F.L. 1989. Lecture notes for IES/CEE 556, Remote image interpretation. University of Wisconsin-Madison, 99 p.

Schluchter Ch. (ed.) 1979. Introduction. Moraines and varves. A.A. Balkema, Rotterdam, p. 441.

Schmugge T.J., Jackson T.J. & McKim H.L. 1980. Survey Methods for Soil Moisture Determination. Water Resources Research, 16 (6), 961 — 979.

Schmugge T.J. 1980. Effect of Texture on Microwave Emission from Soils. IEEE Transactions on Geoscience and Remote Sensing GE-18 (4), 353 — 361.

Schneider. A.F. 1983. Wisconsinan stratigraphy and glacial sequence in southeastern Wisconsin. Geoscience Wisconsin 7, 59 — 85.

Schwarzer T.F. & Adams J.A.S. 1973. Rock and soil discrimination by low altitude airborne gamma-ray spectrometry in Payne County, Oklahoma. Economic Geology 68, 1297 — 1312.

Selig E.T. & Mansukhani A.M. 1975. Relationship of Soil Moisture to the Dielectric Property. Proc. Am. Soc. of Civil Engineers 101, GT8, 755 — 770.

Sellman P.V., Arcone S.A. & Delaney A. 1976. Preliminary evaluation of new LF radiowave and magnetic induction resistivity units- over permafrost terrain. Natl. Res. Council Canada Tech. Mem. 119. Proc. Symposium Permafrost Geophysics. 12 Oct.

Shaw J. 1979. Genesis of the Sveg tills and Rogen moraines of Central Sweden; a model of basal melt out. Boreas 8, 409 — 426.

Shaw J. 1983. Drumlin formation related to inverted meltwater erosional marks. Journal of Glaciology 29 (103), 461 — 477.

Shaw. J. & Kvill D. 1984. A glaciofluvial origin for drumlins of the Livingstone area, Saskatchewan. Can. J. Earth Sci. 21, 1442 — 1459.

Shaw J., Kvill D. & Rains B. 1989. Drumlins and catastrophic subglacial floods. Sedimentary Geology 62 (2/4), 177 — 202.

Shih S.F., Doolittle J.A., Myhre D.L. & Schellentrager G.W. 1986. Using radar for groundwater investigation. Journal of Irrigation and Drainage Engineering 112 (2), 110 — 118.

Smallery I.J. & Unwin D.J. 1968. The formation and shape of drumlins and their distribution and orientation in drumlin fields. J Glaciol. 7, 377 — 390.

Smith-Rose R. L. 1933. The electrical properties of soils for alternating currents at radio frequencies. Proc. Royal Soc. London 140, 359 p.

Stein J. 1985. An Elaboration of Two Methods to Investigate Unfrozen Water Movement in a Snow-soil Environment. Unpubl. Ph.D. Thesis. University of Alaska, Fairbanks. 295 p.

Sutinen R. 1977. Keski-Lapin harjujen rakenteista ja raekoostumuksesta. Unpubl. M.S. thesis. University of Oulu, 98 p.

Sutinen R. 1984. On the Glacial Stratigraphy in Pudasjärvi Area, Peräpohjola. *In* Ten Years of Nordic Till Research, ed. by L-K. Königsson. Striae 20, 91 — 94.

Sutinen R. 1985a. On the Subglacial Sedimentation of Hummocky Moraines and Eskers in Northern Finland. *In* Glaciofluvium, ed. by L.-K. Königsson. Striae 22, 21 — 25.

Sutinen R. 1985b. Application of impulse radar profiling to structural studies of morainic landforms in Northern Finland. *In* Glacial tills 85, ed. by M. C. Forde. Proc. Internal Conference on construction in glacial tills and boulder clays. Engineering technics press ltd. Edinburgh. 31 — 37.

Sutinen R. 1985c. Geological map of Finland 1 : 400 000, Quaternary deposits. Sheet 35, Pudasjärvi. Geol. Surv. Finland, Espoo.

Sutinen R. 1989. Electrical resistivity and permittivity of glacial deposits and radar study of drumlin stratigraphy in southern Wisconsin. GSA Abstracts with Programs 21 (4) p. 48.

Sutinen R. & Pollari R. 1979. General geological map of Finland 1 : 400 000, Quaternary deposits. Sheet 45, Kuusamo. Geol. Surv. Finland, Espoo.

Sutinen R. & Hänninen, Pekka 1990. Radar profiling and dielectrical properties of glacial deposits in North Finland. Proc. VI IAEG Congress, Amsterdam, 2, 1045 — 1051.

Taanila P. 1976. Seisminen tutkimus. *In* Maa- ja kalliorakennus. RIL 98. Suomen Rakennusinsinöörien liitto, Helsinki. 229 — 232.

Tanner V. 1915. Studier öfver kvartärsystemet i Fennoskandias nordliga delar. III. Bull. Comm. géol. Finlande 38. 815 p.

Taylor L.D. 1962. Ice structures, Burroughs Glacier, southeast Alaska. Ph.D. dissertation, The Ohio State Univ., Columbus, 202 p.

Tervo. T. 1986. Glasiaalistratigrafiasta Koillis-Kittilässä. Unpubl. M.S. thesis, University of Oulu. 121 p.

Todd D.K. 1964. Groundwater. Handbook of Applied Hydrology. Ch. 13. ed. by V.T. Chow. McGraw Hill, New York.

Topp G.C. & Davis J.L. 1982. Measurement of Soil Water Content Using Time Domain Reflectometry. Proc. Canadian Hydrology Symposium: 82. Fredericton, New Brunswick, 269 — 287.

Topp G.C., Davis J.L. & Annan A.P. 1980. Electromagnetic Determination of Soil Water content: Measuremets in Coaxial Transmission Lines. Water Resources Research 16 (3), 574 — 582.

Topp G.C., Davis J.L. & Annan A.P. 1982. Electromagnetic determination of soil water content using TDR: II Applications to wetting fronts and steep gradients. Soil Sci. Soc. Am. J. 46, 672 — 678.

Topp G.C., Davis J.L., Bailey W.G. & Zebchuk W.D. 1984. The measurement of soil water content using a portable TDR hand probe. Can. J. Sci. 64, 313 — 321.

Ulaby F.T., Moore R.K. & Fung A.K. 1986. Microwave Remote Sensing. Active and Passive. III. Artech House. 2119 p.

Ulriksen P. 1982. Application of impulse radar to civil engineering. Doctoral thesis, Lund Institute of Technology, Sweden. LUTVDG/TVTG-1001/1—75.

Upham W. 1894. The Madison type of drumlins. American Geologist 14, 68 — 83.

Vanhanen E. 1989. Uraniferous mineralizations in the Kuusamo schist belt, northeastern Finland. Proc. Metallogenesis of uranium deposits, IAEA, Vienna 1987, 169 — 186.

Virkkala K. 1969. Suomen moreenien rakeisuusluokitus. Summary: Classification of Finnish Tills according to Grain Size. Terra 81 (3), 273 — 278.

Von Hippel A. 1954. Dielectric Materials and Applications. Cambridge. Massachusetts. MIT Press. 438 p.

Wang J.R. & Schmugge T.J. 1980. An Empirical Model for the Complex Dielectric Permittivity of Soils as a Function of Water Content. IEEE Transactions on Geoscience and Remote Sensing, GE-18 (4), 228 — 295.

Ward S.H. 1990. Resistivity and induced polarization methods. *In* Investigations in geophysics 5: Geotechnical and environmental geophysics, ed. by S.H Ward. Soc. Expl. Geoph., Tulsa, 191 — 218.

Whittecar G. R. & Mickelson D. M. 1979. Composition, internal structures, and hypothesis of formation for drumlins. Waukesha County, Wisconsin, U.S.A. Journal of Glaciology 22, 357 — 371.

Wilcox S. W. 1944. Sand and gravel prospecting by the earth resistivity method. Geophysics 9, 36 — 45.

Wobschall D. 1977. A theory of the complex dielectric permittivity of soil containing water, the semidispersive model. IEEE Trans. Geosci. Electron., GE-15, 29 — 58.

Woodworth J.B. 1899. The ice-contact in the classification of glacial deposits. Am. Geol. 23, 80 — 86.

Wright H.E.Jr. 1973. Tunnel valleys, glacial surges and subglacial hydrology of the Superior lobe, Minnesota. *In* The Wisconsinan Stage, ed. by R.F.Black, R.P. Golgthwait & G.P. Willman. Geol. Soc. Am. Mem. 136, 251 — 276.